

UNCLASSIFIED

AD NUMBER

AD882110

LIMITATION CHANGES

TO:

Approved for public release; distribution is unlimited.

FROM:

Distribution: Further dissemination only as directed by Electromagnetic Compatability Analysis Center, Annapolis, MD 21402, DEC 1970, or higher DoD authority.

AUTHORITY

ECAC ltr 20 Sep 1972

THIS PAGE IS UNCLASSIFIED

✓
ESD-TR-70-207

AD882110

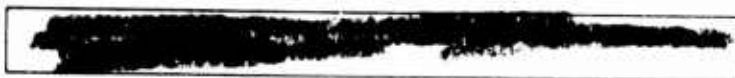
DEPARTMENT OF DEFENSE

ELECTROMAGNETIC COMPATIBILITY ANALYSIS CENTER

ANALYSIS OF PULSED INTERFERENCE TO AMPLITUDE MODULATED RECEIVERS, VOLUME II

Prepared by W. Hatch, R. Hinkle, R. Mayher
of the IIT Research Institute

December 1970



**Best
Available
Copy**

ESD-TR-70-207

When U.S. Government drawings, specifications, or other data are used for any purpose other than a definitely related government procurement operation, the government thereby incurs no responsibility nor any obligation whatsoever, and the fact that the government may have formulated, furnished, or in any way supplied the said drawings, specifications, or other data is not to be regarded by implication or otherwise, or in any manner licensing the holder or any other person or corporation, or conveying any rights or permission to manufacture, use or sell any patented invention that may in any way be related thereto.

Do not return this copy. When not needed, destroy.

ESD-TR-70-207

ANALYSIS OF PULSED INTERFERENCE TO
AMPLITUDE MODULATED RECEIVERS,
VOLUME II

Technical Report

No. ESD-TR-70-207

December 1970

DEPARTMENT OF DEFENSE
Electromagnetic Compatibility Analysis Center

Prepared by W. Hatch, R. Hinkle, R. Mayher
of the IIT Research Institute

DOD DISTRIBUTION STATEMENT

This document may be further distributed by any holder
only with specific prior approval of ECAC.

Published by
Electromagnetic Compatibility Analysis Center
North Severn
Annapolis, Maryland 21402

FOREWORD

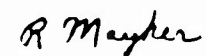
The Electromagnetic Compatibility Analysis Center (ECAC) is a Department of Defense facility, established to provide advice and assistance on electromagnetic compatibility matters to the Secretary of Defense, the Joint Chiefs of Staff, the military departments and other DOD components. The Center, located at North Severn, Annapolis, Maryland 21402, is under executive control of the Director of Defense Research and Engineering and the Chairman, Joint Chiefs of Staff or their designees who jointly provide policy guidance, assign projects, and establish project priorities. ECAC functions under the direction of the Secretary of the Air Force and the management and technical direction of the Center are provided by military and civil service personnel. The technical operations function is provided through an Air Force sponsored contract with the IIT Research Institute (IITRI).

This report was prepared as part of AF Project 649E under Contract F-19628-70-C 0291 by the staff of the IIT Research Institute at the Department of Defense Electromagnetic Compatibility Analysis Center.

To the extent possible, all abbreviations and symbols used in this report are taken from American Standard Y10.19 (1967) "Units Used in Electrical Science and Electrical Engineering" issued by the United States of America Standards Institute.

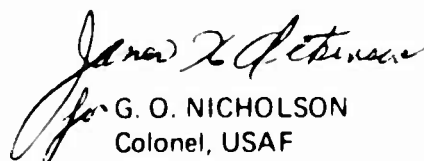
Users of this report are invited to submit comments which would be useful in revising or adding to this material to the Director, ECAC, North Severn, Annapolis, Maryland 21402, Attention ACX.


Reviewed by:


R. Mayher
Project Engineer


J. M. DETERDING
Director of Technical Operations

Approved:


G. O. NICHOLSON
Colonel, USAF
Director


Clarence E. Apple
Lieutenant Colonel, USA
Deputy Director

APPENDIX I

EQUIVALENT LOW PASS FILTER ANALYSIS

This analysis will consider the effect of a linear time invariant bandpass filter on the pulsed interference. The interfering pulsed spectrum at the output of the IF filter will be symmetrical or unsymmetrical depending upon the input pulse parameters. The Fourier transform of the output spectrum will give the output time waveform (references 29 and 30).

To determine the output time waveform analytically, it is necessary to show that for any given narrowband spectrum of a real signal, the real and imaginary bandpass and low pass equivalent can be obtained. This will enable one to determine the amplitude and phase modulation with respect to a particular frequency within the narrowband spectrum.

First it will be shown that the impulse response of a symmetrical bandpass filter is a modulated signal that can be derived from an appropriately chosen low pass filter. These results can then be used to derive the output time waveform for a given symmetrical narrowband spectrum. Second, these results will be extended to show that given any narrowband spectrum of a real signal, the real and imaginary bandpass and low pass equivalent can be obtained. From this the amplitude and phase modulation with respect to a particular frequency can be obtained.

The bandpass filter is defined as a system function whose spectral density has significant values only in a region not containing the origin (Figure I-1a). The Fourier transform of the impulse response of a symmetrical filter is defined as the system function, $G_s(\omega)$. That is:

$$G_s(\omega) = \int_{-\infty}^{\infty} g_s(t) e^{-j\omega t} dt \quad (I-1)$$

$$= X(\omega) + jY(\omega) \quad (I-2)$$

$$= A(\omega)e^{j\theta_s(\omega)} \quad (I-3)$$

Since $G_s(\omega)$ and $g_s(t)$ are Fourier transform pairs

$$g_s(t) = \frac{1}{2\pi} \int_{-\infty}^{\infty} G_s(\omega) e^{j\omega t} d\omega \quad (I-4)$$

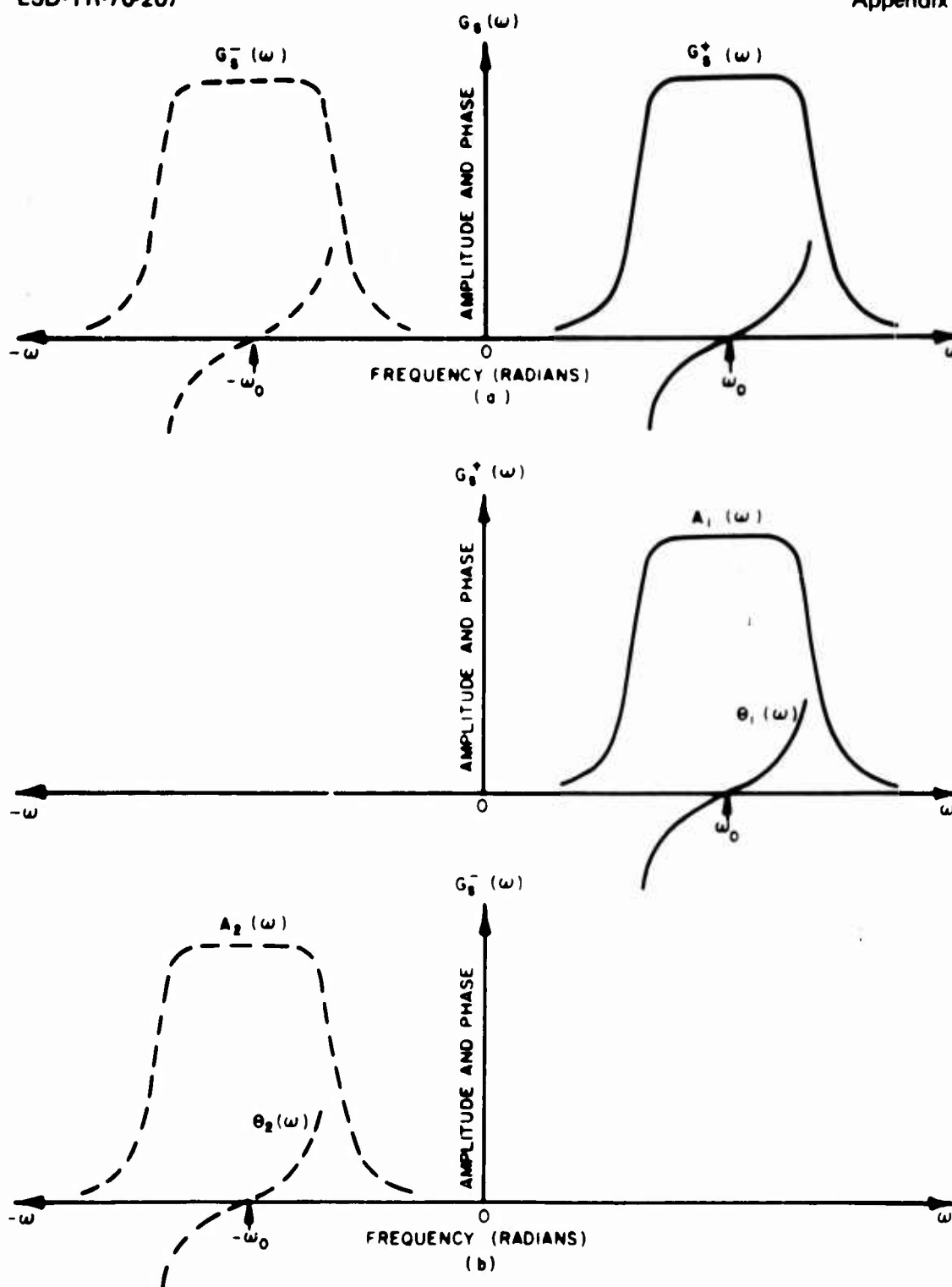


Figure I-1. Symmetrical Bandpass Filter System Function

Considering a system function $G_s(\omega)$ as a sum

$$G_s(\omega) = G_s^+(\omega) + G_s^-(\omega) \quad (I-5)$$

where

$$G_s^+(\omega) = G_s(\omega) U(\omega) = A_1(\omega) e^{-j\theta_1(\omega)} \quad (I-6a)$$

$$G_s^-(\omega) = G_s(\omega) U(-\omega) = A_2(\omega) e^{-j\theta_2(\omega)} \quad (I-6b)$$

as shown in Figure I-1b.

Since $g_s(t)$ is a real function of time

$$G_s(\omega) = G_s^*(-\omega) \quad (I-7)$$

and therefore,

$$G_s^+(\omega) = G_s^{+*}(\omega) \quad (I-8)$$

where $*$ denotes the complex conjugate.

If the system function is symmetrical, then

$$G_s^+(\omega + \omega_0) = G_s^{+*}(\omega_0 - \omega) \quad (I-9)$$

$$G_s^-(\omega - \omega_0) = G_s^{-*}(-\omega_0 - \omega) \quad (I-10)$$

where ω_0 is the center frequency.

Therefore, with

$$G_s^+(\omega) = A_1(\omega) e^{-j\theta_1(\omega)} \quad (I-11)$$

$$G_s^-(\omega) = A_2(\omega) e^{-j\theta_2(\omega)} \quad (I-12)$$

one obtains

$$A_1(\omega + \omega_0) = A_1(\omega_0 - \omega) \quad \theta_1(\omega + \omega_0) = -\theta_1(-\omega_0 - \omega) \quad (I-13)$$

$$A_2(\omega - \omega_0) = A_2(-\omega_0 - \omega) \quad \theta_2(\omega - \omega_0) = -\theta_2(-\omega_0 - \omega) \quad (I-14)$$

Thus, $A_1(\omega)$ and $A_2(\omega)$ are even functions and $\Theta_1(\omega)$ and $\Theta_2(\omega)$ are odd functions about the center frequency ω_0 .

The system function, $G_s(\omega)$, for a symmetrical system can be obtained from the equivalent low pass function. That is, the impulse response of a symmetrical bandpass filter of center frequency ω_0 is given by

$$g_s(t) = 2g_{\ell s}(t) \cos \omega_0 t \quad (I-15)$$

where $g_{\ell s}(t)$ is the equivalent low pass filter function. This is easily shown by considering the fact that the low pass system function $G_{\ell s}(\omega)$ of Figure I-2 is obtained by shifting $G_s^+(\omega)$ in Figure I-2 to the left by ω_0 . That is:

$$G_{\ell s}(\omega) = G_s^+(\omega + \omega_0) \quad (I-16)$$

or

$$G_s^+(\omega) = G_{\ell s}(\omega - \omega_0) \quad (I-17)$$

It is also evident that $G_{\ell s}(\omega)$ can also be obtained by shifting $G_s^-(\omega)$ to the right by ω_0 .

$$G_{\ell s}(\omega) = G_s^-(\omega - \omega_0) \quad (I-18)$$

or

$$G_s^-(\omega) = G_{\ell s}(\omega + \omega_0) \quad (I-19)$$

Due to symmetry

$$G_{\ell s}(-\omega) = G_{\ell s}^*(\omega) \quad (I-20)$$

Using the property of the shifting theorem and Equations 16 and 18 one obtains

$$g_{\ell s}(t) e^{j\omega_0 t} \longleftrightarrow G_s^+(\omega) \quad (I-21)$$

$$g_{\ell s}(t) e^{-j\omega_0 t} \longleftrightarrow G_s^-(\omega) \quad (I-22)$$

$$g_{\ell s}(t) e^{j\omega_0 t} + g_{\ell s}(t) e^{-j\omega_0 t} \longleftrightarrow G_s^+(\omega) + G_s^-(\omega) \quad (I-23)$$

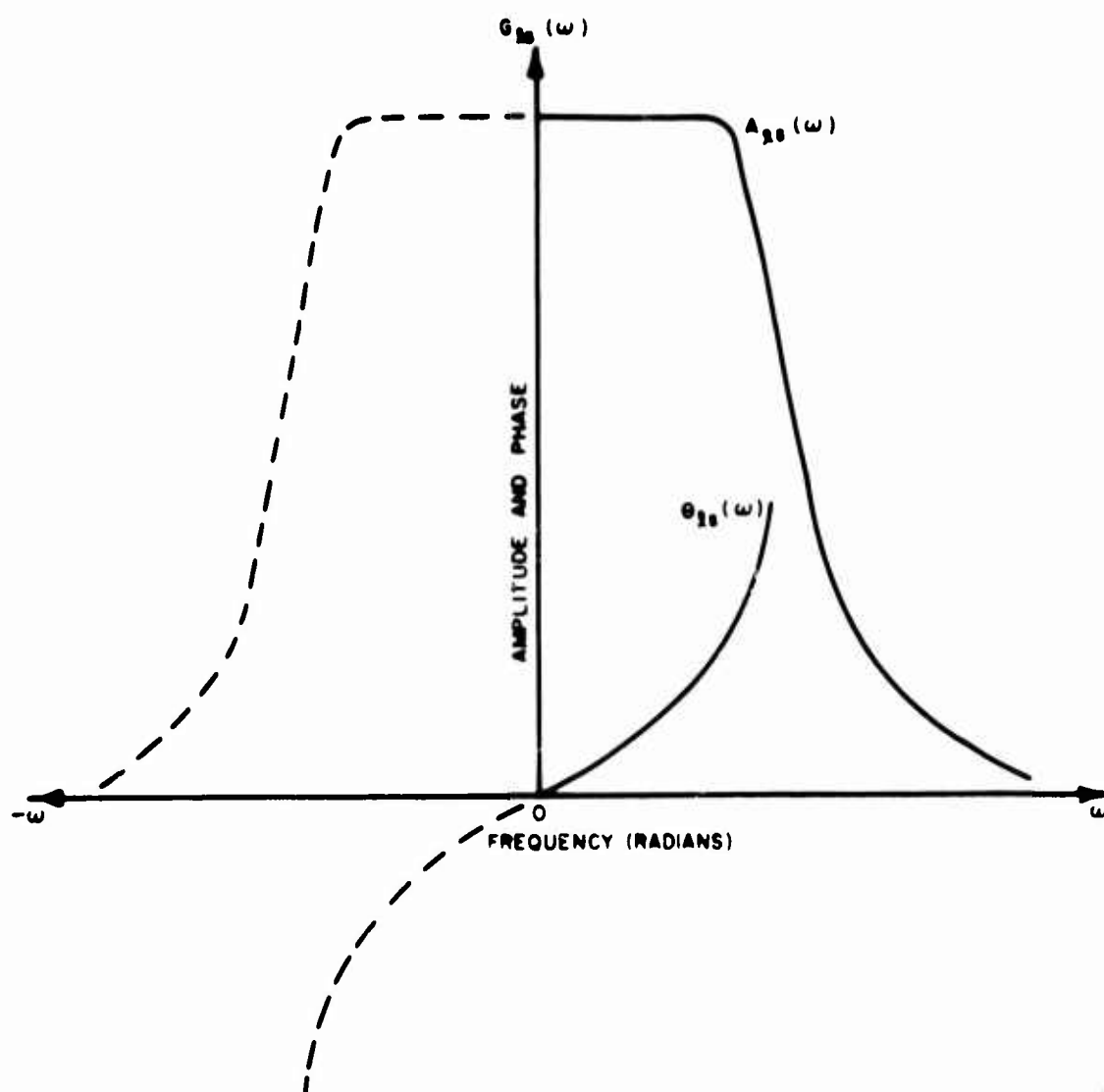


Figure I-2. Equivalent Lowpass Filter System Function

but

$$G_1^+(\omega) + G_1^-(\omega) = G_1(\omega) \longleftrightarrow g_1(t) \quad (I-24)$$

therefore

$$g_1(t) = g_{\ell 1}(t) [e^{j\omega_0 t} + e^{-j\omega_0 t}] = 2g_{\ell 1}(t) \cos \omega_0 t \quad (I-25)$$

The symmetrical system is sufficient for handling on-tune pulse interference since the product of the symmetrical system function and the pulse spectrum will produce a new function symmetrical about ω_0 . However, for off-tuned pulse interference the product of the system function and the pulse spectrum will produce an unsymmetrical function about the center frequency ω_0 .

This can be handled by expanding the result obtained for the symmetrical case. Writing $G(\omega)$ as in the symmetrical case (see Figure I-3) we have

$$G(\omega) = G^+(\omega) + G^-(\omega) \quad (I-26)$$

where $G^+(\omega)$ and $G^-(\omega)$ are defined by Equation (I-6). In order to simplify the drawing only the real part of $G(\omega)$ will be shown. If the system is unsymmetrical then there is no clearly defined center frequency, ω_0 , as in the symmetrical case.

Choosing ω_0 as any frequency in the passband one can write the output signal of a narrowband waveform in complex form as

$$g(t) = \text{Re} [A(t)e^{j\phi_1(t)} e^{j(\omega_0 t + \theta_0)}] \quad (I-27)$$

where Re means take the real part

$$A(t) = \text{slowly varying function as compared to } \omega_0 t$$

$$\phi_1(t) = \text{slowly varying phase function as compared to } \omega_0 t$$

$$\omega_0 = \text{carrier frequency in radians}$$

$$\theta_0 = \text{carrier phase}$$

Rewriting $g(t)$ in quadrature form gives

$$g(t) = A(t) \cos \phi_1(t) \cos (\omega_0 t + \theta_0) - A(t) \sin \phi_1(t) \sin (\omega_0 t + \theta_0) \quad (I-28)$$

$$= 2g_{\ell 1}(t) \cos (\omega_0 t + \theta_0) - 2g_{\ell 2}(t) \sin (\omega_0 t + \theta_0) \quad (I-29)$$

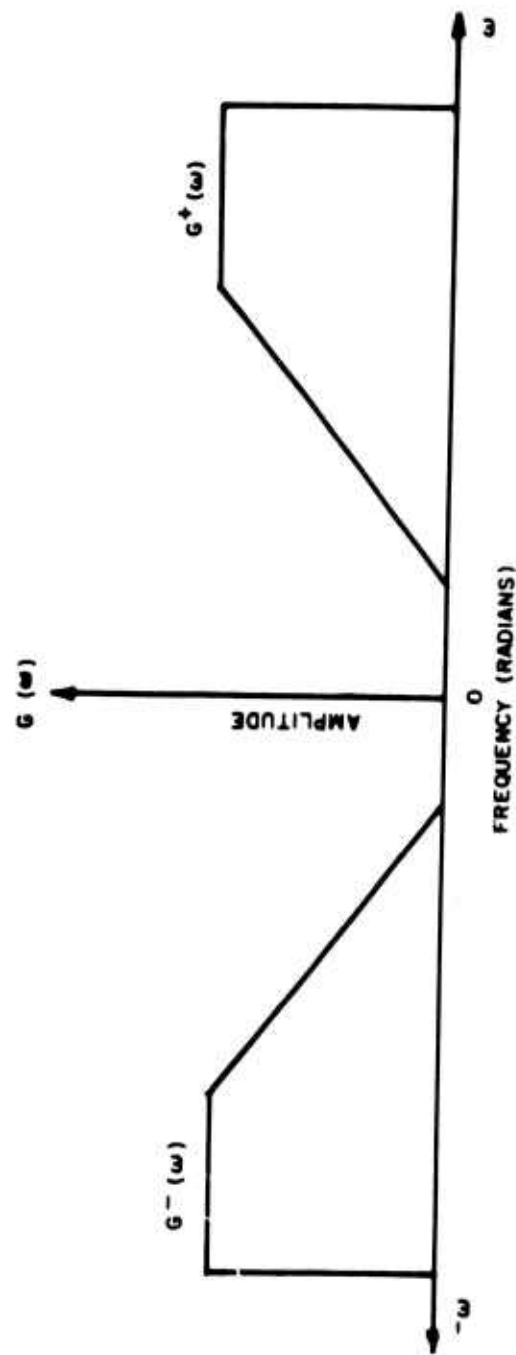


Figure I-3. Narrowband Spectrum of a Real Signal

$$= A(t) \cos [\omega_0 t + \theta_0 + \phi_1(t)] \quad (I-30)$$

where

$$2g_{\ell_1}(t) = A(t) \cos \phi_1(t) \quad (I-31)$$

$$2g_{\ell_2}(t) = A(t) \sin \phi_1(t) \quad (I-32)$$

$$A(t) = 2[g_{\ell_1}^2(t) + g_{\ell_2}^2(t)]^{1/2} \quad (I-33)$$

$$\phi_1(t) = \tan^{-1} g_{\ell_1}(t)/g_{\ell_2}(t) \quad (I-34)$$

letting

$$g_1(t) = 2g_{\ell_1}(t) \cos (\omega_0 t + \theta_0) \quad (I-35)$$

$$g_2(t) = 2g_{\ell_2}(t) \sin (\omega_0 t + \theta_0) \quad (I-36)$$

then

$$g(t) = g_1(t) + g_2(t) \quad (I-37)$$

Since $g(t)$ is a real time function the Fourier transform of $g(t)$ can be written as

$$g(t) \longleftrightarrow G(\omega) = G^+(\omega) + G^-(\omega) \quad (I-38)$$

Since $g(t)$ is a real time function, $g_1(t)$ and $g_2(t)$ are also real time functions whose Fourier transforms are given by

$$g_1(t) \longleftrightarrow G_1(\omega) = G_1^+(\omega) + G_1^-(\omega) = G_{\ell_1}(\omega - \omega_0)e^{j\theta_0} + G_{\ell_1}(\omega + \omega_0)e^{j\theta_0} \quad (I-39)$$

$$g_2(t) \longleftrightarrow G_2(\omega) = G_2^+(\omega) + G_2^-(\omega) = \frac{1}{j} [G_{\ell_2}(\omega - \omega_0)e^{j\theta_0} - G_{\ell_2}(\omega + \omega_0)e^{-j\theta_0}] \quad (I-40)$$

where $G_{1,2}^+(\omega)$ and $G_{1,2}^-(\omega)$ indicate the positive spectrum and negative spectrums and $G_{\ell_1}(\omega)$ and $G_{\ell_2}(\omega)$ are the low pass equivalent of $G_1(\omega)$ and $G_2(\omega)$, respectively.

In order to evaluate $G(\omega)$ with respect to some frequency ω_0 , it is necessary to extract $G_1(\omega)$ and $G_2(\omega)$ from $G(\omega)$ with respect to ω_0 .

In order to evaluate the spectrum at some point other than the carrier, say $\Delta\omega$ from the carrier the following is noted:

$$G_1^+(\omega) \Big|_{\omega=\omega_0+\Delta\omega} = G_{\ell_1}(\Delta\omega)e^{j\theta_0} = G_{\ell_1}^*(-\Delta\omega)e^{j\theta_0} \quad (I-41)$$

$$G_2^+(\omega) \Big|_{\omega=\omega_0+\Delta\omega} = \frac{1}{j} G_{\ell_2}(\Delta\omega)e^{j\theta_0} = \frac{1}{j} G_{\ell_2}^*(-\Delta\omega)e^{j\theta_0} \quad (I-42)$$

Without loss of generality θ_0 can be set equal to zero and the following stated:

$$G_1^+(\omega) \Big|_{\omega=\omega_0+\Delta\omega} = G_1^{+*}(\omega) \Big|_{\omega=\omega_0-\Delta\omega} \quad (I-43)$$

$$G_2^+(\omega) \Big|_{\omega=\omega_0+\Delta\omega} = -G_2^{+*}(\omega) \Big|_{\omega=\omega_0-\Delta\omega} \quad (I-44)$$

This states that the positive frequency content of $G_1(\omega)$ is symmetrical or has conjugate symmetry about ω_0 , whereas $G_2(\omega)$ is unsymmetrical or has anti-conjugate symmetry about ω_0 as depicted in Figure I-4, a and b. $G_1^+(\omega)$ is the real part of $G(\omega)$ and $G_2^+(\omega)$ is the imaginary part of $G(\omega)$. Therefore, $G_1^+(\omega)$ and $G_2^+(\omega)$ can be obtained by performing the following:

$$G_1^+(\omega) \Big|_{\omega=\omega_0+\Delta\omega} = \frac{1}{2}G^+(\omega) \Big|_{\omega=\omega_0+\Delta\omega} + \frac{1}{2}G^{+*}(\omega) \Big|_{\omega=\omega_0-\Delta\omega} \quad (I-45)$$

$$G_2^+(\omega) \Big|_{\omega=\omega_0+\Delta\omega} = \frac{1}{2}G^+(\omega) \Big|_{\omega=\omega_0+\Delta\omega} - \frac{1}{2}G^{+*}(\omega) \Big|_{\omega=\omega_0-\Delta\omega} \quad (I-46)$$

also

$$\begin{aligned} G_1^{+*}(\omega) \Big|_{\omega=\omega_0-\Delta\omega} &= \frac{1}{2}G^{+*}(\omega) \Big|_{\omega=\omega_0-\Delta\omega} + \frac{1}{2}G^+(\omega) \Big|_{\omega=\omega_0+\Delta\omega} \\ &= G_1^+(\omega) \Big|_{\omega=\omega_0+\Delta\omega} \end{aligned} \quad (I-47)$$

$$\begin{aligned} G_2^{+*}(\omega) \Big|_{\omega=\omega_0-\Delta\omega} &= \frac{1}{2}G^{+*}(\omega) \Big|_{\omega=\omega_0-\Delta\omega} - \frac{1}{2}G^+(\omega) \Big|_{\omega=\omega_0+\Delta\omega} \\ &= -G_2^+(\omega) \Big|_{\omega=\omega_0+\Delta\omega} \end{aligned} \quad (I-48)$$

Define

$$G_1^-(\omega) = G_1^{+*}(-\omega) \quad G_2^-(\omega) = G_2^{+*}(-\omega) \quad (I-49)$$

$$G_1(\omega) = G_1^+(\omega) + G_1^-(\omega), \quad G_2(\omega) = G_2^+(\omega) + G_2^-(\omega) \quad (I-50)$$

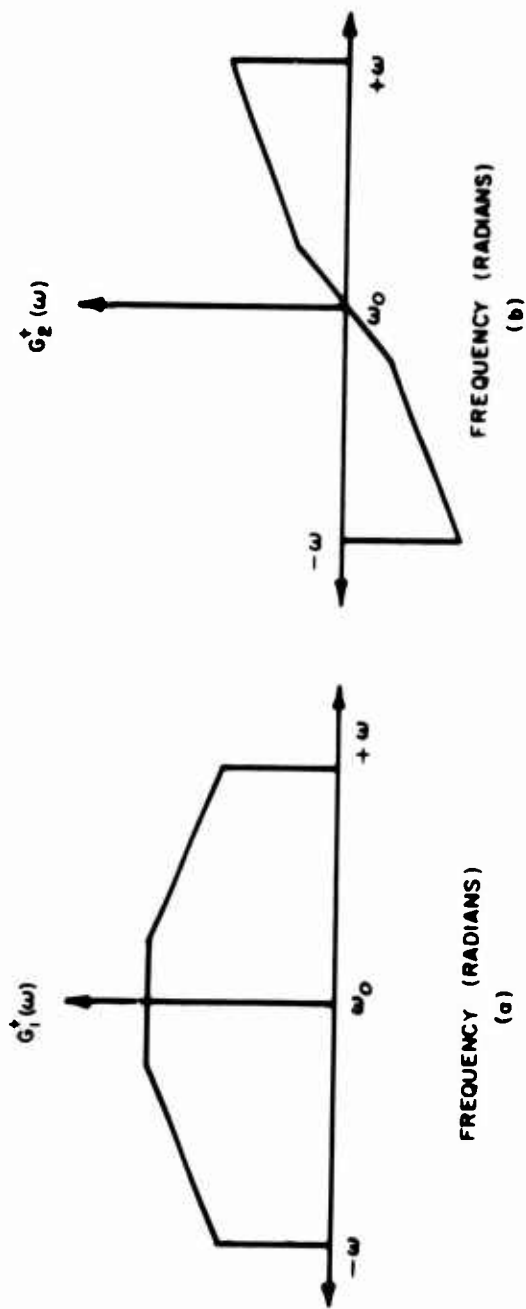


Figure I-4. Symmetrical and Non-Symmetrical Spectrum of a Real Signal

From Equation (I-41) and (I-42) one obtains:

$$2G_{\ell_1}(\omega) = G_1^+(\omega + \omega_0) + G_1^-(\omega - \omega_0) \quad (I-51)$$

$$2G_{\ell_2}(\omega) = G_2^+(\omega + \omega_0) - G_2^-(\omega - \omega_0) \quad (I-52)$$

Thus, $G_{\ell_1}(\omega)$ and $G_{\ell_2}(\omega)$ are spectrum of real signals with $G_{\ell_1}(\omega)$ corresponding to the modulation on $\cos \omega_0 t$ and $G_{\ell_2}(\omega)$ corresponding to the modulation on $\sin \omega_0 t$.

Therefore, given any narrowband spectrum of a real signal, one can obtain the real and imaginary bandpass or low pass equivalent which will give the amplitude and phase modulation with respect to any frequency within the narrowband spectrum. The general equation for the time waveform of the narrowband spectrum is given by Equation (I-30) as:

$$g(t) = A(t) \cos [\omega_0 t + \theta_0 + \phi_1(t)] \quad (I-53)$$

where

$A(t)$ = amplitude modulation

$\phi_1(t)$ = phase modulation

When the spectrum is even $G_2(\omega)$ and thus $G_{\ell_2}(\omega)$ are equal to zero and this gives an output time waveform of the form:

$$g(t) = 2g_{\ell_1}(t) \cos \omega_0 t \quad (I-54)$$

where θ_0 , the carrier phase angle, has been assumed equal to zero. This is the same form as Equation (I-25) which was obtained for the symmetrical system function.

APPENDIX II

DETECTOR ANALYSIS FOR AM RECEIVER

INTRODUCTION

The analysis will consider the effects of a linear envelope detector on pulsed interference and band limited Gaussian noise. The envelope detector is assumed to be ideal in that it responds only to the amplitude variations and not to the phase variations. The appendix is divided into two sections. The first section discusses the derivation of the AM detector equation used in the computer simulation model. The second section discusses the derivation of a series expansion form of an AM detector output for a large interfering carrier-to-noise ratio.

COMPUTER SIMULATION DETECTOR MODEL

The computer simulation model obtains the desired signal at the detector input by taking the inverse Fourier transform of the low pass equivalent IF filter transfer function, $H(\omega)$, multiplied by the IF input low pass equivalent of the desired signal spectrum, $V_s(\omega)$. It can easily be shown that the lowpass equivalent of the desired signal at the detector input is given by:

$$X_s(t) = \mathcal{F}^{-1} H(\omega) V_s(\omega) \quad (II-1)$$

$$= X_R(t) + j X_I(t) \quad (II-1a)$$

where

$$X_R(t) = A_s [1 + M_s \cos(\omega_s t + \psi)] \quad (II-2a)$$

$$X_I(t) = 0 \quad (II-2b)$$

and

$$A_s = \text{The amplitude of the desired signal at IF output}$$

$$m_s = \text{The desired signal modulation index after IF filtering}$$

- ω_s = The frequency of the desired modulating tone in radians
- ψ = The phase shift of the information after IF filtering

The desired bandpass signal (reference 31) is given by:

$$V_s(t) = \text{Re} \left\{ X_s(t) e^{j\omega_s t} \right\} \quad (\text{II-3a})$$

$$= \text{Re} \left\{ [X_R(t) + jX_I(t)] [\cos \omega_0 t + j \sin \omega_0 t] \right\} \quad (\text{II-3b})$$

$$= X_R(t) \cos \omega_0 t \quad (\text{II-3c})$$

$$= A_s [1 + M_s \cos(\omega_s t + \psi)] \cos \omega_0 t \quad (\text{II-3d})$$

where

- ω_0 = The desired signal carrier frequency in radians

The computer simulation model obtains the undesired signal at the detector input by taking the inverse Fourier transform of the low pass equivalent IF filter transfer function, $H(\omega)$, multiplied by the IF input low pass equivalent of the pulsed interfering signal spectrum, $V_I(\omega)$, plus the noise spectrum, $V_N(\omega)$. It can easily be shown that the low pass equivalent of the undesired signal at the detector input is given by

$$Y_{I+N}(t) = \mathcal{F}^{-1} H(\omega) [V_I(\omega) + V_N(\omega)] \quad (\text{II-4})$$

$$= Y_R(t) + jY_I(t) \quad (\text{II-4a})$$

The undesired bandpass signal is given by

$$V_{I+N}(t) = \text{Re} \left\{ Y_{I+N}(t) e^{j\omega_0 t} \right\} \quad (\text{II-5a})$$

$$= \text{Re} \left\{ [Y_R(t) + jY_I(t)] [\cos \omega_0 t + j \sin \omega_0 t] \right\} \quad (\text{II-5b})$$

$$= Y_R(t) \cos \omega_0 t - Y_I(t) \sin \omega_0 t \quad (\text{II-5c})$$

Since $Y_R(t)$ and $Y_I(t)$ represent real and imaginary time dependent vectors in a rectangular coordinate system, they may be written in polar coordinate form as

$$Y_R(t) = A(t) \cos \phi(t) \quad (II-6)$$

$$Y_I(t) = A(t) \sin \phi(t) \quad (II-7)$$

where

$$A(t) = \sqrt{Y_R^2(t) + Y_I^2(t)}$$

Therefore, the undesired bandpass signal is given by

$$V_{I+N}(t) = A(t) [\cos \phi(t) \cos \omega_0 t - \sin \phi(t) \sin \omega_0 t] \quad (II-8)$$

Equation (II-8) may be rewritten as

$$V_{I+N}(t) = A(t) \cos [\omega_0 t + \phi(t)] \quad (II-9)$$

where

$$\phi(t) = \Delta\omega t + \theta_0 + \theta_1^1(t)$$

$$\theta_1^1(t) = \phi_1(t) - \Delta\omega t$$

and

$A(t)$ = The undesired signal amplitude modulation after IF filtering

$\Delta\omega$ = The frequency difference between the desired and undesired carriers in radians

θ_0 = Phase difference between desired and undesired carriers after IF filtering (phase angle of desired carrier = 0°)

$\phi_1(t)$ = Undesired signal phase modulation after IF filtering

Therefore, the undesired bandpass signal is an amplitude and phase modulated signal.

The desired plus undesired signal at the detector input is obtained by adding Equations (II-3d) and (II-5c), and is given by

$$V(t) = V_s(t) + V_{I+N}(t) \quad (II-10a)$$

$$= [X_R(t) + Y_R(t)] \cos \omega_0 t - Y_I(t) \sin \omega_0 t \quad (II-10b)$$

The output of the linear detector will then be the envelope of $V(t)$ and is given by

$$V_d(t) = \left\{ [X_R(t) + Y_R(t)]^2 + Y_I^2(t) \right\}^{1/2} \quad (II-11a)$$

$$= \left\{ [A_S |1 + M_S \cos(\omega_S t + \psi)| + A(t) \cos \phi(t)]^2 + [A(t) \sin \phi(t)]^2 \right\}^{1/2} \quad (II-11b)$$

SERIES EXPANSION OF DETECTION OUTPUT

In order to obtain a better understanding of the degradation caused by the pulsed interference, Equation (II-11) should be in a form that separates the pulsed interference components from the desired signal components. This can be accomplished by considering a large interfering carrier-to-noise ratio so that noise may be neglected and arranging the detector output equation in a form that can be expanded in a series for $A_S > A_I$ and $A_I > A_S$.

For $A_S > A_I$

The equation for the interfering signal at the detector input is given by

$$V_I(t) = A(t) \cos [\omega_0 t + \phi(t)] \quad (II-12)$$

where

$$A(t) = A_I p(t)$$

$$A_I = \text{The amplitude of the interfering signal at IF output}$$

$$p(t) = \text{The amplitude modulation of the pulsed interfering signal plus the amplitude transients caused by the IF filter}$$

Expanding $V_I(t)$ and adding the desired signal given in Equation (II-3d) gives

$$V(t) = V_S(t) + V_I(t) = [A_S[1 + M_S \cos(\omega_S t + \psi)] + A_I p(t) \cos \phi(t)] \cos \omega_O t - [A_I p(t) \sin \phi(t)] \sin \omega_O t \quad (\text{II-13})$$

The output of the linear detector will then be the envelope of $V(t)$ and is given by

$$V_d(t) = \left\{ [A_S[1 + M_S \cos(\omega_S t + \psi)] + A_I p(t) \cos \phi(t)]^2 + [A_I p(t) \sin \phi(t)]^2 \right\}^{1/2} \quad (\text{II-14})$$

Multiplying Equation (II-14) inside the square root by

$$V_d(t) = \left[\frac{A_S[1 + M_S \cos(\omega_S t + \psi)]}{A_S[1 + M_S \cos(\omega_S t + \psi)]} \right]^2 \text{ gives} \\ = A_S[1 + M_S \cos(\omega_S t + \psi)] \left\{ \left[1 + \frac{A_I p(t) \cos \phi(t)}{A_S[1 + M_S \cos(\omega_S t + \psi)]} \right]^2 + \left[\frac{A_I p(t) \sin \phi(t)}{A_S[1 + M_S \cos(\omega_S t + \psi)]} \right]^2 \right\}^{1/2} \quad (\text{II-15})$$

Equation (II-15) can be expanded in a power series in (A_I/A_S) and the higher order terms neglected since we let $A_S > A_I$. The Taylor expansion of the square root term of $V_d(t)$ can be represented as

$$[(1+ax)^2 + b^2 x^2]^{1/2} = 1 + ax + \frac{b^2 x^2}{2} + \dots \quad (\text{II-16})$$

Therefore, $V_d(t)$ becomes

$$V_d(t) \approx A_S[1 + M_S \cos(\omega_S t + \psi)] \left\{ 1 + \frac{A_I p(t) \cos \phi(t)}{A_S[1 + M_S \cos(\omega_S t + \psi)]} + \frac{1}{2} \left[\frac{A_I p(t) \sin \phi(t)}{A_S[1 + M_S \cos(\omega_S t + \psi)]} \right]^2 \right\} \quad (\text{II-17a})$$

And:

$$V_d(t) \approx \left\{ A_s [1 + M_s \cos(\omega_s t + \psi)] + A_i p(t) \cos \phi(t) + \frac{A_i^2 p^2(t)}{2A_s} \left[\frac{\sin^2 \phi(t)}{1 + M_s \cos(\omega_s t + \psi)} \right] \right\} \quad (II-17b)$$

The third term of $V_d(t)$ can be expanded using a power series and the following trigometric identities.

$$\frac{1}{1 + M_s \cos(\omega_s t + \psi)} \approx 1 - M_s \cos(\omega_s t + \psi) + M_s^2 \cos^2(\omega_s t + \psi) + \dots \quad (II-18a)$$

$$\sin^2 \phi(t) = \frac{1}{2} - \frac{1}{2} \cos 2\phi(t) \quad (II-18b)$$

$$\cos^2(\omega_s t + \psi) = \frac{1}{2} + \frac{1}{2} \cos 2(\omega_s t + \psi) \quad (II-18c)$$

$$\cos X \cos Y = \frac{1}{2} [\cos(X+Y) + \cos(X-Y)] \quad (II-18d)$$

Applying the power series expansion and trigometric identities listed above the third term becomes

$$\begin{aligned} & \frac{A_i^2 p^2(t)}{2A_s} \left\{ \frac{1}{2} \left(1 + \frac{M_s^2}{2} \right) - \frac{M_s}{2} \cos(\omega_s t + \psi) + \frac{M_s^2}{4} \cos 2(\omega_s t + \psi) \right. \\ & - \frac{1}{2} \left(1 + \frac{M_s^2}{2} \right) \cos 2\phi(t) + \frac{M_s}{4} \cos [2\phi(t) + (\omega_s t + \psi)] \\ & + \frac{M_s}{4} \cos [2\phi(t) - (\omega_s t + \psi)] - \frac{M_s^2}{8} \cos 2[\phi(t) + (\omega_s t + \psi)] \\ & \left. - \frac{M_s^2}{8} \cos 2[\phi(t) - (\omega_s t + \psi)] \right\} \end{aligned}$$

Normalizing $V_d(t)$ by A_s and substituting for $\phi(t)$ the detector output equation becomes

$$\frac{V_d(t)}{A_s} \approx [1 + M_s \cos(\omega_s t + \psi)] + R_i p(t) \cos [\Delta \omega t + \theta_o + \phi_i(t)]$$

$$\begin{aligned}
& + \frac{R_I^2 p^2(t)}{2} \left\{ \frac{1}{2} \left(1 + \frac{M_s^2}{2} \right) - \frac{M_s}{2} \cos(\omega_s t + \psi) \right. \\
& + \frac{M_s^2}{4} \cos 2(\omega_s t + \psi) - \frac{1}{2} \left(1 + \frac{M_s^2}{2} \right) \cos 2[\Delta\omega t + \Theta_0 + \phi_1(t)] \\
& + \frac{M_s}{4} \cos [2(\Delta\omega t + \Theta_0 + \phi_1(t)) + (\omega_s t + \psi)] \\
& + \frac{M_s}{4} \cos [2(\Delta\omega t + \Theta_0 + \phi_1(t)) - (\omega_s t + \psi)] \\
& + \frac{M_s^2}{8} \cos 2[(\Delta\omega t + \Theta_0 + \phi_1(t)) + (\omega_s t + \psi)] \\
& \left. + \frac{M_s^2}{8} \cos 2[(\Delta\omega t + \Theta_0 + \phi_1(t)) - (\omega_s t + \psi)] \right\} \quad (II-19)
\end{aligned}$$

where $R_I = A_I/A_S$

For $A_I > A_S$

In order to get the detector output equation in proper form for power series expansion in A_S/A_I the desired signal equation must be written as

$$V_S(t) = A_S [1 + M_s \cos(\omega_s t + \psi)] \cos [\omega_0 t + \phi(t) - \phi(t)] \quad (II-20)$$

The undesired pulse signal is given by

$$V_I(t) = A_I p(t) \cos [\omega_0 t + \phi(t)] \quad (II-21)$$

Expanding $V_S(t)$ gives

$$\begin{aligned}
V_S(t) = A_S [1 + M_s \cos(\omega_s t + \psi)] & \left\{ \cos \phi(t) \cos [\omega_0 t + \phi(t)] \right. \\
& \left. + \sin \phi(t) \sin [\omega_0 t + \phi(t)] \right\} \quad (II-22)
\end{aligned}$$

The desired plus undesired signal is given by

$$\begin{aligned}
V(t) = V_S(t) + V_I(t) = & \left\{ A_I p(t) + A_S [1 + M_s \cos(\omega_s t + \psi)] \cos \phi(t) \right\} \cos [\omega_0 t + \phi(t)] \\
& + A_S [1 + M_s \cos(\omega_s t + \psi)] \sin \phi(t) \sin [\omega_0 t + \phi(t)] \quad (II-23)
\end{aligned}$$

The output of the linear detector will then be the envelope of $V(t)$ and is given by

$$V_d(t) = \left\{ [A_1 p(t) + A_s [1 + M_s \cos(\omega_s t + \psi)] \cos \phi(t)]^2 + [A_s [1 + M_s \cos(\omega_s t + \psi)] \sin \phi(t)]^2 \right\}^{1/2} \quad (II-24)$$

Multiplying Equation (II-24) inside the square root by $\left[\frac{A_1 p(t)}{A_1 p(t)} \right]^2$ gives

$$V_d(t) = A_1 p(t) \left\{ \left[1 + \frac{A_s [1 + M_s \cos(\omega_s t + \psi)] \cos \phi(t)}{A_1 p(t)} \right]^2 + \left[\frac{A_s [1 + M_s \cos(\omega_s t + \psi)] \sin \phi(t)}{A_1 p(t)} \right]^2 \right\}^{1/2} \quad (II-25)$$

Equation (II-25) can be expanded in a power series in (A_s/A_1) and the higher order terms neglected since we let $A_1 > A_s$. The Taylor expansion of the square root term of $V_d(t)$ can be represented as

$$[(1 + ax)^2 + b^2 x^2]^{1/2} = 1 + ax + \frac{b^2 x^2}{2} + \dots \quad (II-26)$$

Therefore, $V_d(t)$ becomes

$$V_d(t) \approx A_1 p(t) \left\{ 1 + \frac{A_s [1 + M_s \cos(\omega_s t + \psi)] \cos \phi(t)}{A_1 p(t)} + \frac{1}{2} \left[\frac{A_s [1 + M_s \cos(\omega_s t + \psi)] \sin \phi(t)}{A_1 p(t)} \right]^2 \right\} \quad (II-27)$$

And:

$$V_d(t) \approx A_1 p(t) + A_s [1 + M_s \cos(\omega_s t + \psi)] \cos \phi(t) + \frac{A_s^2}{2 A_1 p(t)} [(1 + M_s \cos(\omega_s t + \psi))]^2 \sin^2 \phi(t) \quad (II-28)$$

Equation (II-28) can be reduced using the following trigometric identities:

$$\cos(\omega_s t + \psi) \cos \phi(t) = \frac{1}{2} \left\{ \cos [(\omega_s t + \psi) + \phi(t)] \right. \quad (\text{II-29a})$$

$$\left. + \cos [(\omega_s t + \psi) - \phi(t)] \right\} \quad (\text{II-29b})$$

$$\cos^2(\omega_s t + \psi) = \frac{1}{2} + \frac{1}{2} \cos 2(\omega_s t + \psi) \quad (\text{II-29c})$$

$$\sin^2 \phi(t) = \frac{1}{2} - \frac{1}{2} \cos 2\phi(t) \quad (\text{II-29d})$$

Then:

$$\begin{aligned} V_d(t) \approx & A_1 p(t) + A_s \left\{ \cos \phi(t) + \frac{M_s}{2} \cos [(\omega_s t + \psi) + \phi(t)] \right. \\ & \left. + \frac{M_s}{2} \cos [(\omega_s t + \psi) - \phi(t)] \right\} \\ & + \frac{A_s^2}{2A_1 p(t)} \left\{ \frac{1}{2} \left(1 + \frac{M_s^2}{2} \right) + M_s \cos(\omega_s t + \psi) + \frac{M_s^2}{4} \cos 2(\omega_s t + \psi) \right. \\ & - \frac{1}{2} \left(1 + \frac{M_s^2}{2} \right) \cos 2\phi(t) - \frac{M_s}{2} \cos [(\omega_s t + \psi) + 2\phi(t)] \\ & - \frac{M_s}{2} \cos [(\omega_s t + \psi) - 2\phi(t)] - \frac{M_s^2}{8} \cos 2[(\omega_s t + \psi) + \phi(t)] \\ & \left. - \frac{M_s^2}{8} \cos 2[(\omega_s t + \psi) - \phi(t)] \right\} \quad (\text{II-30}) \end{aligned}$$

Normalizing $V_d(t)$ by A_1 and substituting for $\phi(t)$ the detector output equation becomes

$$\begin{aligned} \frac{V_d(t)}{A_1} \approx & p(t) + R_s \left\{ \cos [\Delta\omega t + \Theta_0 + \phi_1'(t)] + \frac{M_s}{2} \cos [(\omega_s t + \psi) + (\Delta\omega t + \Theta_0 + \phi_1'(t))] \right. \\ & \left. + \frac{M_s}{2} \cos [(\omega_s t + \psi) - (\Delta\omega t + \Theta_0 + \phi_1'(t))] \right\} \\ & + \frac{R_s^2}{2p(t)} \left\{ \frac{1}{2} \left(1 + \frac{M_s^2}{2} \right) + M_s \cos(\omega_s t + \psi) \right. \\ & \left. + \frac{M_s^2}{4} \cos 2(\omega_s t + \psi) - \frac{1}{2} \left(1 + \frac{M_s^2}{2} \right) \cos [\Delta\omega t + \Theta_0 + \phi_1'(t)] \right\} \end{aligned}$$

$$\begin{aligned}
& - \frac{M_s}{2} \cos [(\omega_s t + \psi) + 2(\Delta\omega t + \theta_0 + \phi_1'(t))] \\
& - \frac{M_s}{2} \cos [(\omega_s t + \psi) - 2(\Delta\omega t + \theta_0 + \phi_1'(t))] \\
& - \frac{M_s^2}{8} \cos 2[(\omega_s t + \psi) + (\Delta\omega t + \theta_0 + \phi_1'(t))] \\
& - \frac{M_s^2}{8} \cos 2[(\omega_s t + \psi) - (\Delta\omega t + \theta_0 + \phi_1'(t))] \Bigg\} \quad (II-31)
\end{aligned}$$

$$\text{where } R_s = \frac{A_s}{A_I} = \frac{1}{R_I}$$

APPENDIX III

BASIC AM PULSED DEGRADATION DATA

This appendix documents the basic pulsed degradation data obtained in this investigation. Table 6-1 summarizes the data parameters and the figure numbers corresponding to their location.

TABLE III-1
THRESHOLD LEVEL OF RECTANGULAR PULSED INTERFERENCE
IN A NARROWBAND AM VOICE SYSTEM (RECEIVER NO. 1)

Pulse Width	PRF (PPS)	Δf (MHz)	S/I (dB)	Δf (MHz)	S/I (dB)	Δf (MHz)	S/I (dB)	Δf (MHz)	S/I (dB)	Δf (MHz)	S/I (dB)	Δf (MHz)	S/I (dB)	Δf (MHz)	S/I (dB)
5 μ s	300	0	+5	.003	+5	.025	+3	.100	0	.500	-17	1.000	-26		
5 μ s	1000	0	+16	.003	+8	.025	+8	.100	+7	.500	-14	1.000	-24		
100 μ s	40	0	+21	.003	+20	.025	+1	.100	-15	.500	-29				
100 μ s	80	0	+22	.003	+21	.025	-2	.100	-6	.500	-24				
100 μ s	300	0	+28												
100 μ s	400	0	+30	.003	+32	.025	+8	.100	-2	.500	-17				
200 μ s	40	0	+24	.003	+25	.025	+3	.100	-11	.500	-25				
200 μ s	80	0	+25	.003	+23	.025	+14	.100	-9	.500	-25				
200 μ s	400	0	+32	.003	+34	.025	+13	.100	-2	.500	-18				
400 μ s	10	0	+24	.003	+24	.025	-3	.100	-13	.500	-28	1.000	-42		
400 μ s	40	0	+24	.003	+25	.025	+2	.100	-9	.500	-25	1.000	-38		
400 μ s	80	0	+30	.003	+28	.025	+2	.100	-10	.500	-23	1.000	-33		
400 μ s	400	0	+31	.003	+31	.025	+8	.100	-1	.500	-16	1.000	-26		
1000 μ s	10	0	+29	.003	+29	.025	+4	.100	-7	.500	-24				
1000 μ s	40	0	+25	.003	+25	.025	+5	.100	-11	.500	-27				
1000 μ s	80	0	+30	.003	+28	.025	+2	.100	-9	.500	-24				
1000 μ s	400	0	+27	.003	+37	.025	+10	.100	-1	.500	-13				

TABLE III-2
THRESHOLD LEVELS OF CHIRPED RECTANGULAR PULSED INTERFERENCE
IN A NARROWBAND AM VOICE SYSTEM (RECEIVER NO. 1)

Pulse Width	PRF (PPS)	CHIRP (kHz)	Δf (MHz)	S/I (dB)	Δf (MHz)	S/I (dB)	Δf (MHz)	S/I (dB)	Δf (MHz)	S/I (dB)
100 μ s	40	500	0	+5	.003	+5	.1	+5	1.0	-35
100 μ s	80	500	0	+6	.003	+6	.1	+6	1.0	-34
100 μ s	400	500	0	+9	.003	+9	.1	+9	1.0	-32
200 μ s	40	500	0	+6	.003	+6	.1	+9	1.0	-32
200 μ s	80	500	0	+28	.003	+28	.1	+9	1.0	-33
200 μ s	400	500	0	+10	.003	+10	.1	-	1.0	-30
400 μ s	10	250	0	+13	.003	+13	.1	+13	1.0	-40
400 μ s	40	250	0	+15	.003	+15	.1	+15	1.0	-40
400 μ s	80	250	0	+17	.003	+17	.1	+17	1.0	-37

TABLE III-3
THRESHOLD LEVEL OF RECTANGULAR PULSED INTERFERENCE
IN A NARROWBAND AM VOICE SYSTEM (RECEIVER NO. 2)

Pulse Width	PRF (PPS)	Δf (MHz)	S/I (dB)	Δf (MHz)	S/I (dB)	Δf (MHz)	S/I (dB)	Δf (MHz)	S/I (dB)	Δf (MHz)	S/I (dB)	Δf (MHz)	S/I (dB)	Δf (MHz)	S/I (dB)
200 μ s	40	0	+12			.1	-3	1	-39	10	-34	20	-57		
200 μ s	80	0	+16			.1	-3	1	-35	10	-27	20	-56		
200 μ s	400	0	+31			.1	-21	1	-27	10	-27	20	-63		
400 μ s	10	0	+20	.003	+13	.1	-42	1	-52	10	-43	20	-65		
400 μ s	40	0	+23	.003	+16	.1	-34	1	-48	10	-36	20	-58		
400 μ s	80	0	+27	.003	+17	.1	-23	1	-45	10	-32	20	-59		
400 μ s	400	0	+24	.003	+25	.1	-12	1	-33	10	-29	20	-56		
1000 μ s	10	0	+25	.003	+9			1	-51	10	-39	20	-69		
1000 μ s	40	0	+28	.003	+16			1	-46	10	-28	20	-60		
1000 μ s	80	0	+29	.003	+22			1	-45	10	-31	20	-57		
1000 μ s	400	0	+25	.003	+30			1	-42	10	-22	20	-47		
5 μ s	300	0	-1	.1	0	.75	-11	1	-26	10	-63	20	-79		
5 μ s	1000	0	+2	.1	+4	.75	-18	1	-37	10	-66	20	-91		
100 μ s	40	0	-3	.1	-33			1	-53	10	-44	20	-75		
100 μ s	80	0	0	.1	-26			1	-50	10	-44	20	-65		
100 μ s	300	0	+14												
100 μ s	400	0	+16	.1	-18			1	-36	10	-38	20	-61		

TABLE III-4
THRESHOLD LEVEL OF RECTANGULAR PULSED INTERFERENCE IN A
NARROWBAND AM VOICE SYSTEM FOR CHIRPED RECTANGULAR
INTERFERENCE (RECEIVER NO. 2)

Pulse Width	PRF (PPS)	CHIRP (kHz)	Δf (MHz)	S/I (dB)	Δf (MHz)	S/I (dB)	Δf (MHz)	S/I (dB)	Δf (MHz)	S/I (dB)
100 μ s	40	1000	0	-63	1.0	-51	10	-55	20	-83
100 μ s	80	1000	0	-23	1.0	-50	10	-53	20	-80
100 μ s	400	1000	0	-23	1.0	-52	10	-44	20	-76
200 μ s	40	1000	0	-37	.1	-37	10	-46	20	-79
200 μ s	80	1000	0	-37	.1	-36	10	-46	20	-81
200 μ s	400	1000	0	-1	.1	-30	10	-43	20	-80
400 μ s	10	250	0	-5	.1	-35	10	-64	20	-83
400 μ s	40	250	0	+7	.1	-26	10	-53	20	-78
400 μ s	80	250	0	+7	.1	-22	10	-51	20	-78

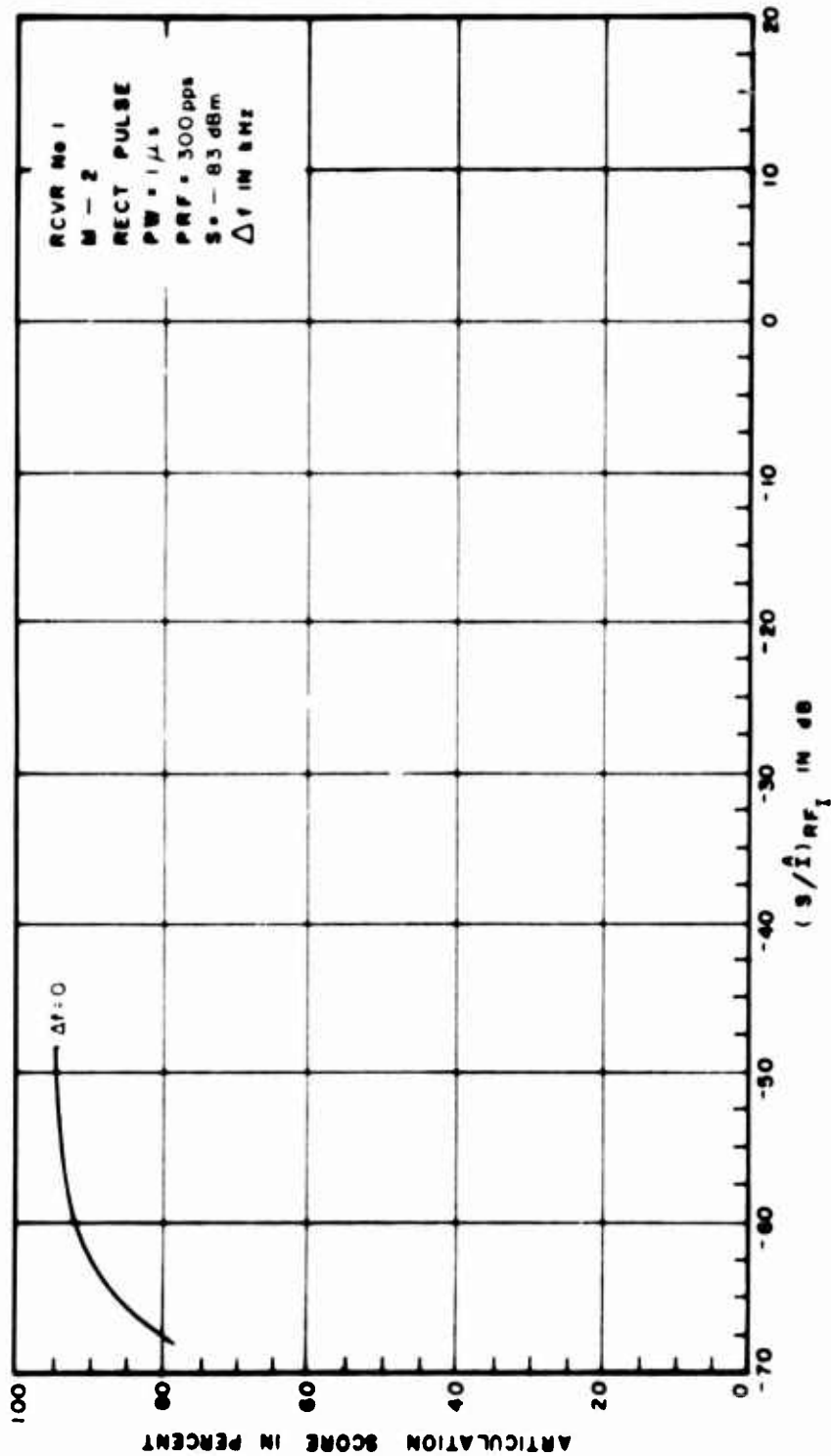


Figure III-1. Articulation Score for Pulsed Interference to an AM Receiver

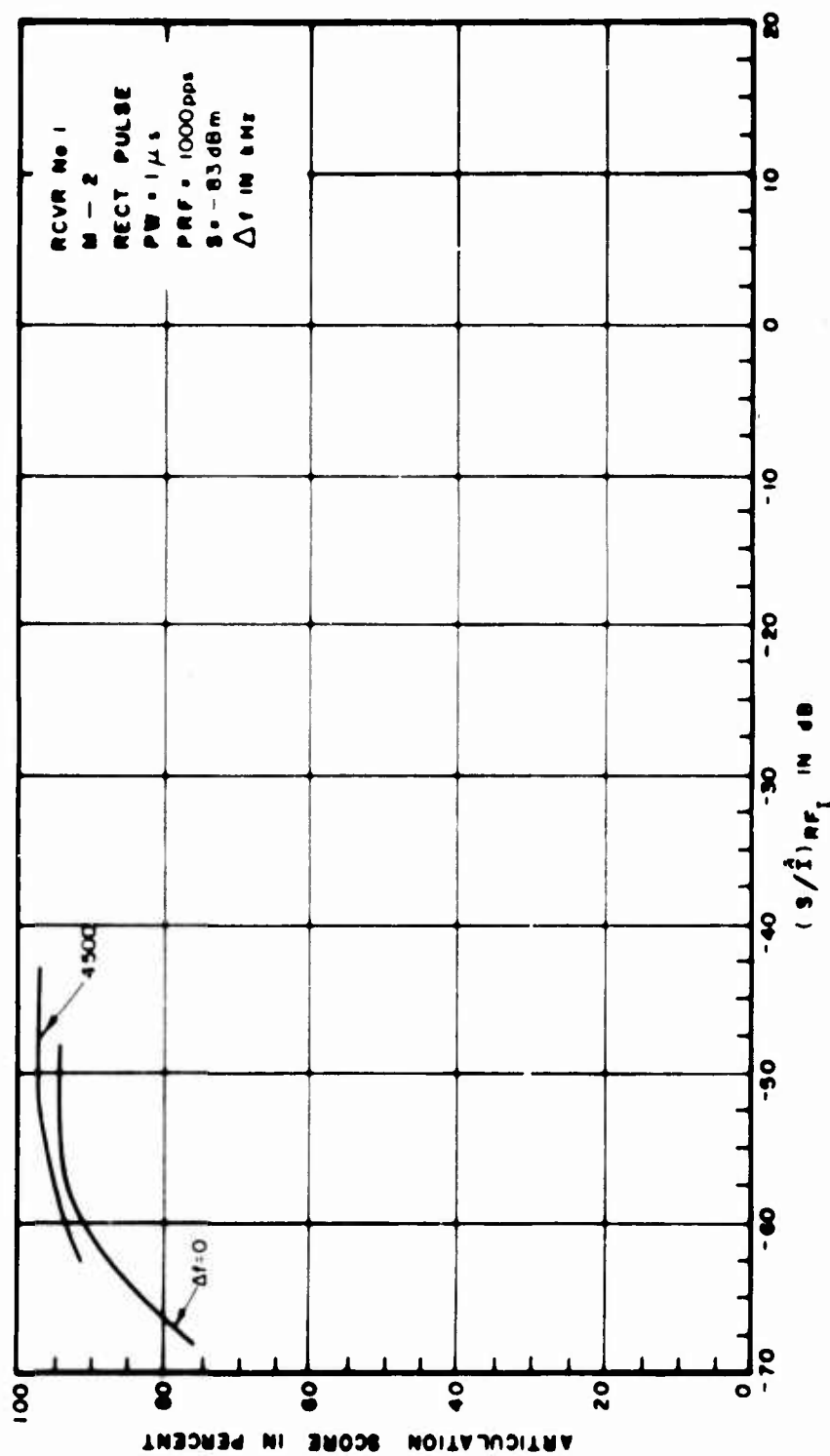


Figure III-2. Articulation Score for Pulsed Interference to an AM Receiver

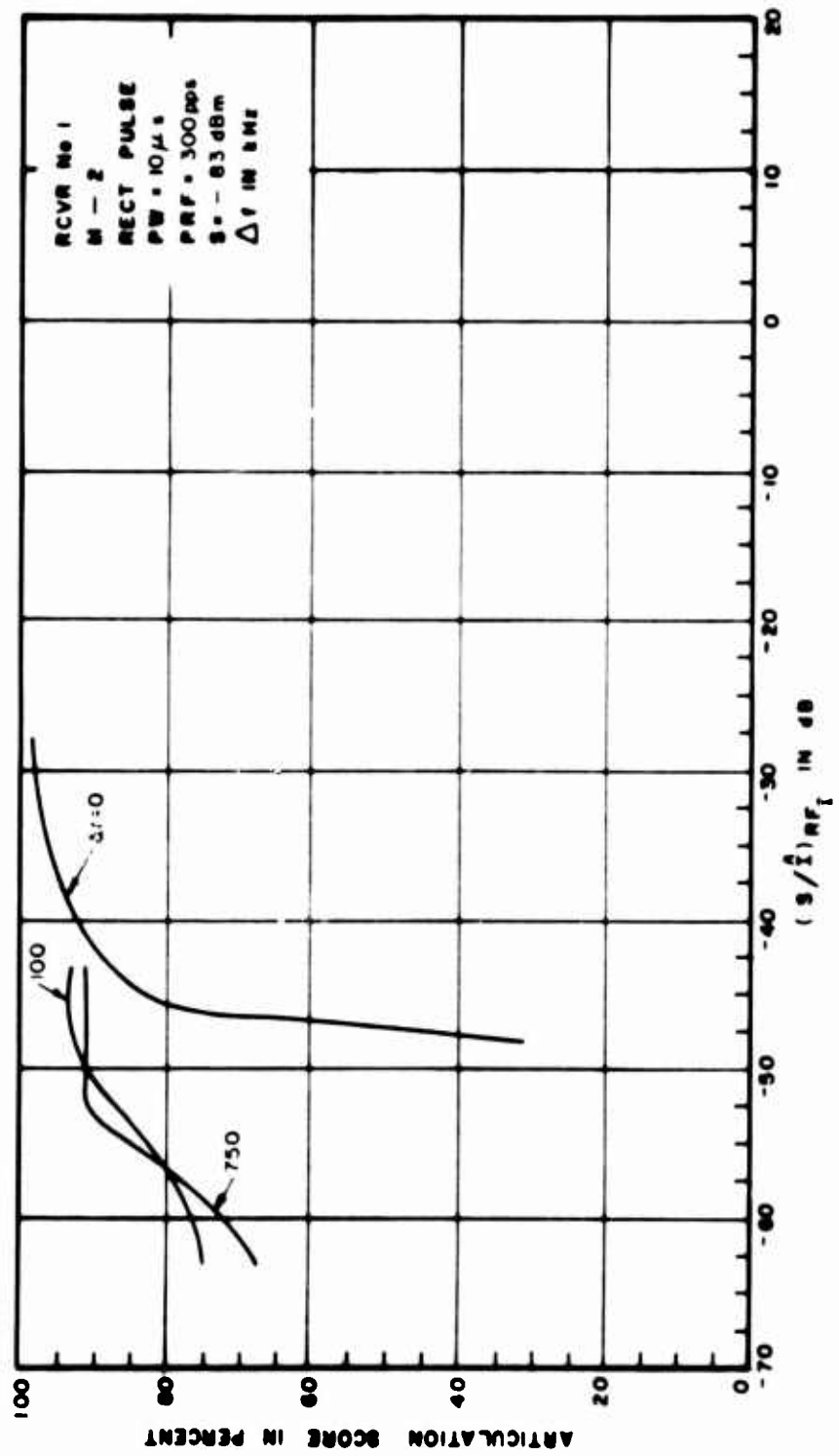


Figure III-3. Articulation Score for Pulsed Interference to an AM Receiver

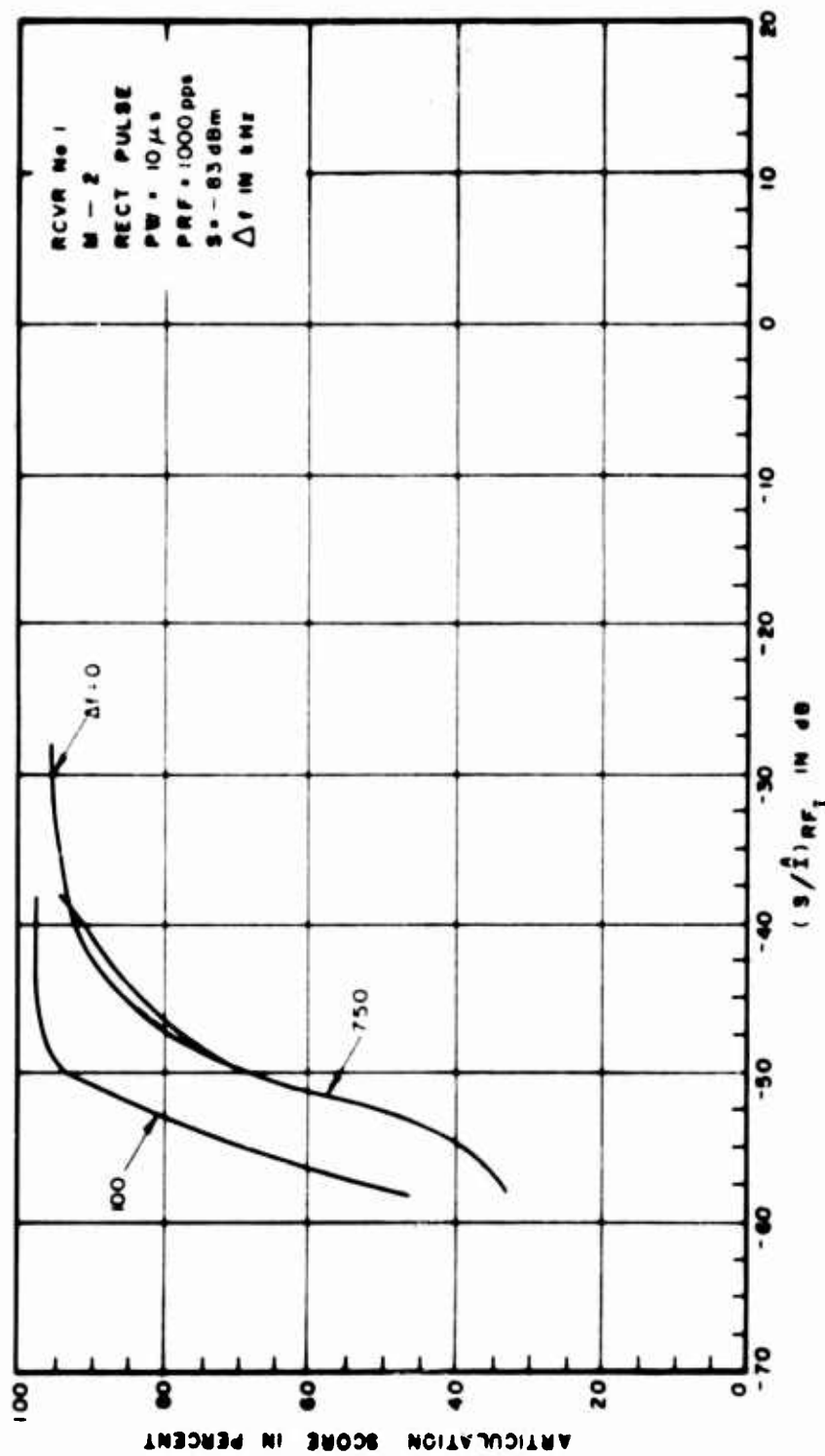


Figure III-4. Articulation Score for Pulsed Interference to an AM Receiver

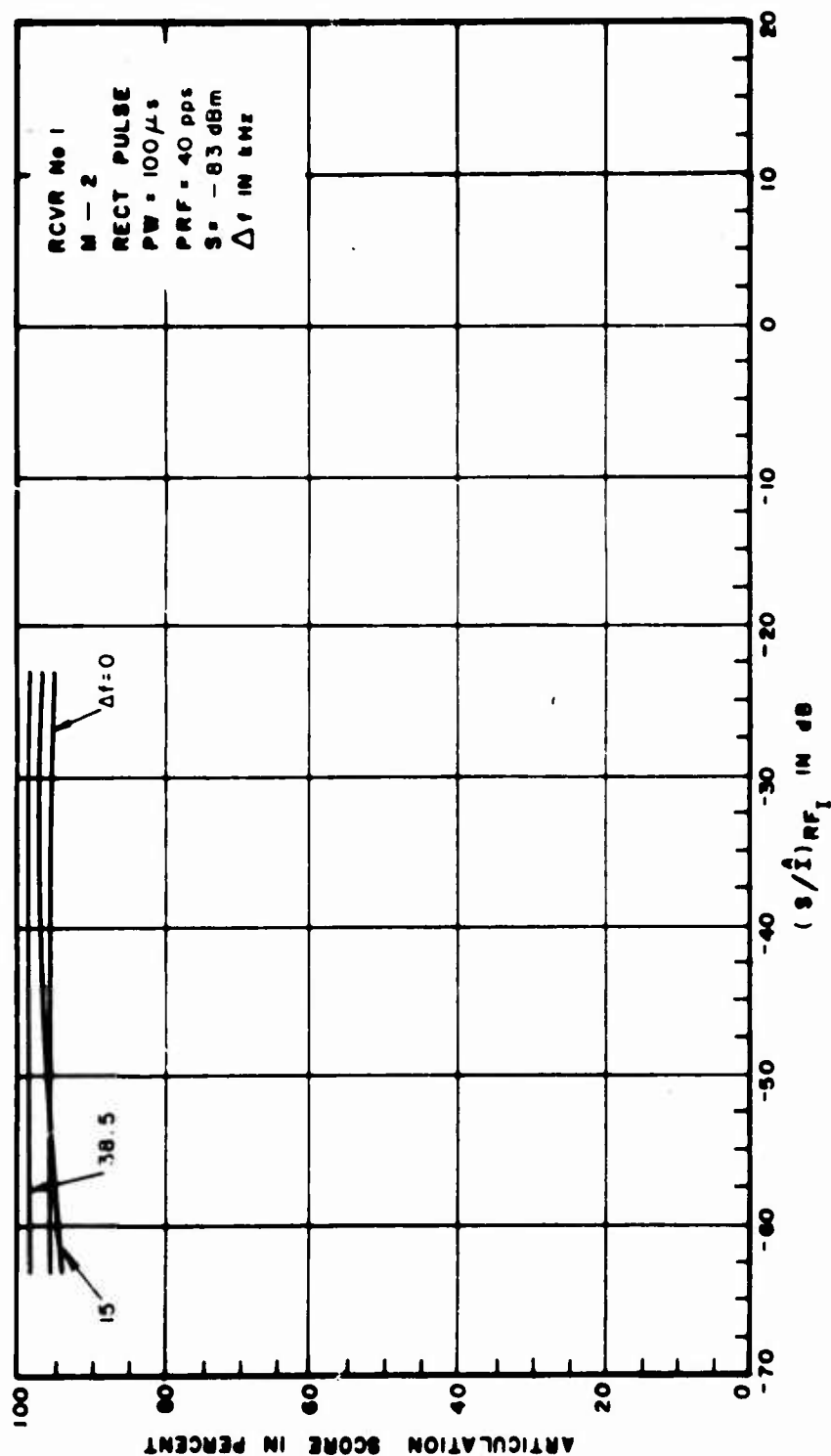


Figure III-5. Articulation Score for Pulsed Interference to an AM Receiver

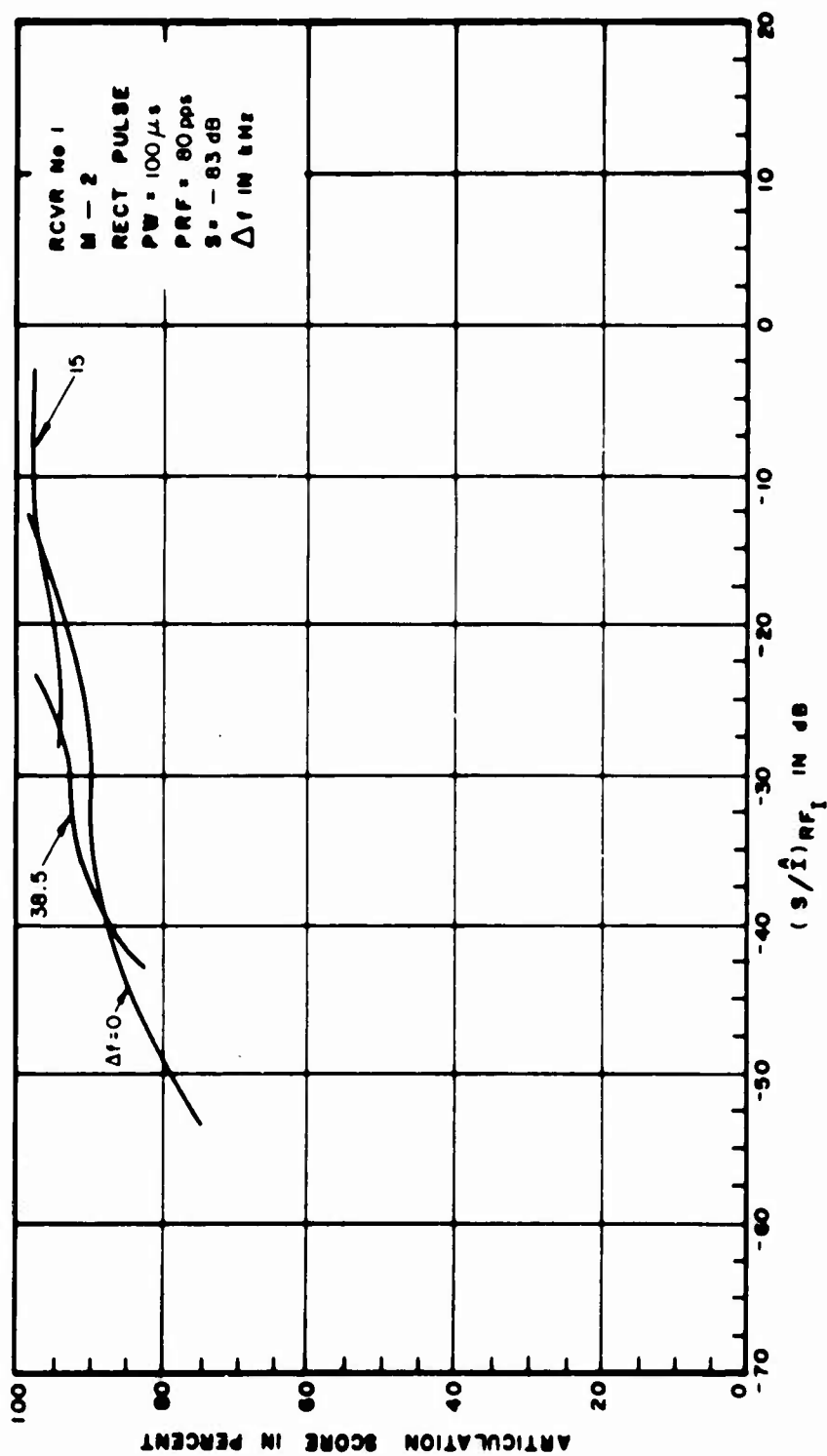


Figure III-6. Articulation Score for Pulsed Interference to an AM Receiver

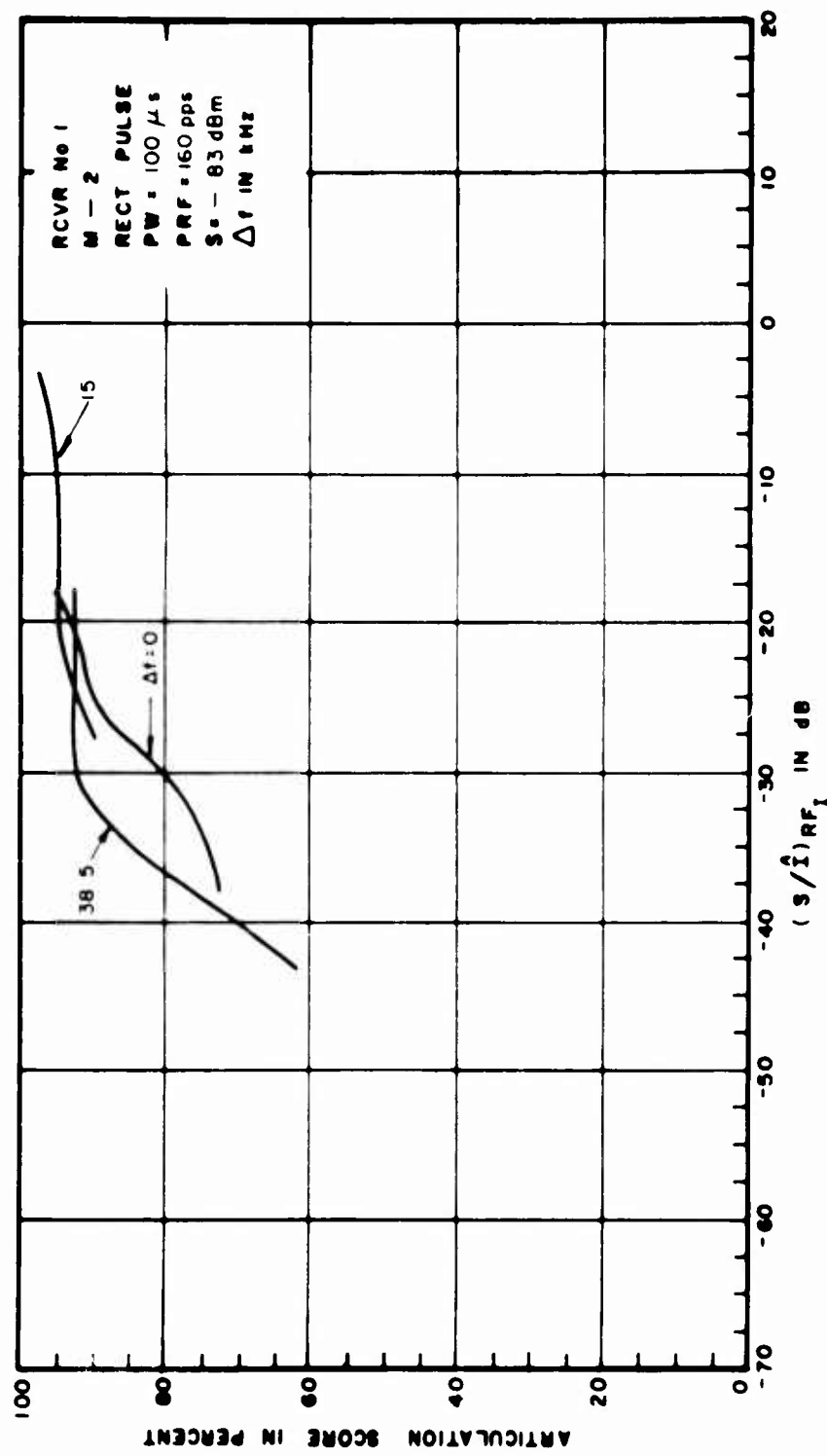


Figure III-7. Articulation Score for Pulsed Interference to an AM Receiver

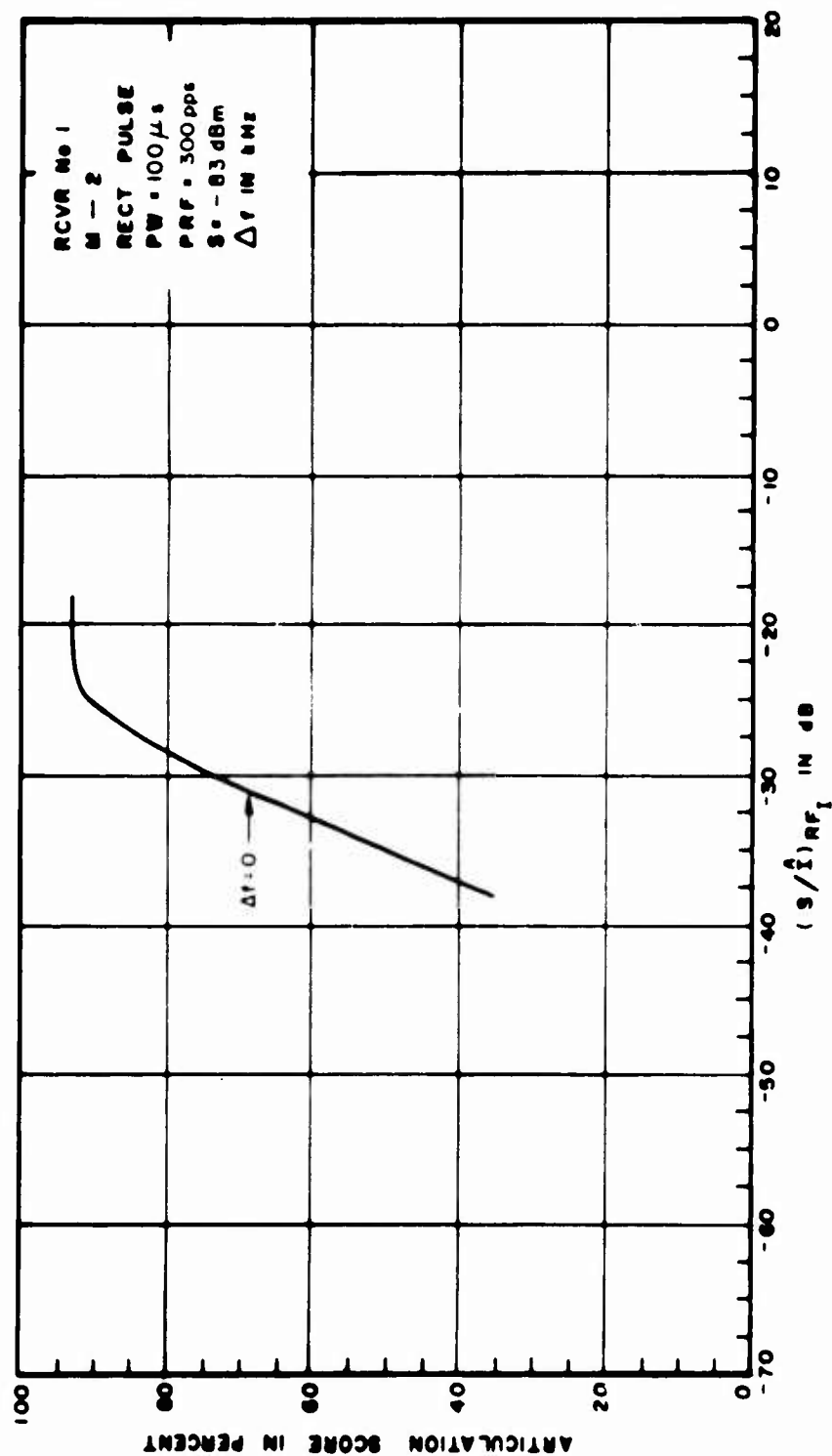


Figure III-8. Articulation Score for Pulsed Interference to an AM Receiver

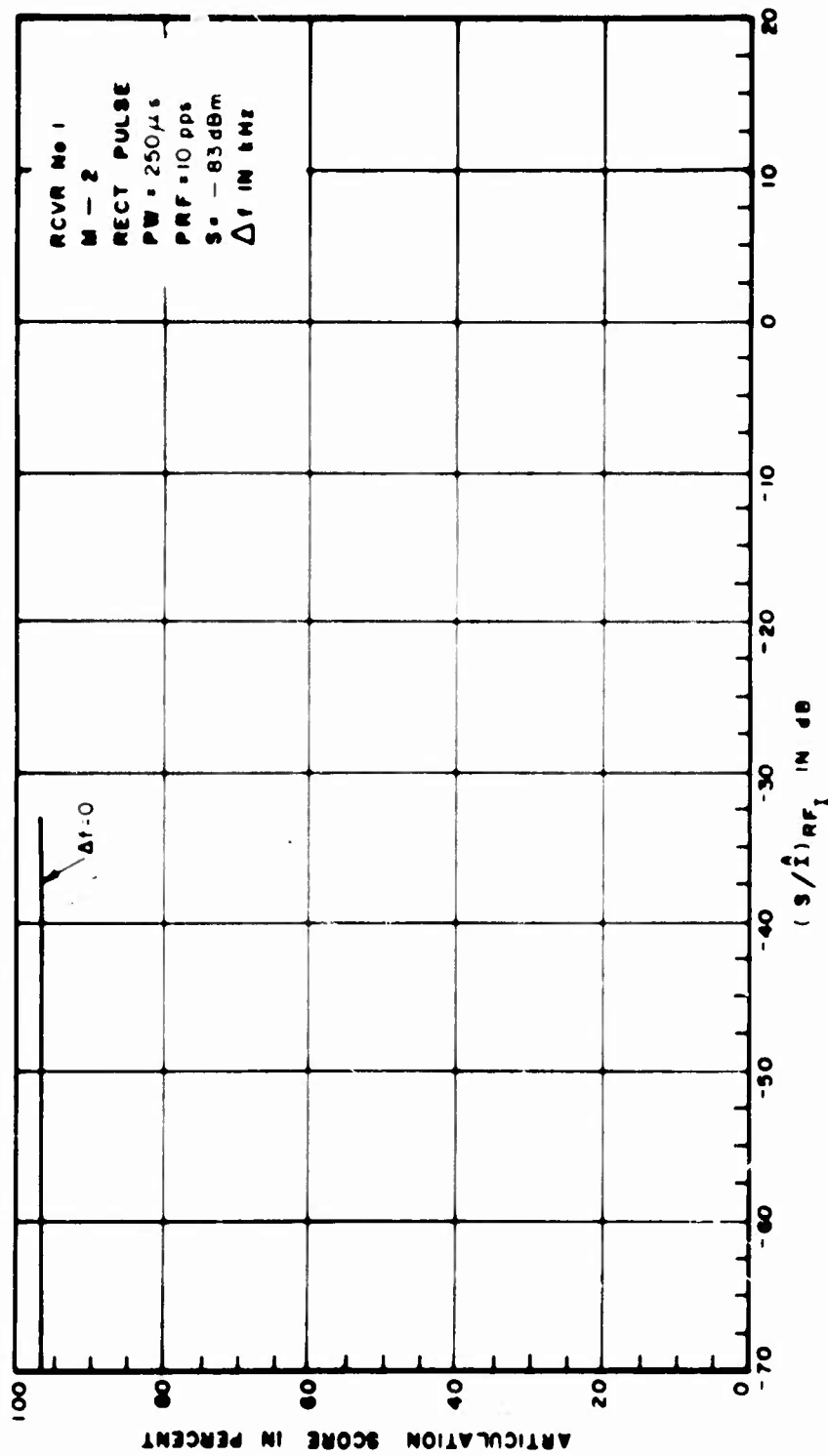


Figure III-9. Articulation Score for Pulsed Interference to an AM Receiver

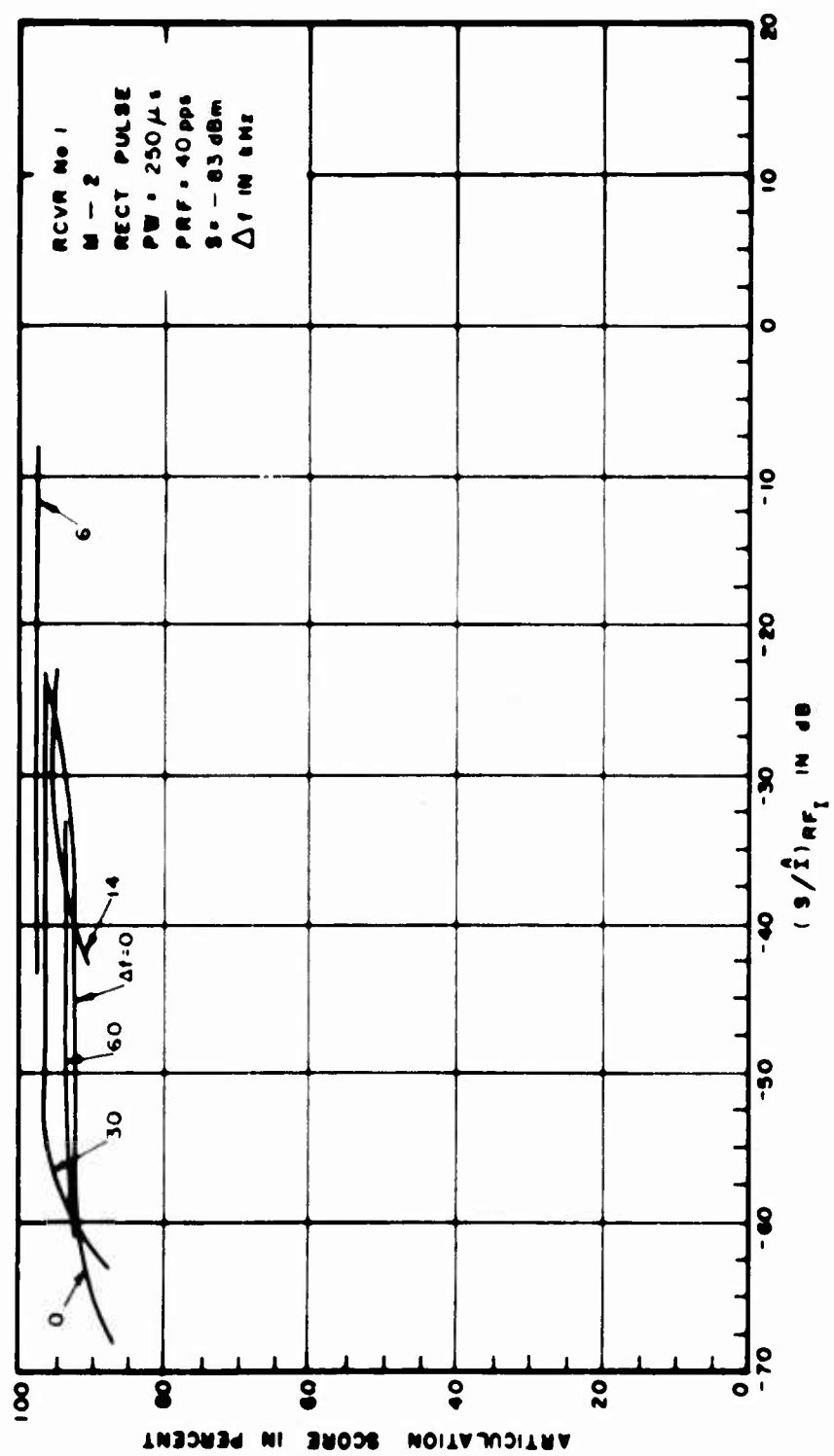


Figure III-10. Articulation Score for Pulsed Interference to an AM Receiver

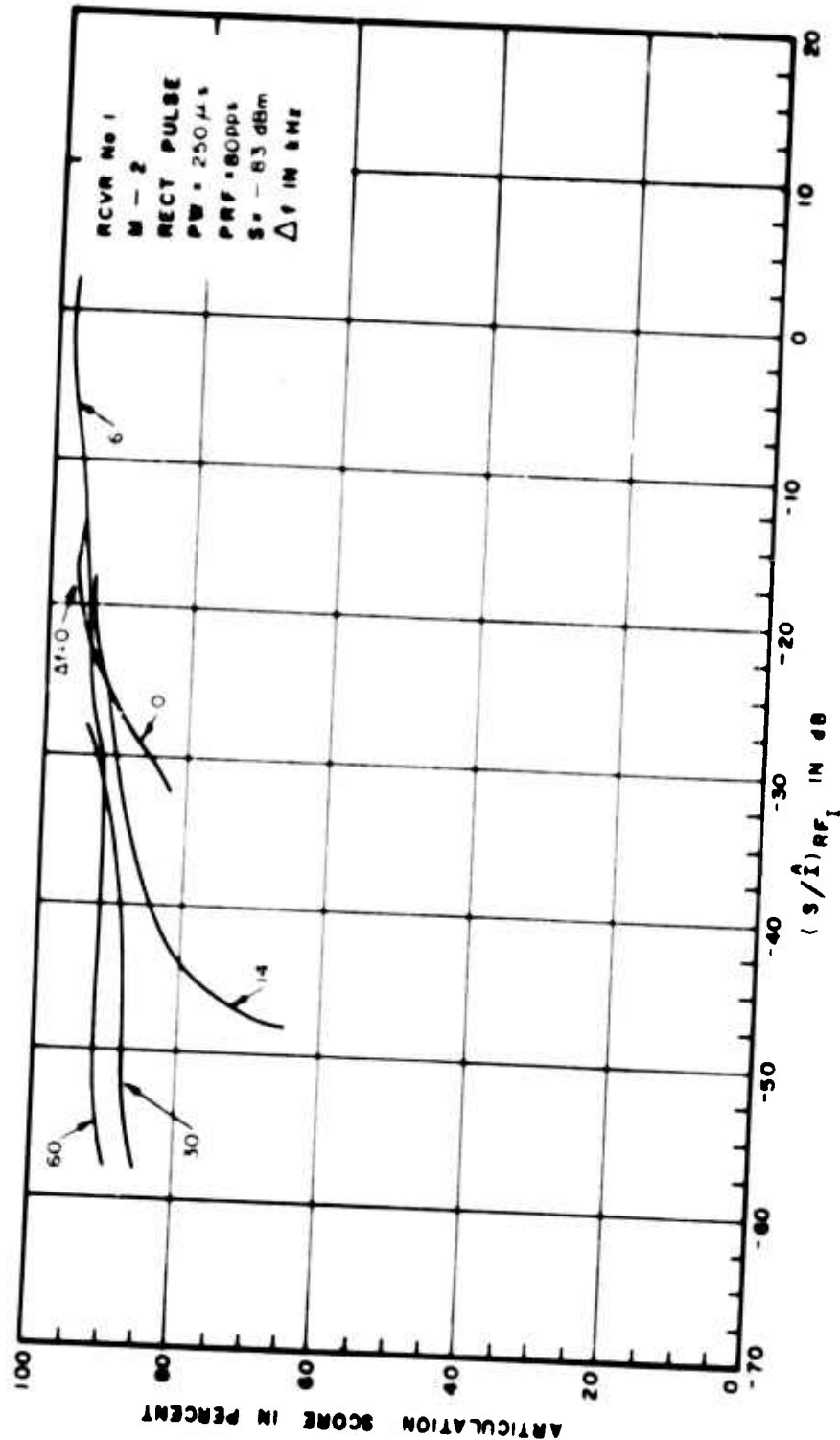


Figure III-11. Articulation Score for Pulsed Interference to an AM Receiver

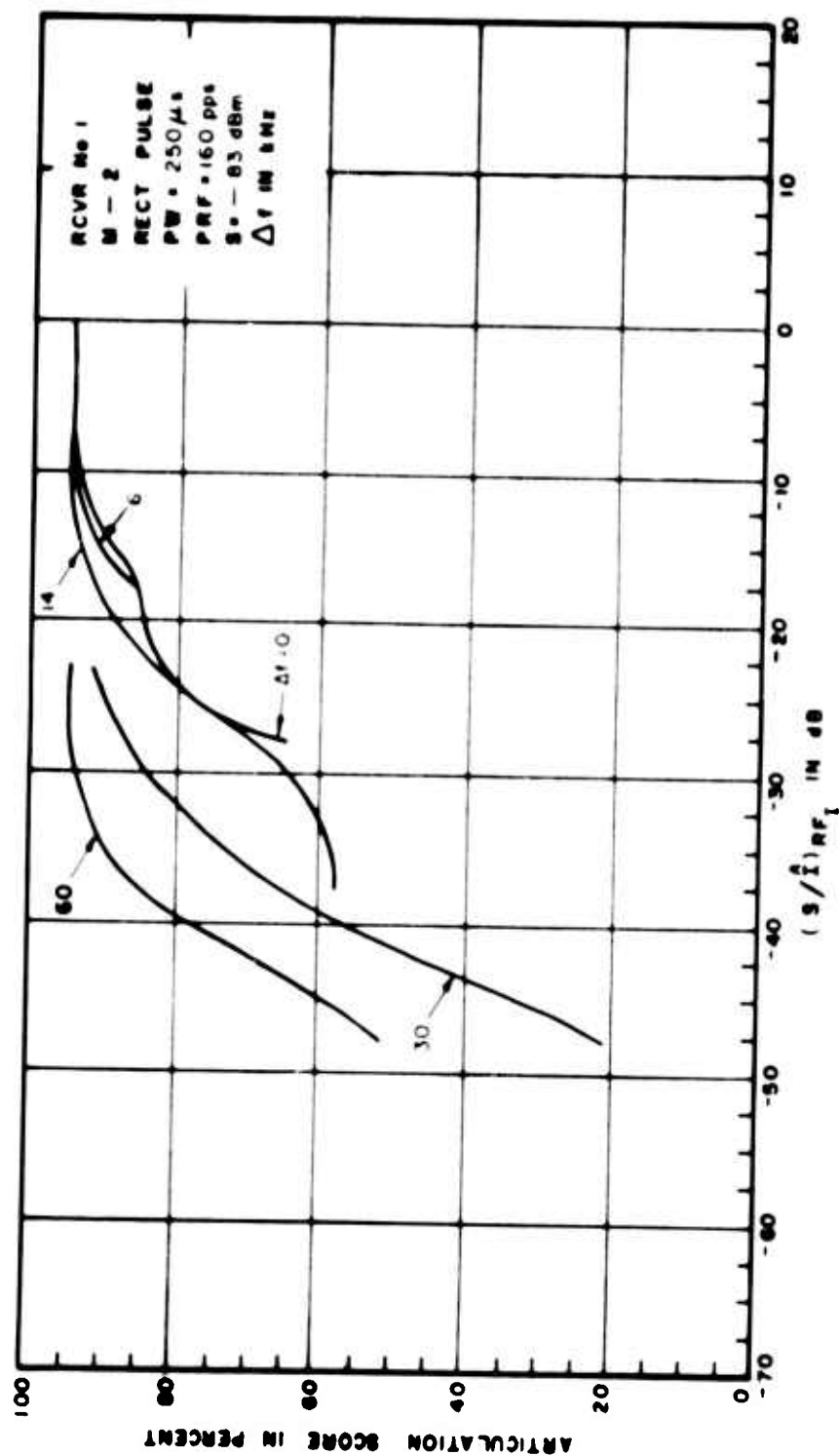


Figure III-12. Articulation Index for Pulsed Interference to an AM Receiver

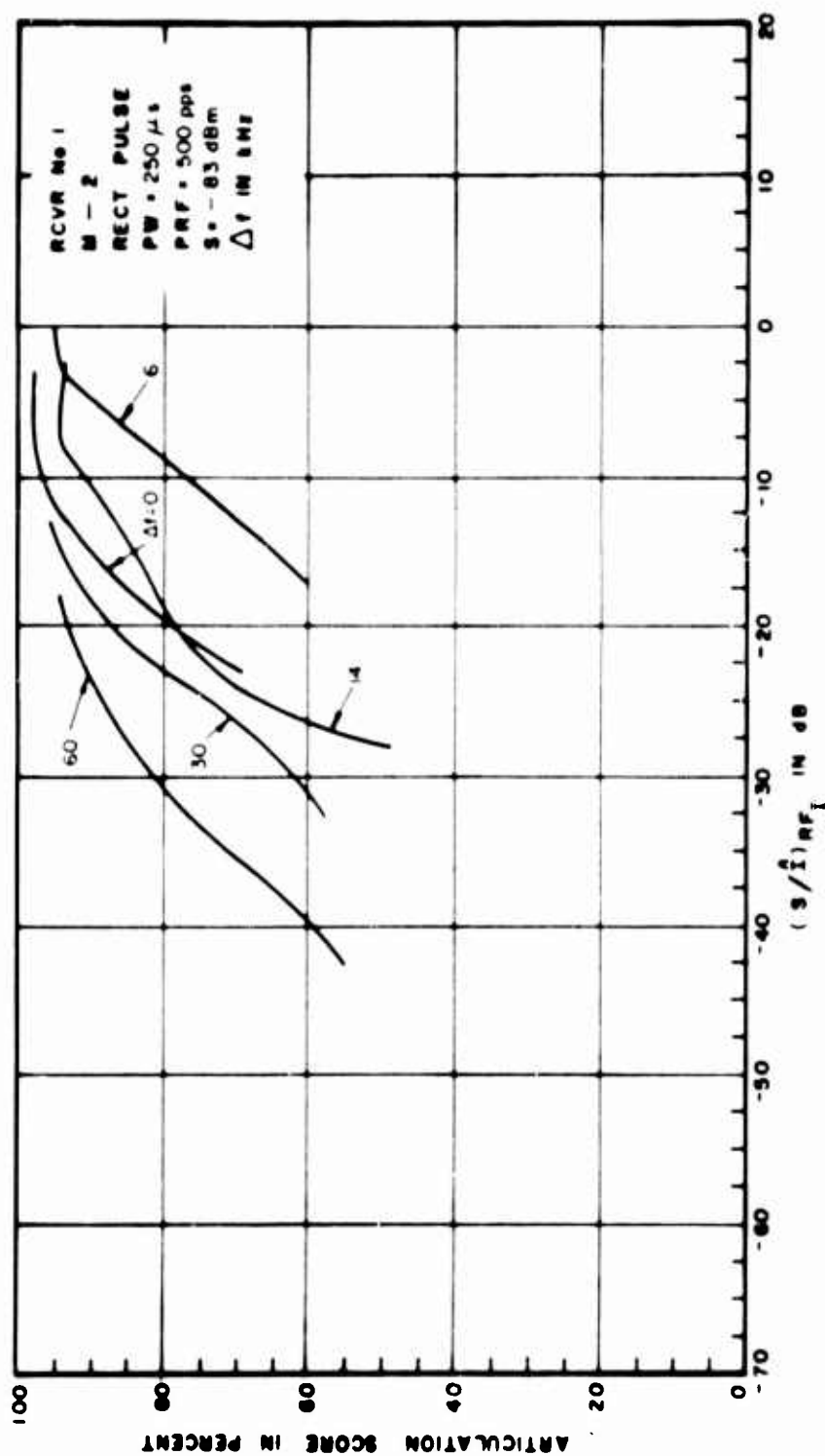


Figure III-13. Articulation Score for Pulsed Interference to an AM Receiver

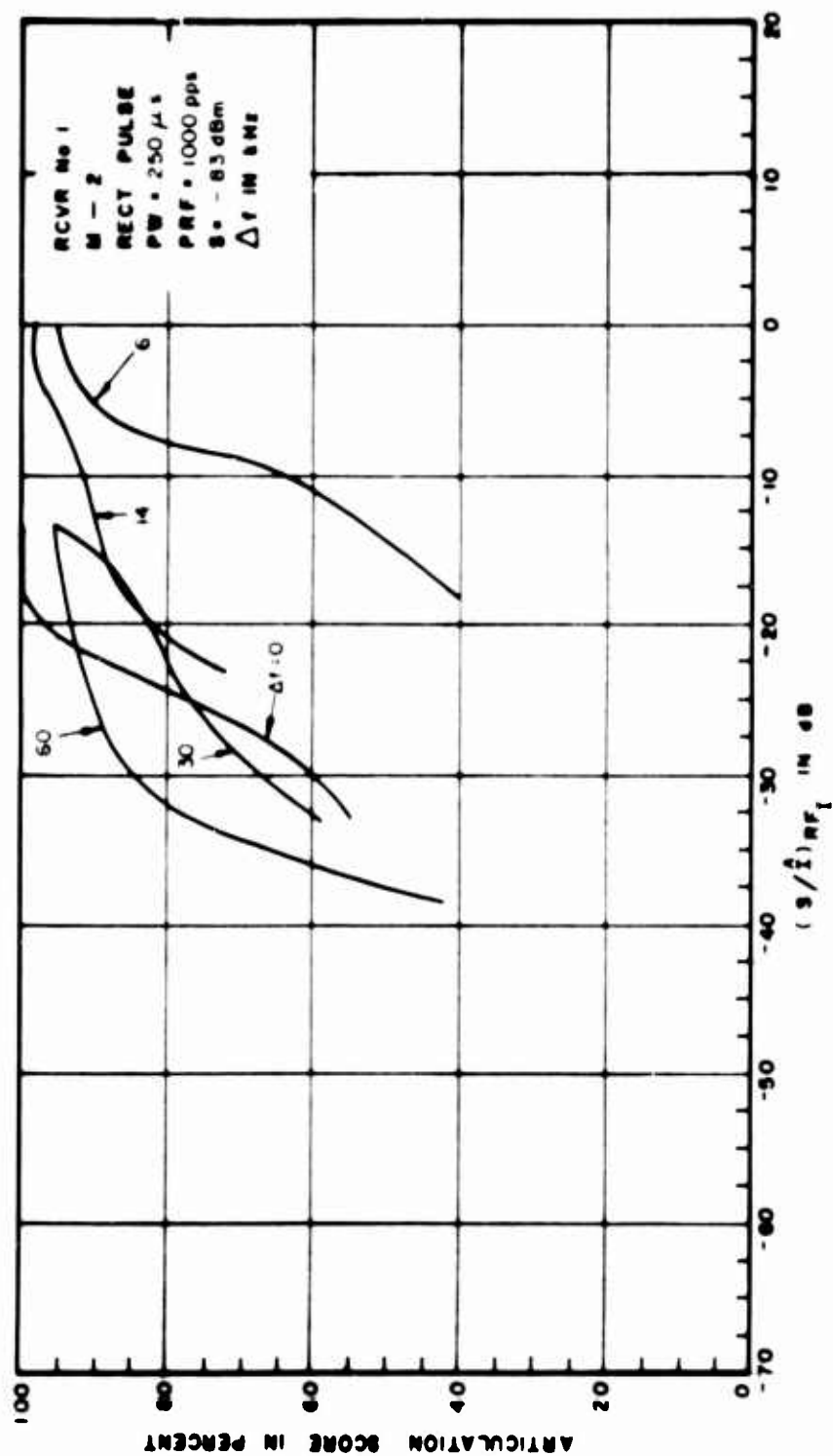


Figure III-14. Articulation Score for Pulsed Interference to an AM Receiver

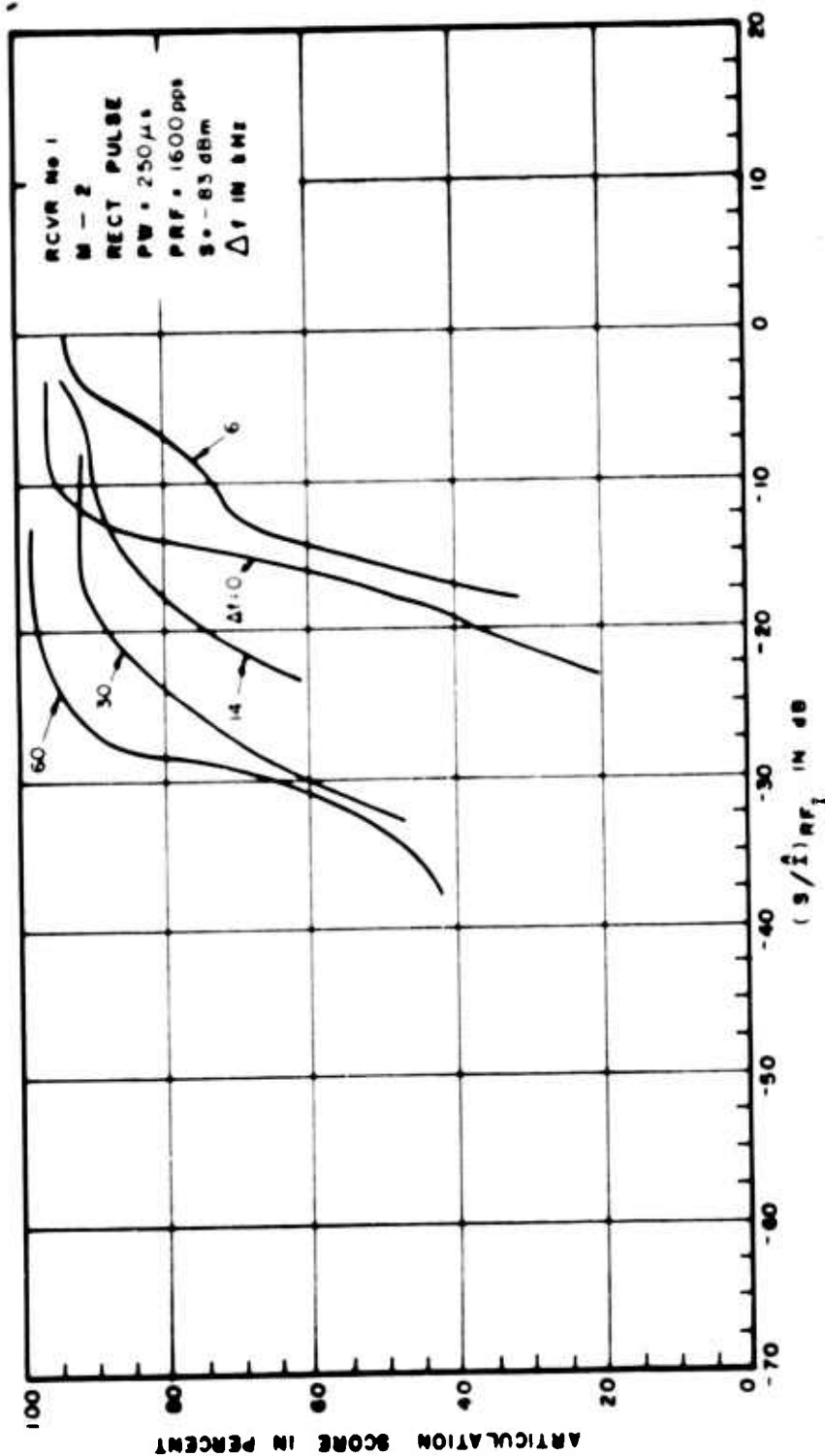


Figure III-15. Articulation Score for Pulsed Interference to an AM Receiver

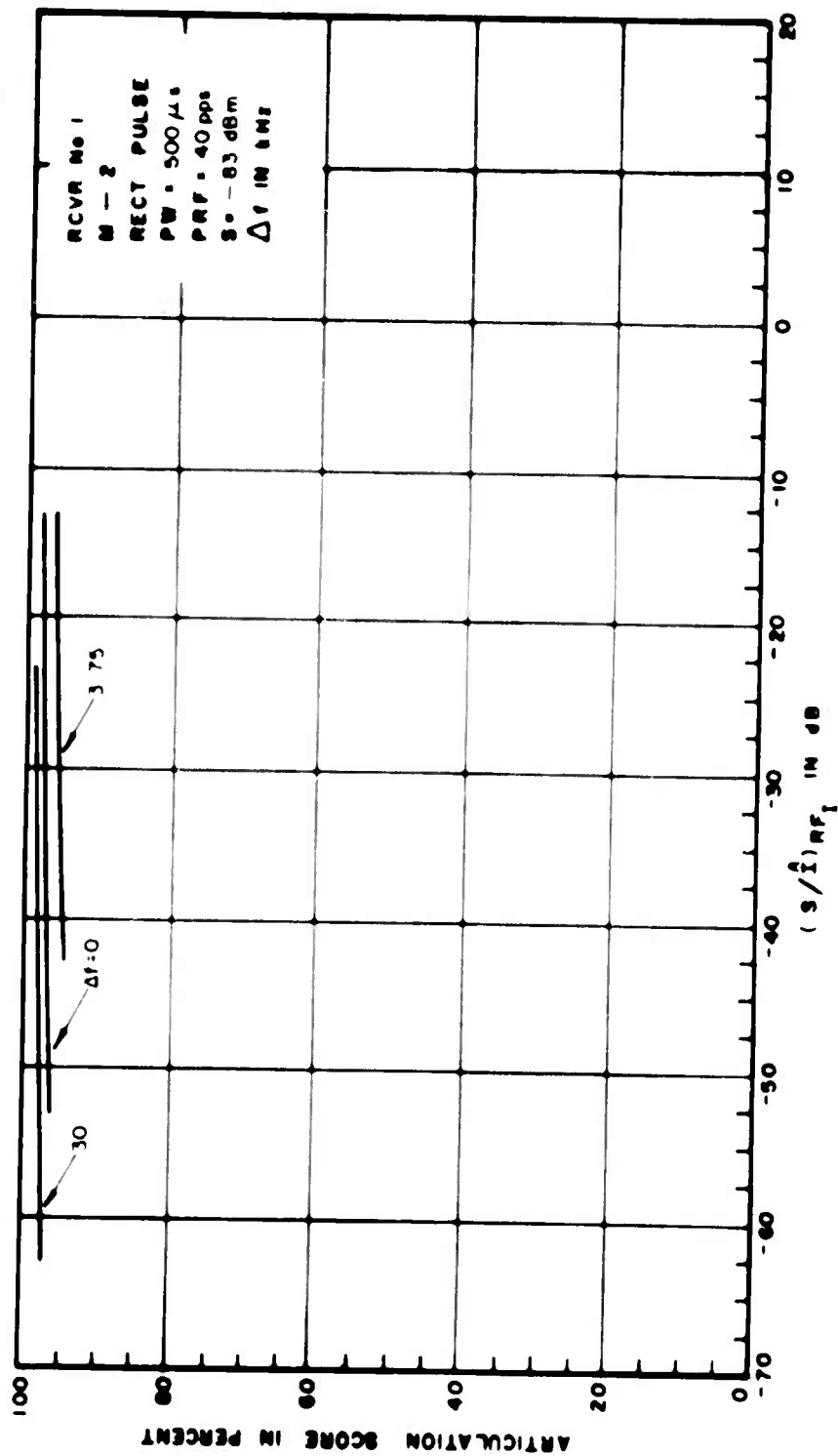


Figure III-16. Articulation Score for Pulsed Interference to an AM Receiver

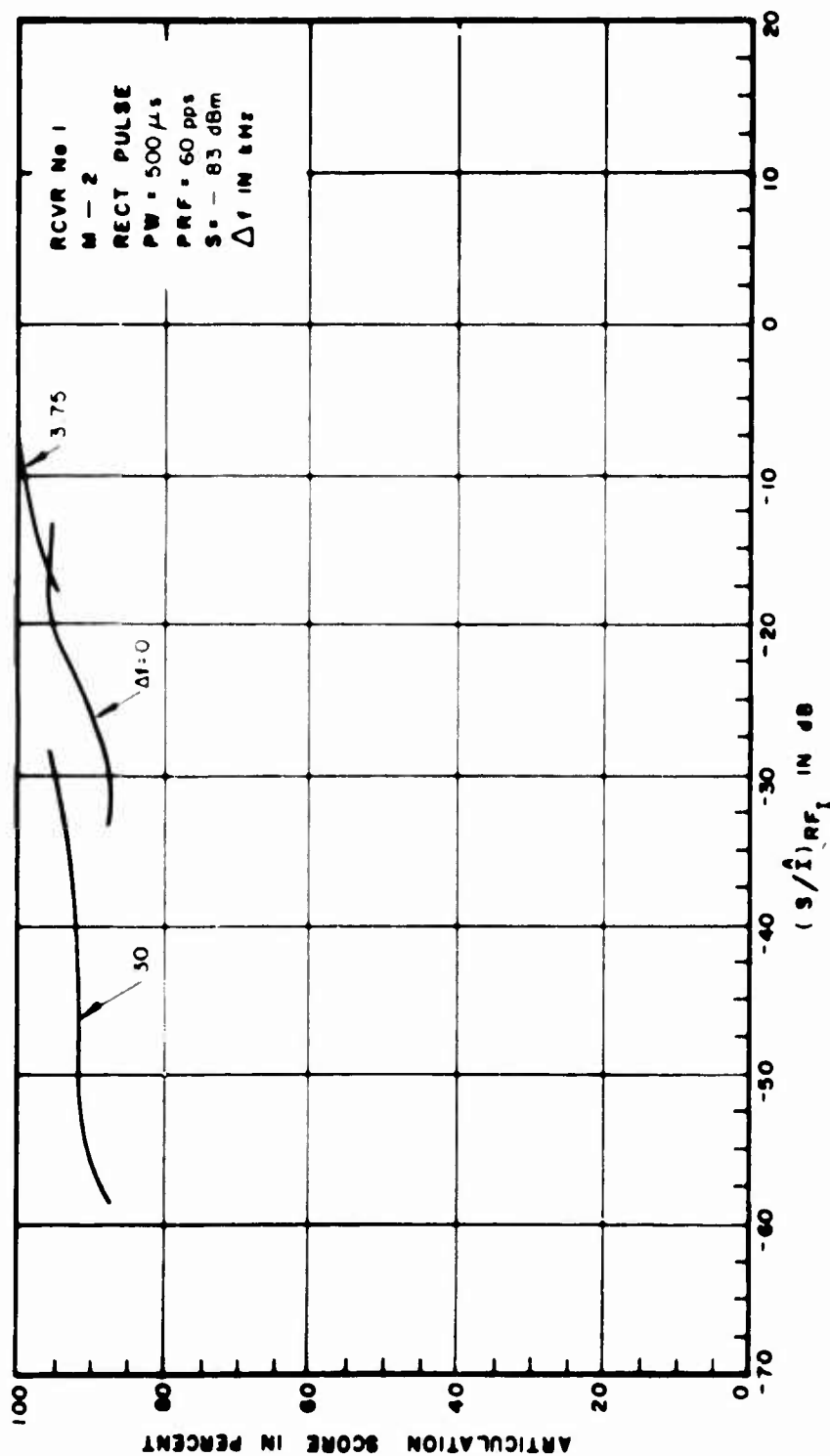


Figure III-17. Articulation Score for Pulsed Interference to an AM Receiver

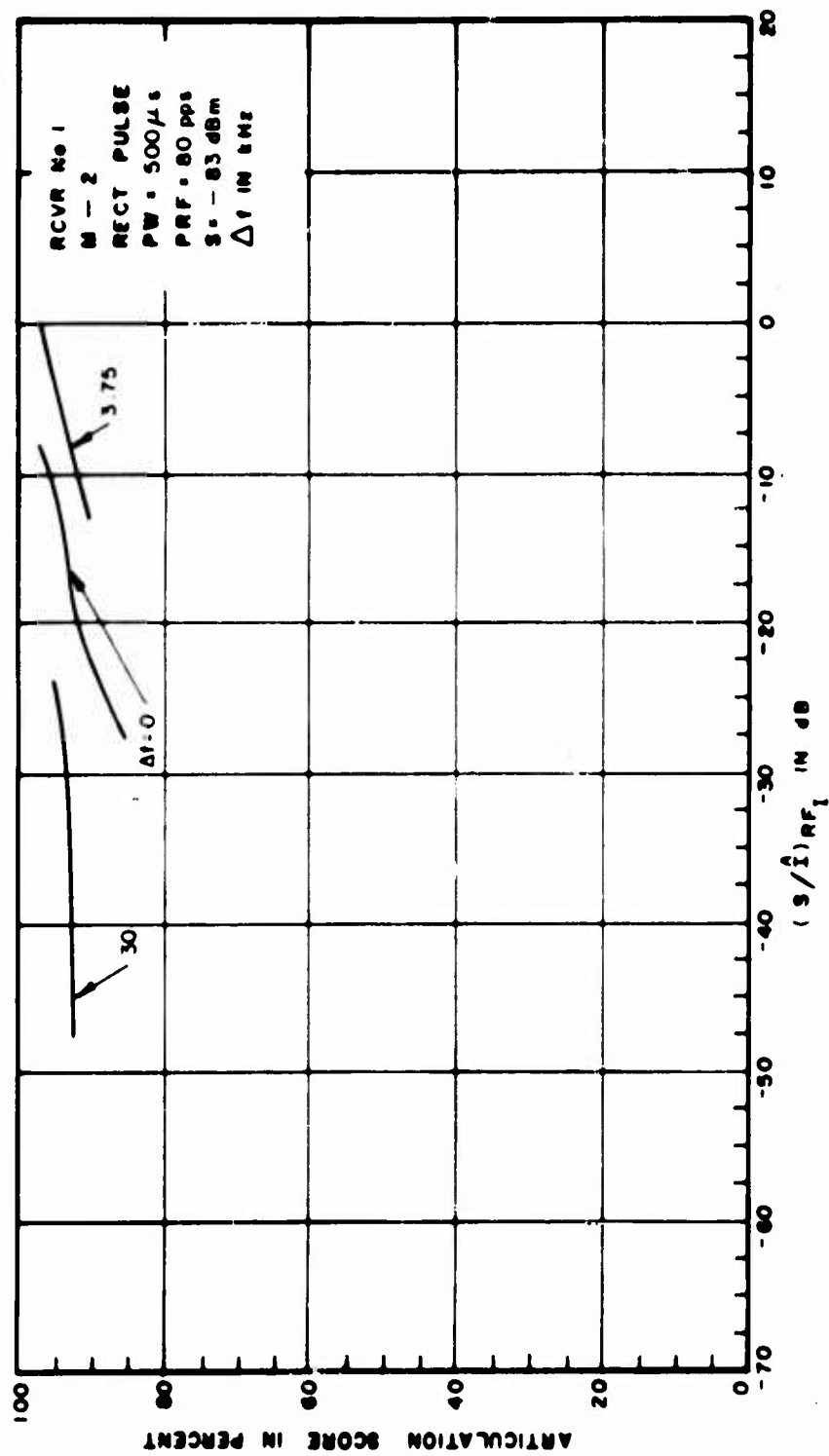


Figure III-18. Articulation Score for Pulsed Interference to an AM Receiver

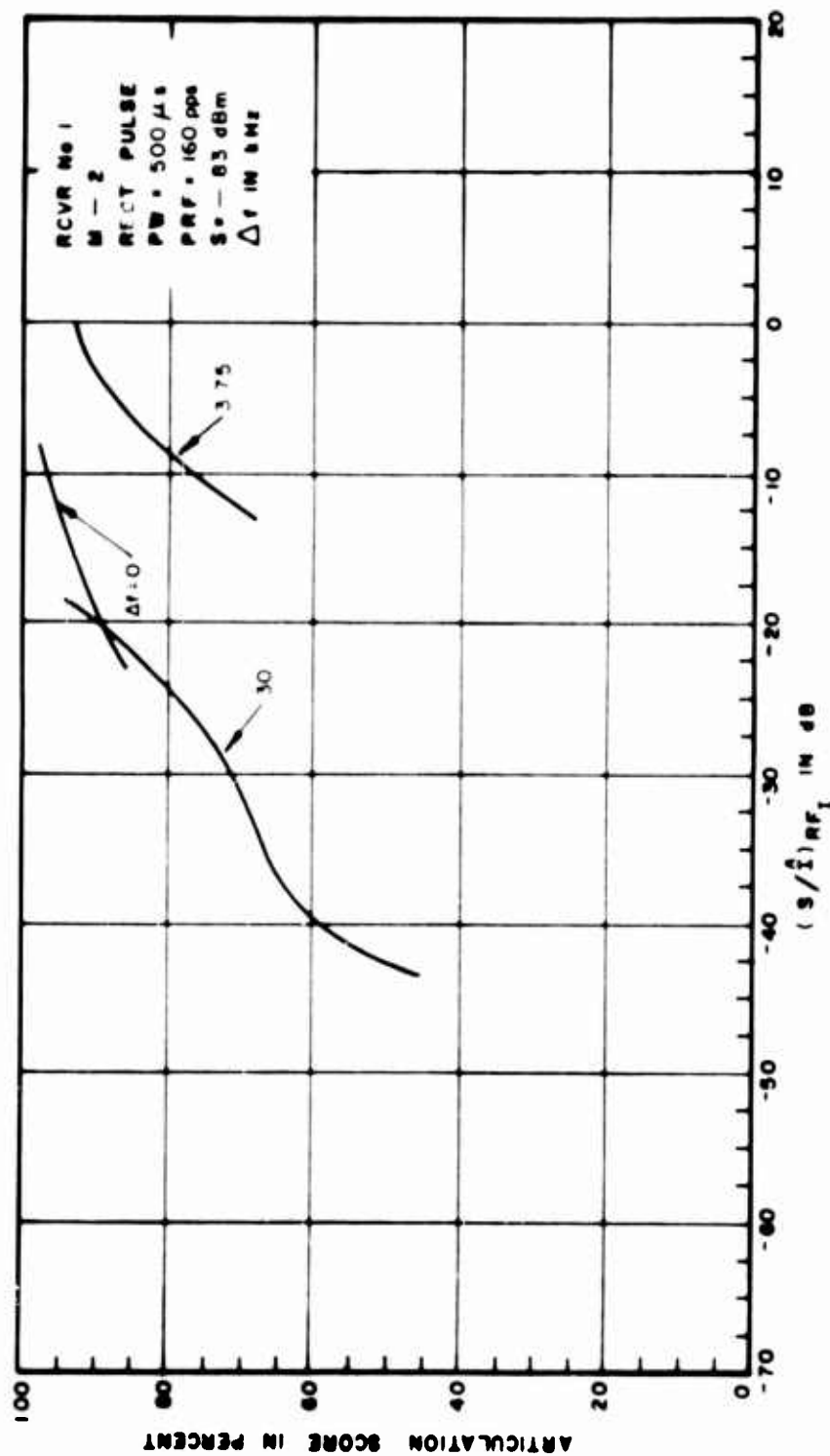


Figure III-19. Articulation Score for Pulsed Interference to an AM Receiver

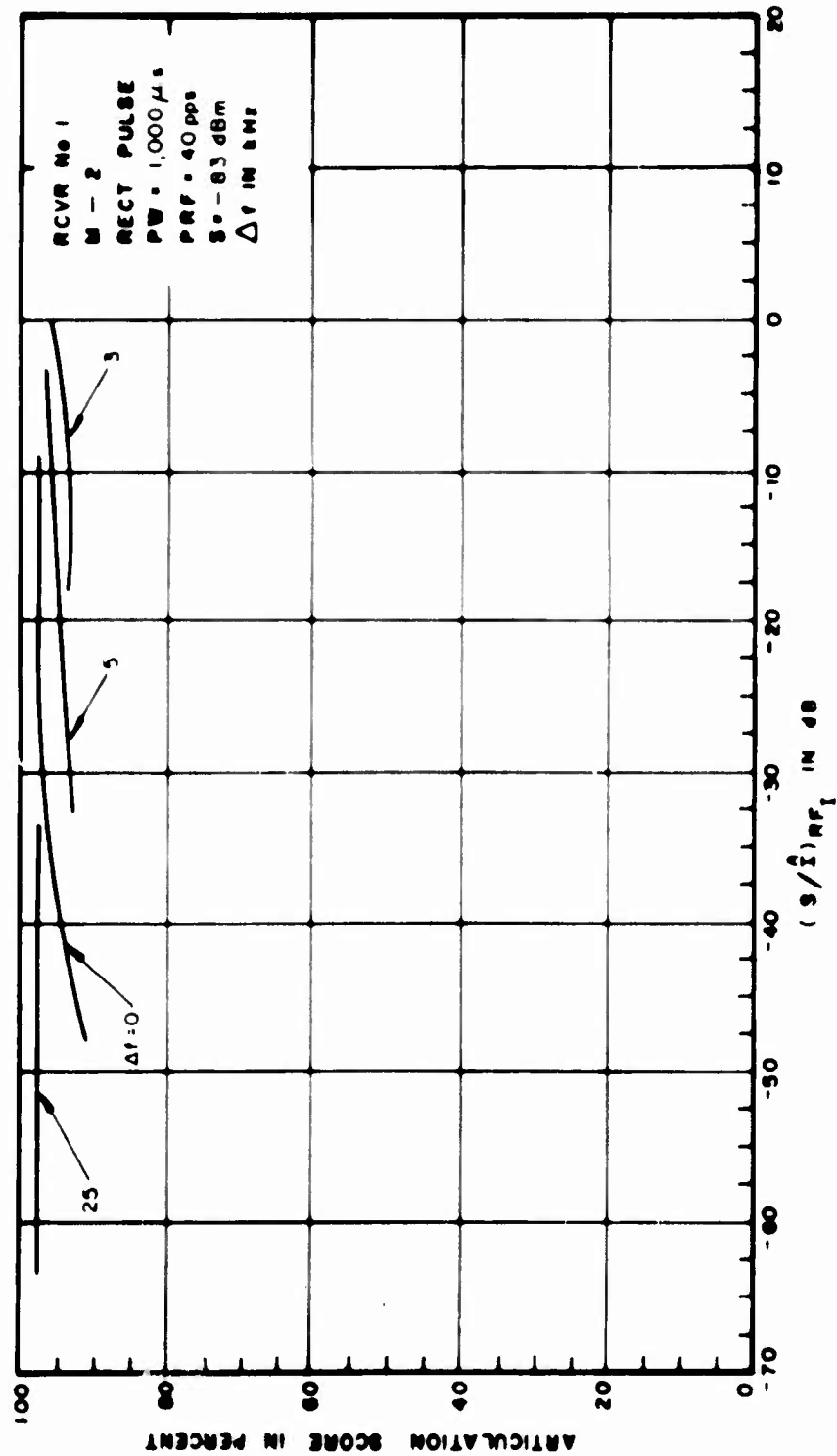


Figure III-20. Articulation Score for Pulsed Interference to an AM Receiver

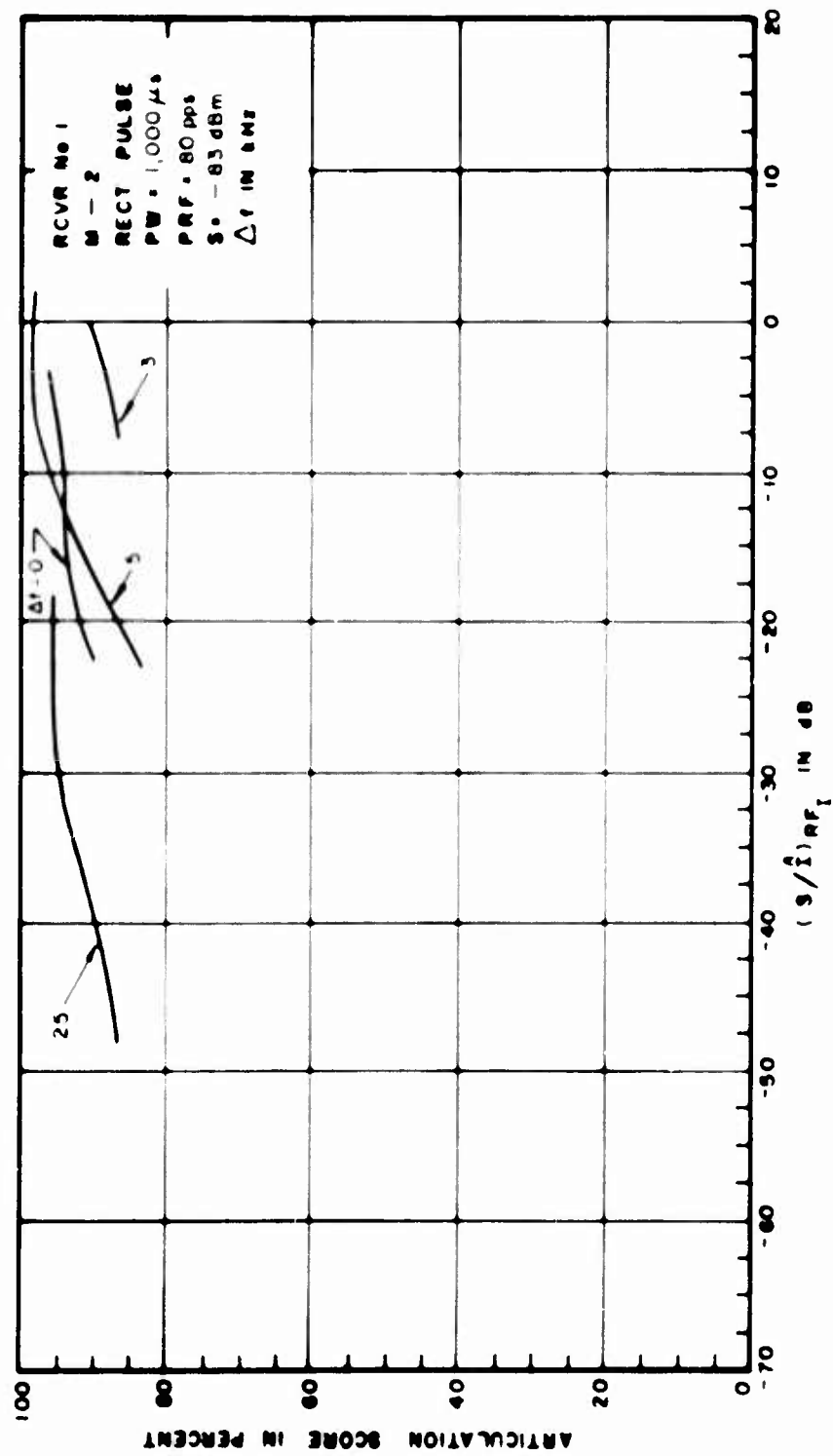


Figure III-21. Articulation Score for Pulsed Interference to an AM Receiver

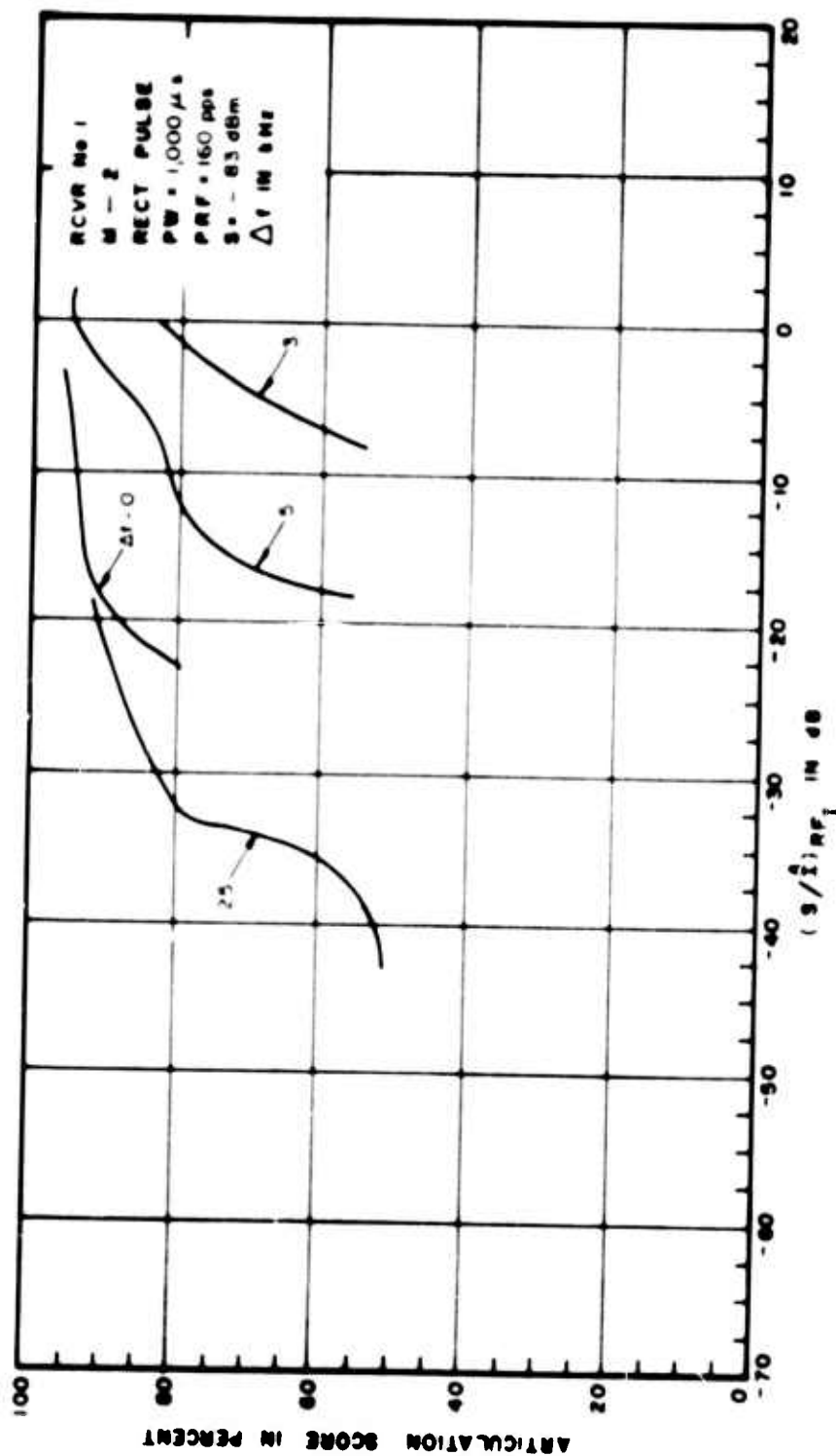


Figure III-22. Articulation Score for Pulsed Interference to an AM Receiver

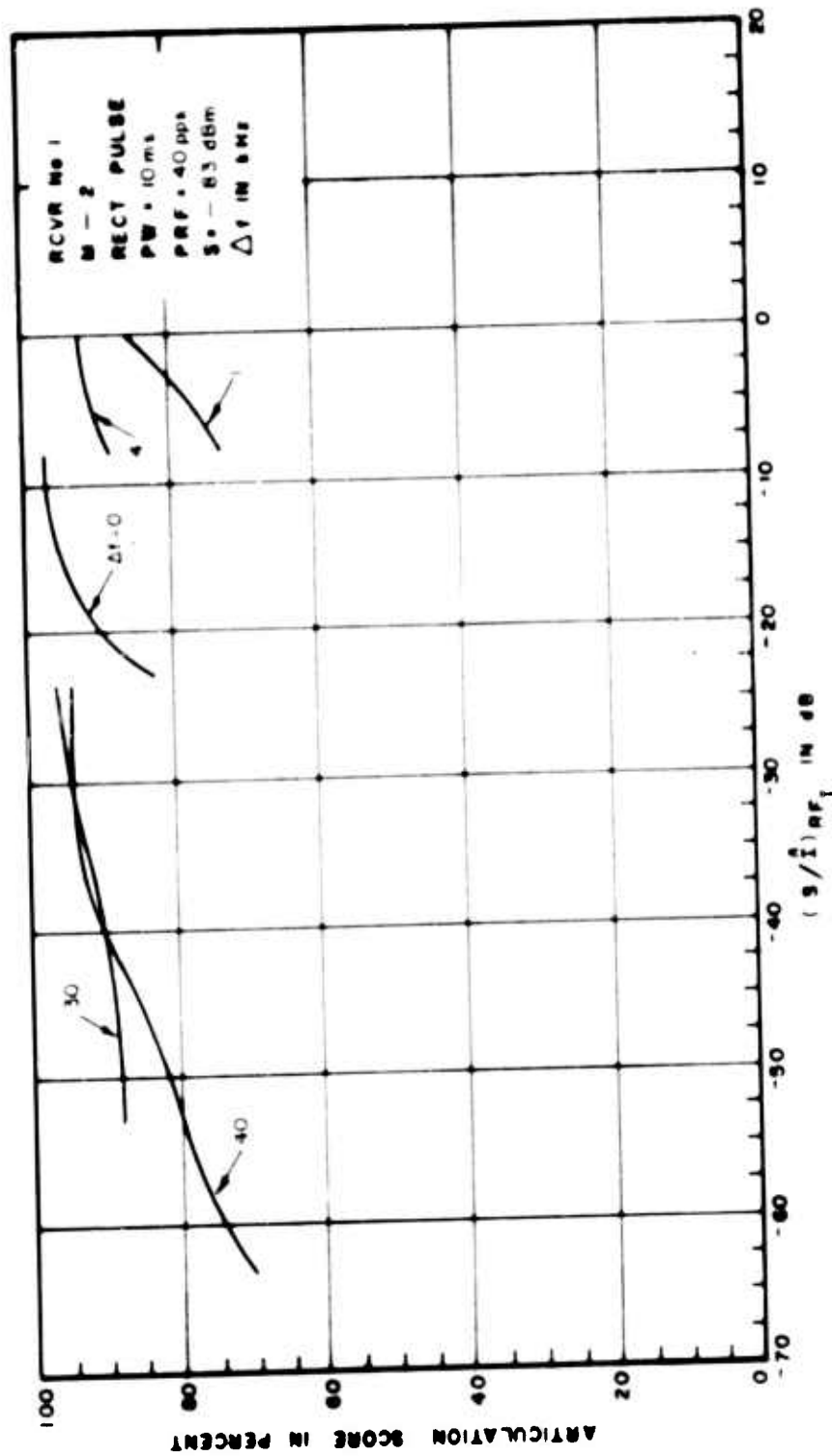


Figure III-23. Articulation Score for Pulsed Interference to an AM Receiver

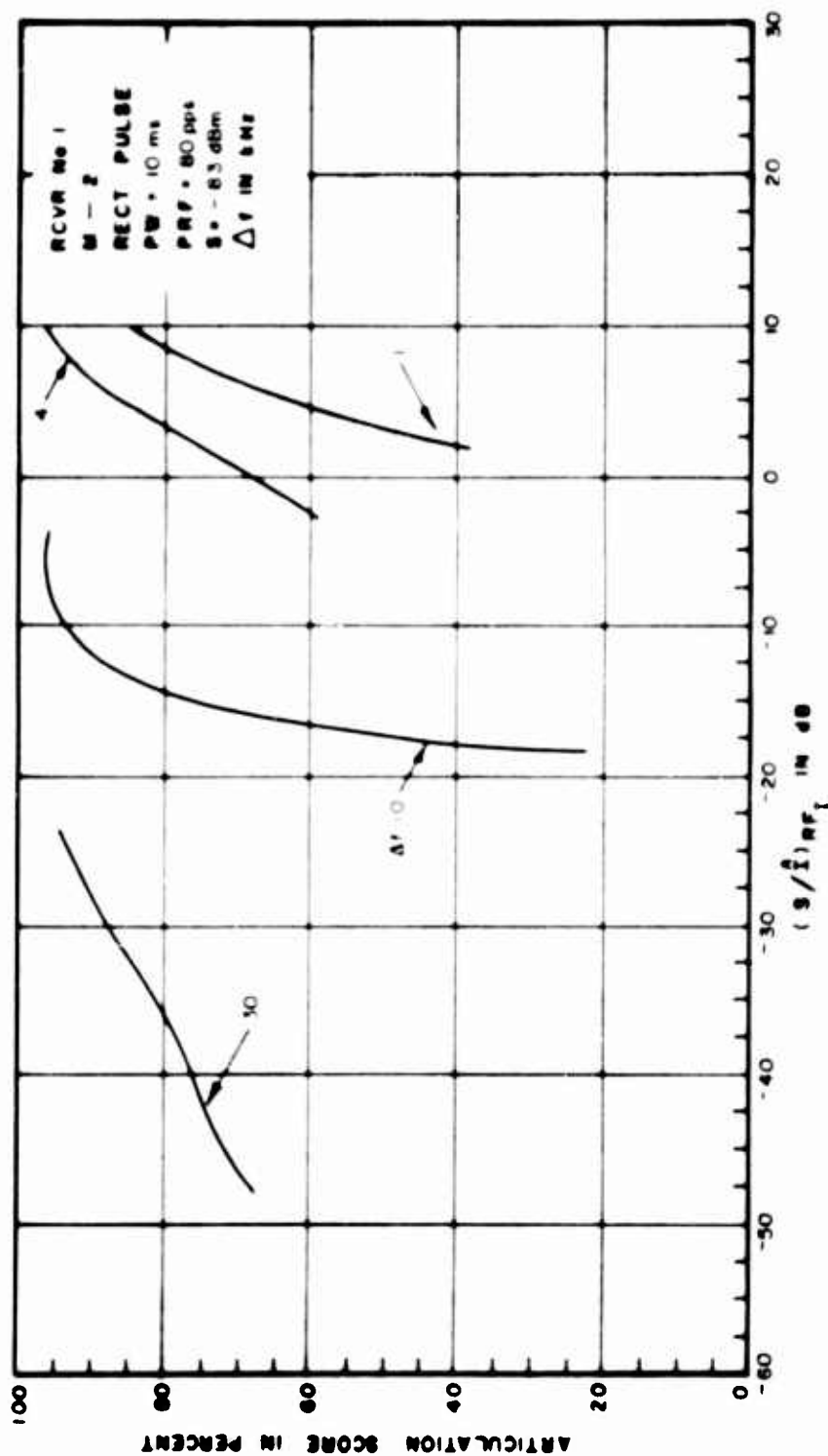


Figure III-24. Articulation Score for Pulsed Interference to an AM Receiver

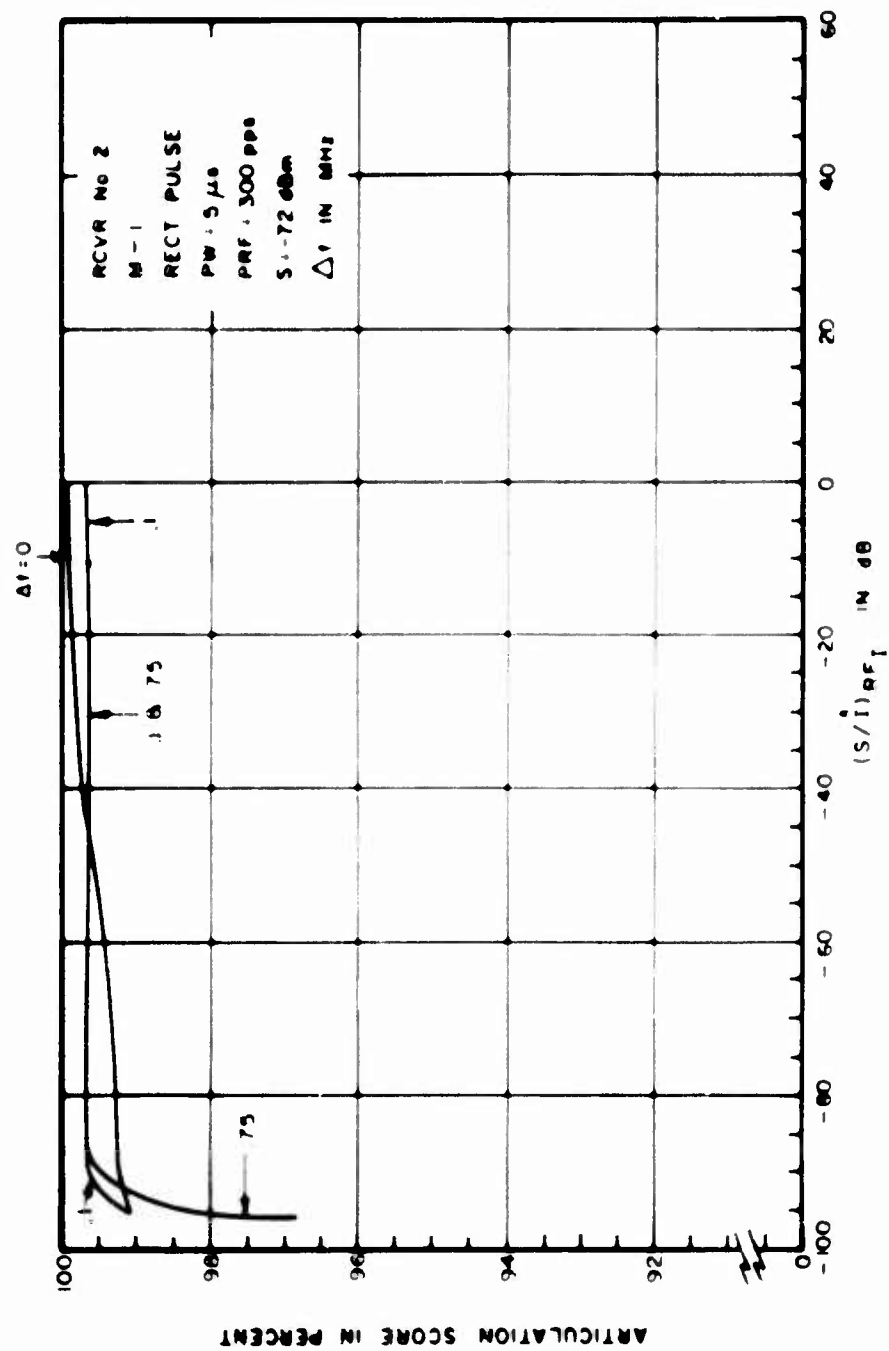


Figure III-25. Articulation Score for Pulsed Interference to an AM Receiver

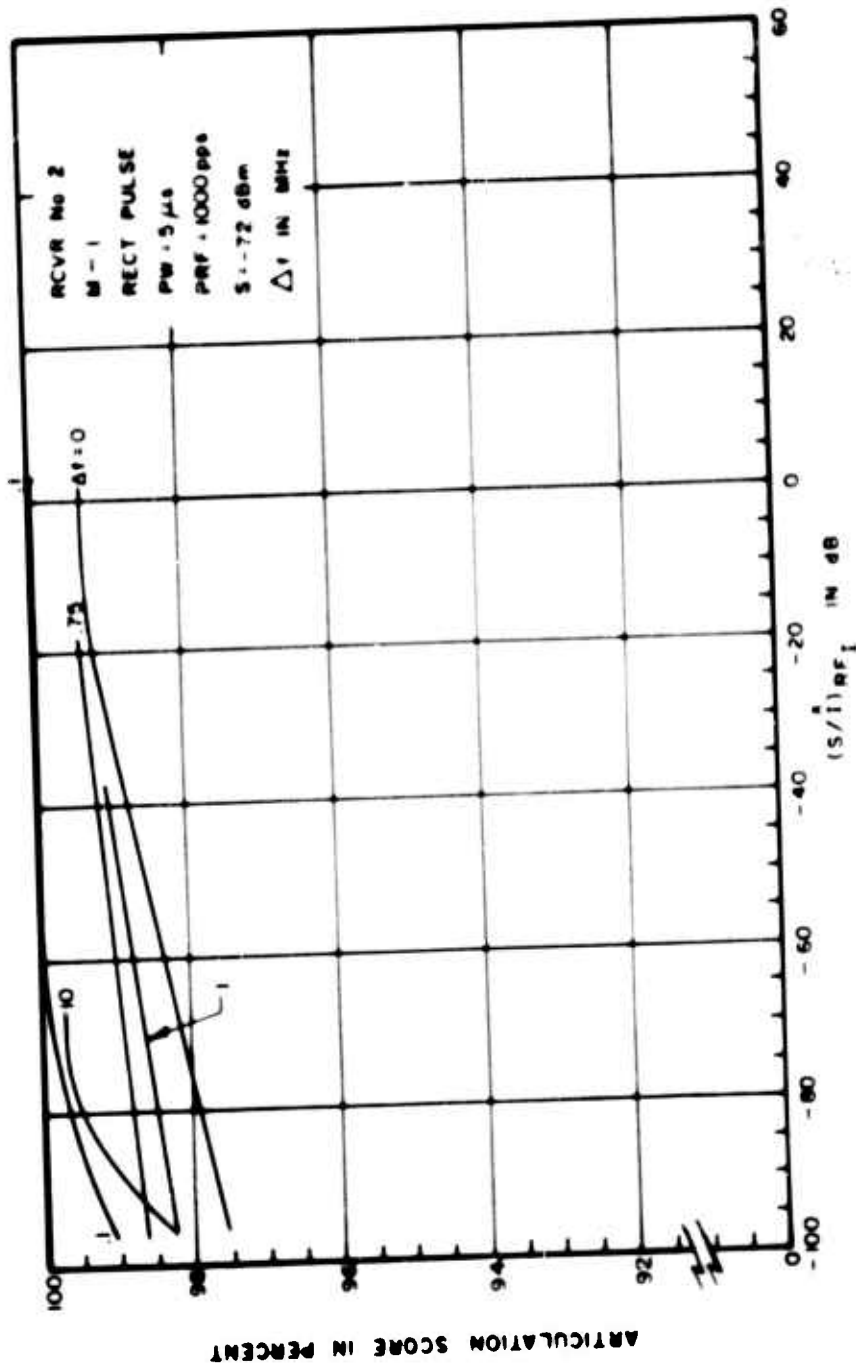


Figure III-26. Articulation Score for Pulsed Interference to an AM Receiver

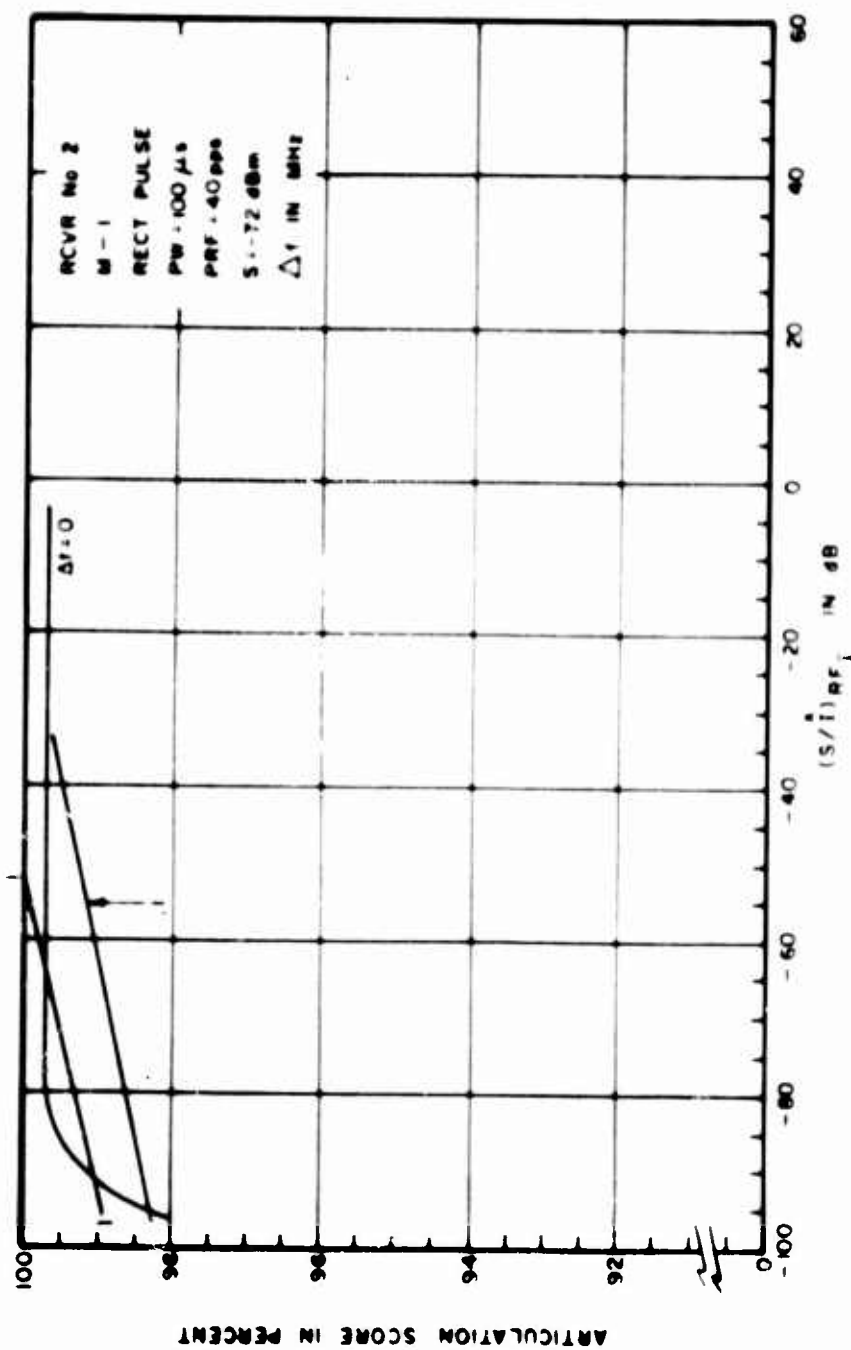


Figure III-27. Articulation Score for Pulsed Interference to an AM Receiver

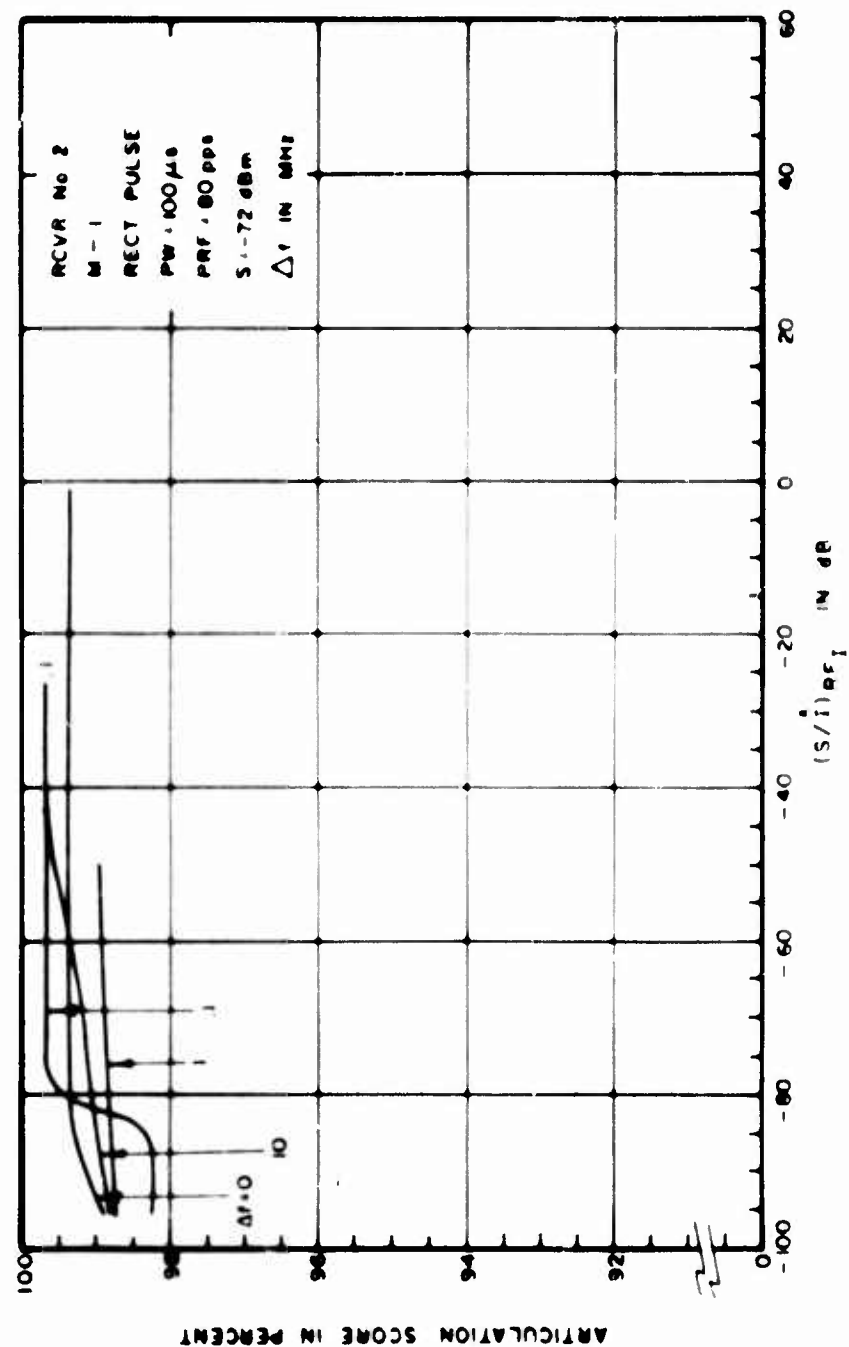


Figure III 28. Articulation Score for Pulsed Interference to an AM Receiver

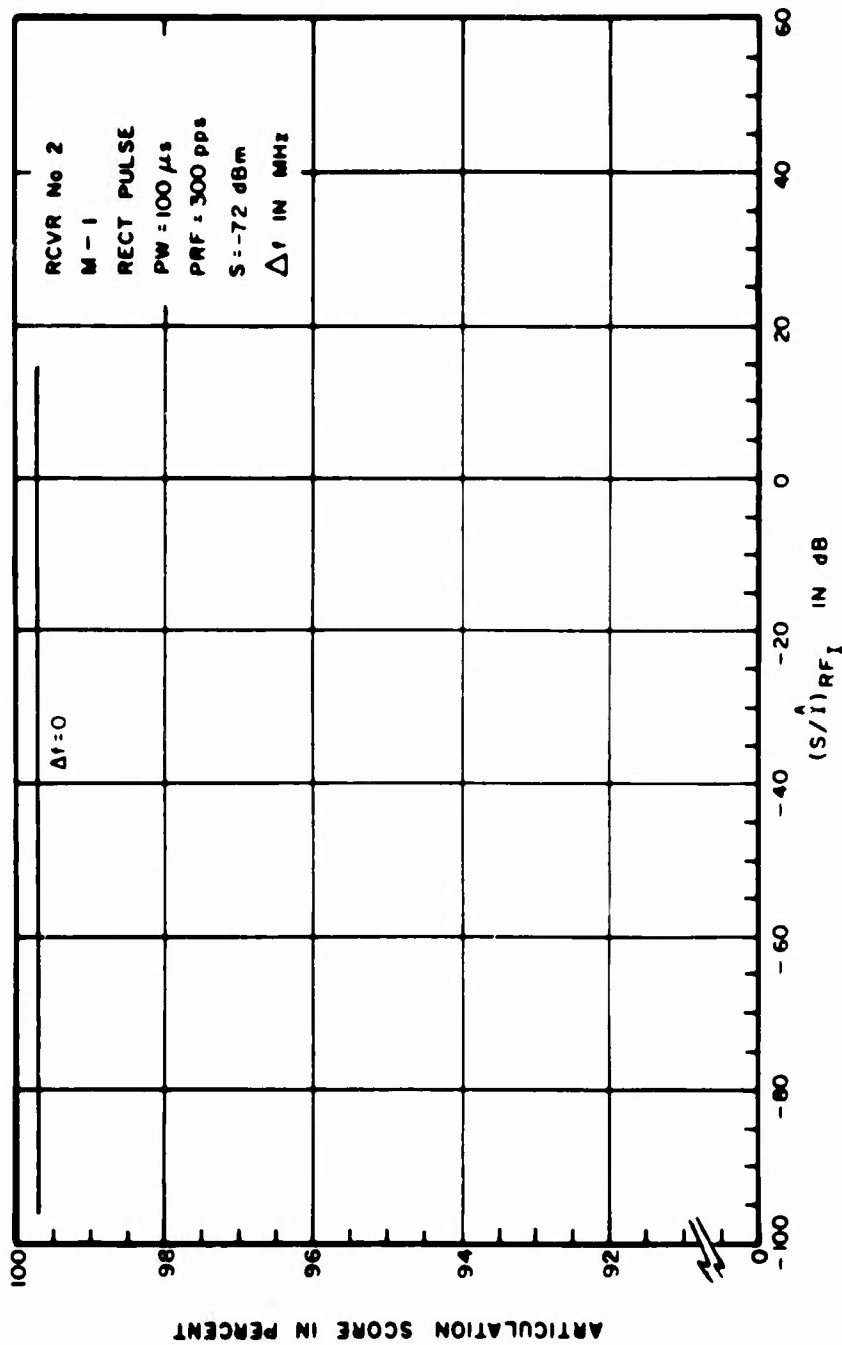


Figure III-29. Articulation Score for Pulsed Interference to an AM Receiver

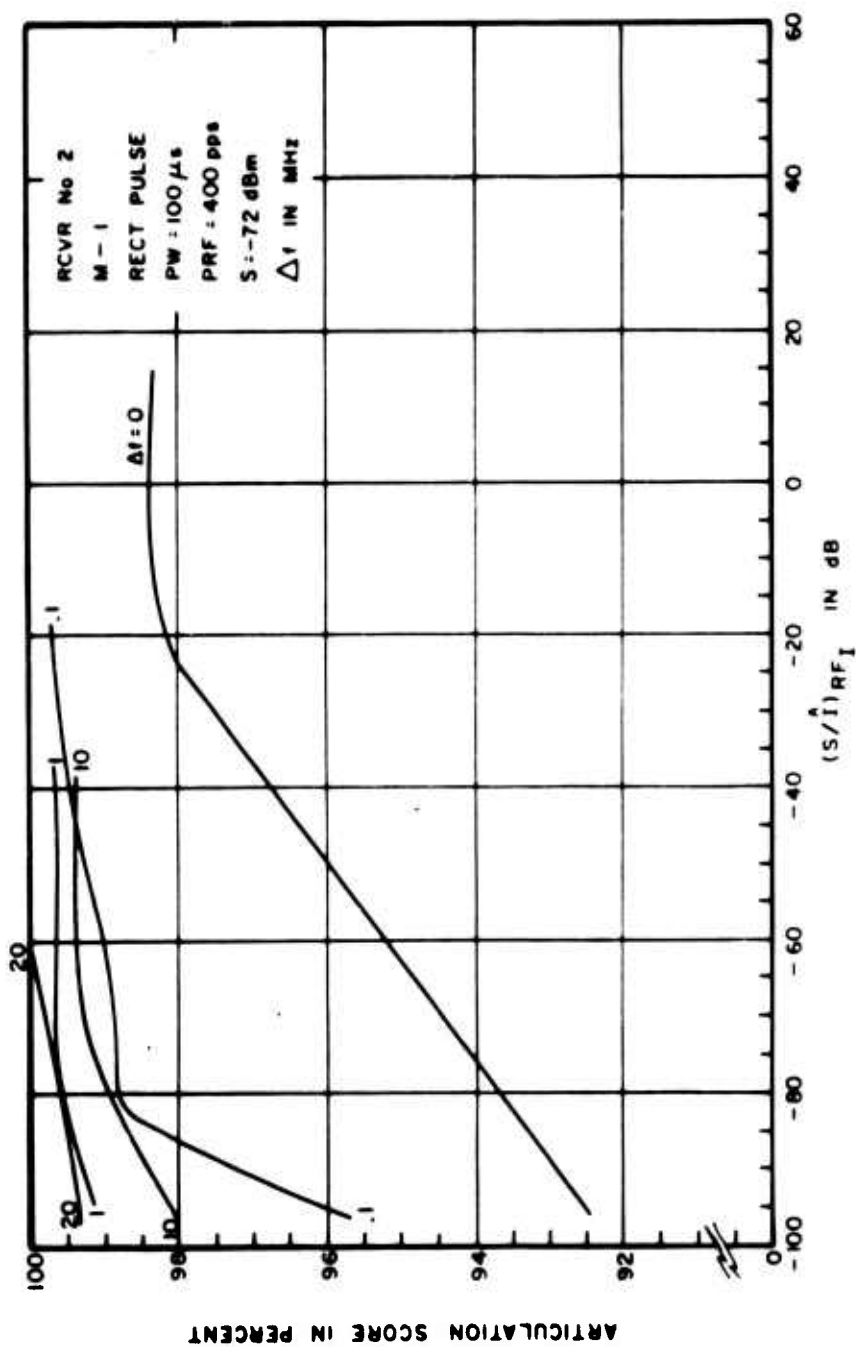


Figure III-30. Articulation Score for Pulsed Interference to an AM Receiver

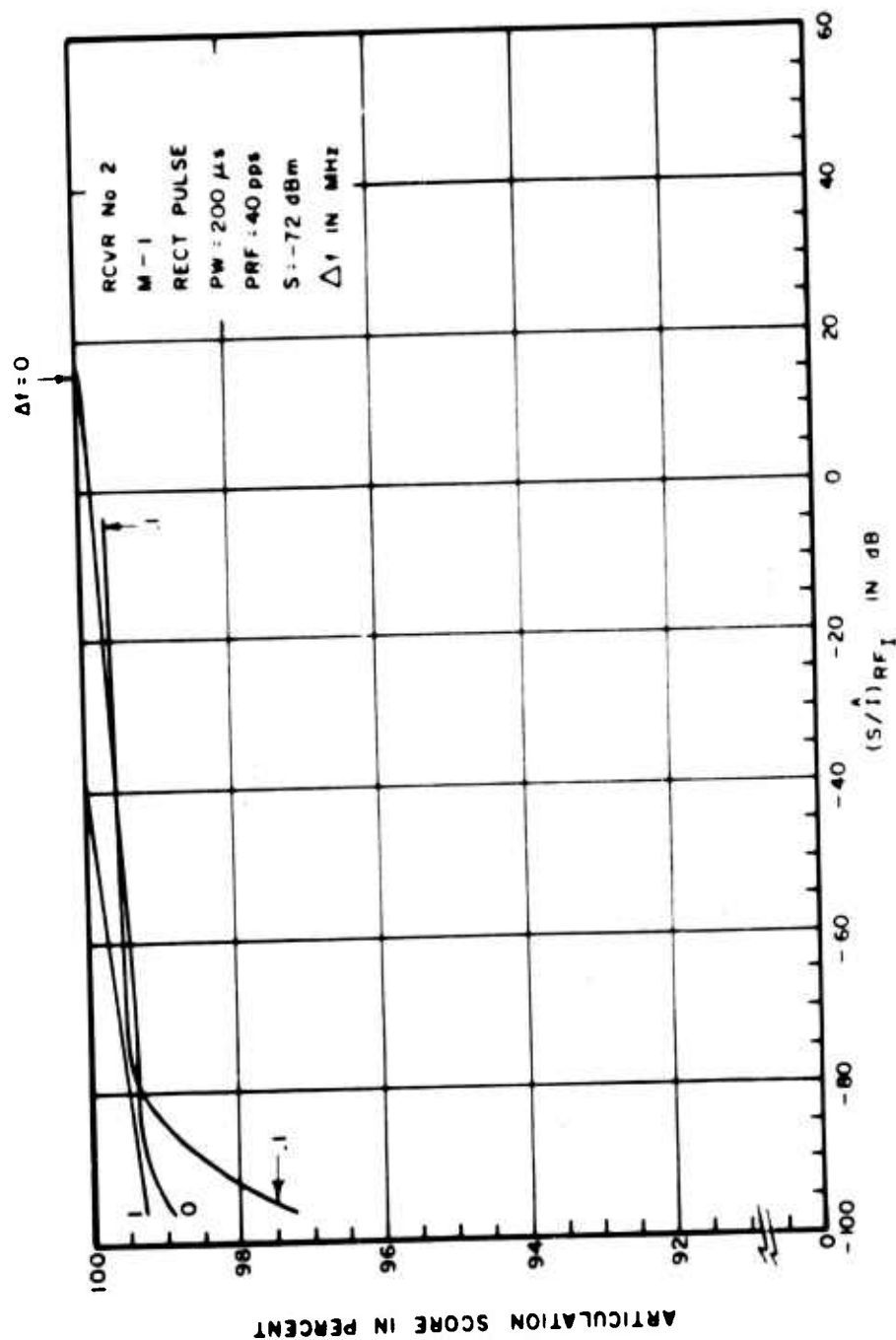


Figure III-31. Articulation Score for Pulsed Interference to an AM Receiver

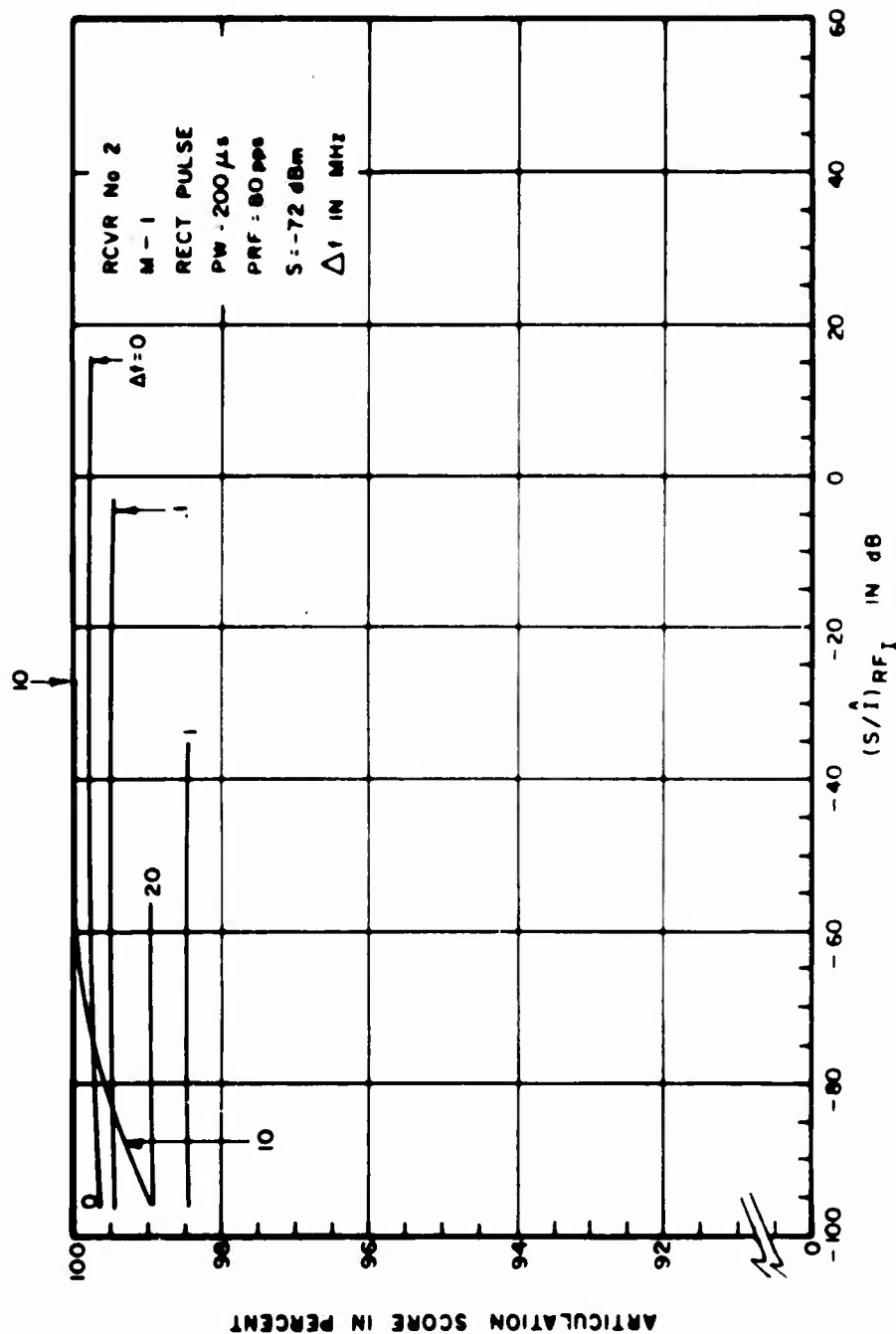


Figure III-32. Articulation Score for Pulsed Interference to an AM Receiver

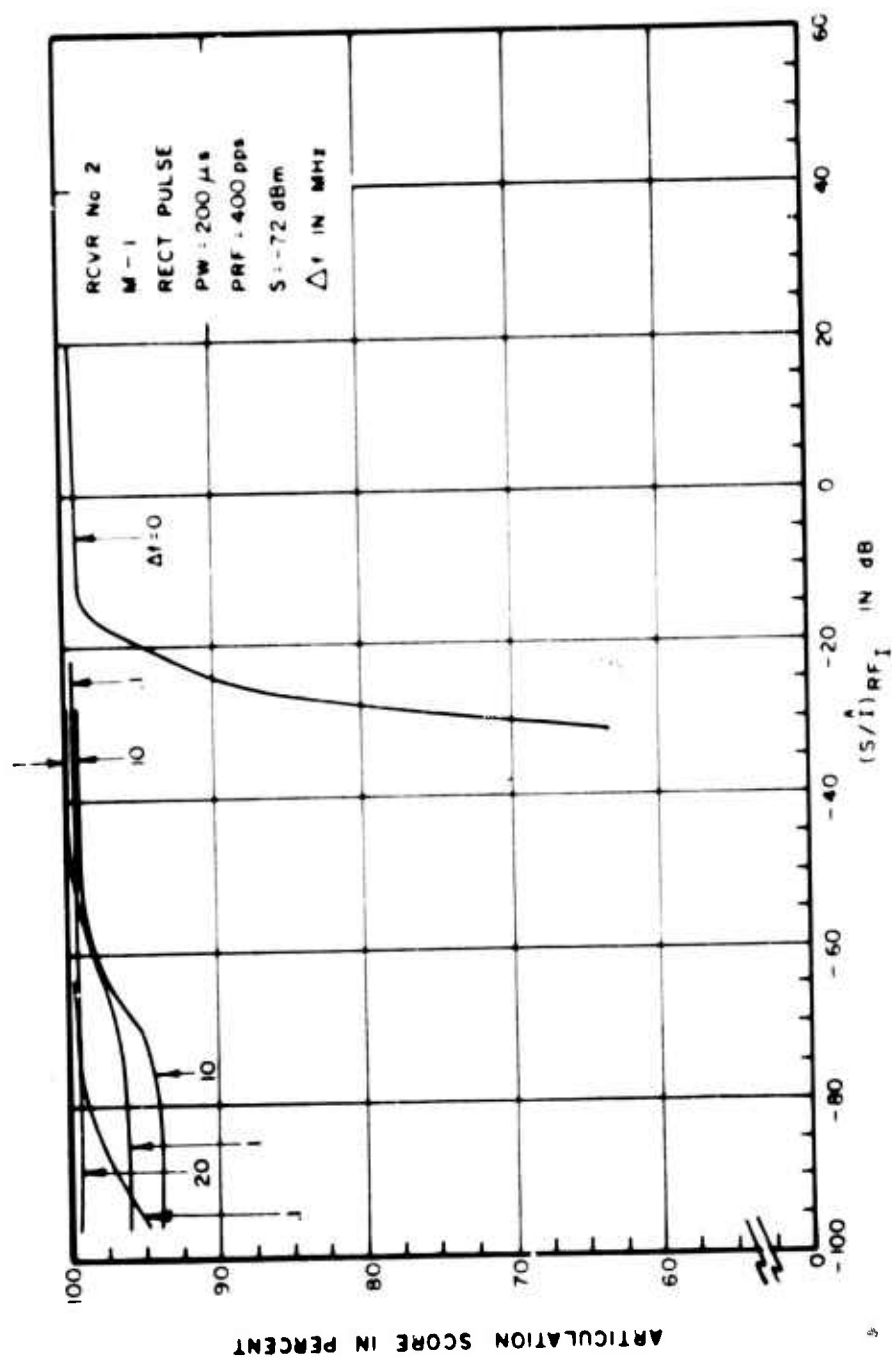


Figure III-33. Articulation Score for Pulsed Interference to an AM Receiver

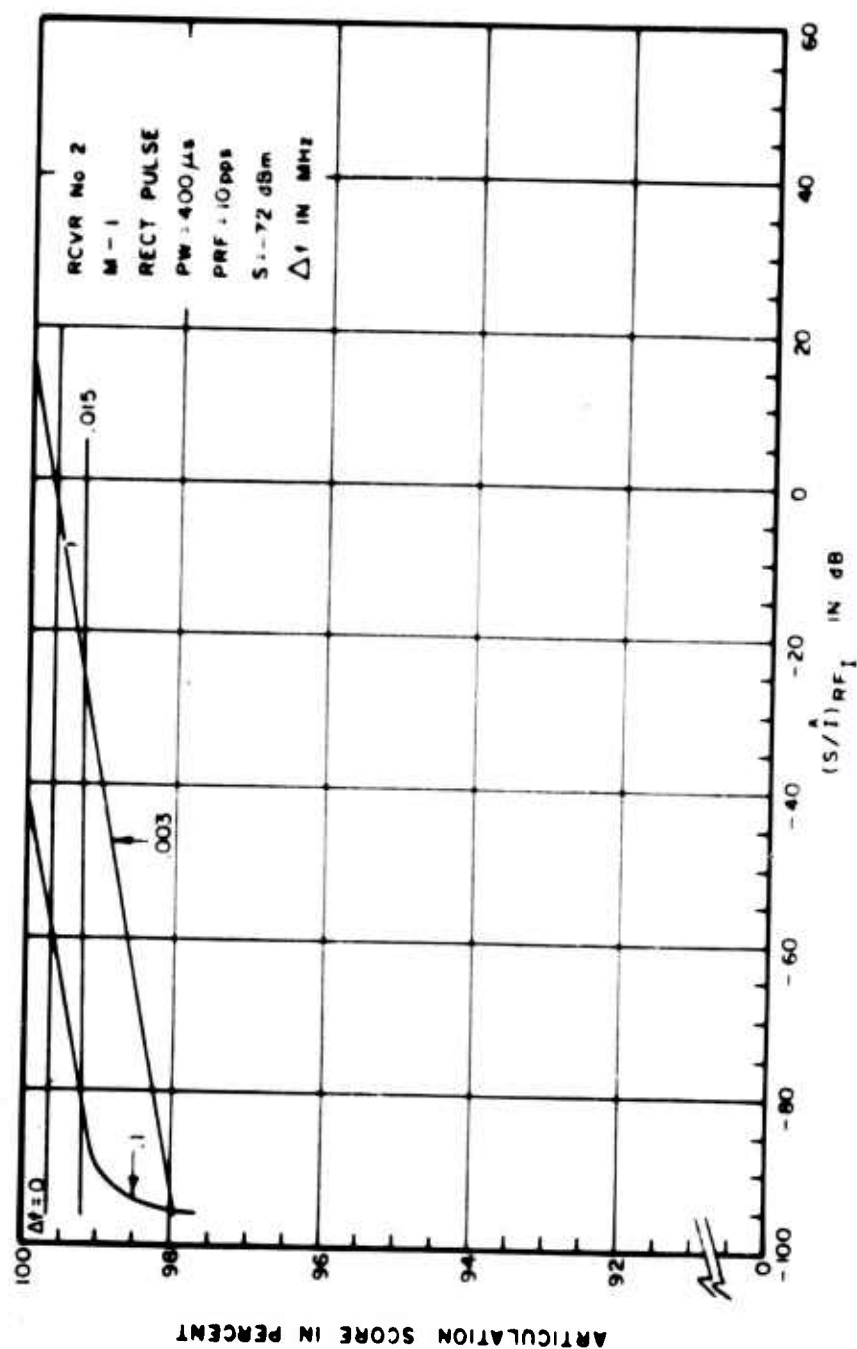


Figure III-34. Articulation Score for Pulsed Interference to an AM Receiver

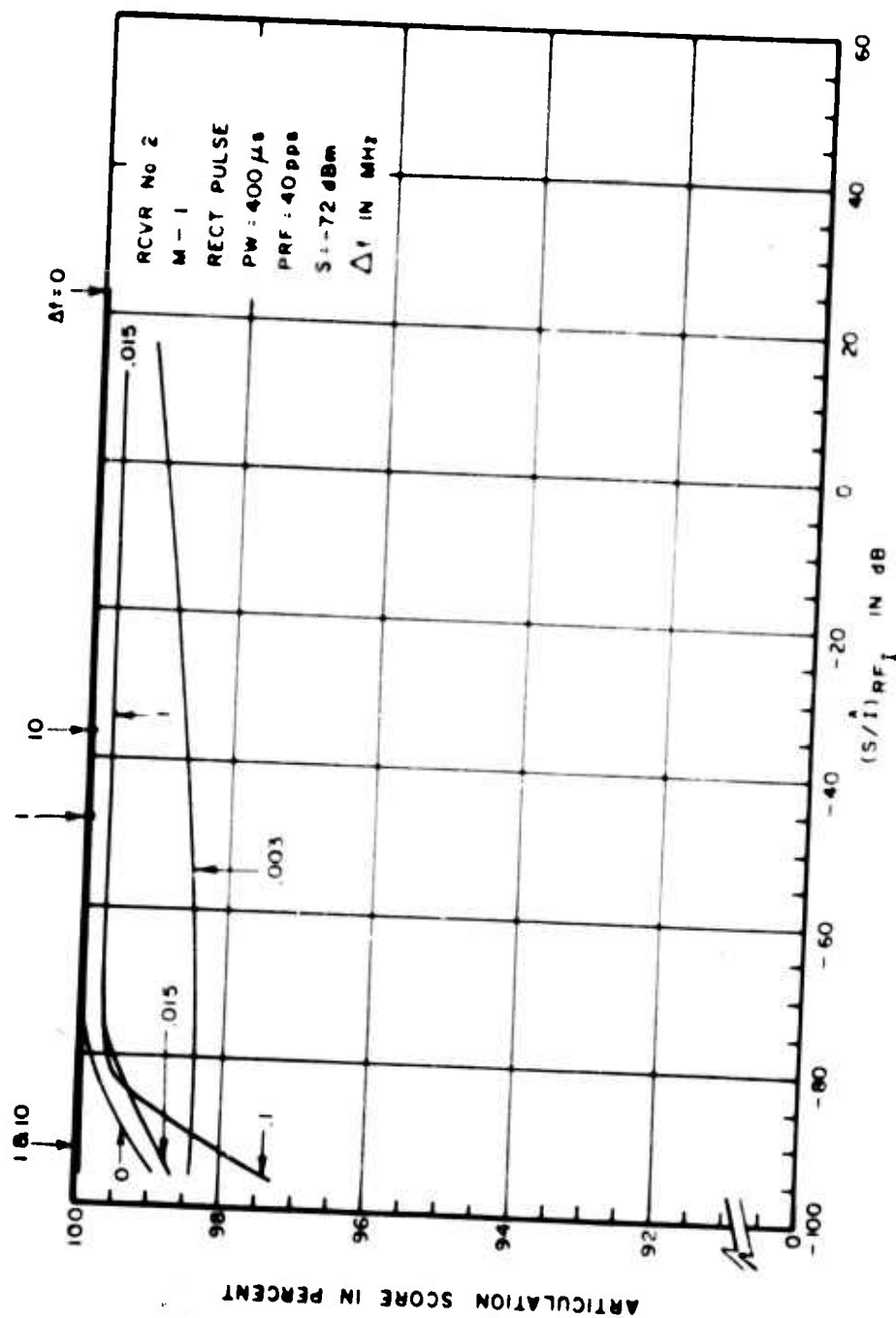


Figure III-35. Articulation Score for Pulsed Interference to an AM Receiver

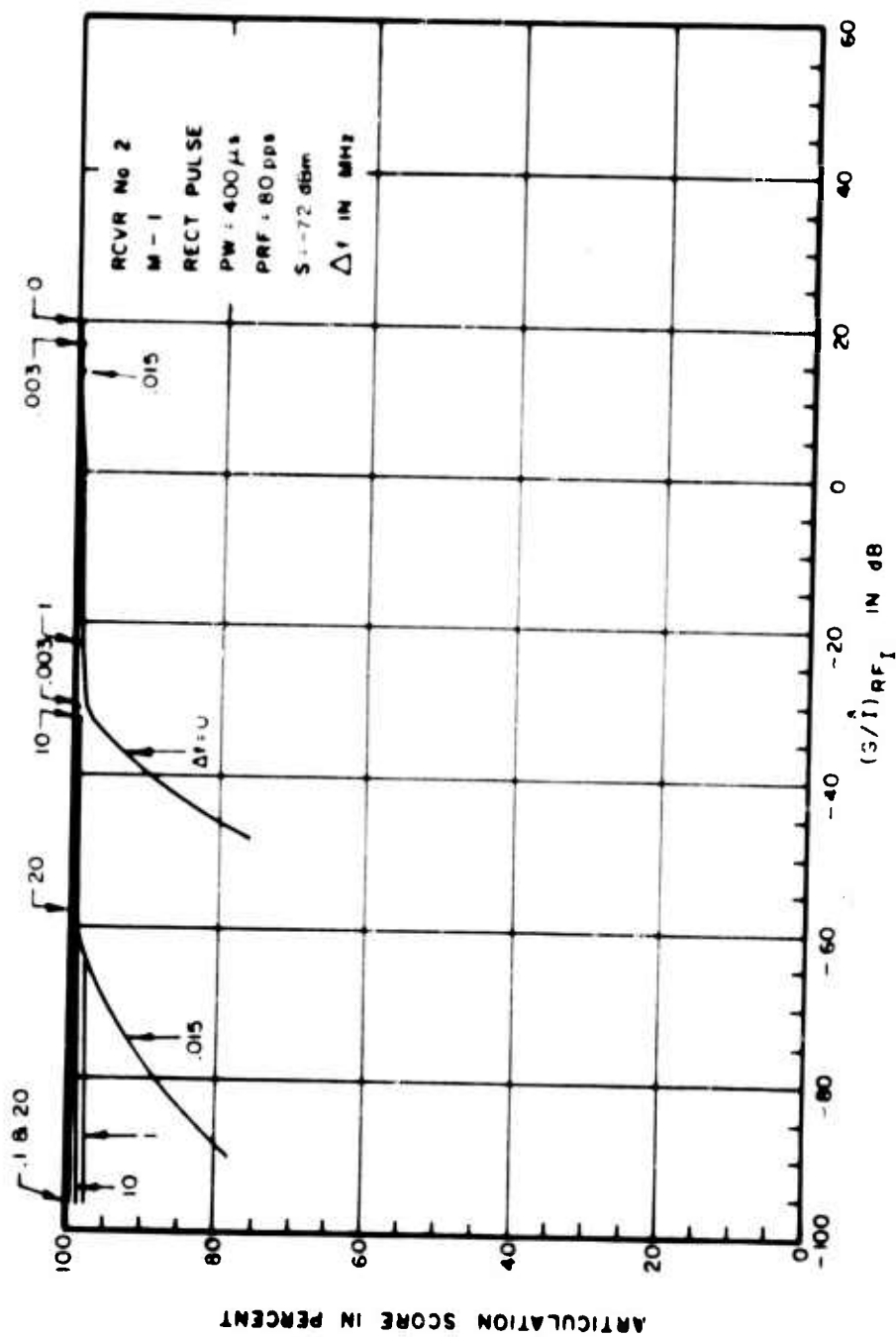


Figure III-36. Articulation Score for Pulsed Interference to an AM Receiver

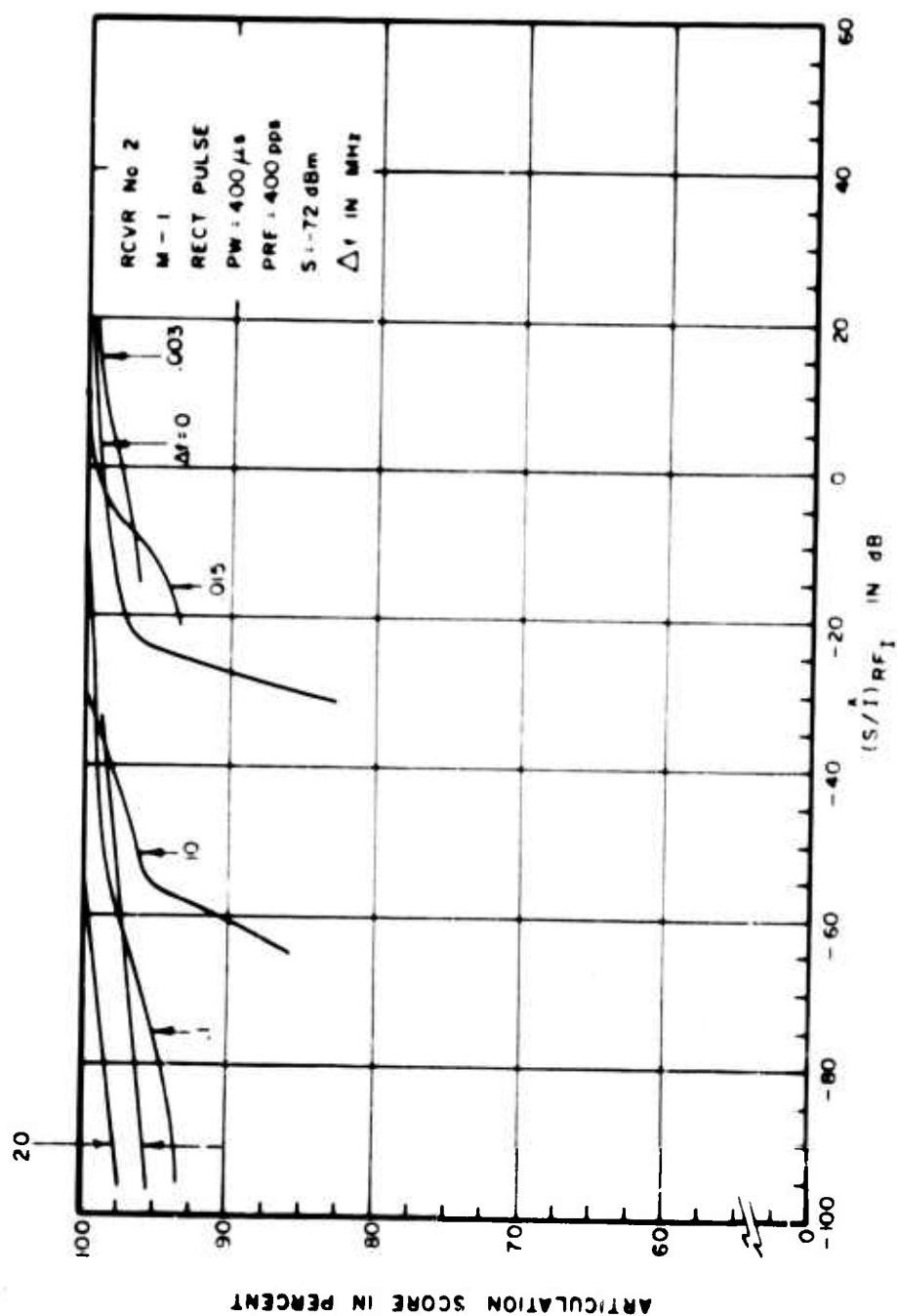


Figure III-37. Articulation Score for Pulsed Interference to an AM Receiver

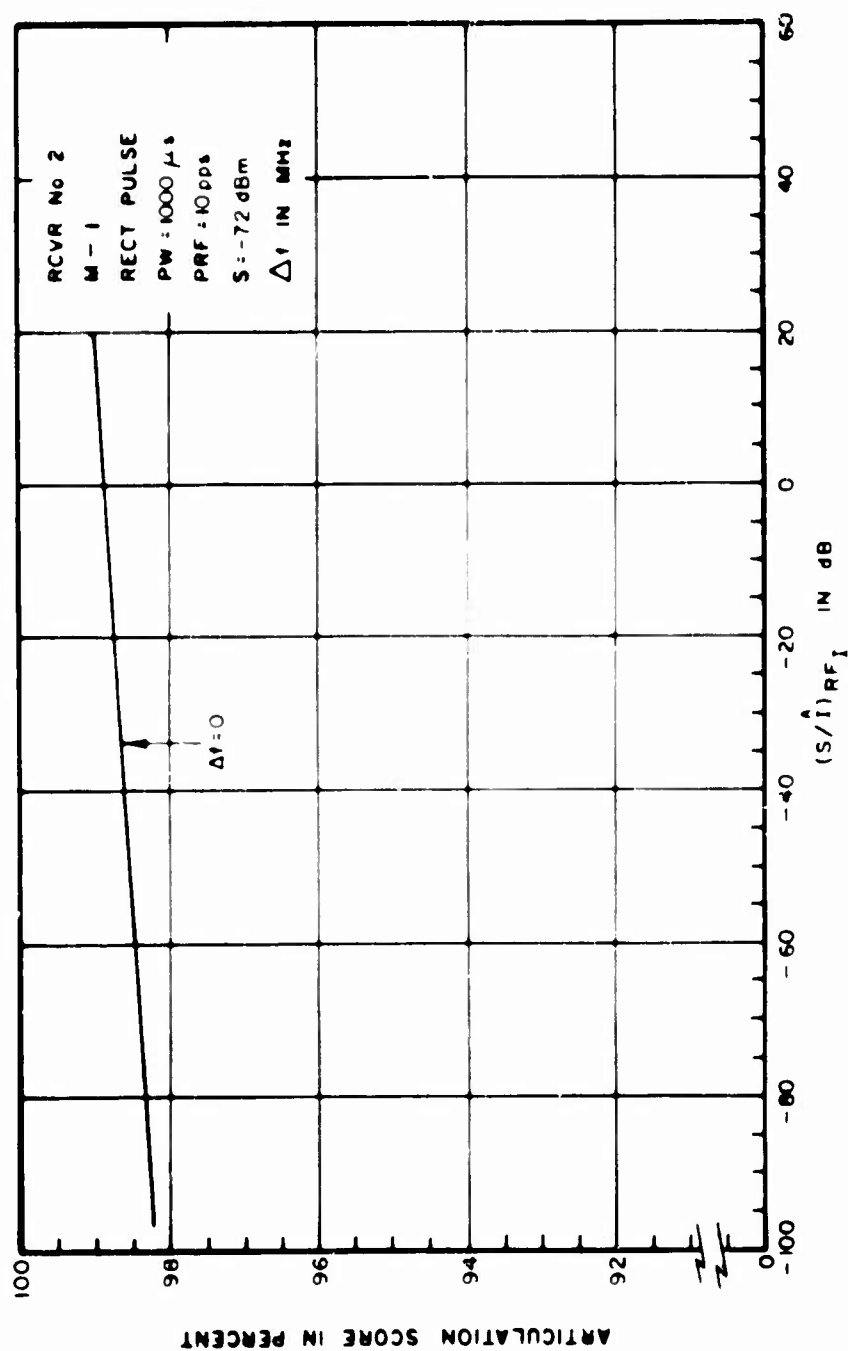


Figure III-38. Articulation Score for Pulsed Interference to an AM Receiver

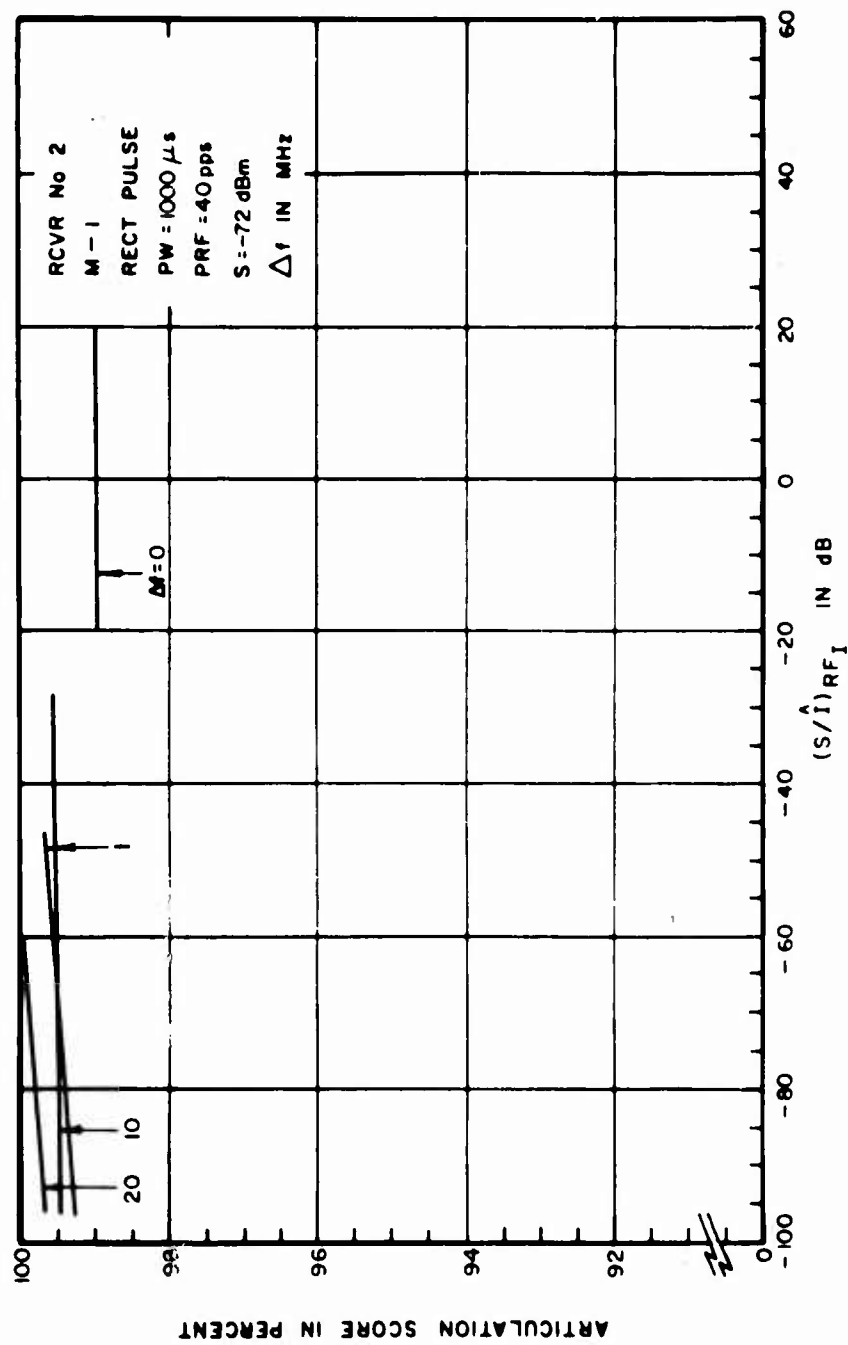


Figure III-39. Articulation Score for Pulsed Interference to an AM Receiver

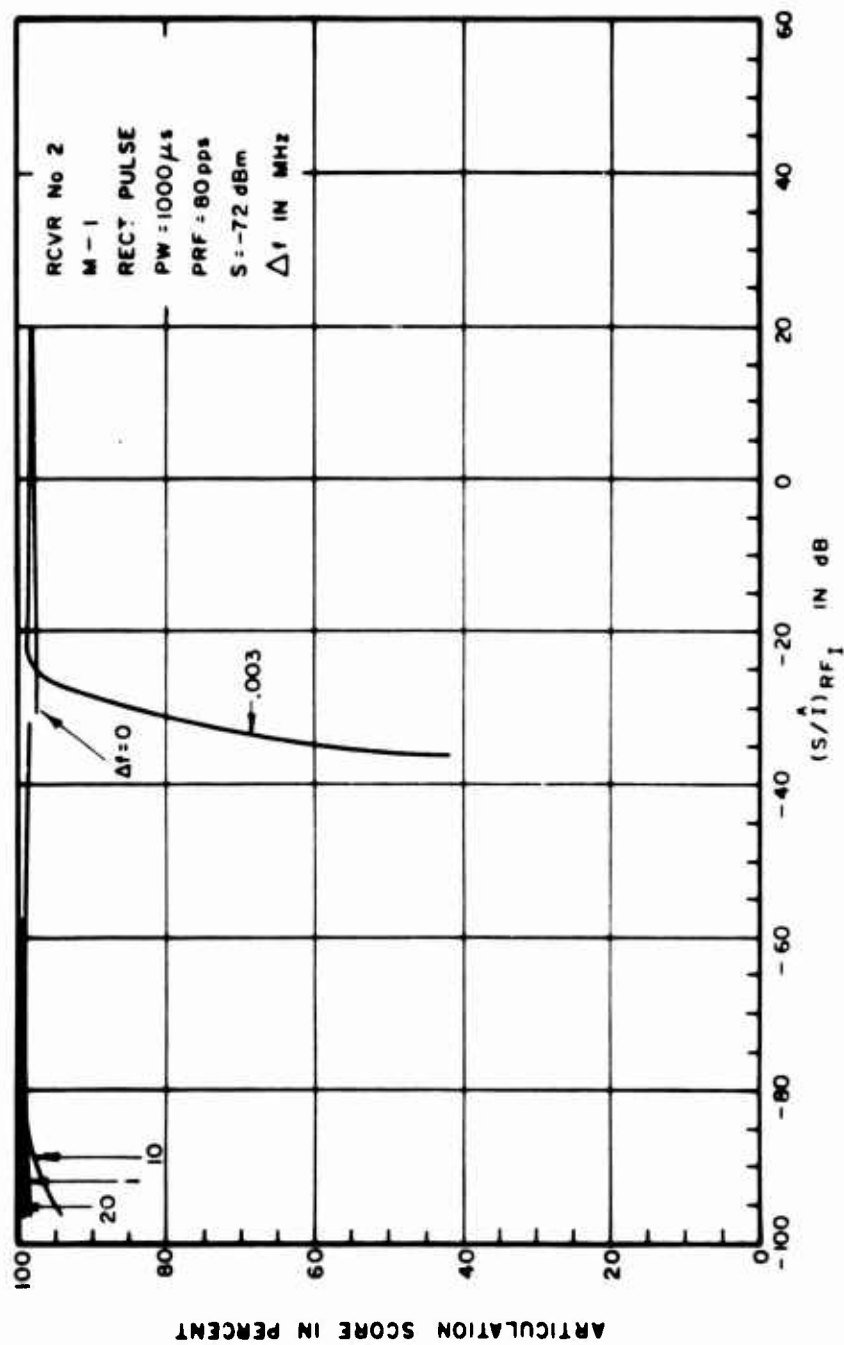


Figure III-40. Articulation Score for Pulsed Interference to an AM Receiver

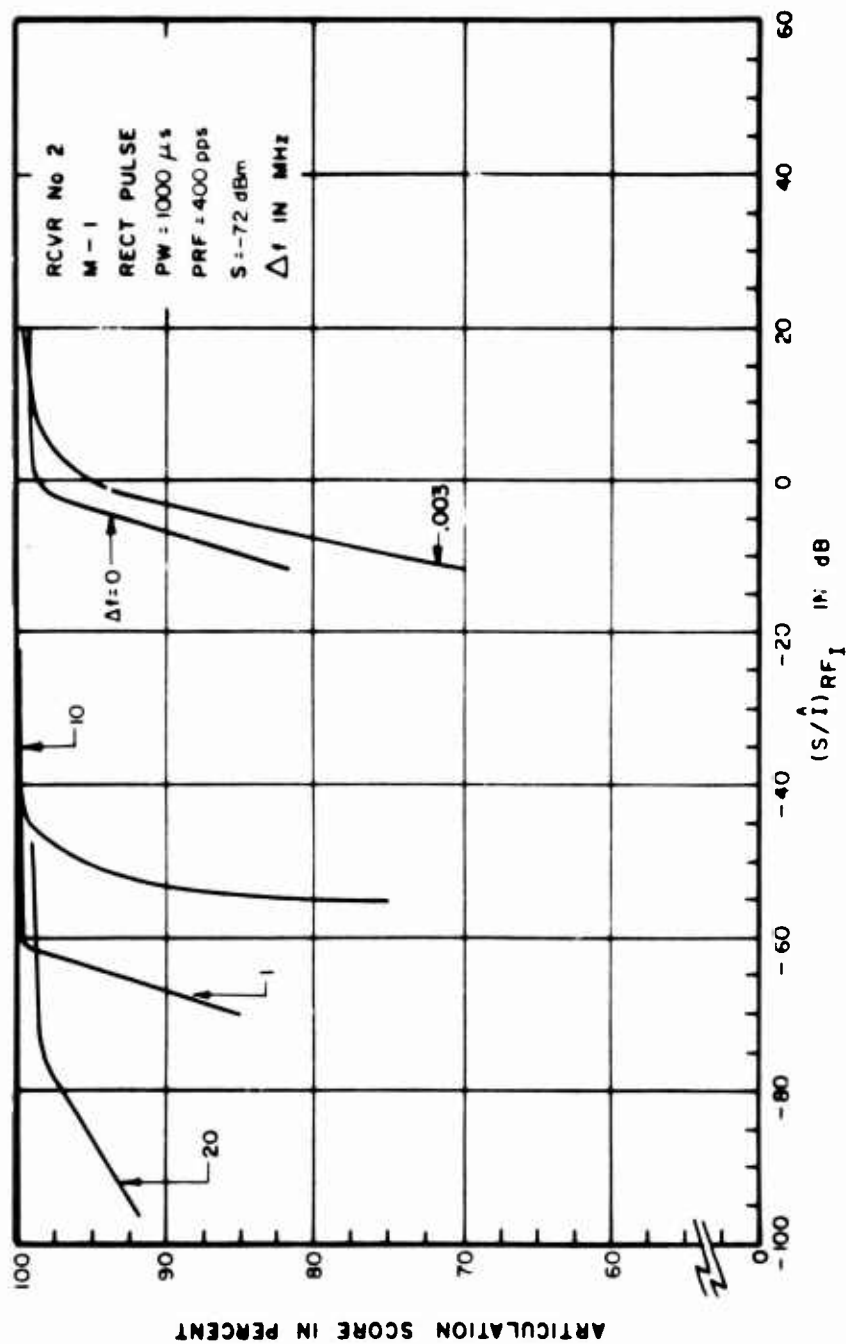


Figure III-41. Articulation Score for Pulsed Interference to an AM Receiver

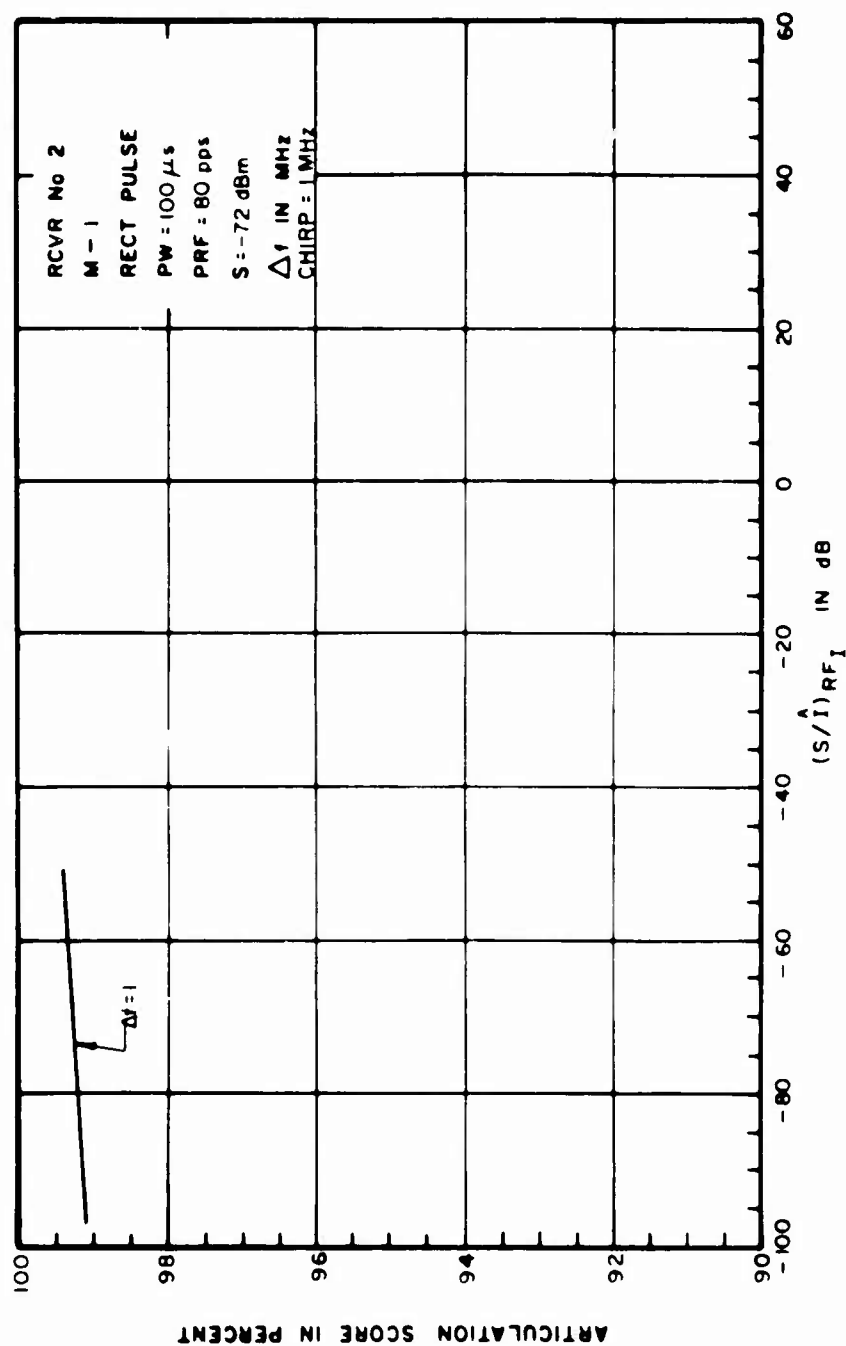


Figure III-42. Articulation Score for Pulsed Interference to an AM Receiver

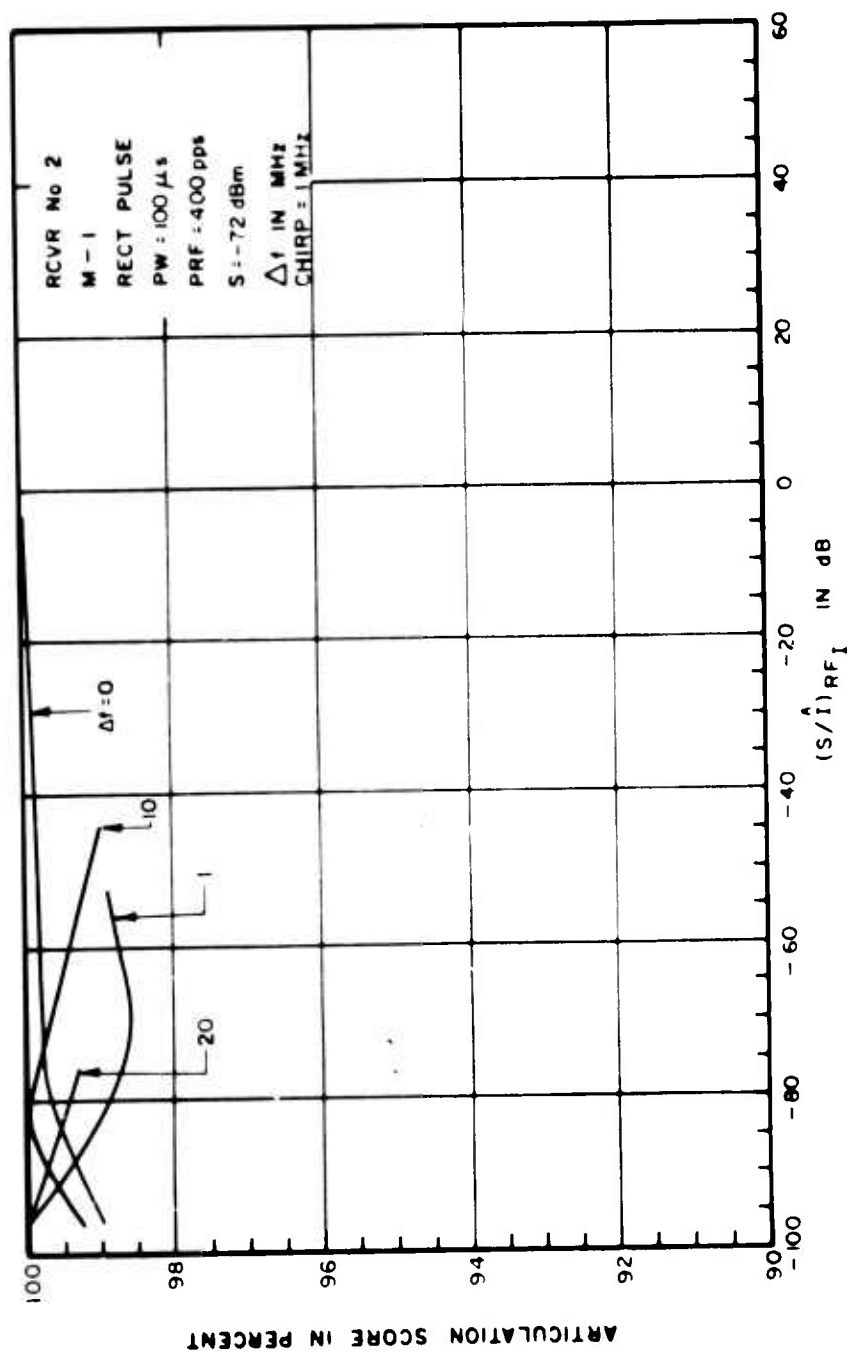


Figure III-43. Articulation Score for Pulsed Interference to an AM Receiver

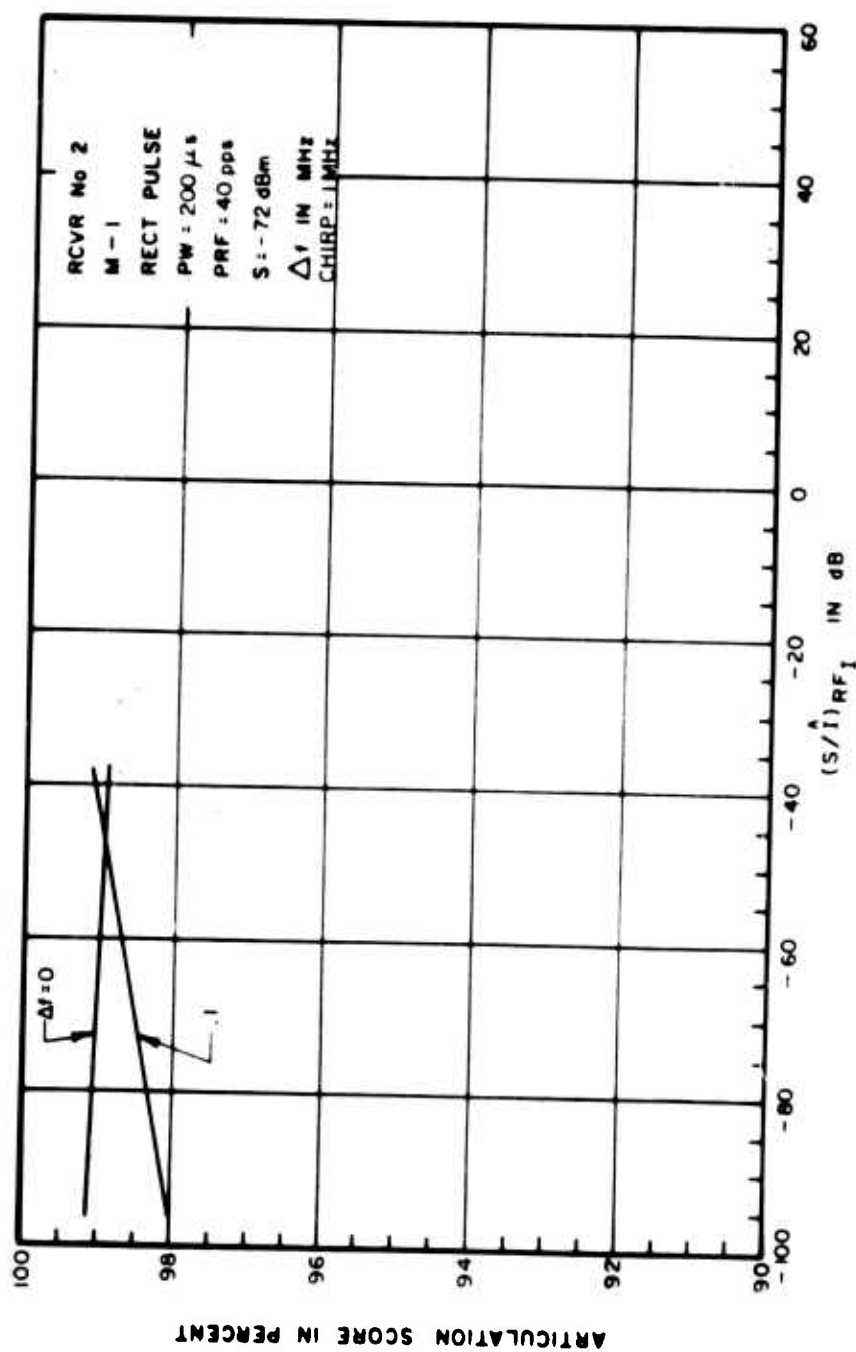


Figure III-44. Articulation Score for Pulsed Interference to an AM Receiver

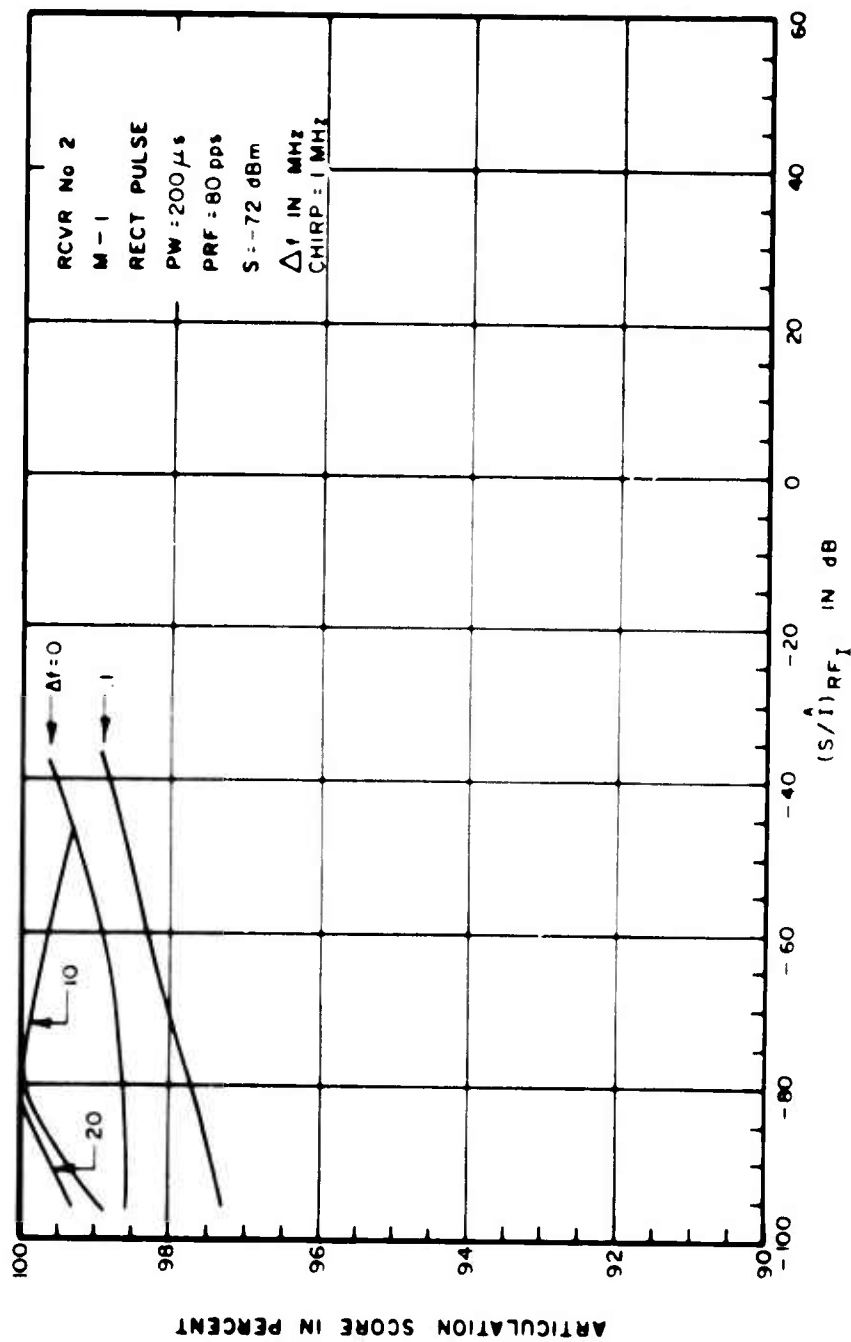


Figure III-45. Articulation Score for Pulsed Interference to an AM Receiver

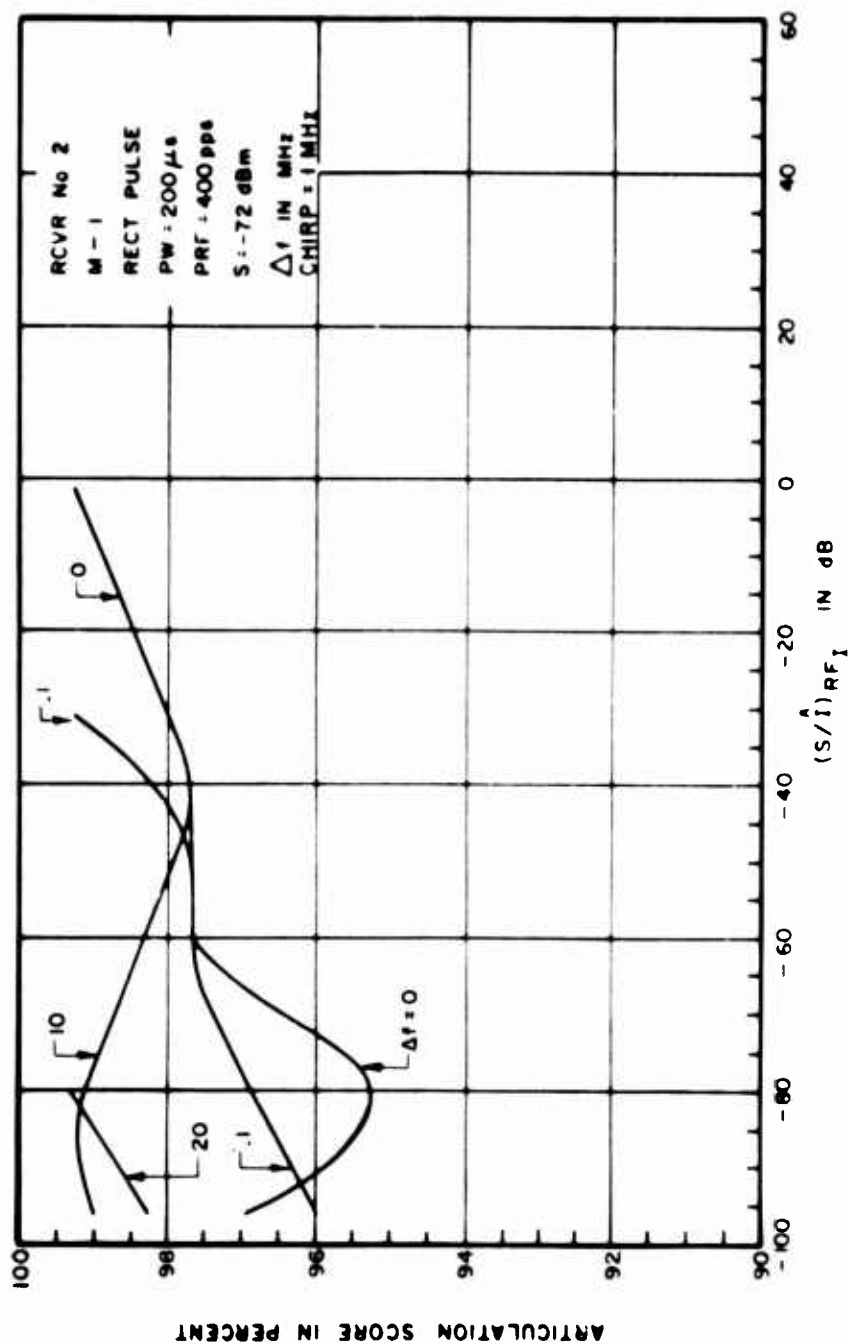


Figure III-46. Articulation Score for Pulsed Interference to an AM Receiver

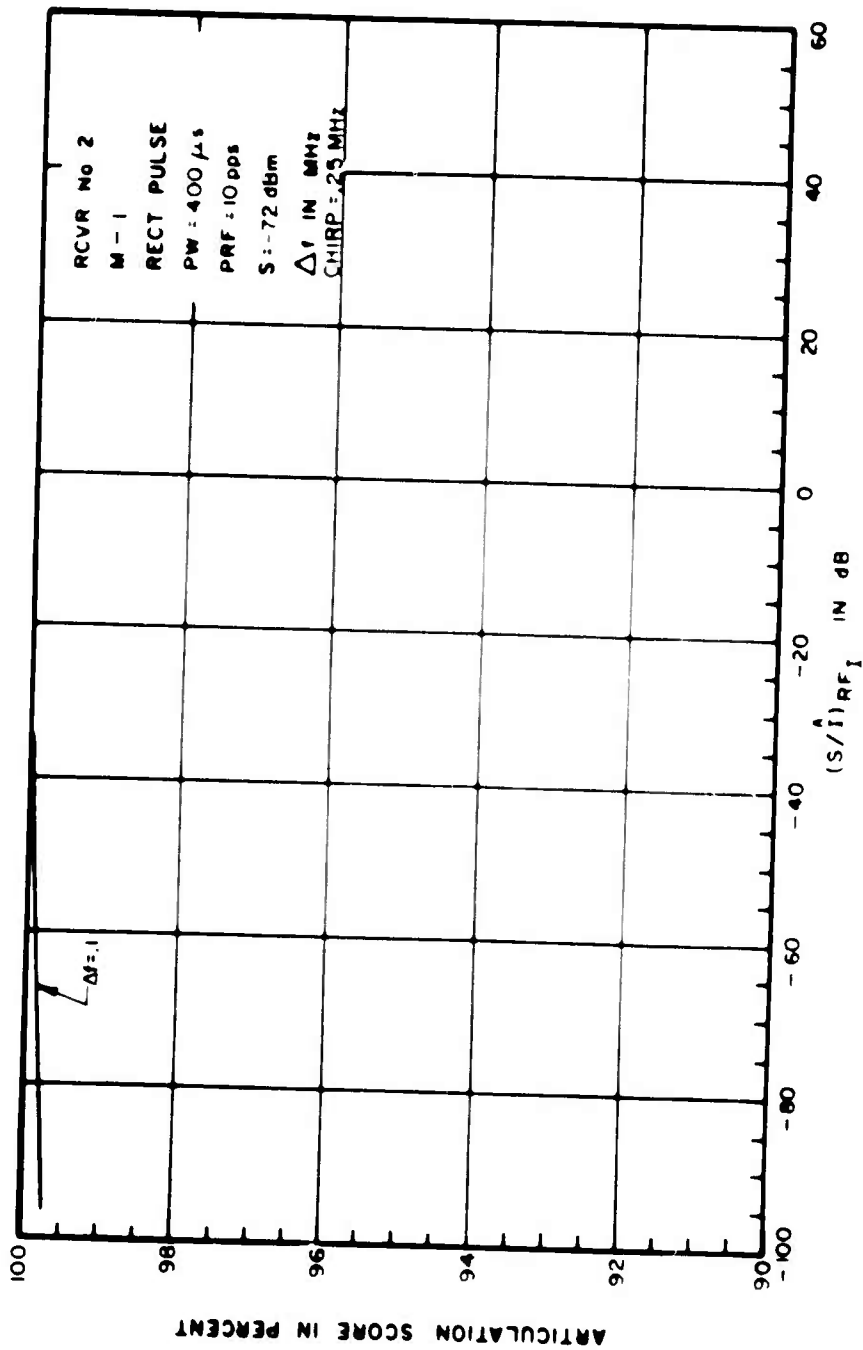


Figure III-47. Articulation Score for Pulsed Interference to an AM Receiver

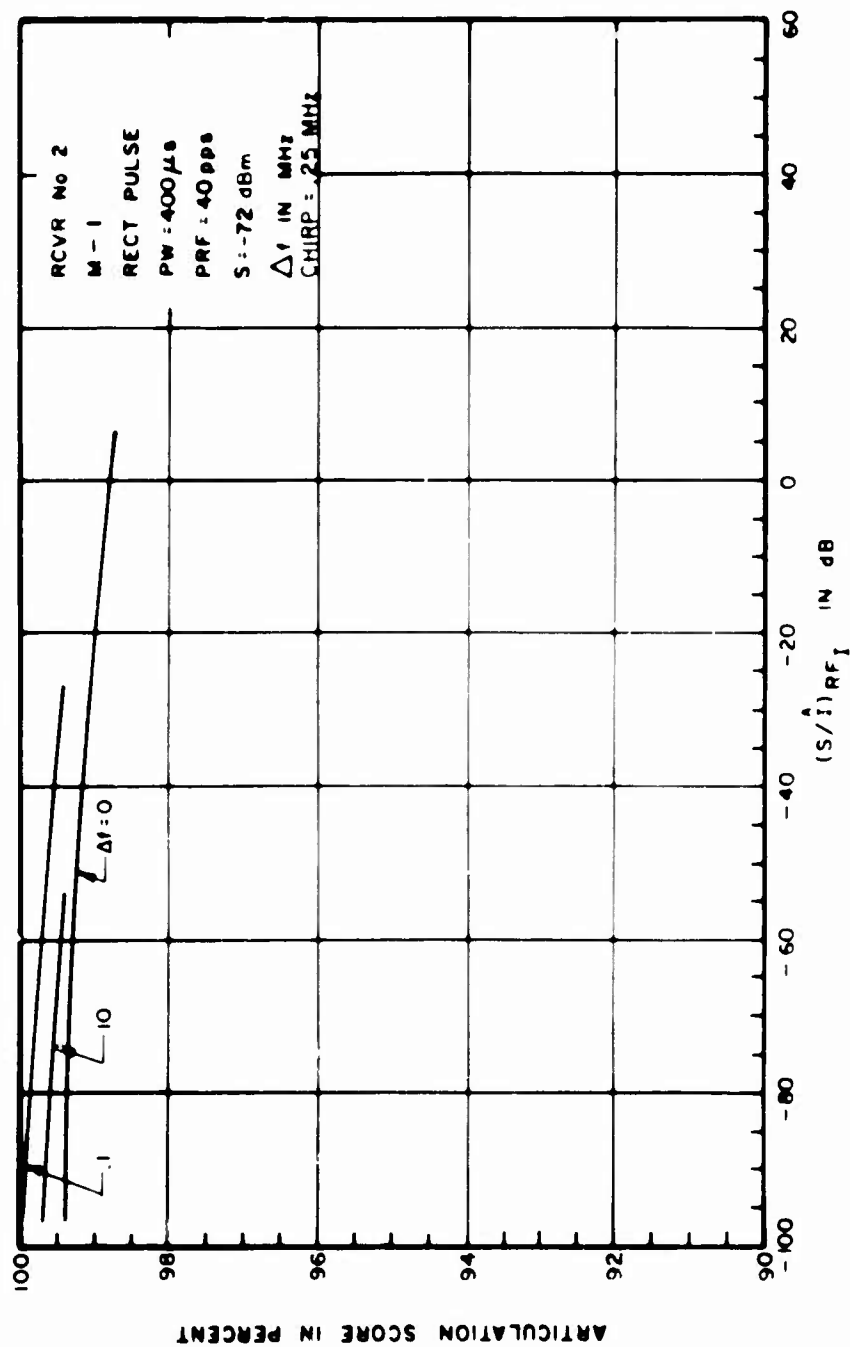


Figure III 48. Articulation Score for Pulsed Interference to an AM Receiver

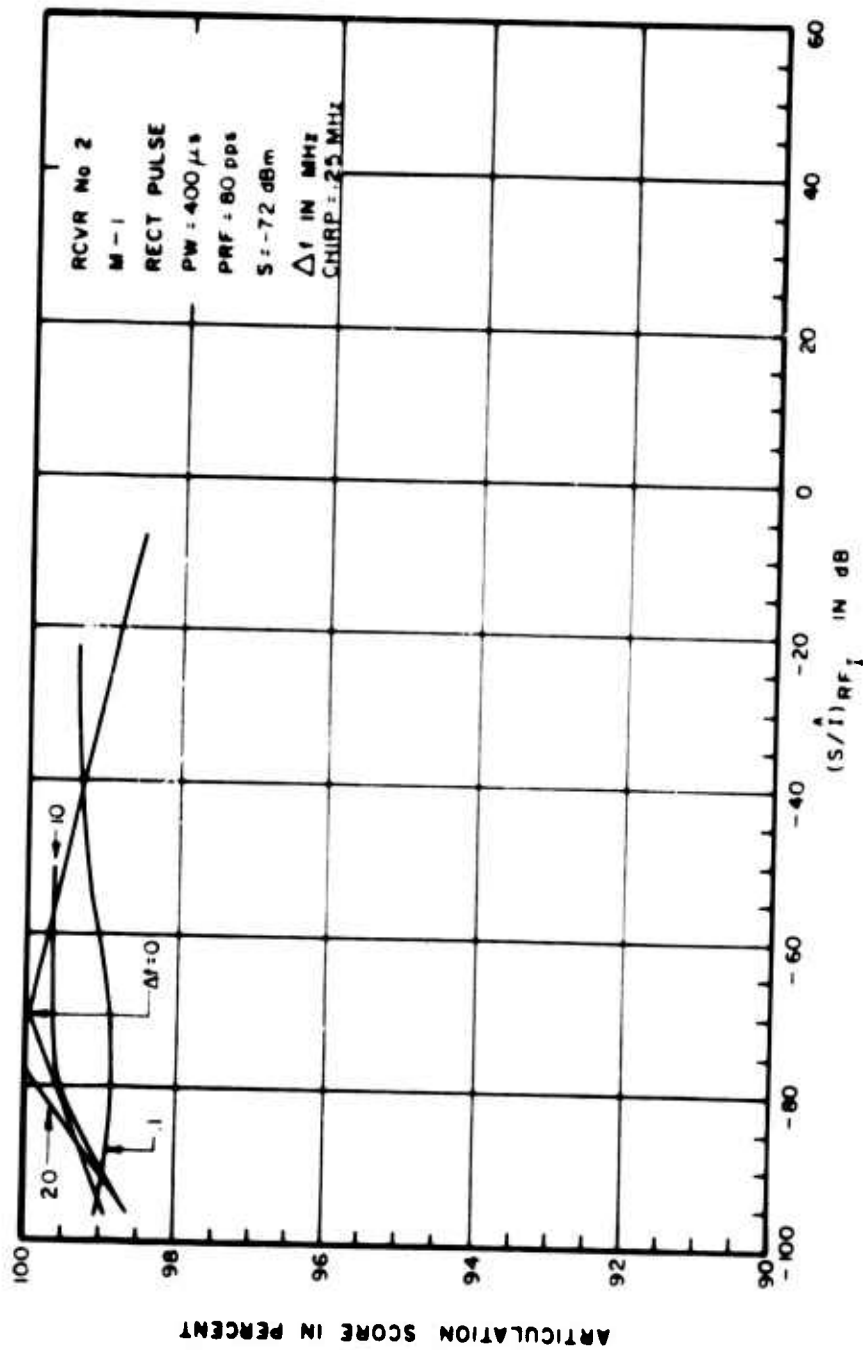


Figure III-49. Articulation Score for Pulsed Interference to an AM Receiver

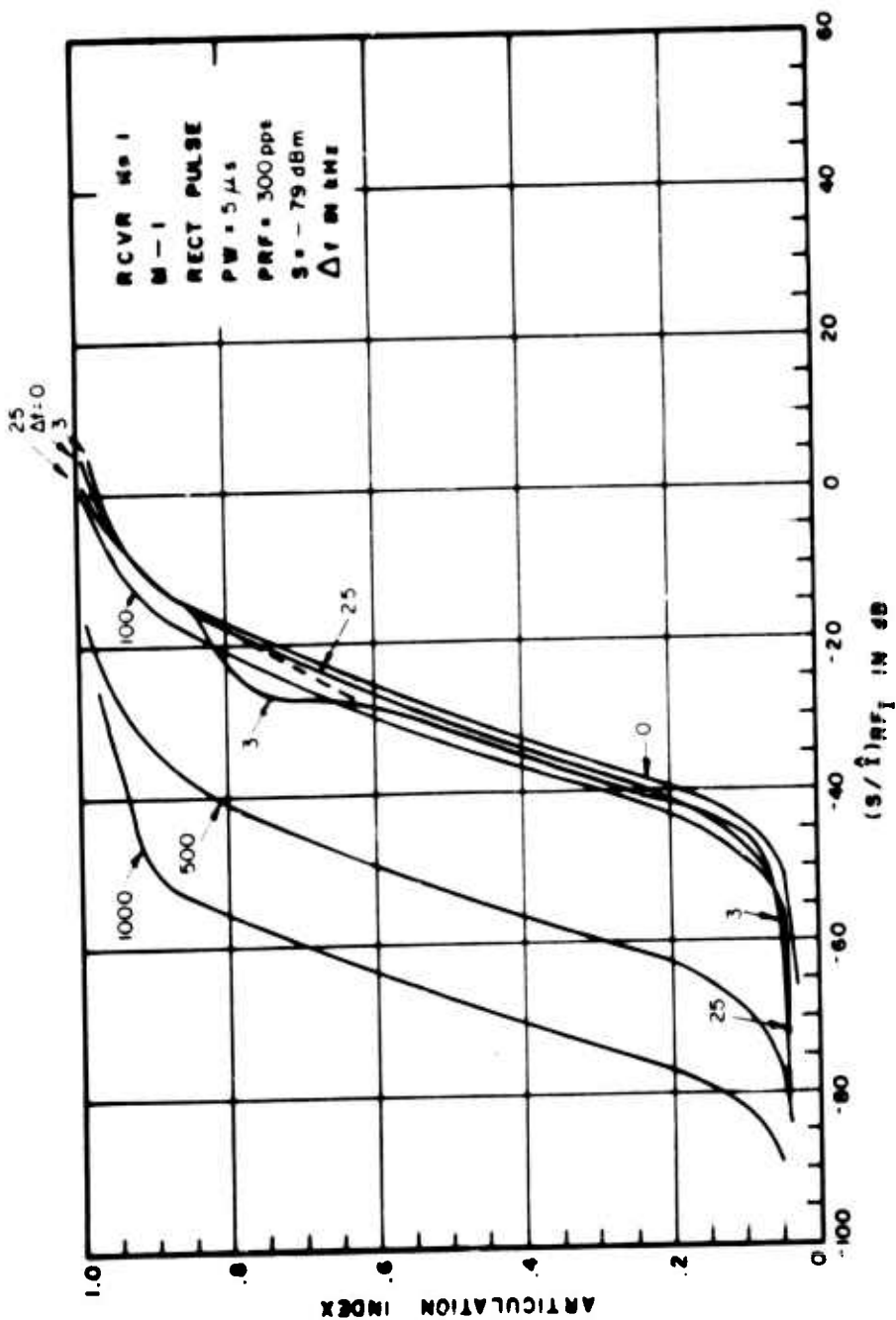


Figure III-50. Articulation Index for Pulsed Interference to an AM Receiver

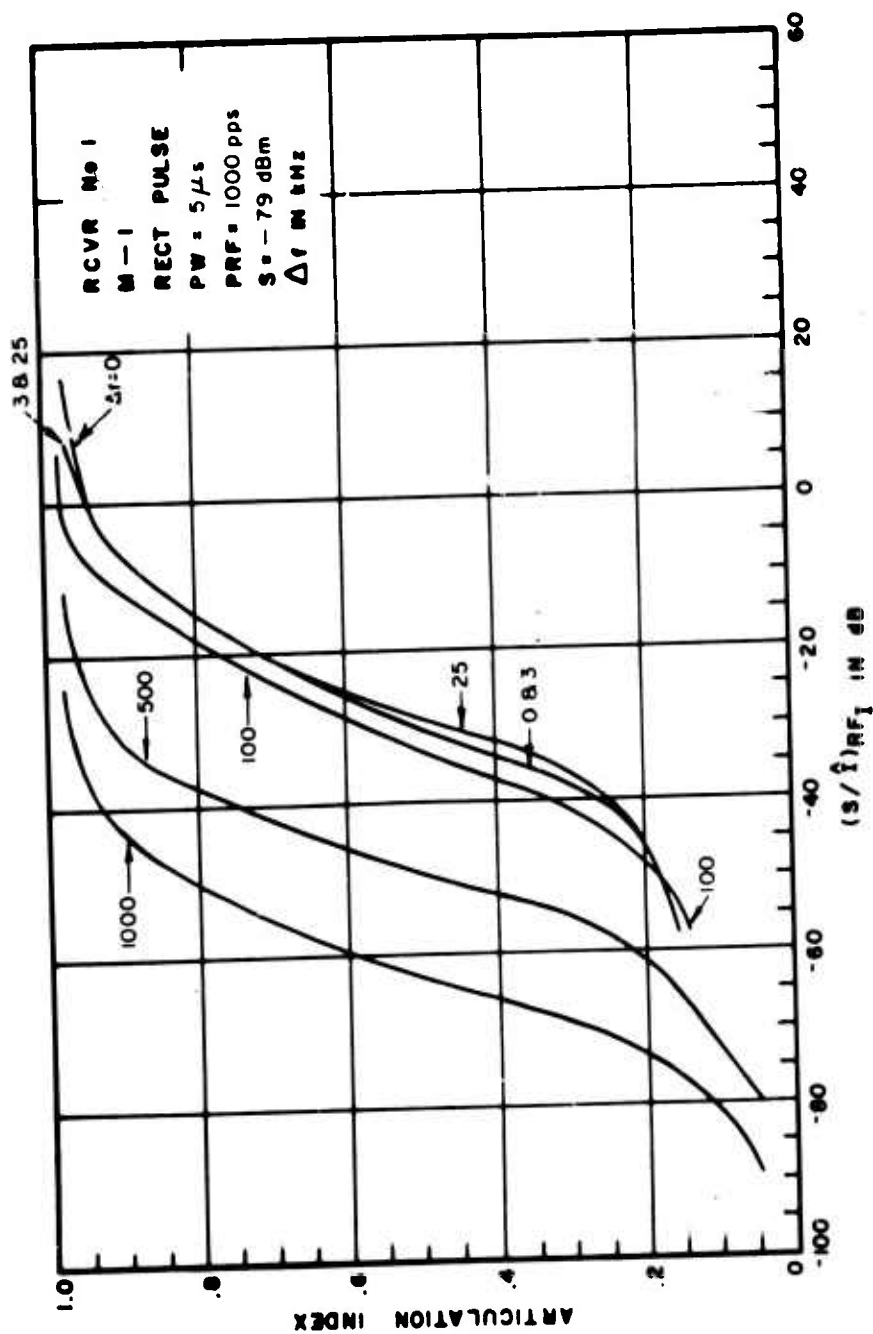


Figure III-51. Articulation Index for Pulsed Interference to an AM Receiver

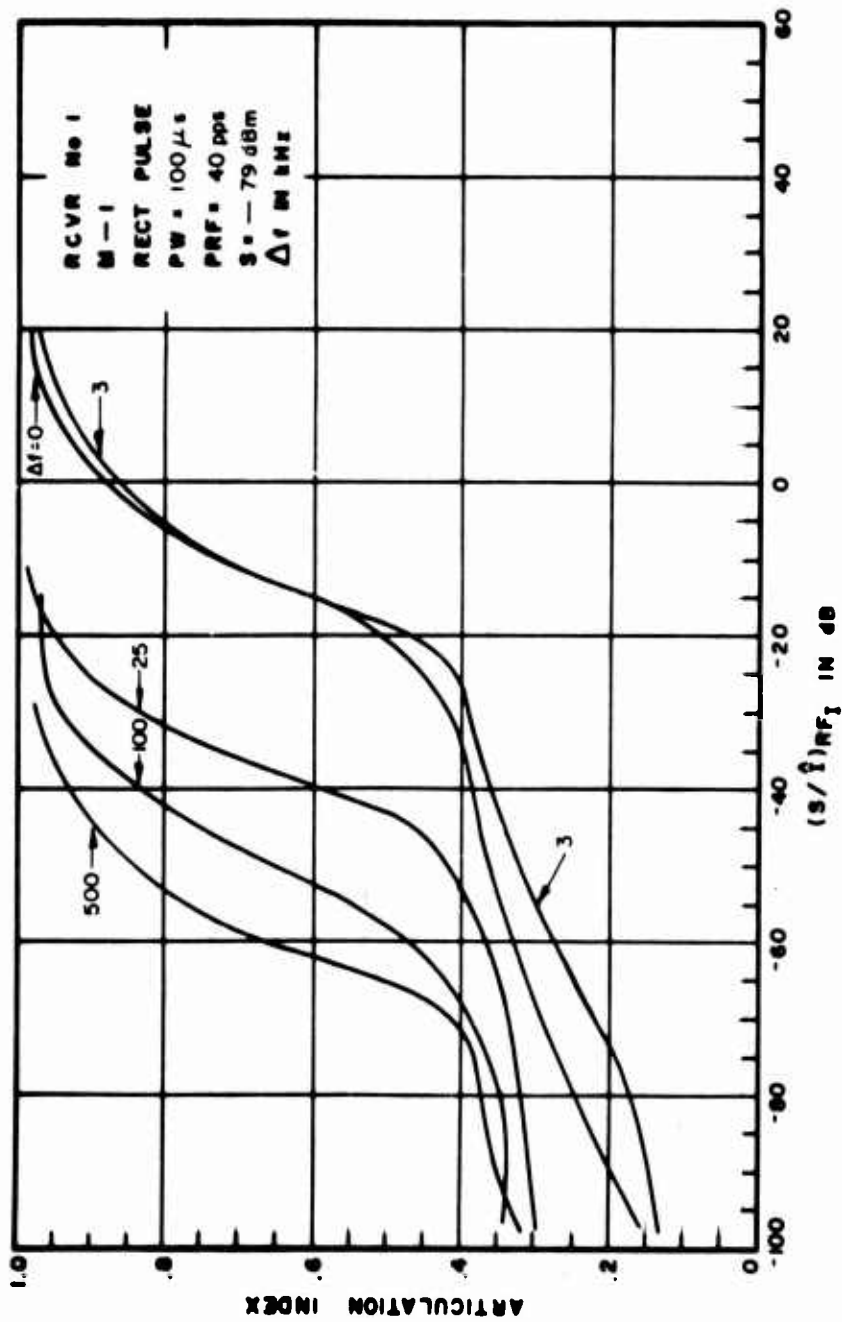


Figure III-52. Articulation Index for Pulsed Interference to an AM Receiver

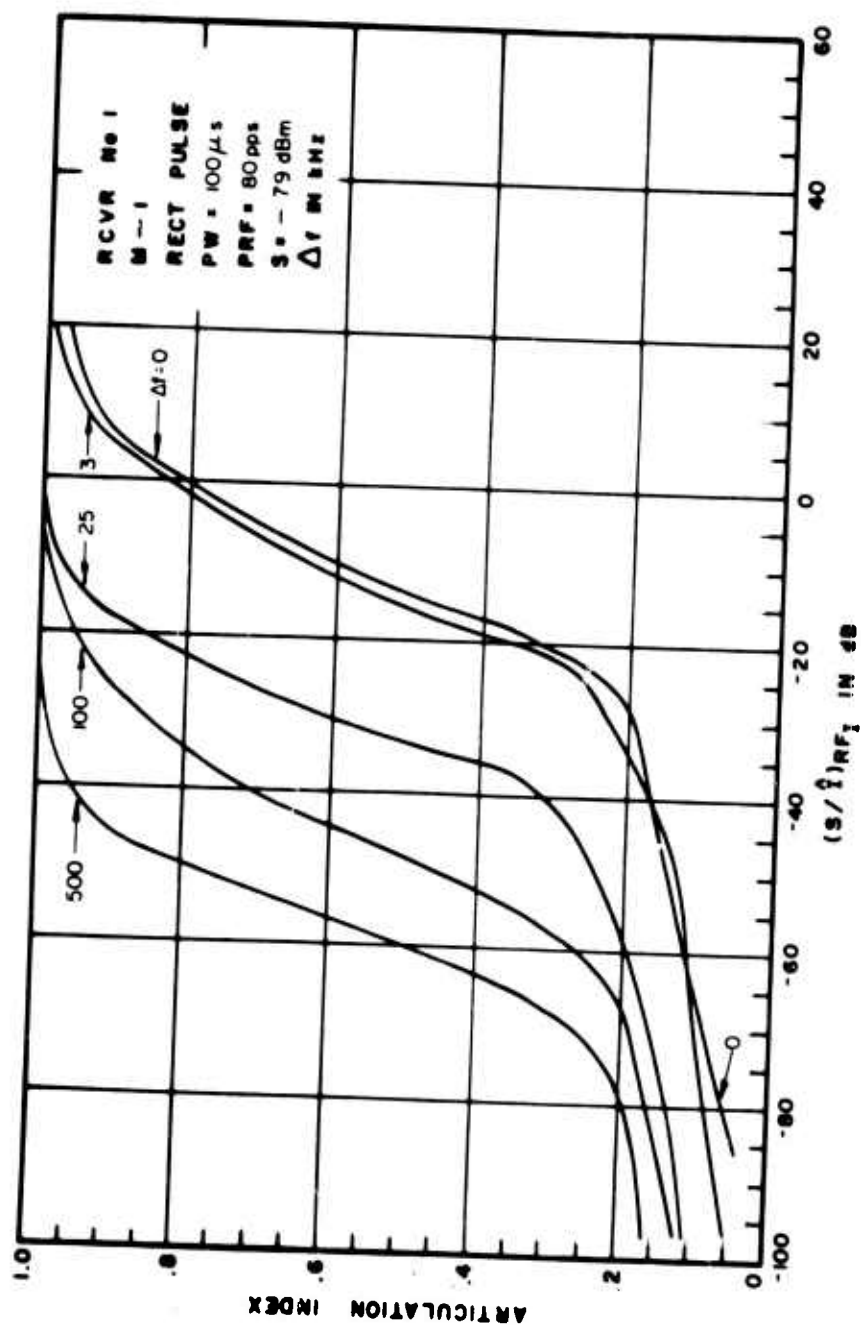


Figure III-53. Articulation Index for Pulsed Interference to an AM Receiver

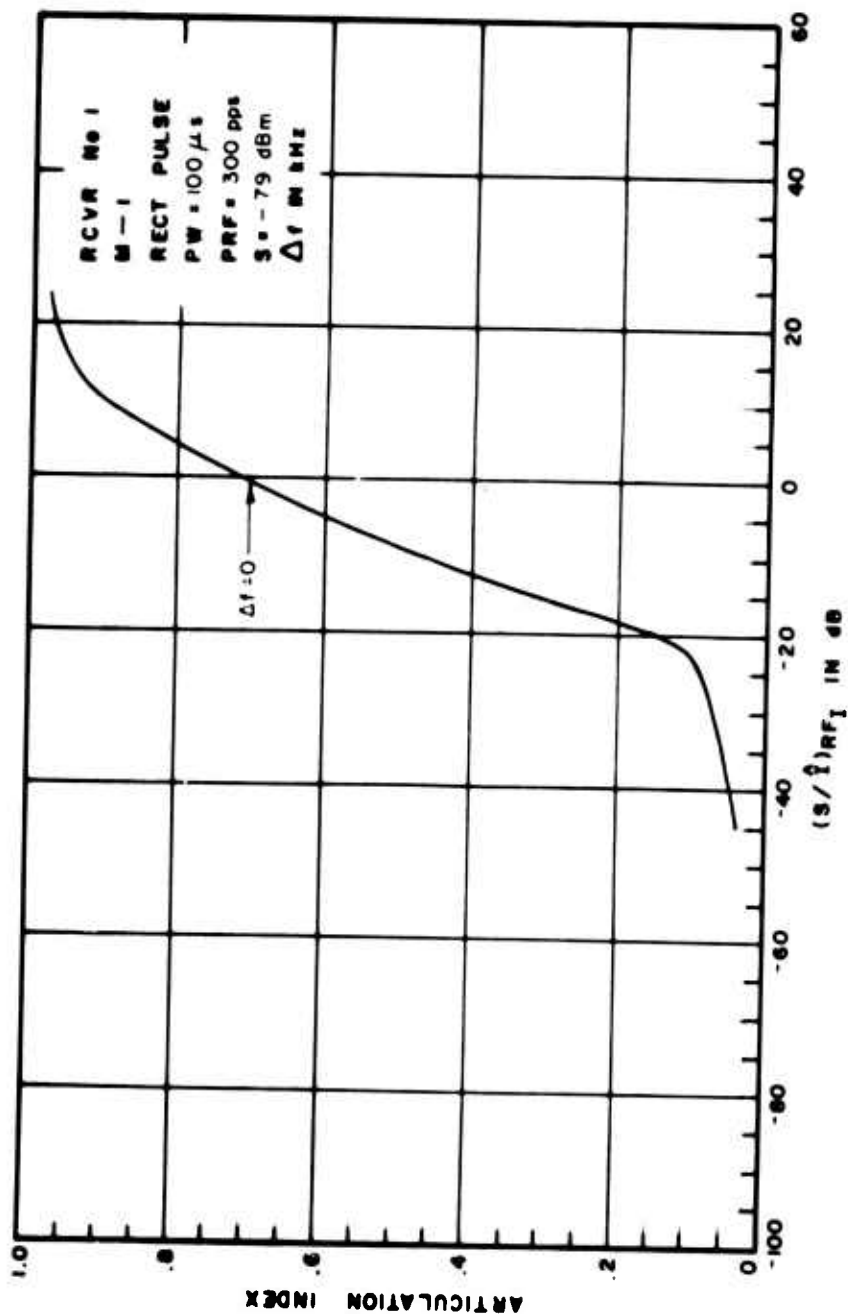


Figure III-54. Articulation Index for Pulsed Interference to an AM Receiver

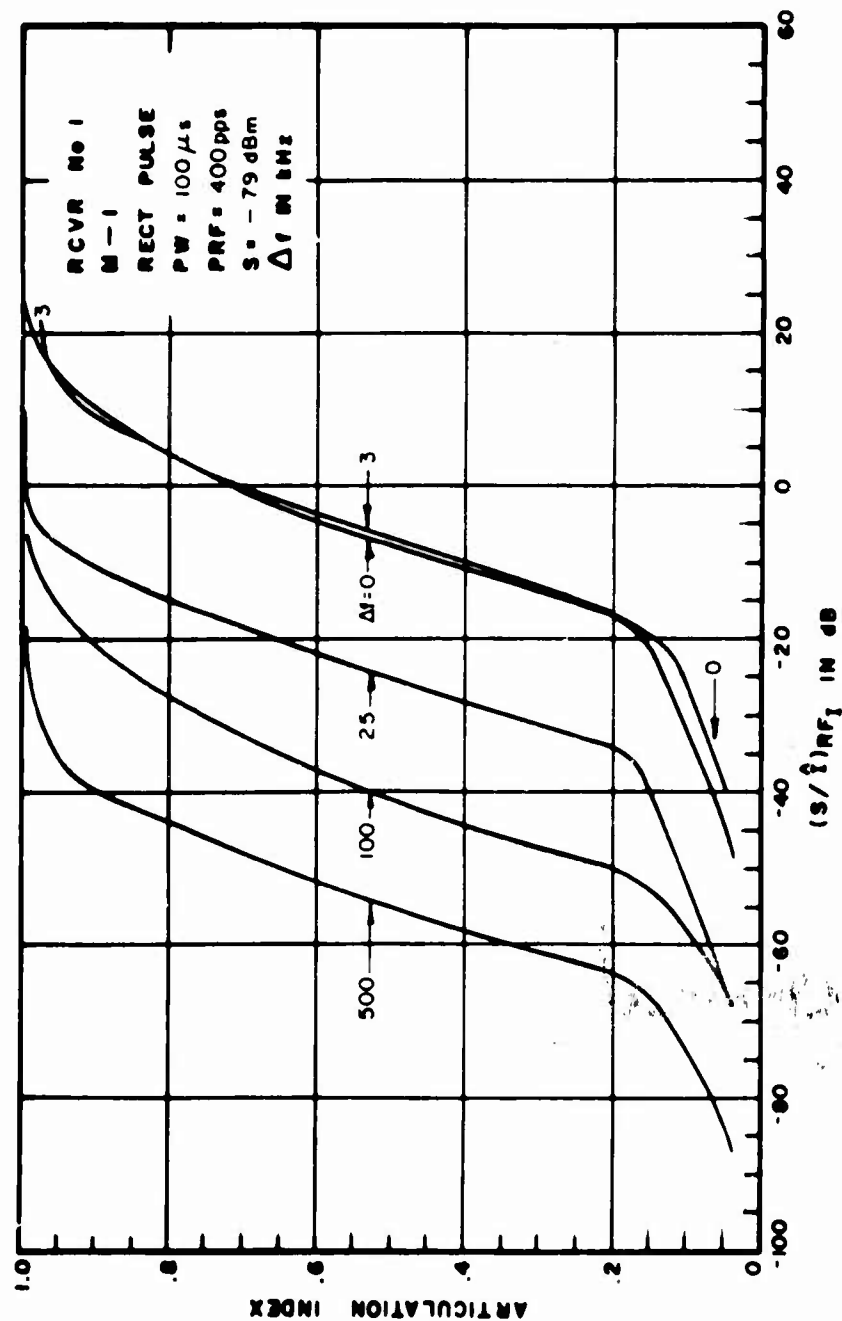


Figure III-55. Articulation Index for Pulsed Interference to an AM Receiver

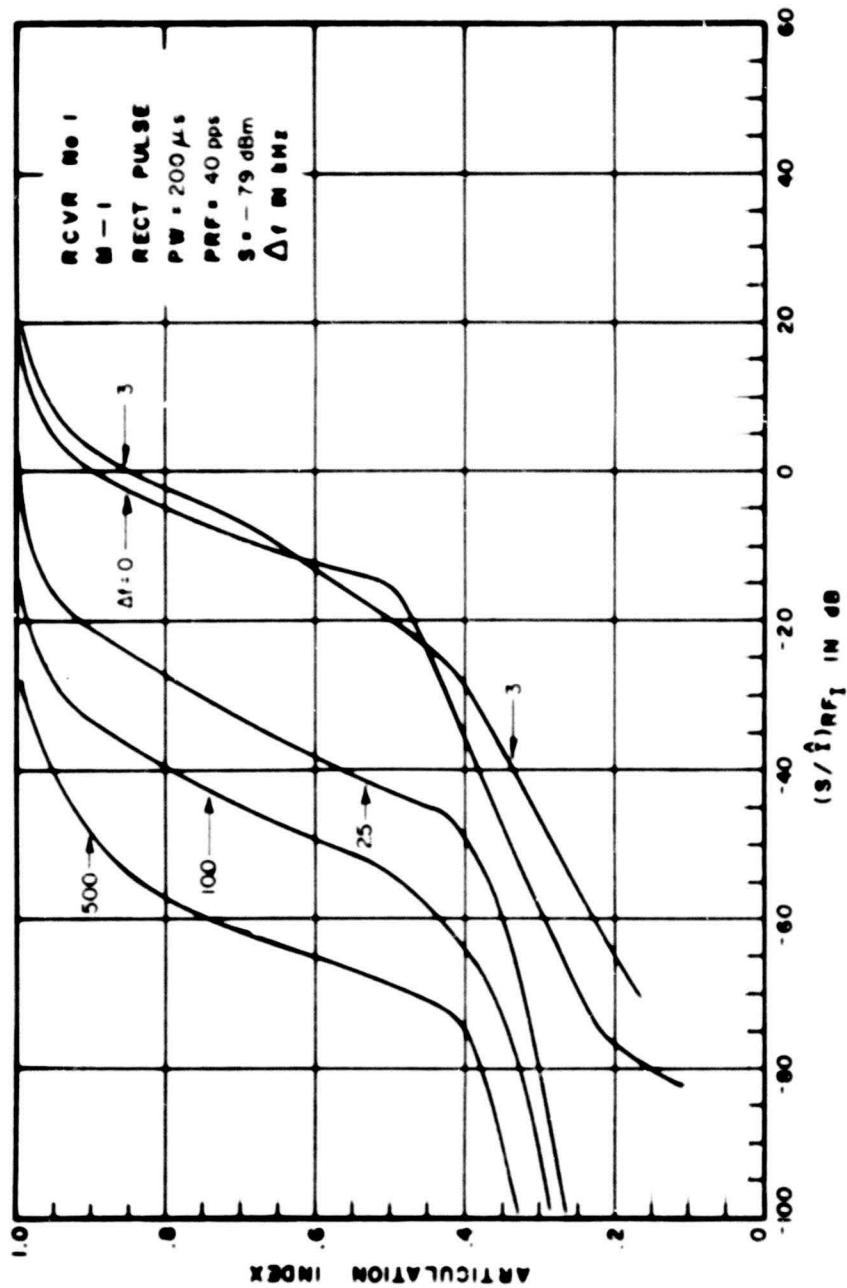


Figure III-56. Articulation Index for Pulsed Interference to an AM Receiver

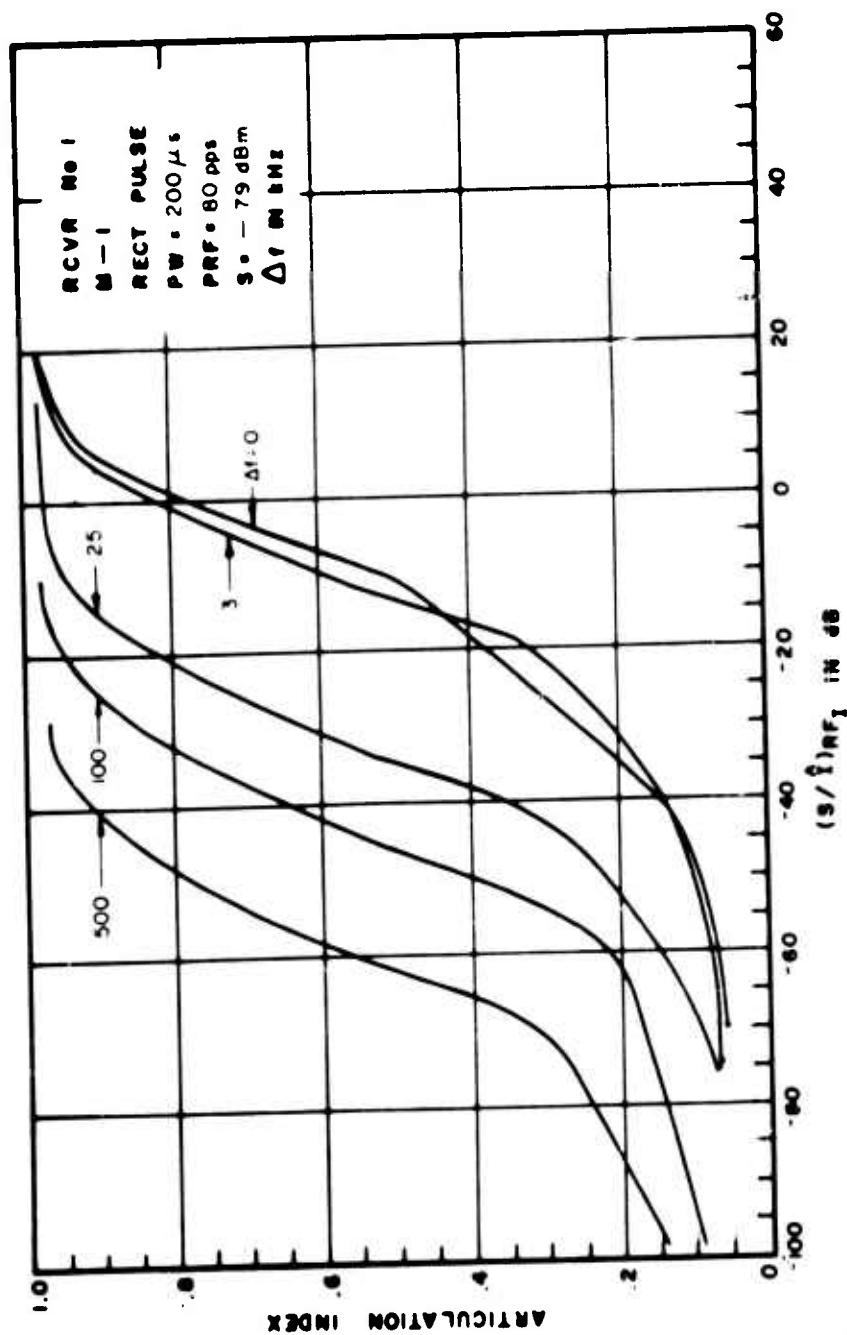


Figure III-57. Articulation Index for Pulsed Interference to an AM Receiver

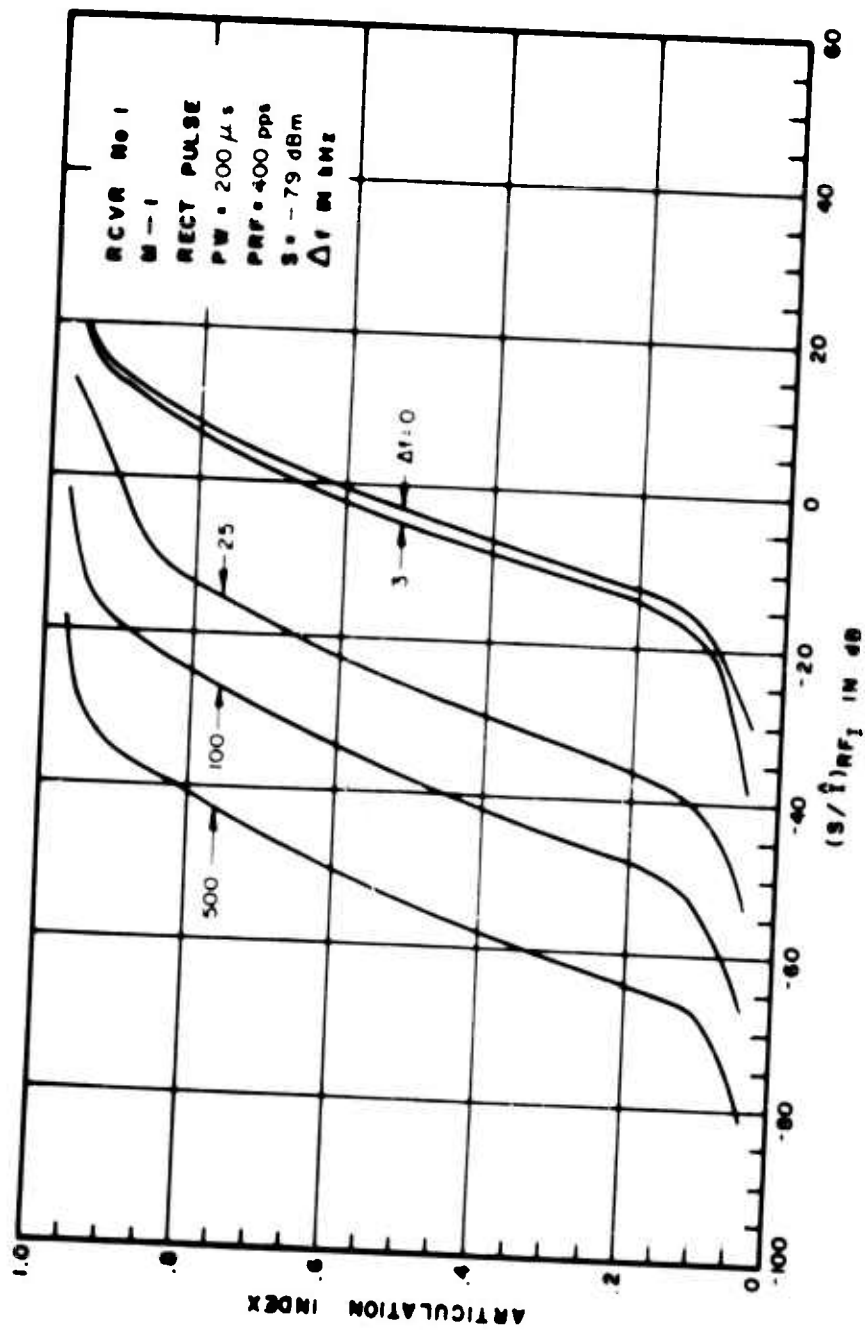


Figure III-58. Articulation Index for Pulsed Interference to an AM Receiver

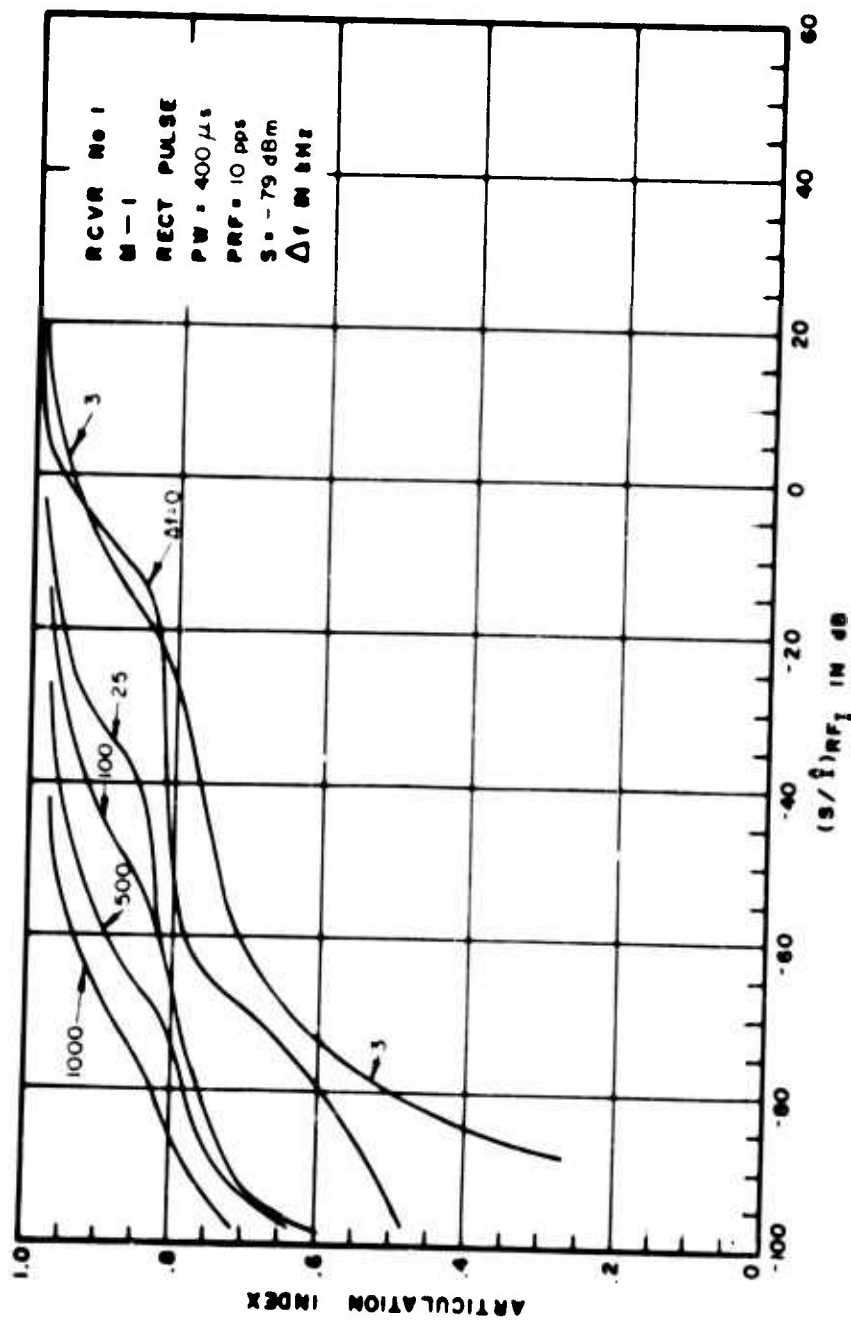


Figure III-59. Articulation Index for Pulsed Interference to an AM Receiver

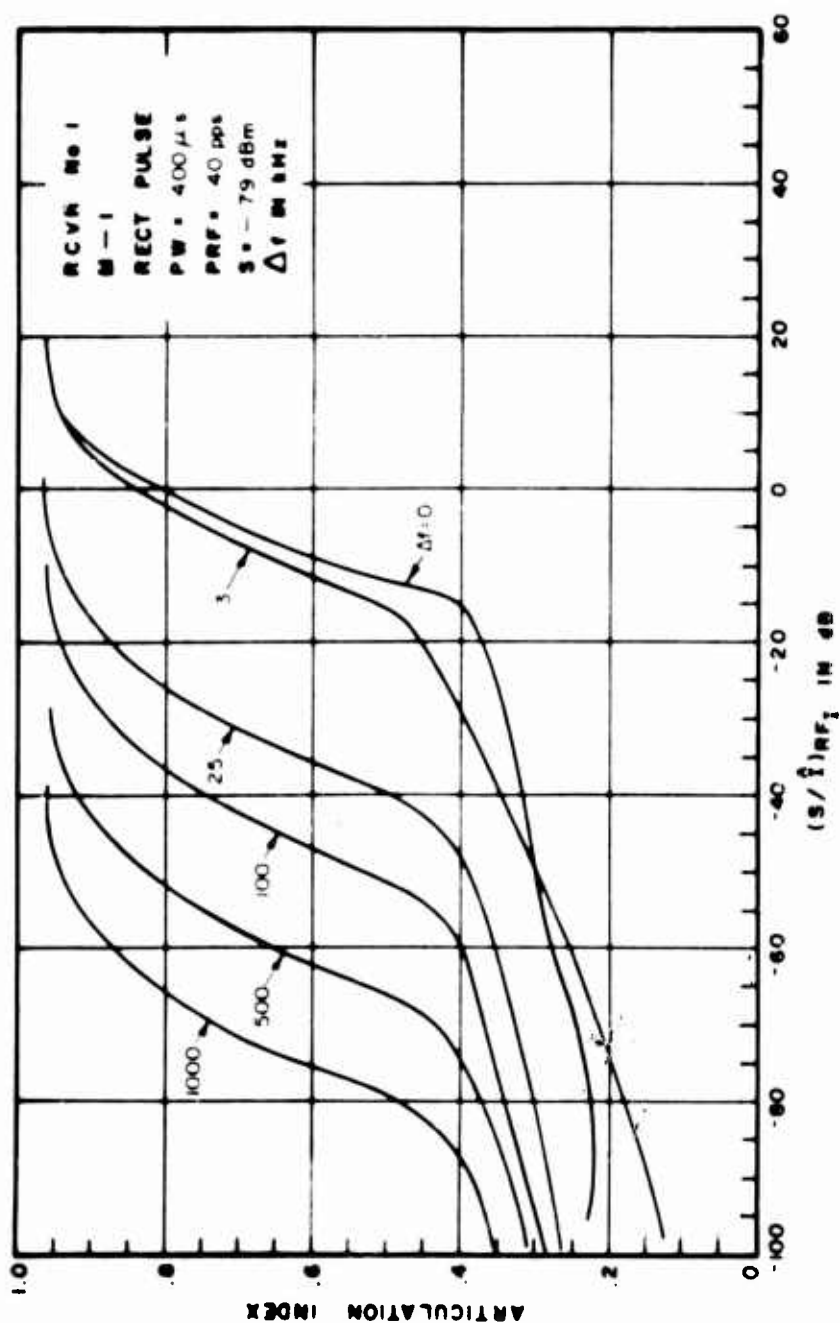


Figure III-60. Articulation Index for Pulsed Interference to an AM Receiver

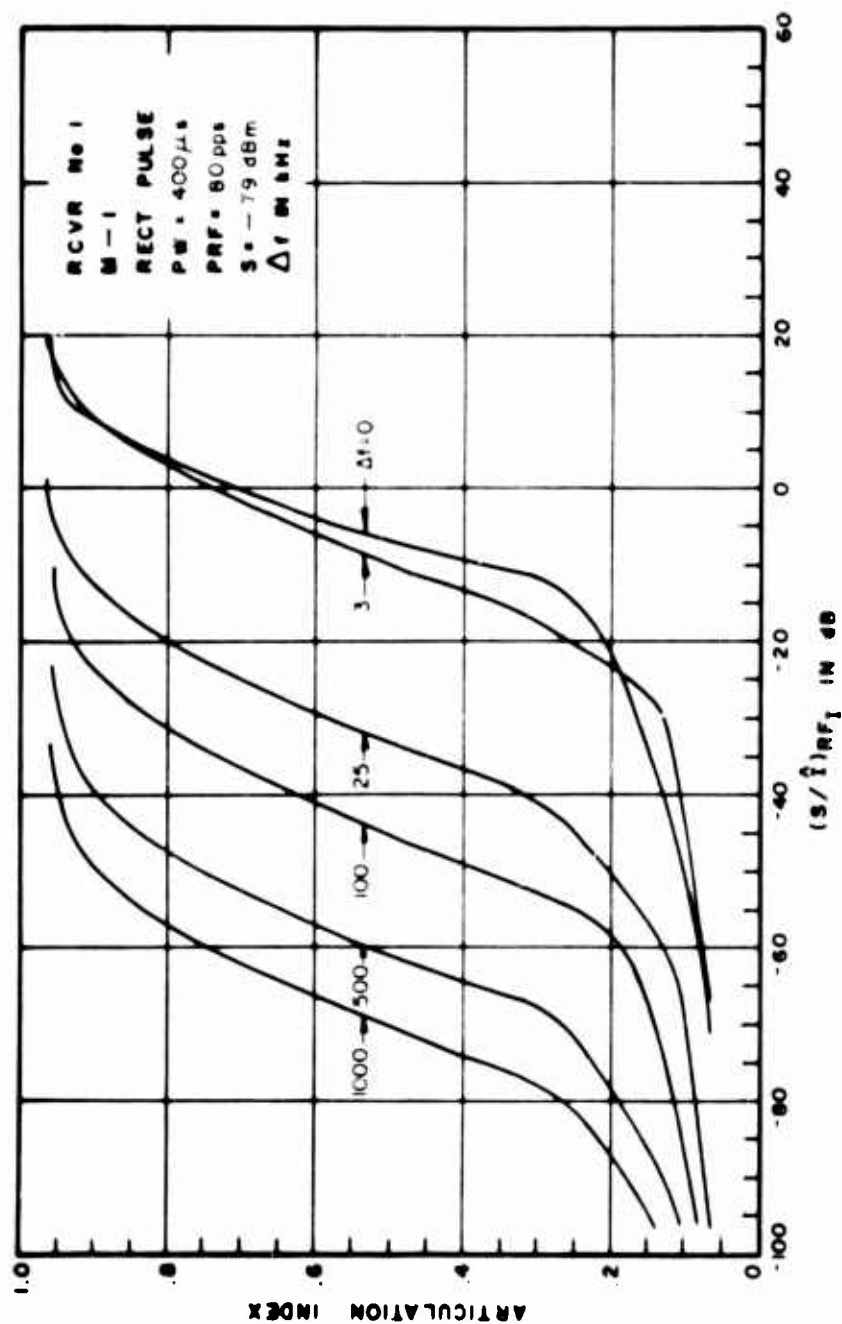


Figure III-61. Articulation Index for Pulsed Interference to an AM Receiver

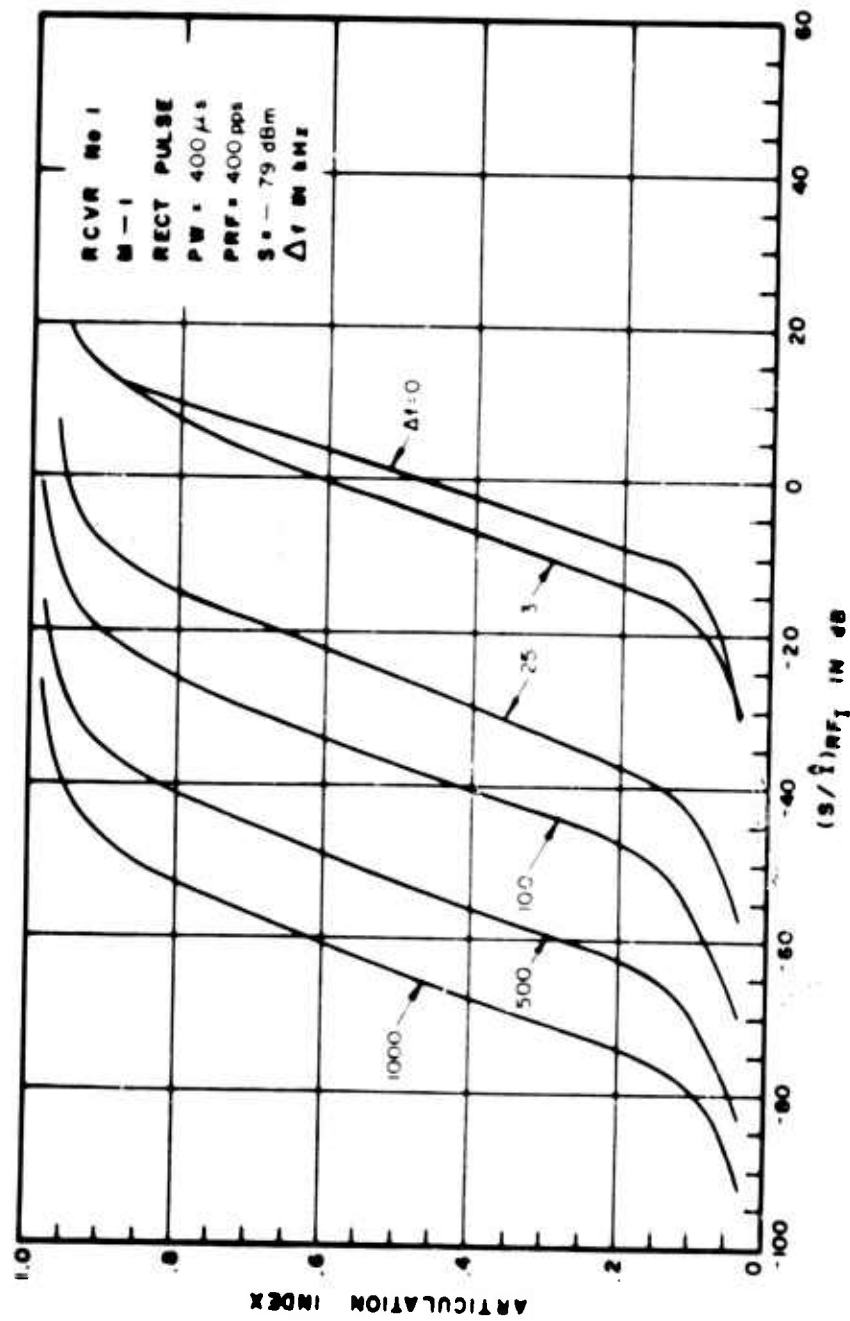


Figure III-62. Articulation Index for Pulsed Interference to an AM Receiver

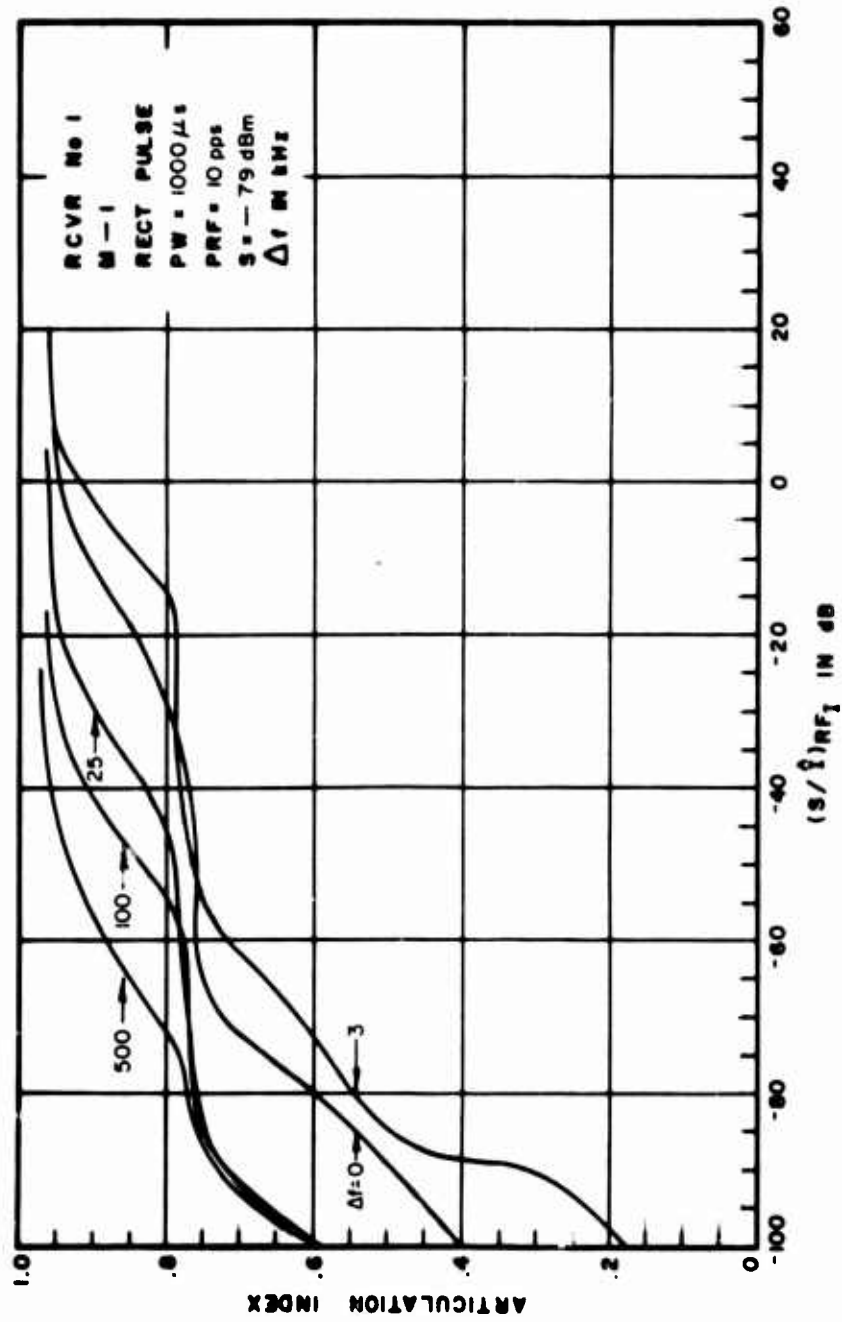


Figure III-63. Articulation Index for Pulsed Interference to an AM Receiver

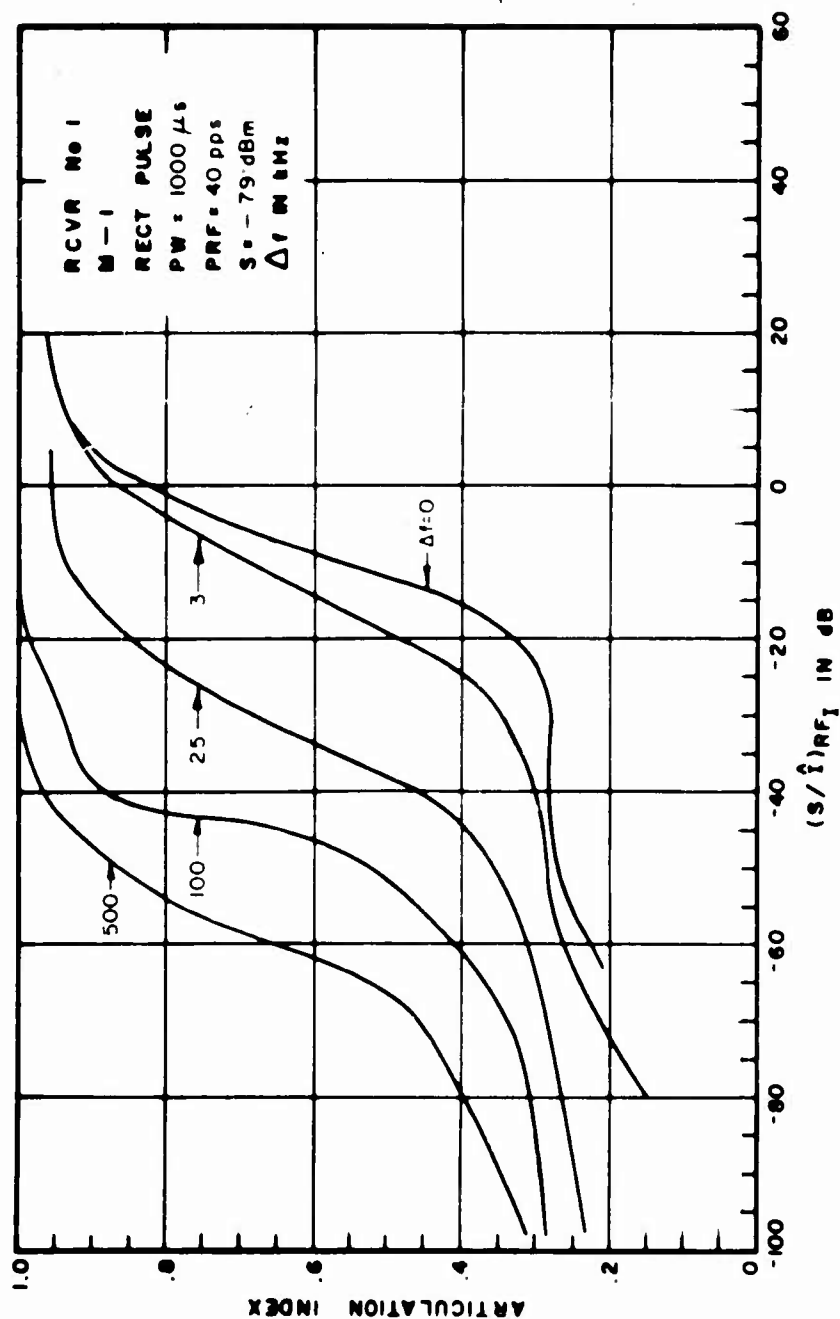


Figure III-64. Articulation Index for Pulsed Interference to an AM Receiver

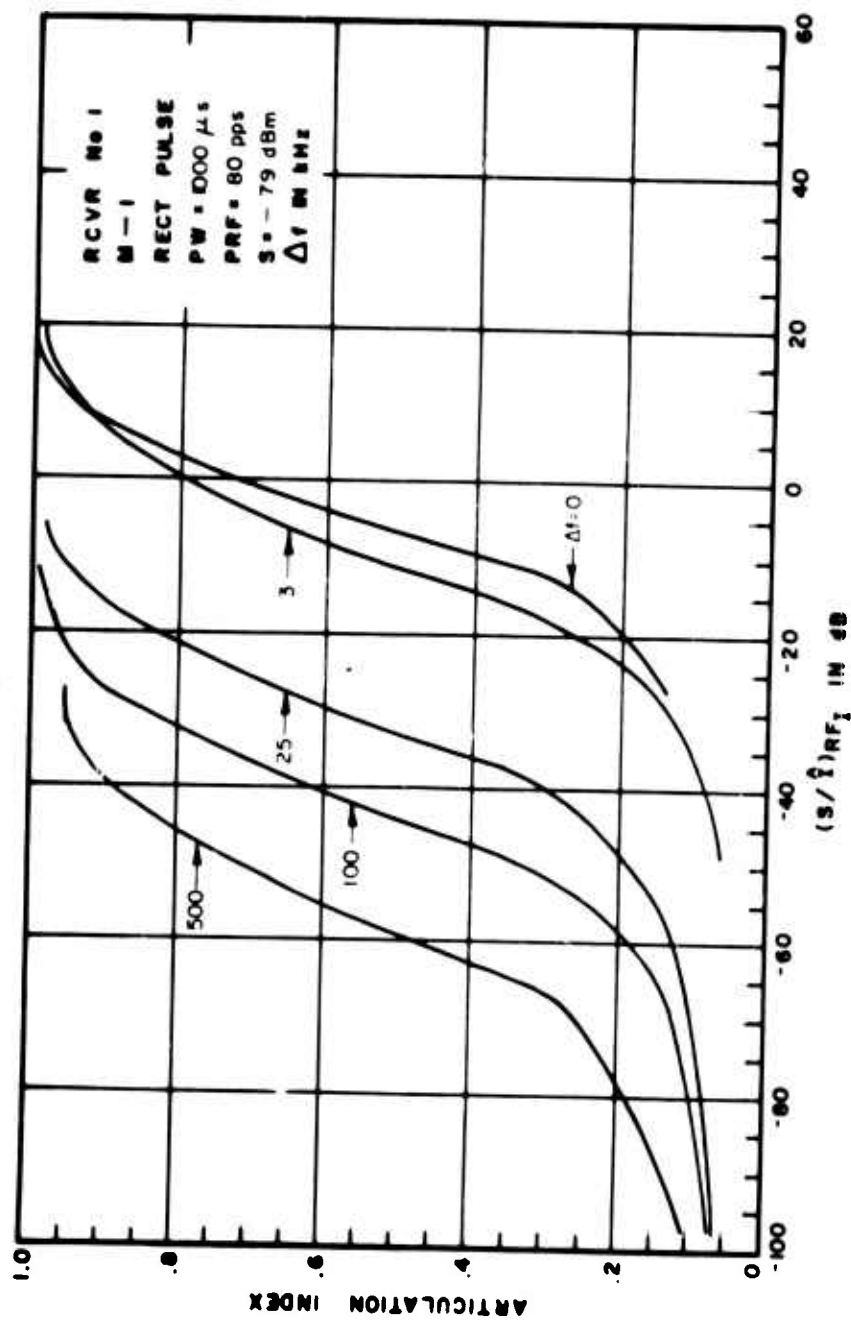


Figure III-65. Articulation Index for Pulsed Interference to an AM Receiver

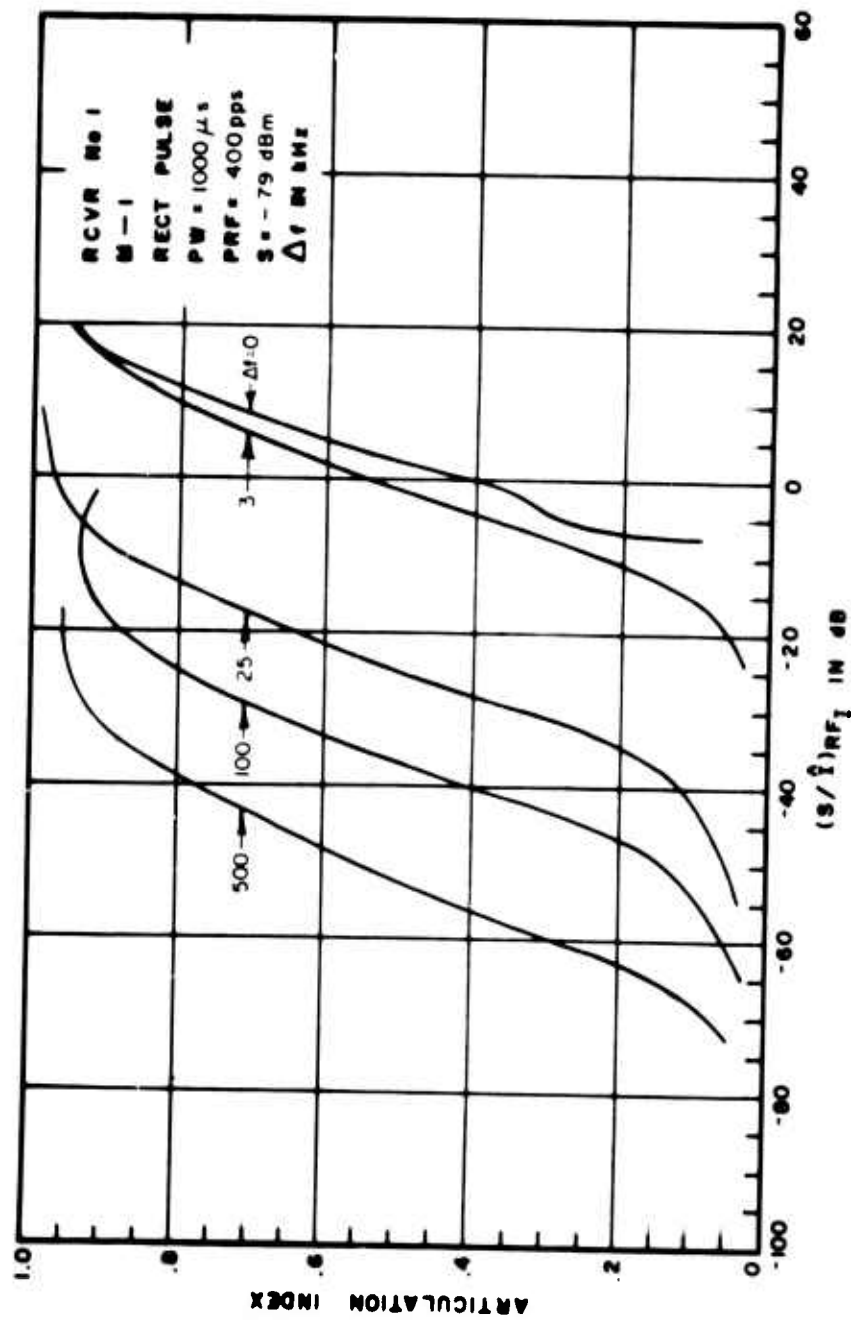


Figure III-66. Articulation Index for Pulsed Interference to an AM Receiver

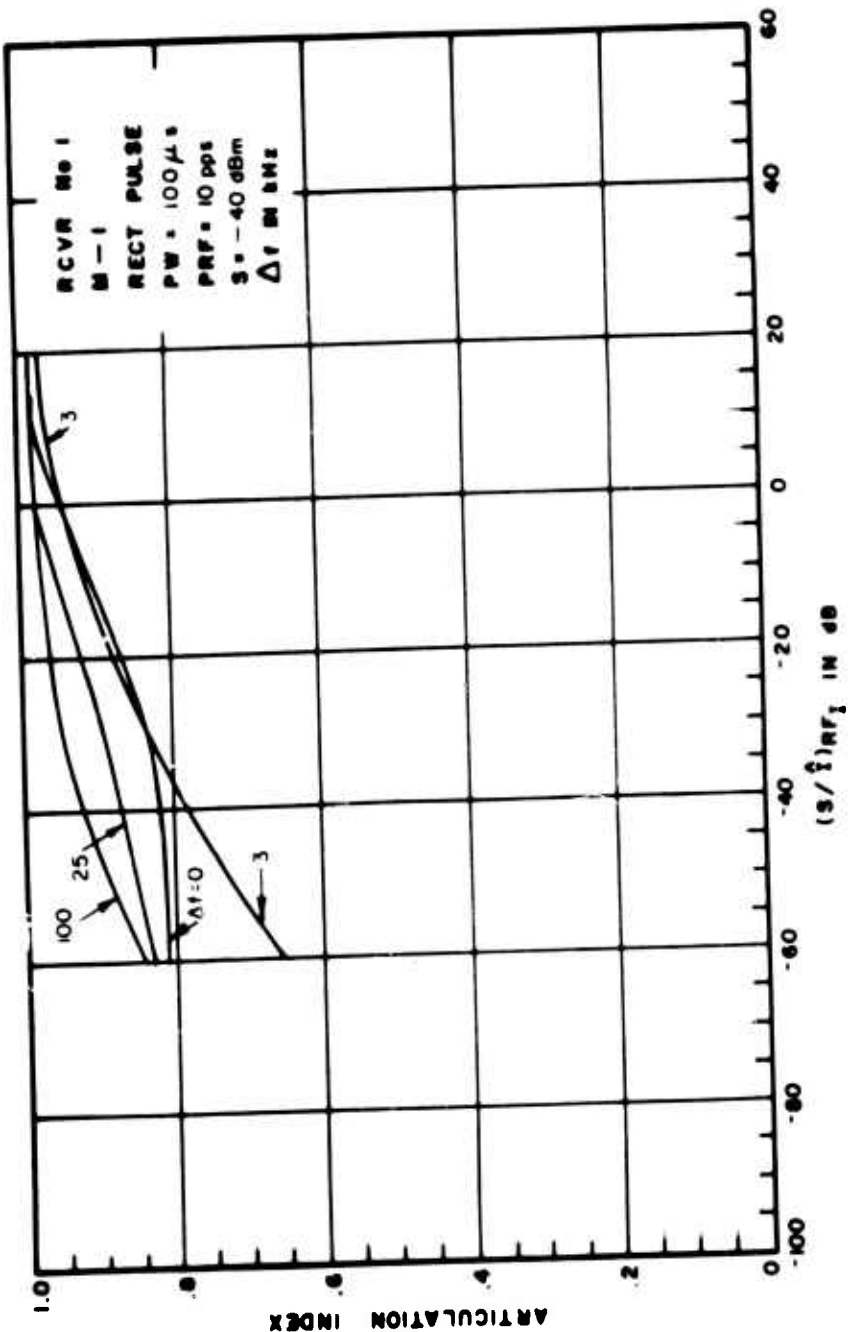


Figure III-67. Articulation Index for Pulsed Interference to an AM Receiver

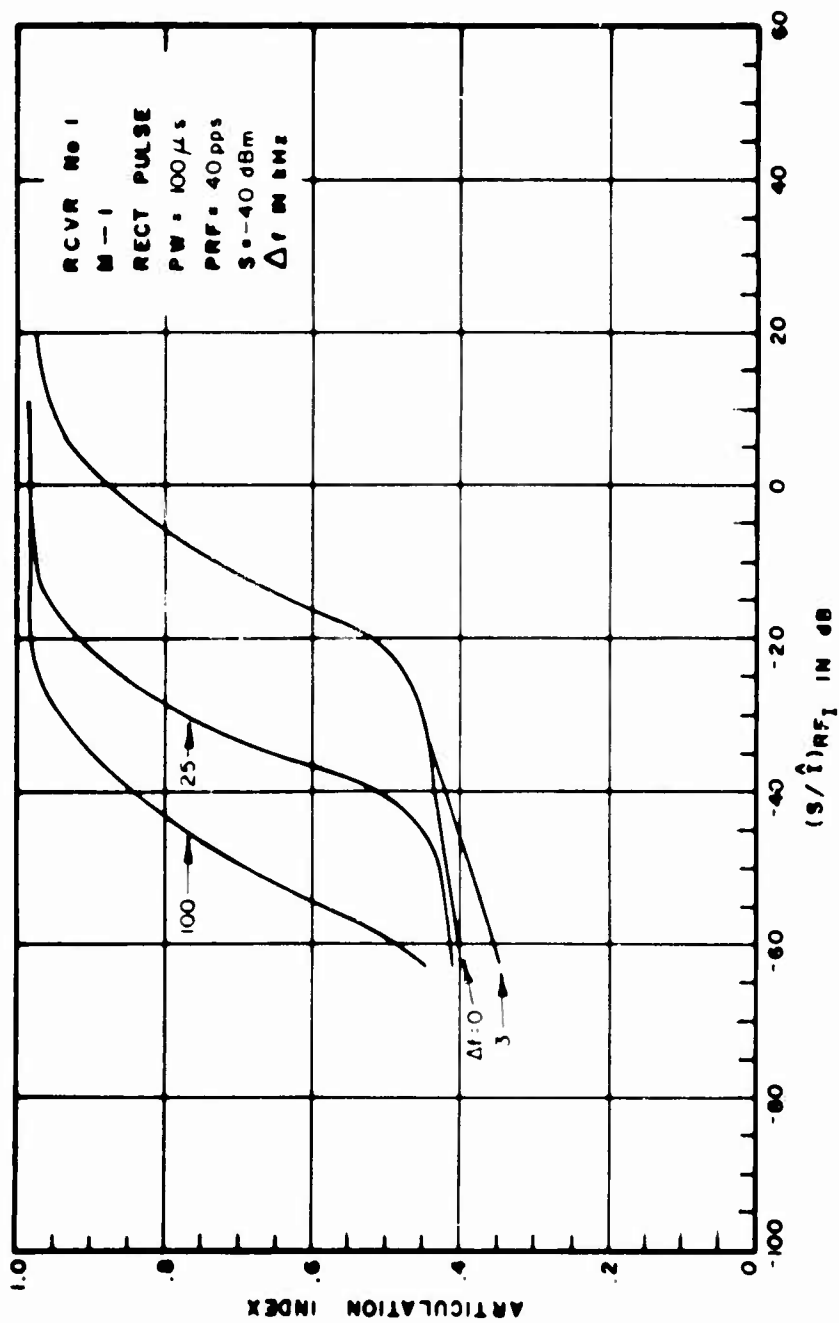


Figure III-68. Articulation Index for Pulsed Interference to an AM Receiver

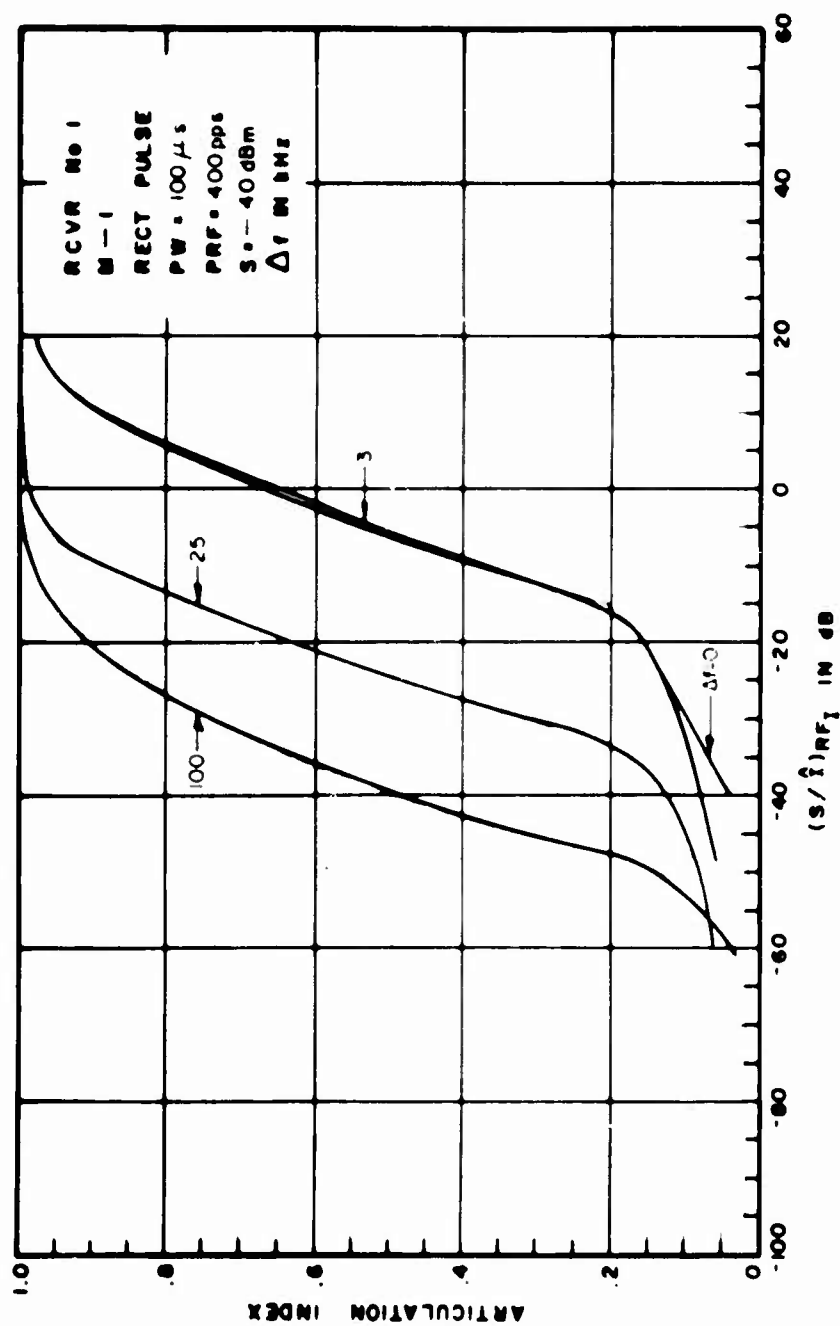


Figure III-69. Articulation Index for Pulsed Interference to an AM Receiver

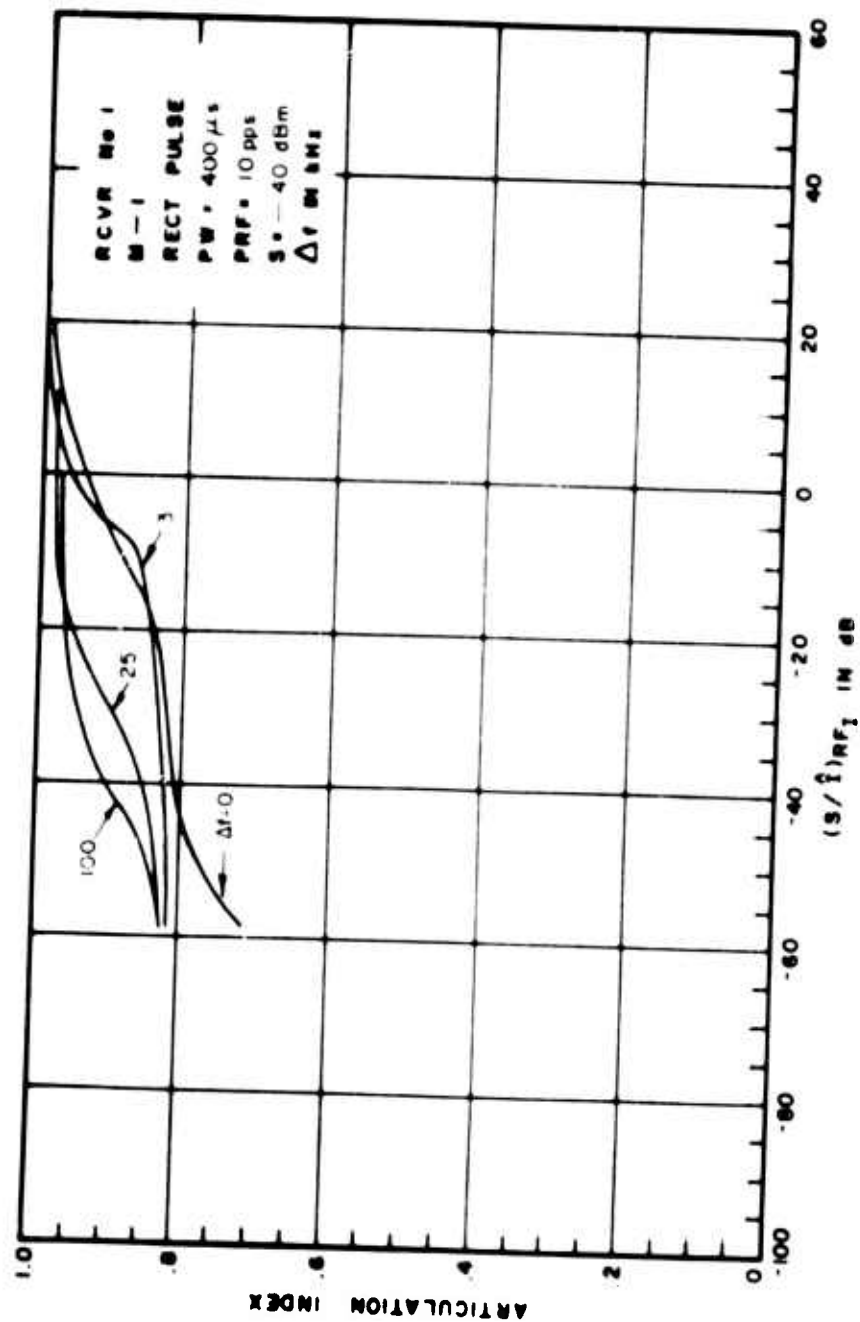


Figure III 70. Articulation Index for Pulsed Interference to an AM Receiver

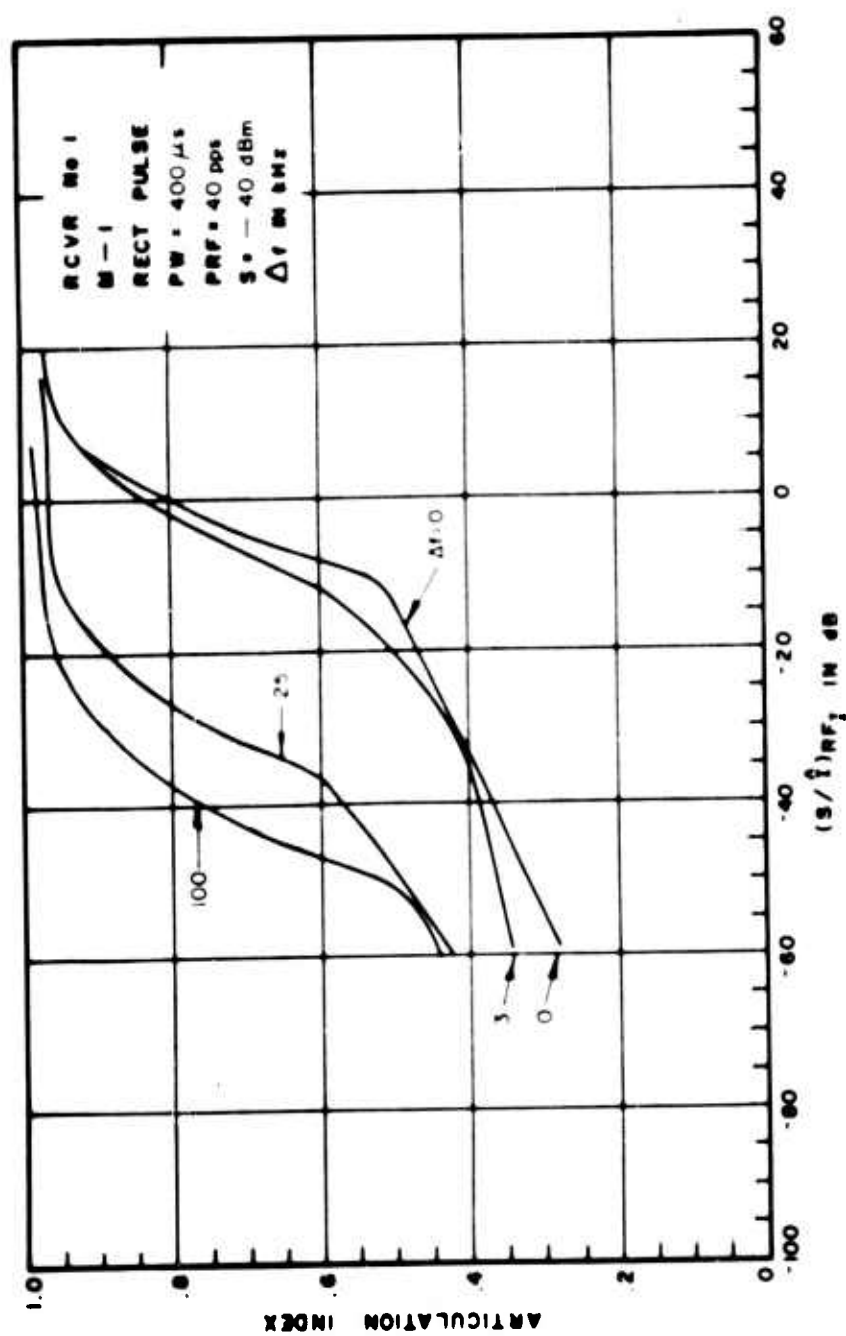


Figure III-71. Articulation Index for Pulsed Interference to an AM Receiver

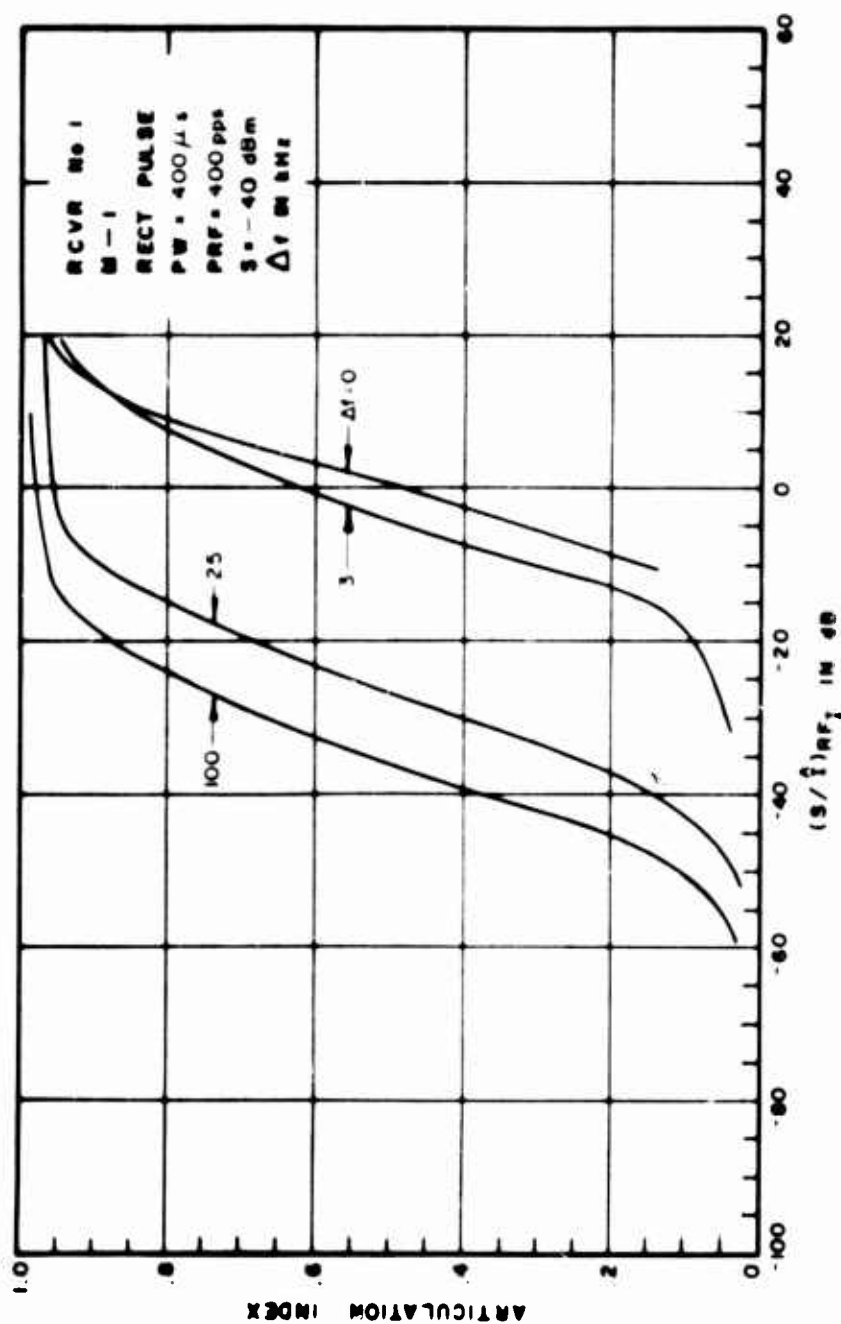


Figure III-72. Articulation Index for Pulsed Interference to an AM Receiver

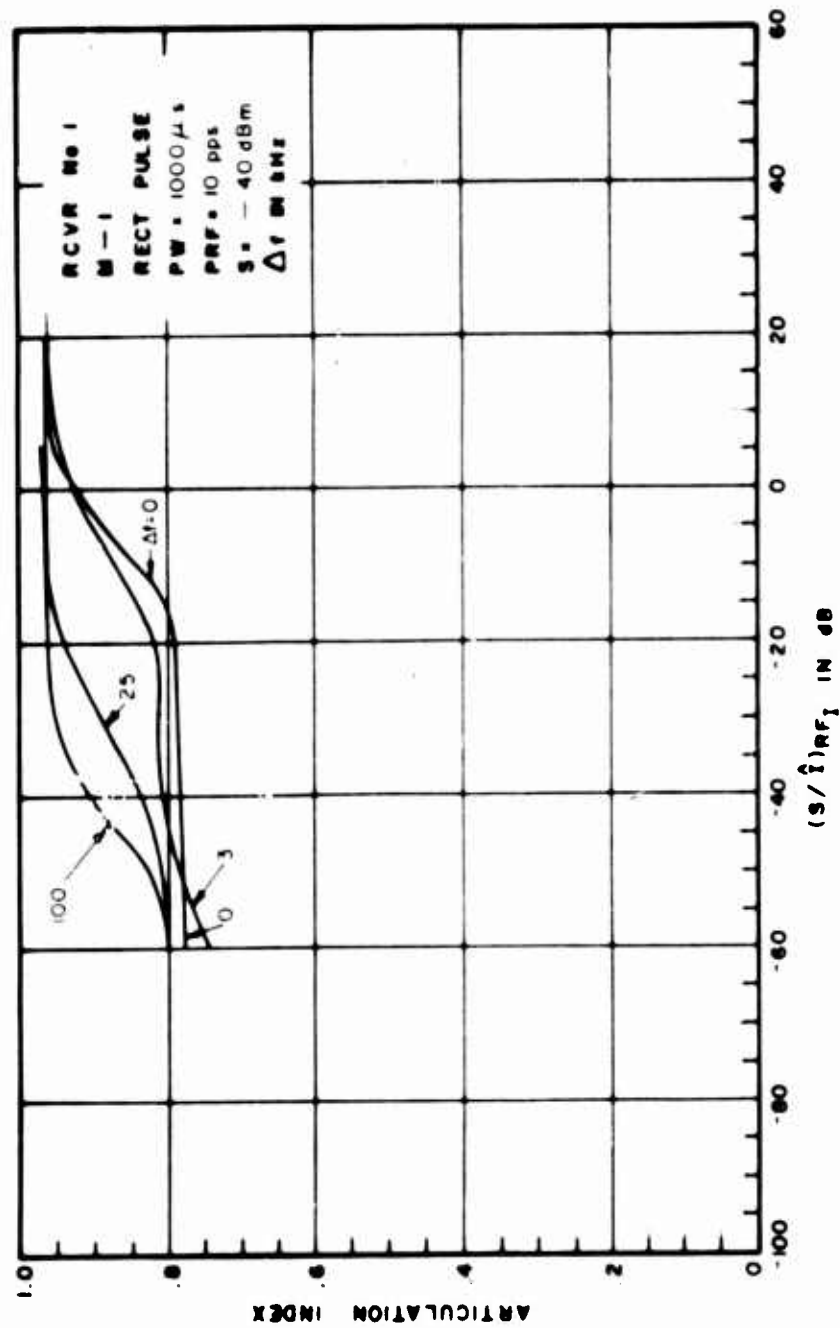


Figure III-73. Articulation Index for Pulsed Interference to an AM Receiver

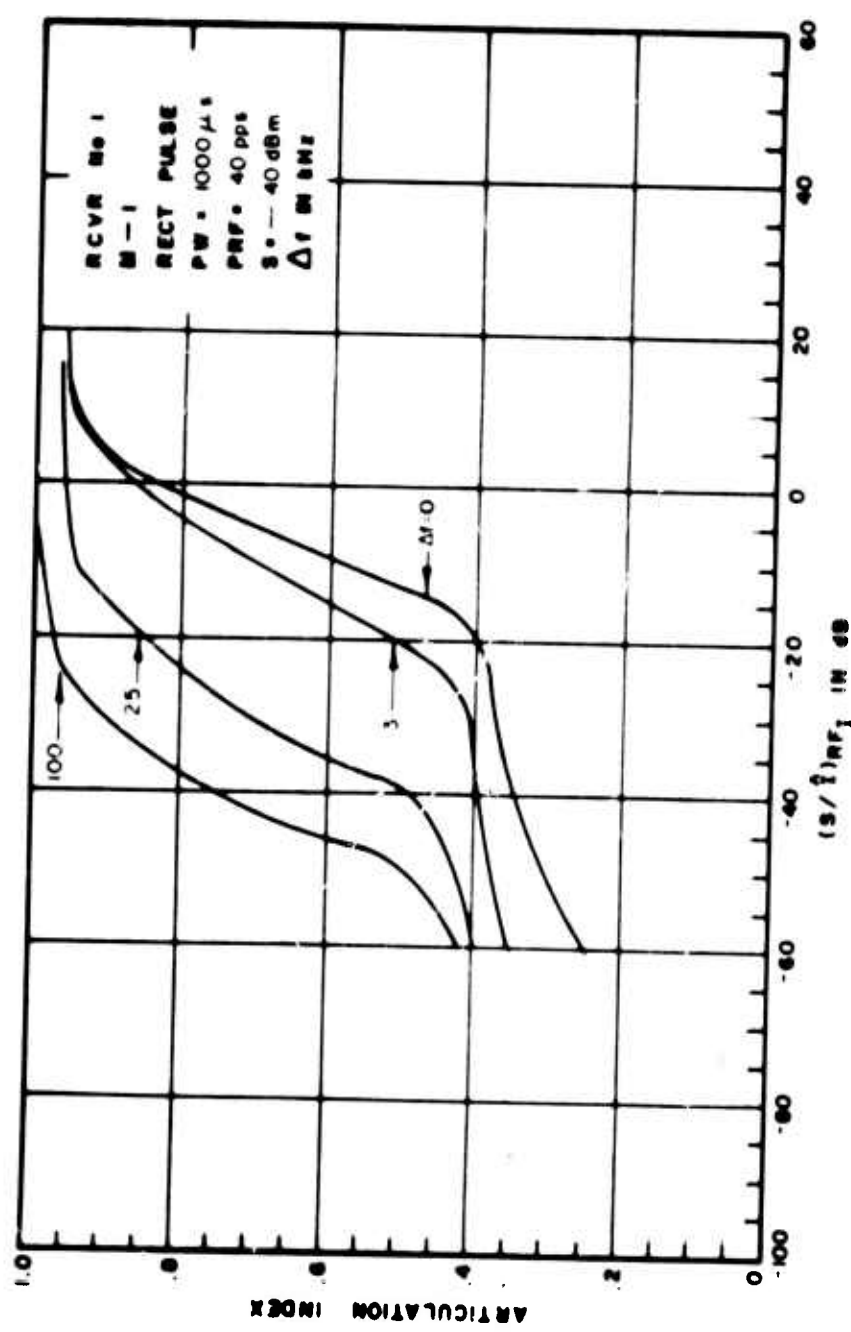


Figure III-74. Articulation Index for Pulsed Interference to an AM Receiver

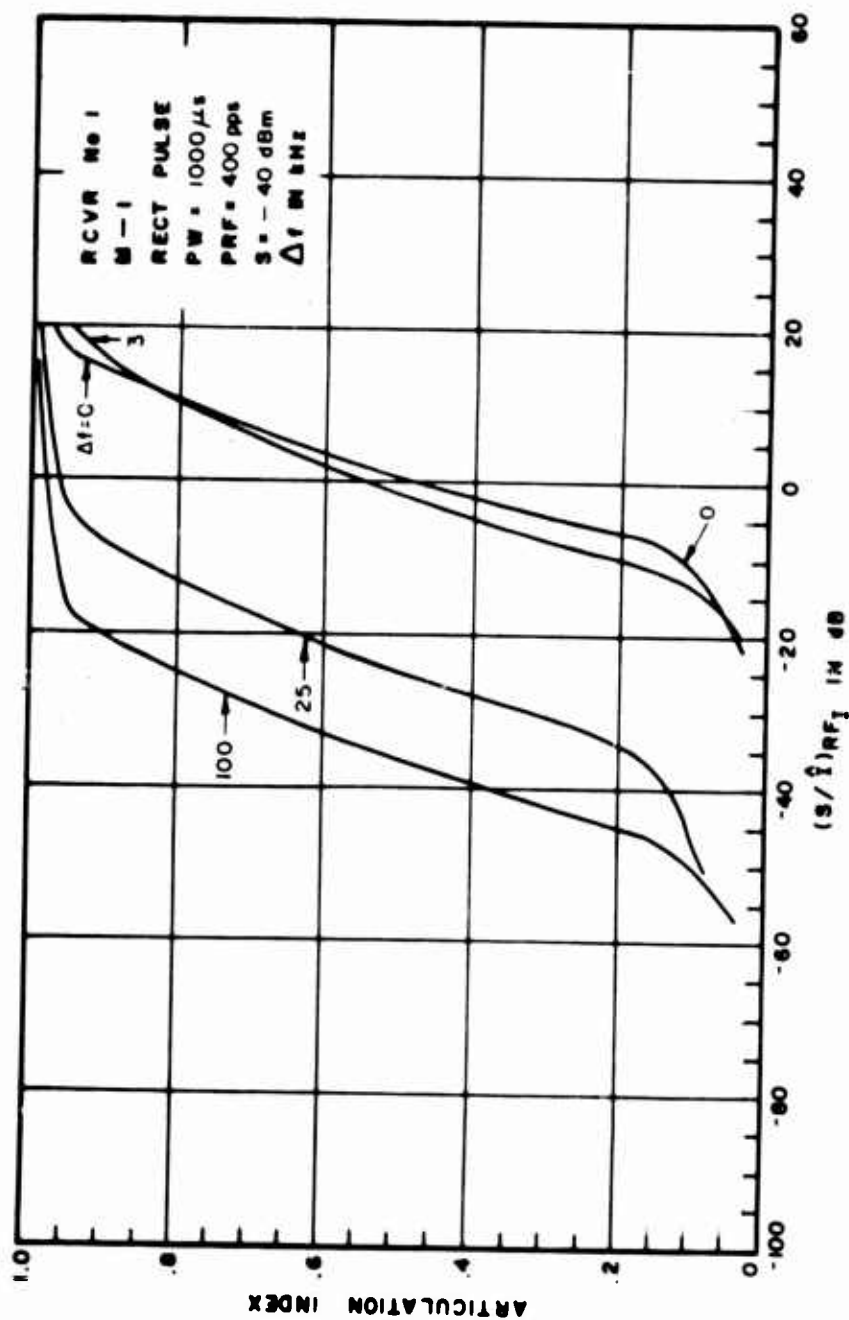


Figure III-75. Articulation Index for Pulsed Interference to an AM Receiver

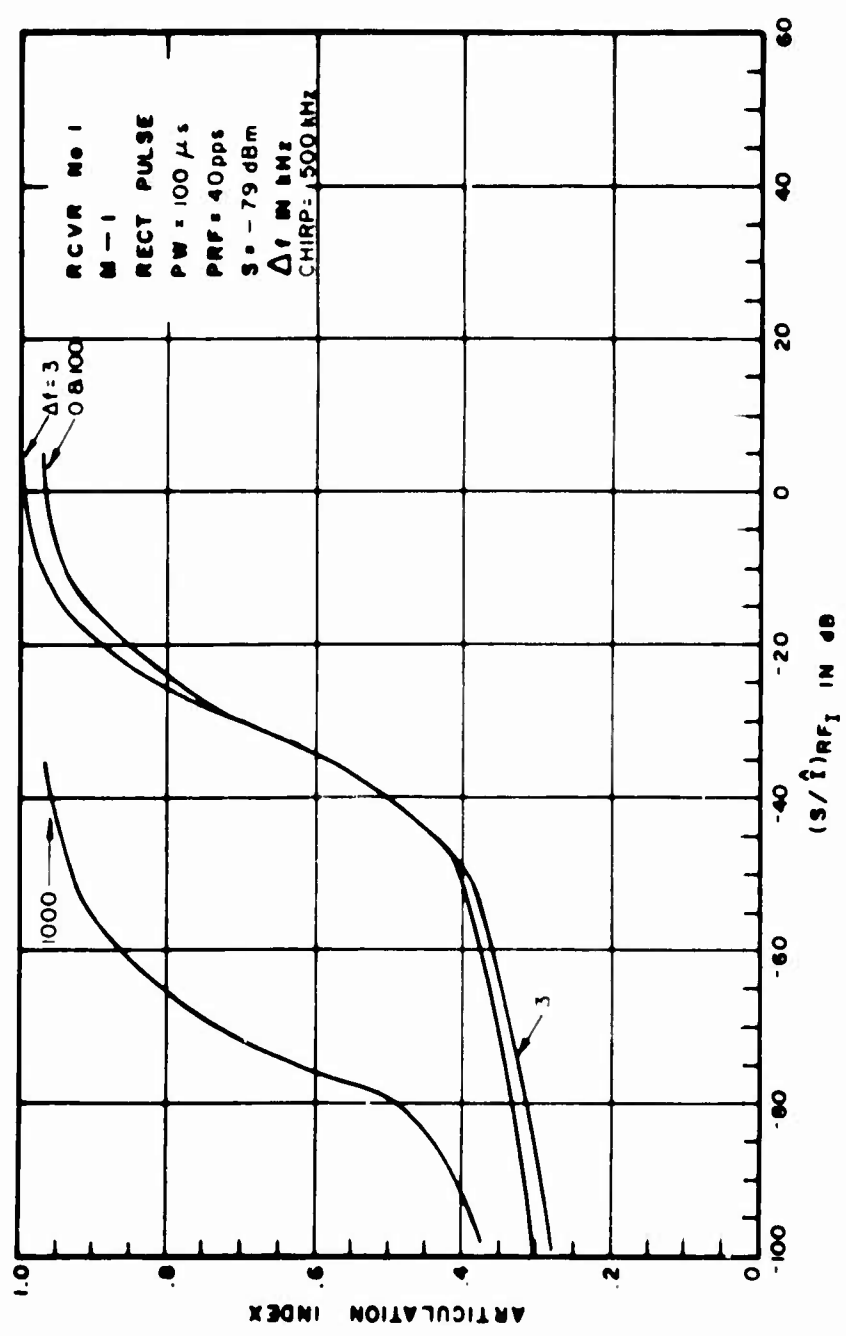


Figure III-76. Articulation Index for Pulsed Interference to an AM Receiver

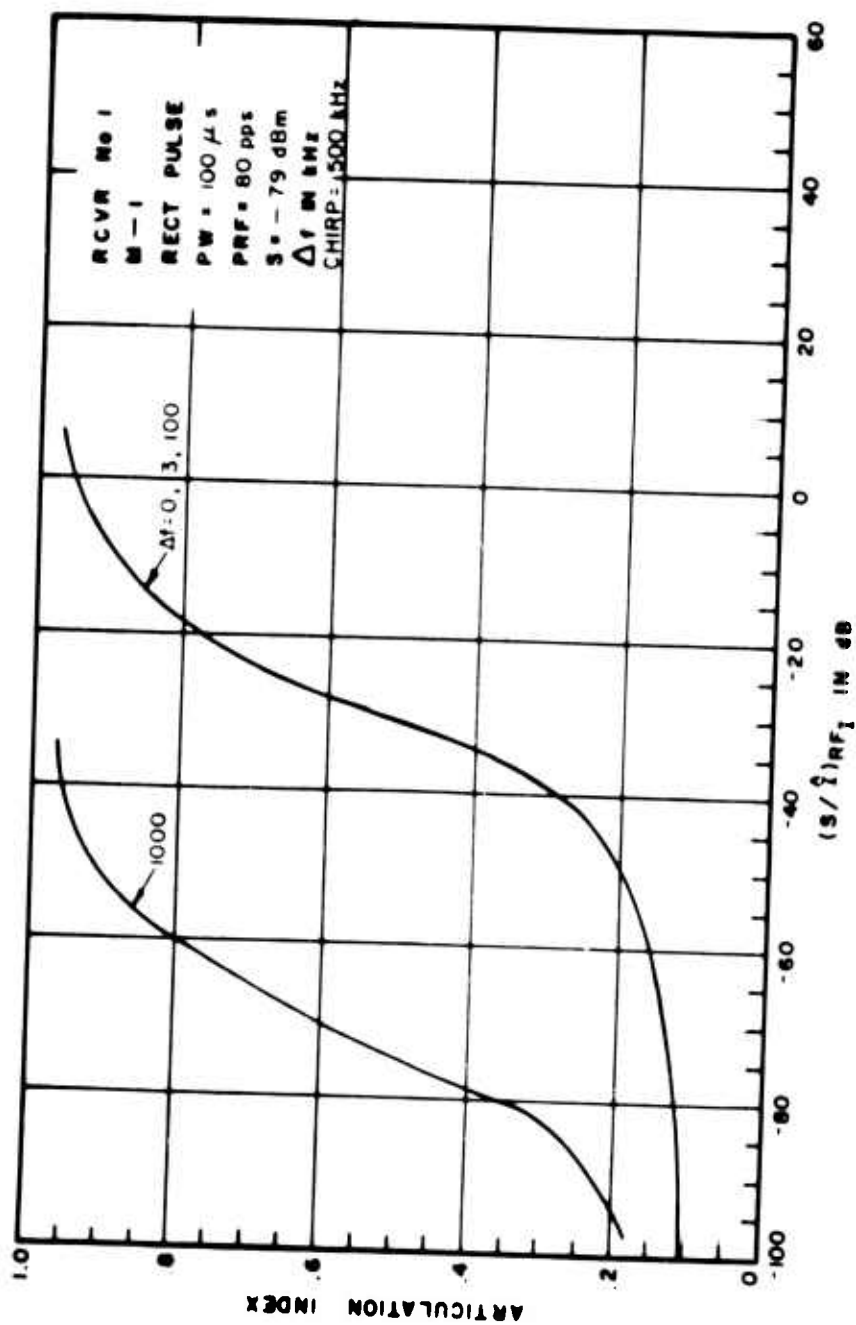


Figure III-77. Articulation Index for Pulsed Interference to an AM Receiver

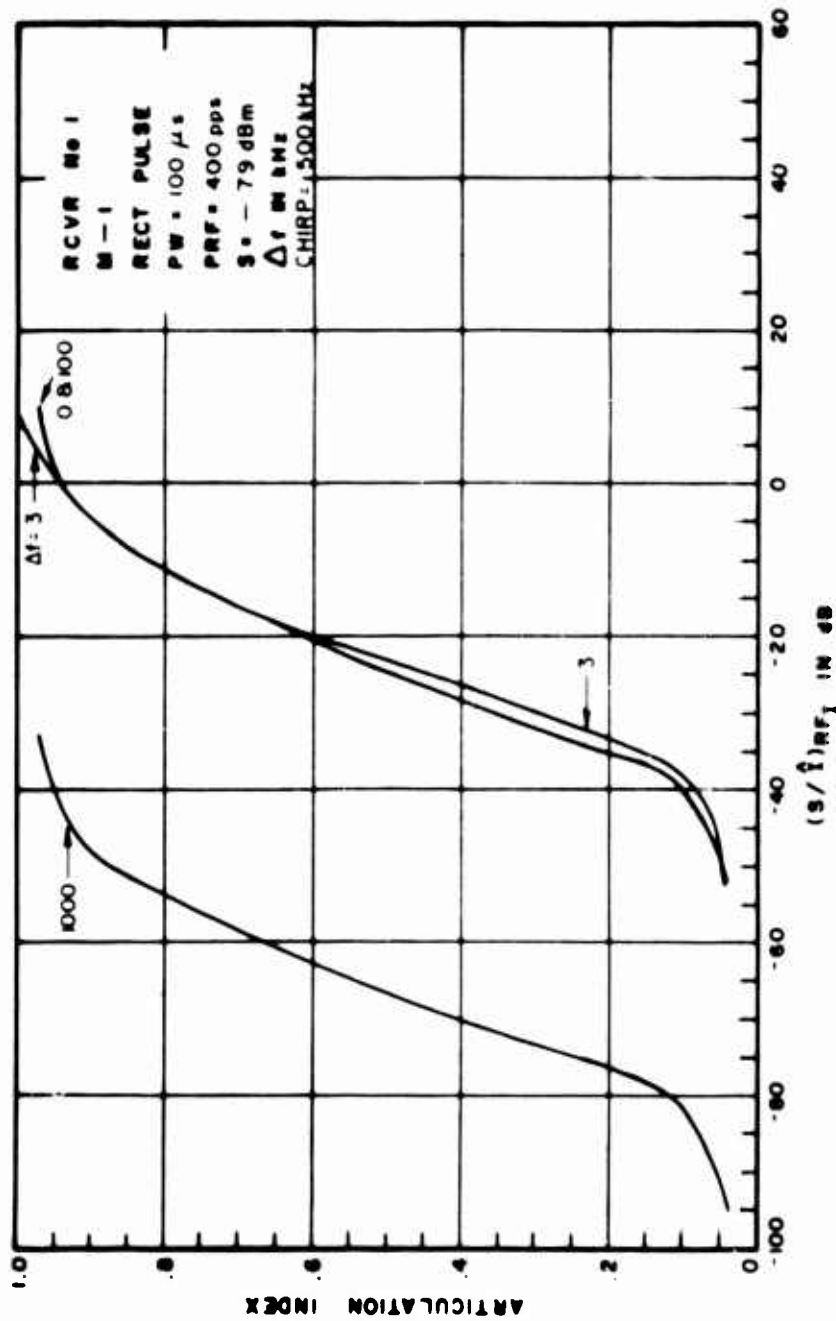


Figure III-78. Articulation Index for Pulsed Interference to an AM Receiver

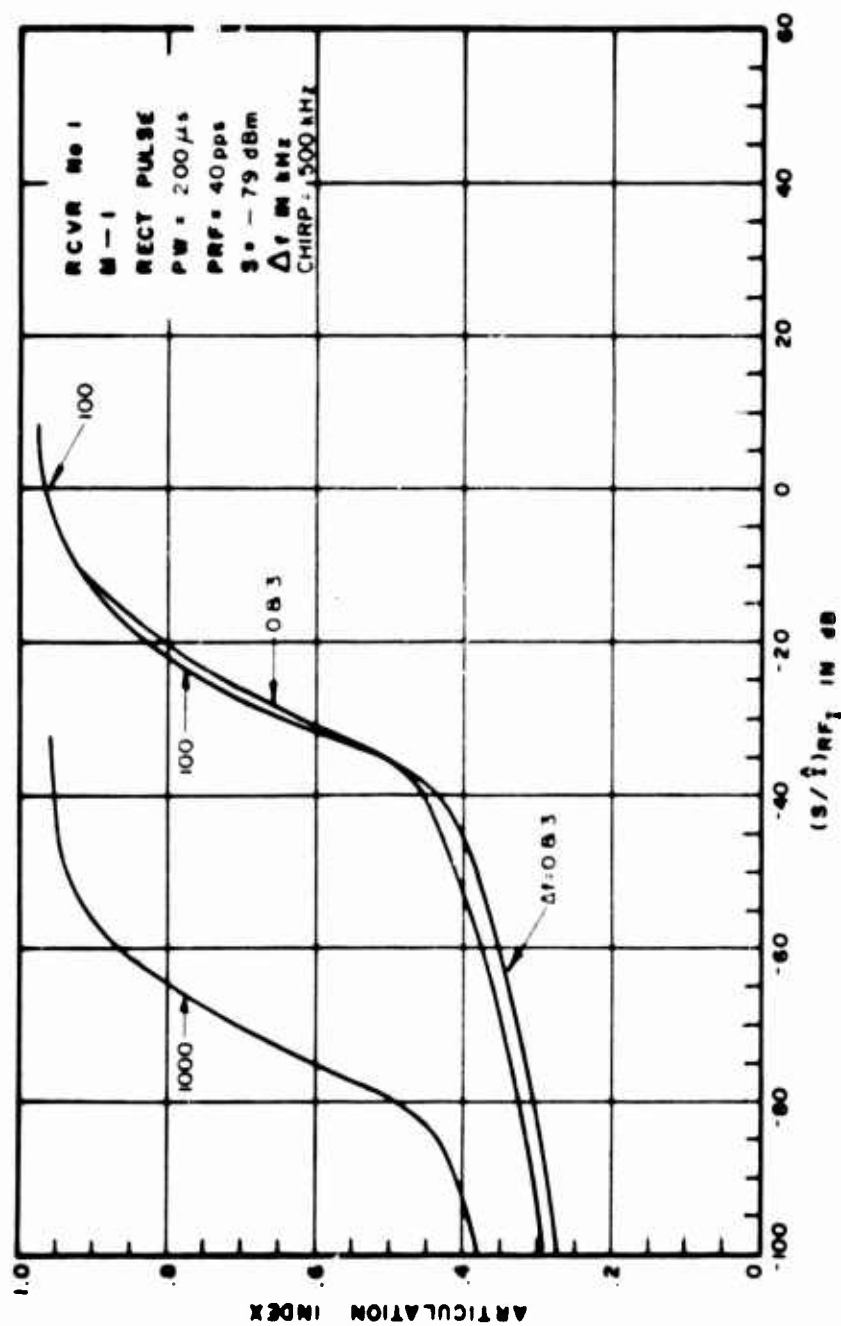


Figure III-79. Articulation Index for Pulsed Interference to an AM Receiver

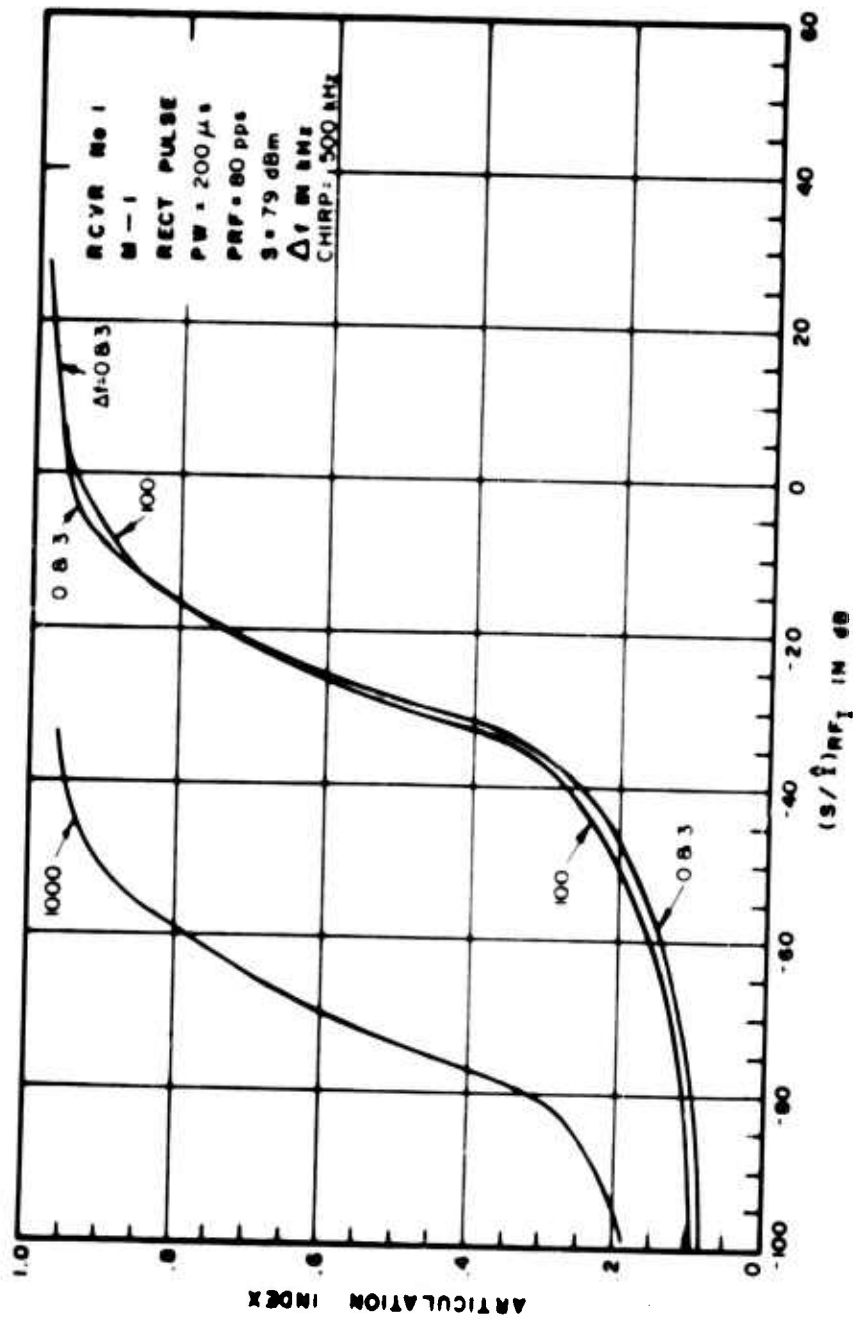


Figure III-80. Articulation Index for Pulsed Interference to an AM Receiver

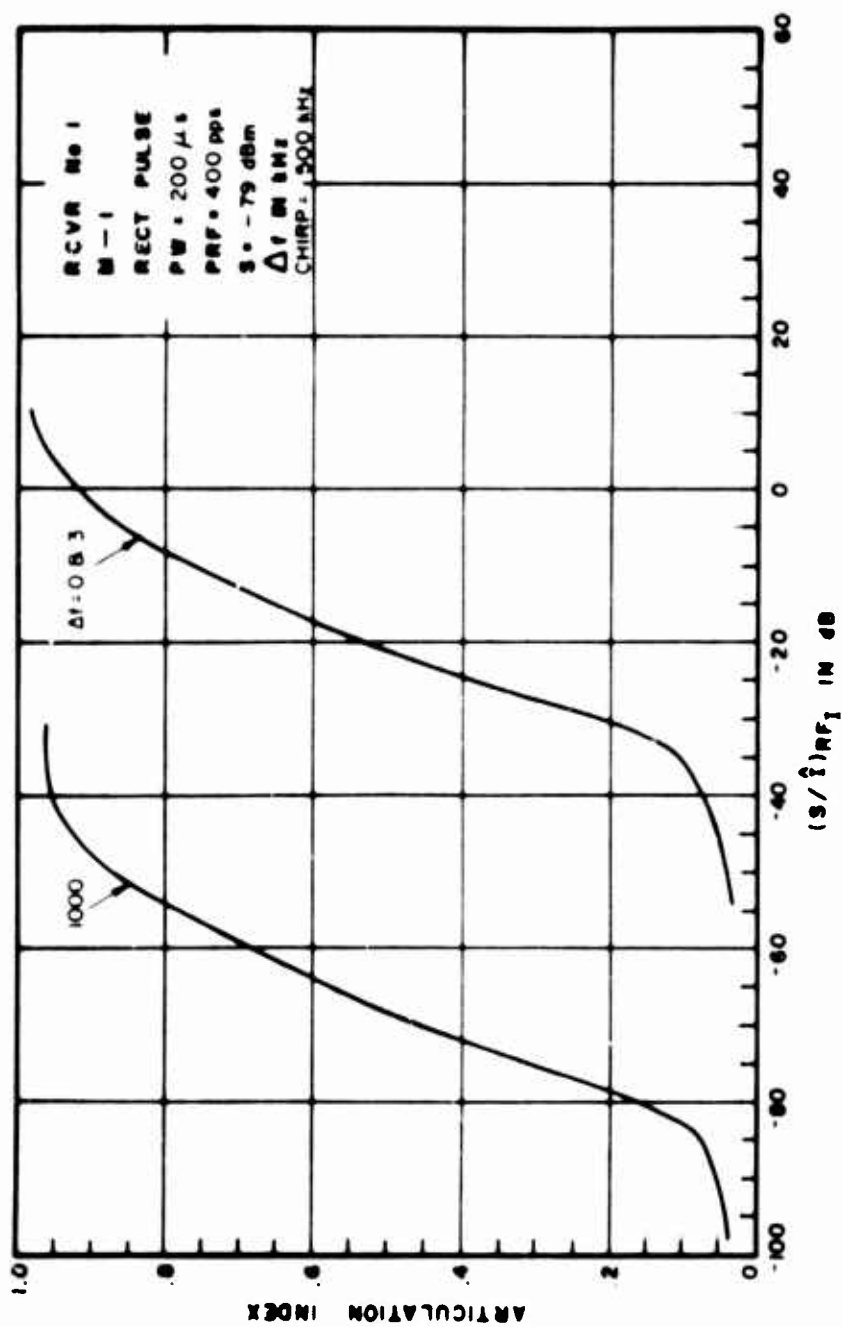


Figure III-81. Articulation Index for Pulsed Interference to an AM Receiver

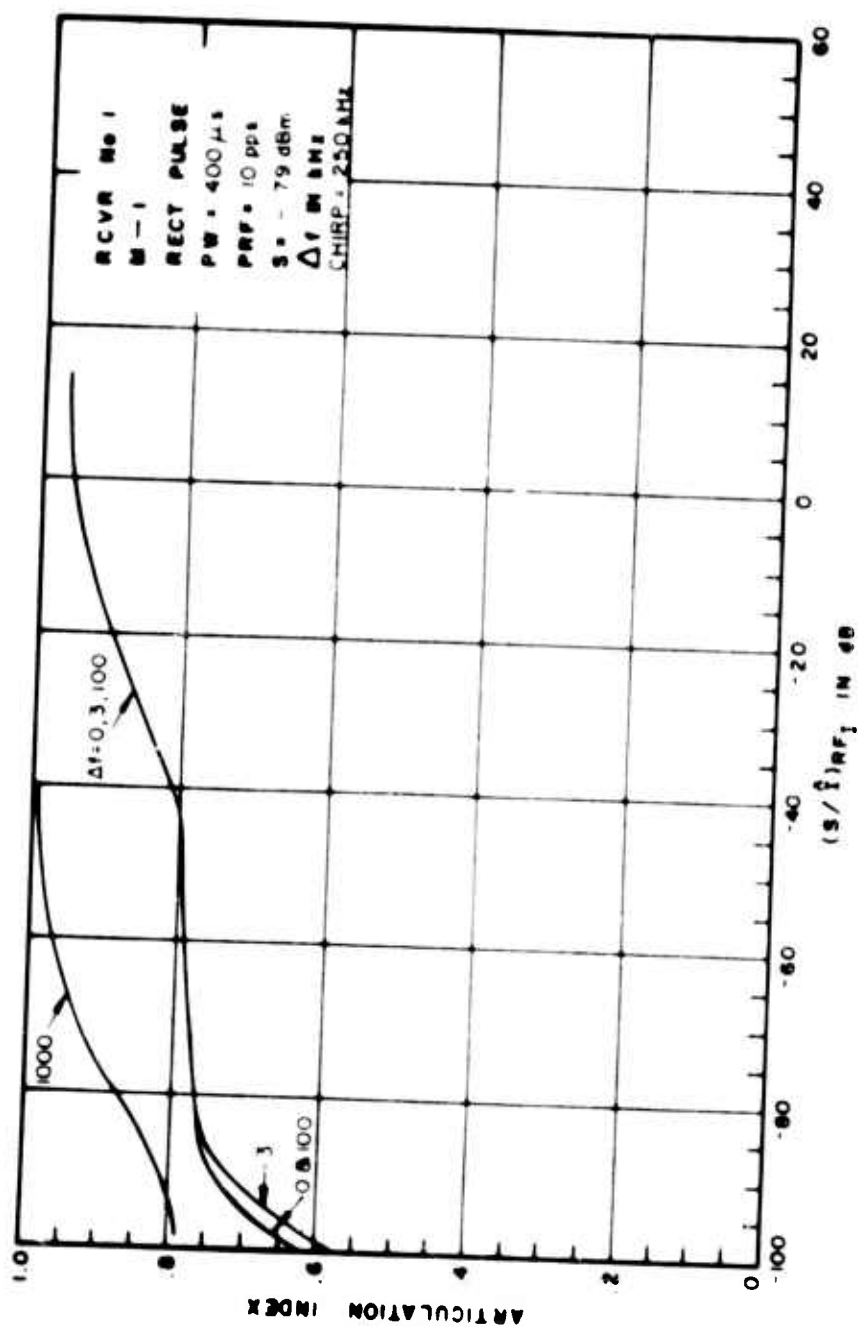


Figure III-82. Articulation Index for Pulsed Interference to an AM Receiver

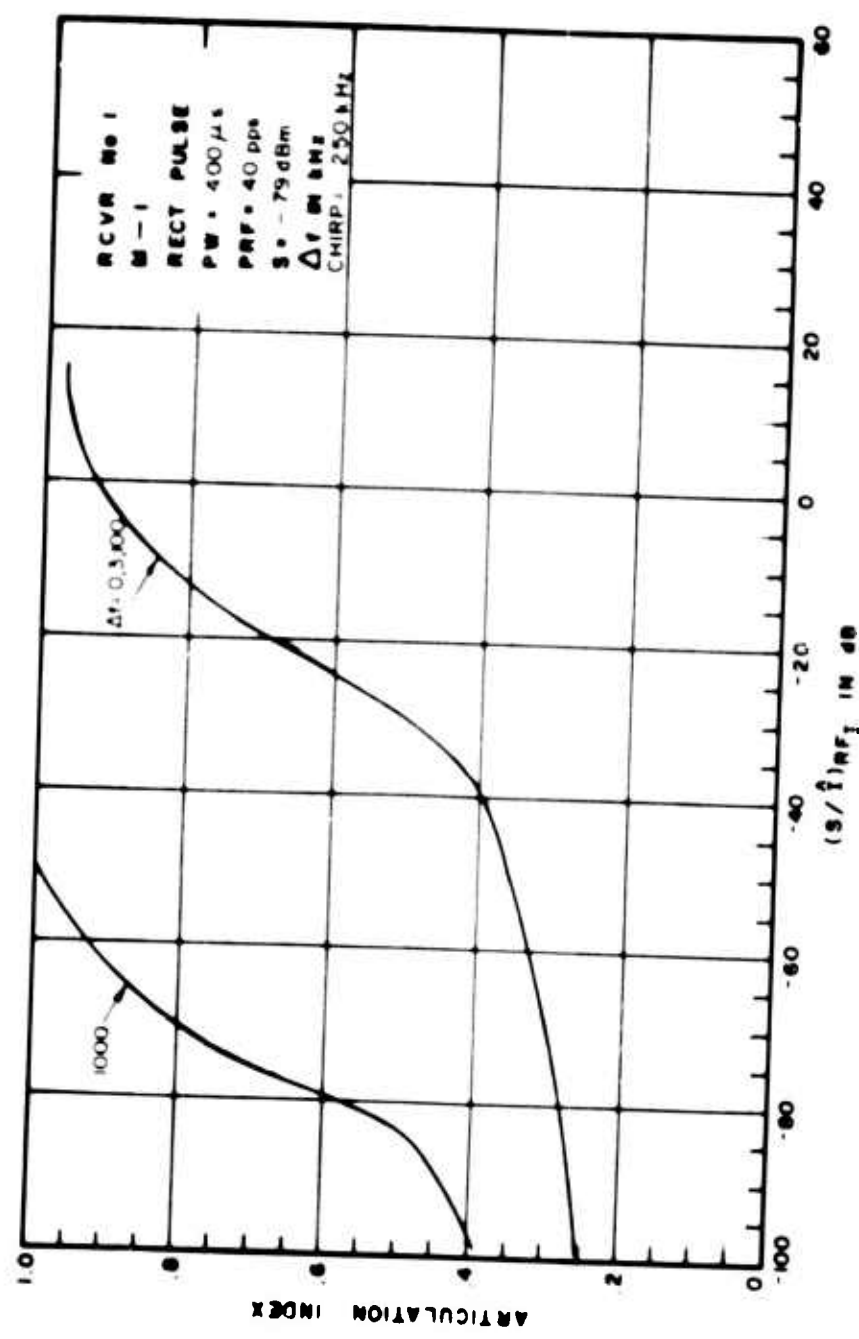


Figure III-83. Articulation Index for Pulsed Interference to an AM Receiver

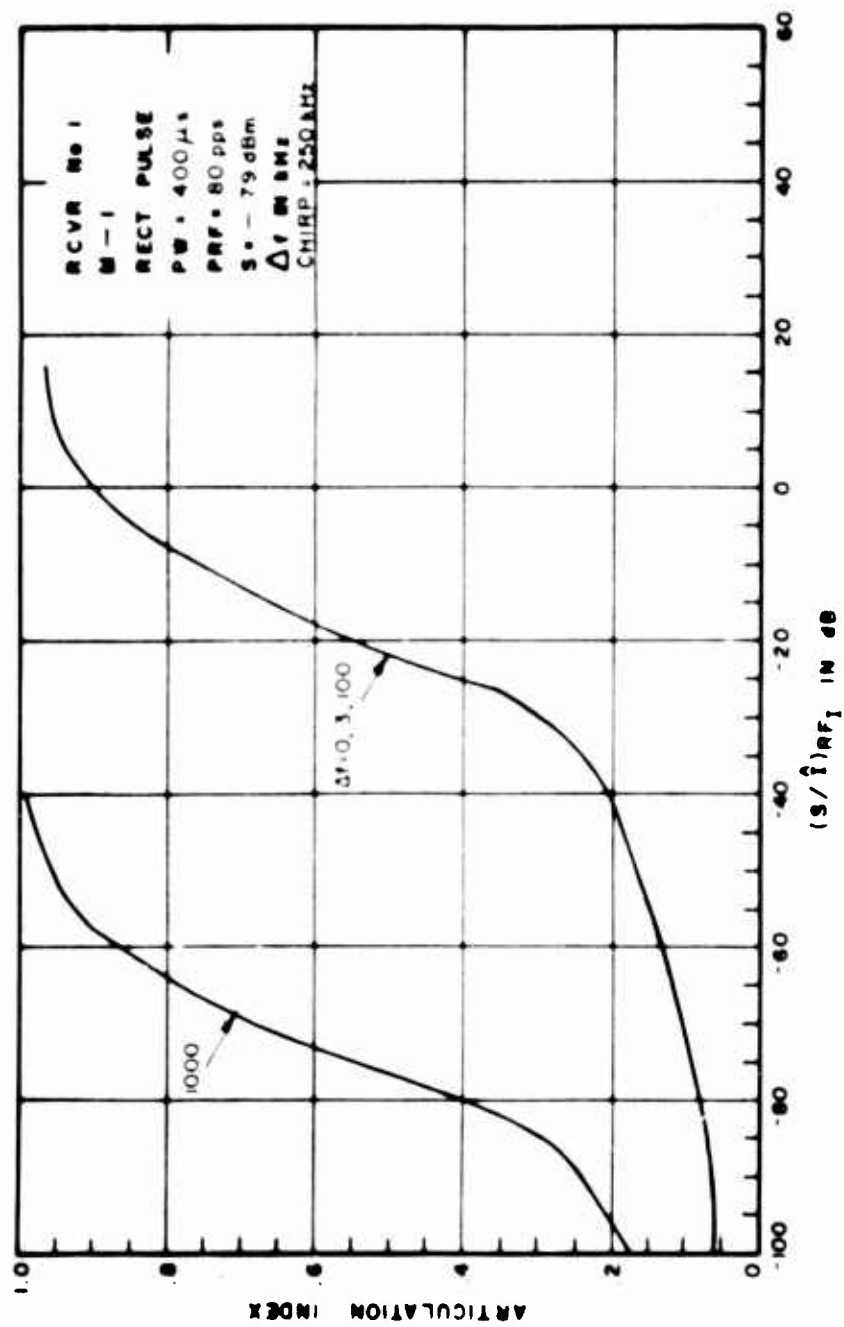


Figure III.84. Articulation Index for Pulsed Interference to an AM Receiver

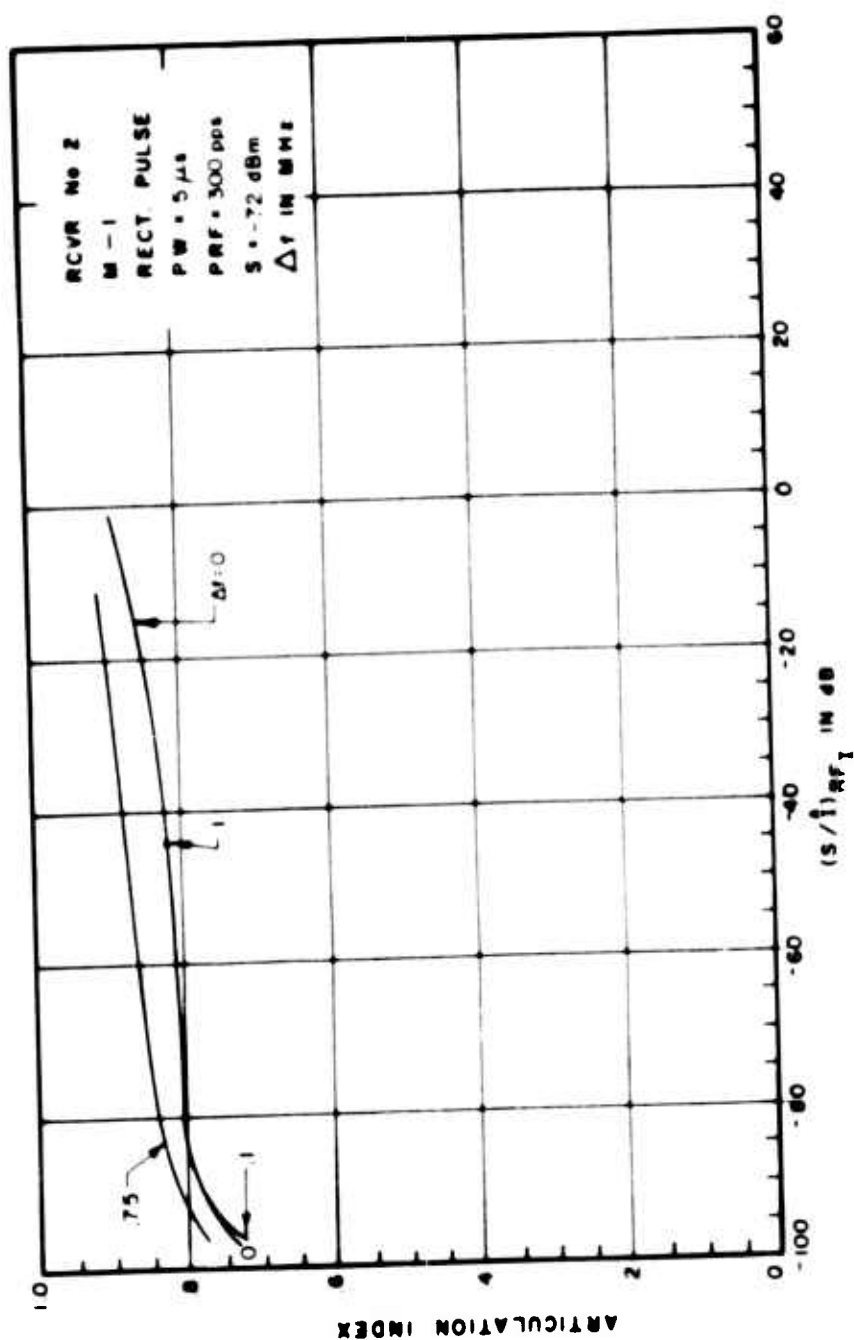


Figure III 85. Articulation Index for Pulsed Interference to an AM Receiver

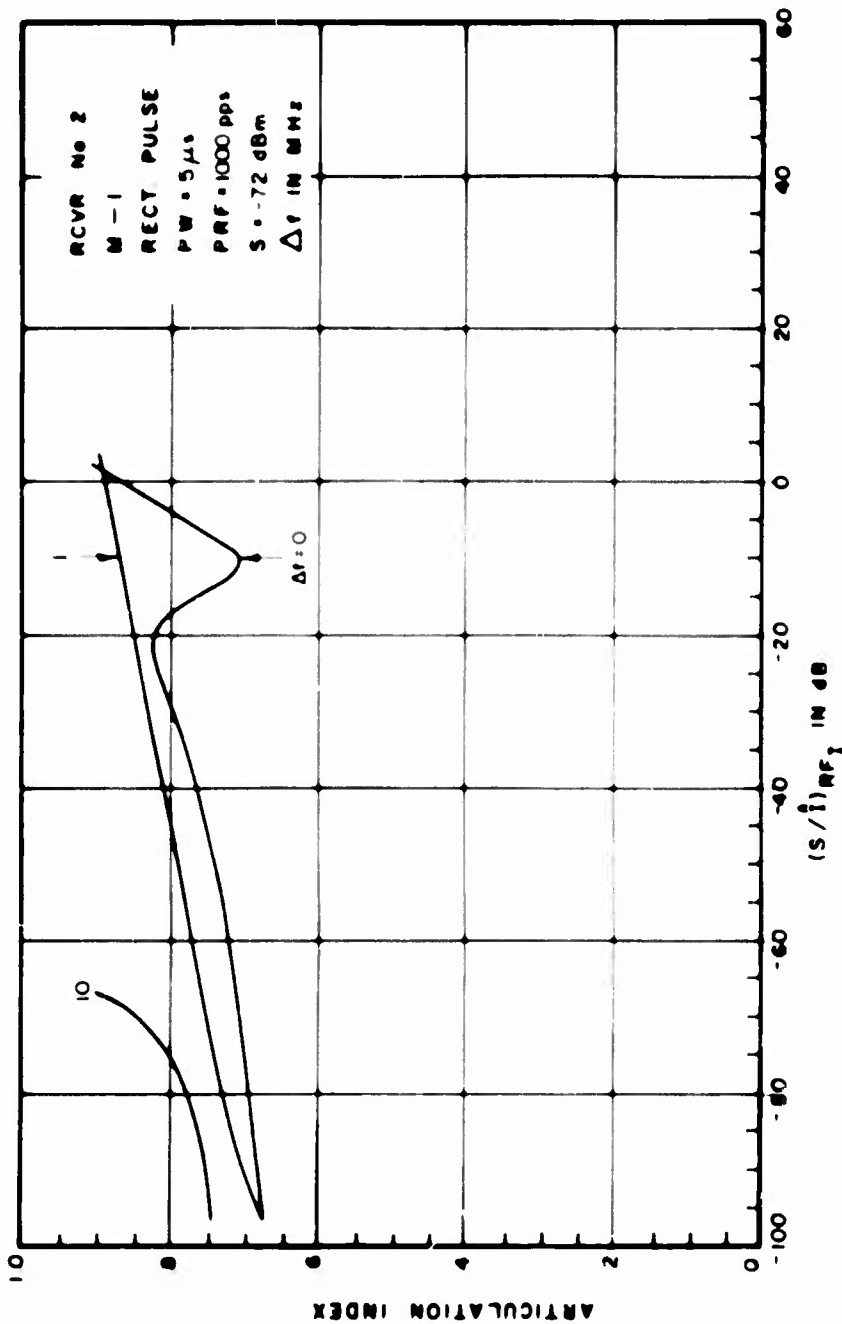


Figure III-86. Articulation Index for Pulsed Interference to an AM Receiver

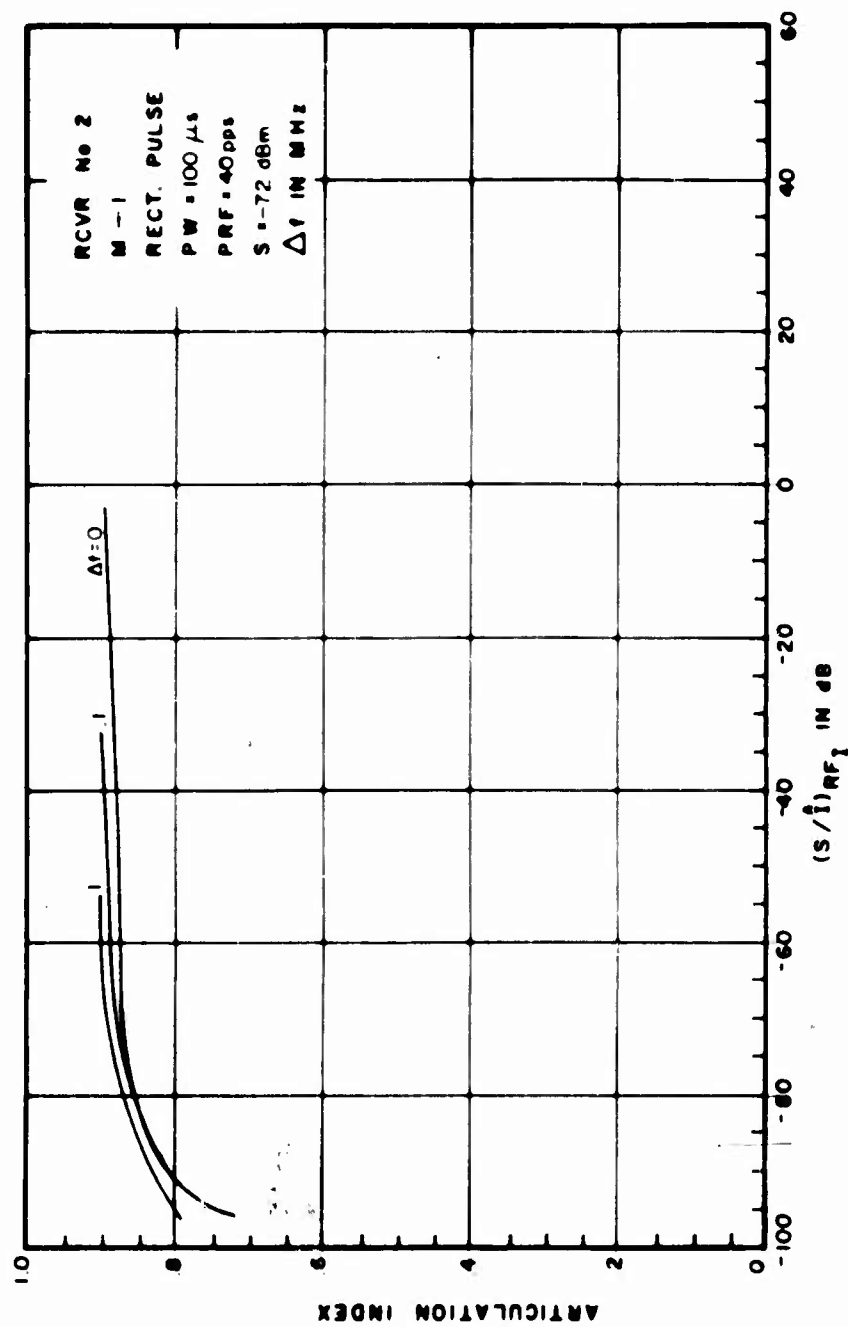


Figure III-87. Articulation Index for Pulsed Interference to an AM Receiver

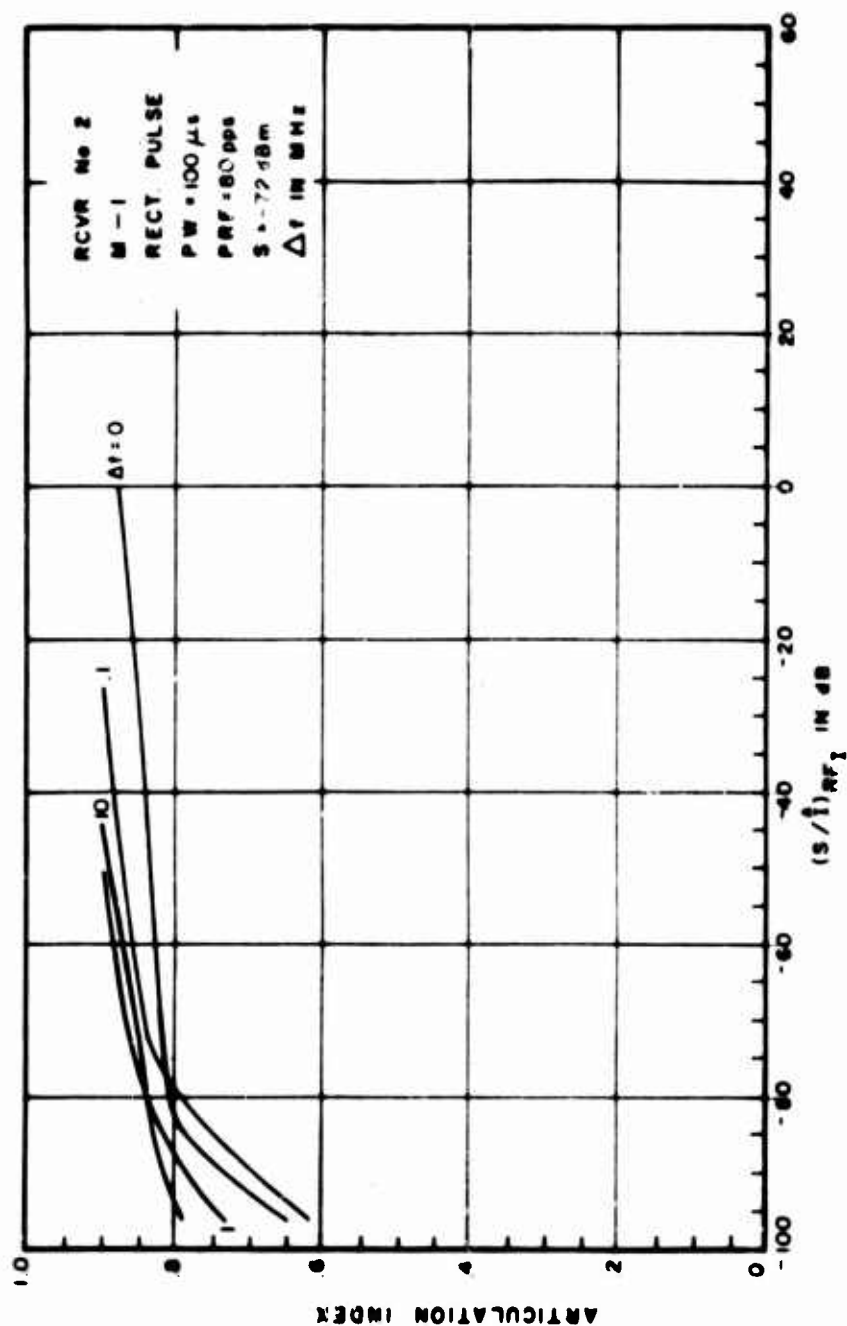


Figure III-88. Articulation Index for Pulsed Interference to an AM Receiver

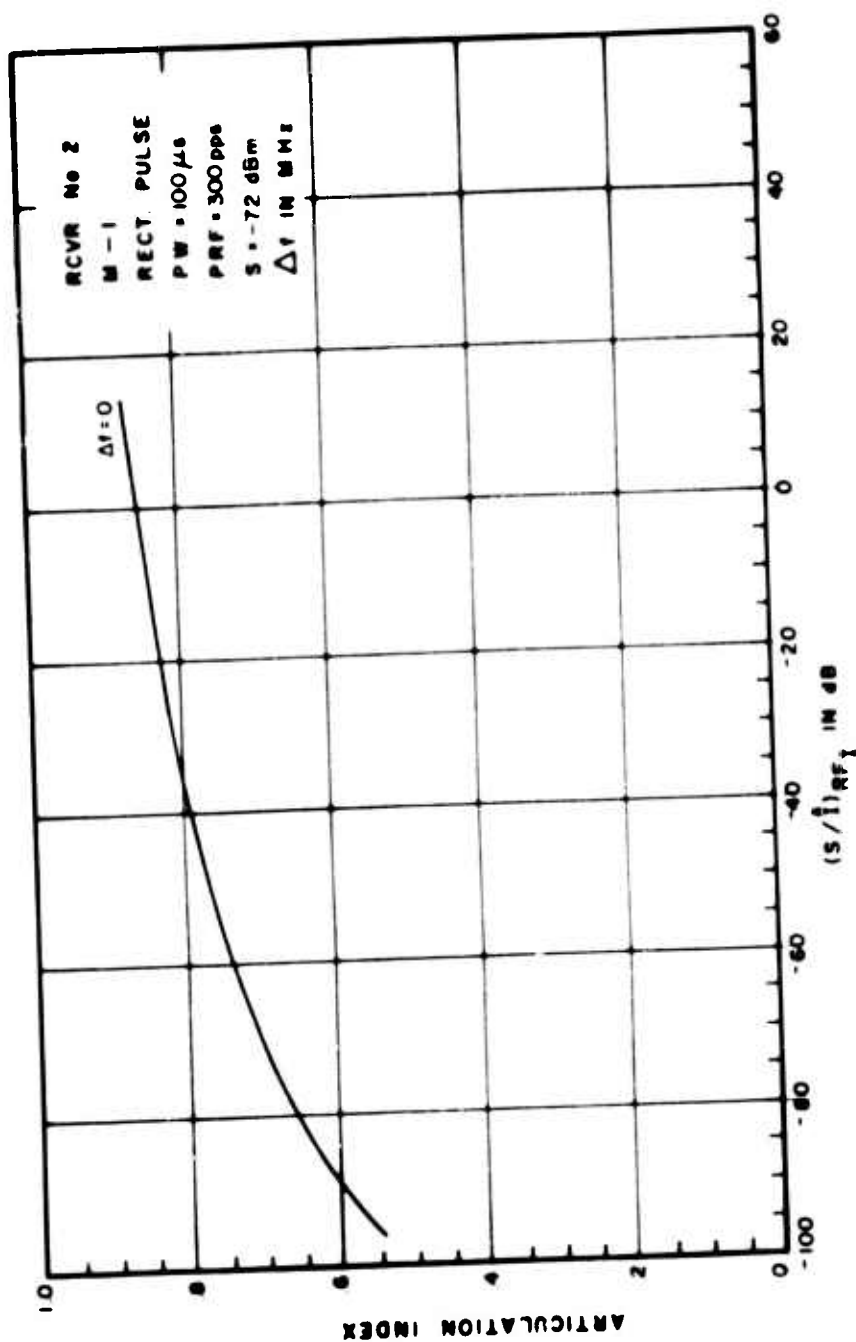


Figure III-89. Articulation Index for Pulsed Interference to an AM Receiver

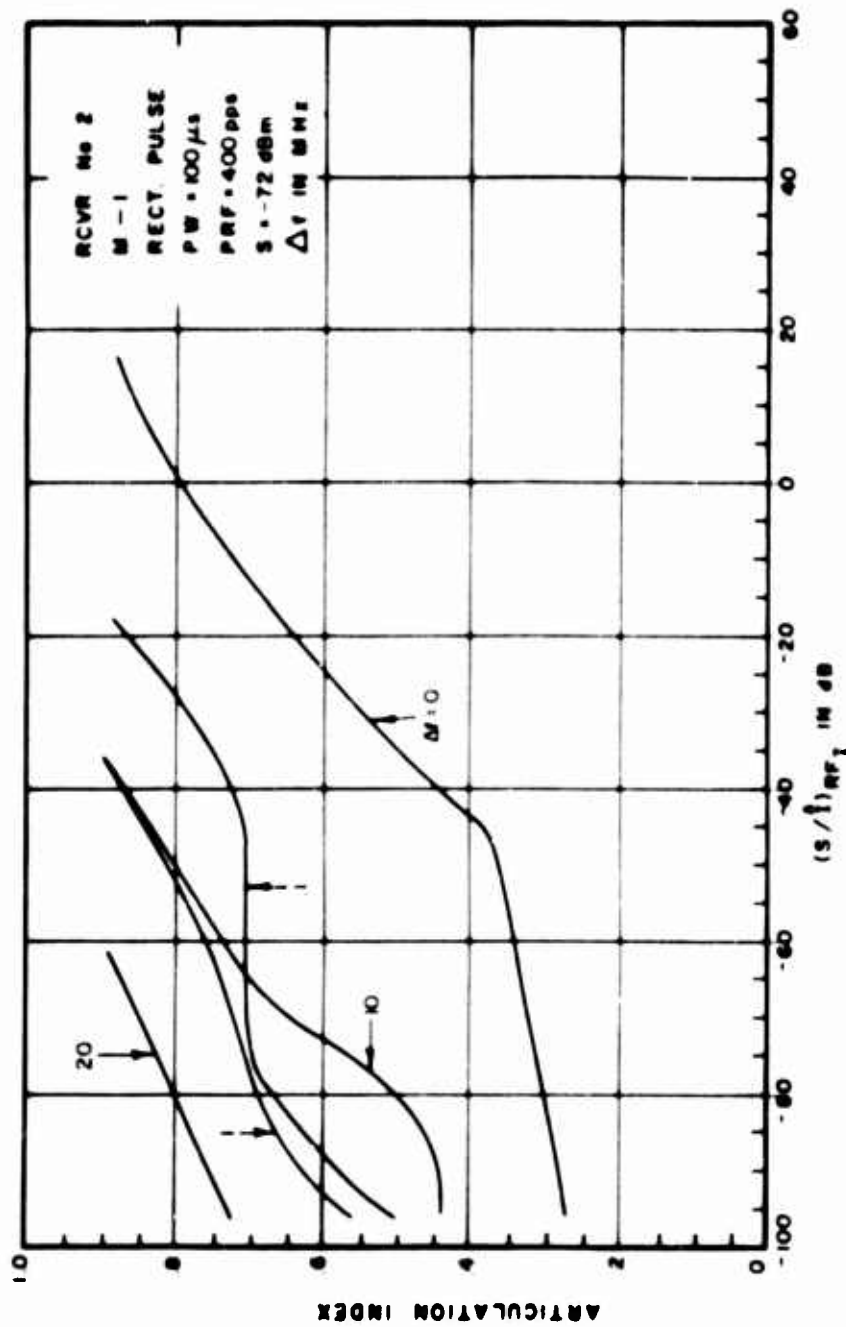


Figure III-90. Articulation Index for Pulsed Interference to an AM Receiver

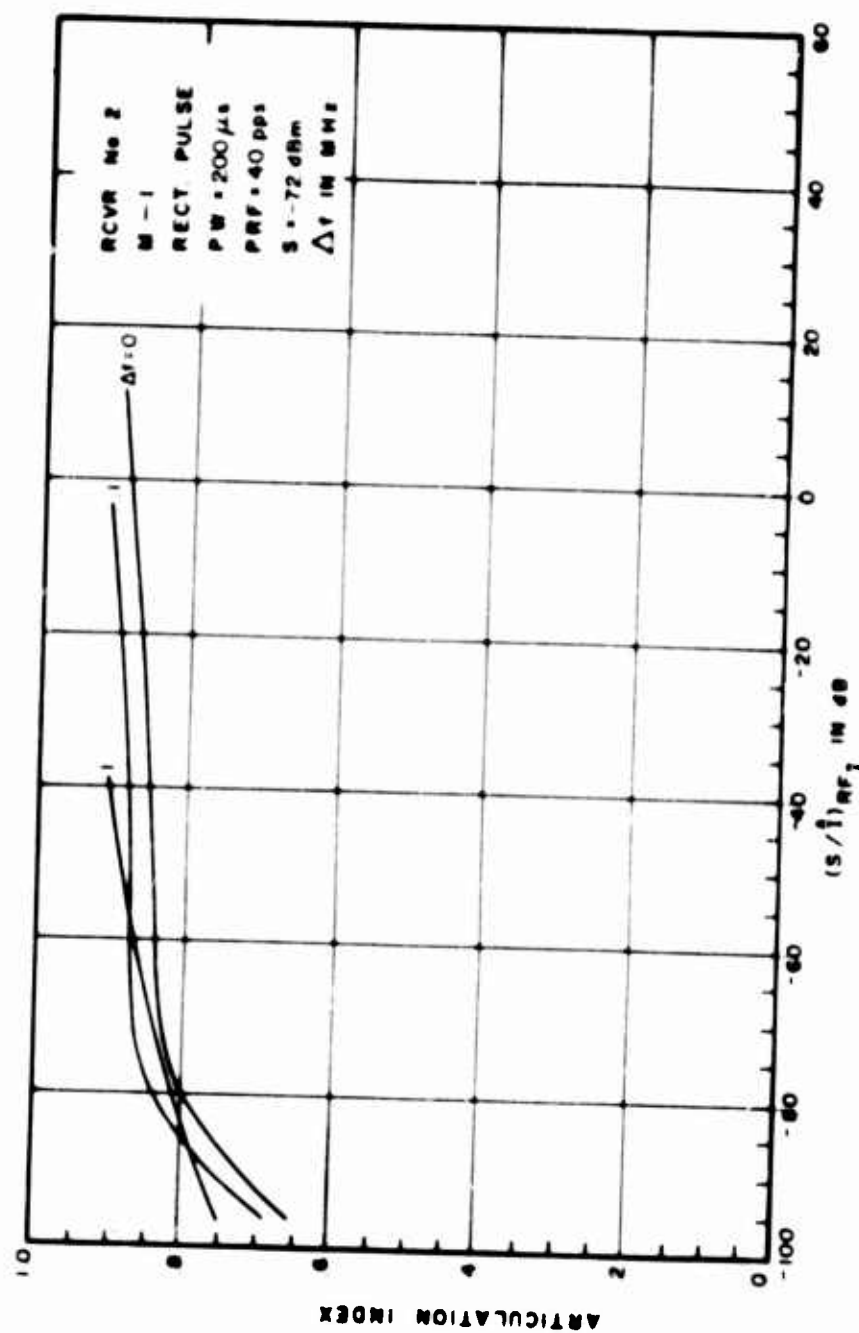


Figure III-91. Articulation Index for Pulsed Interference to an AM Receiver

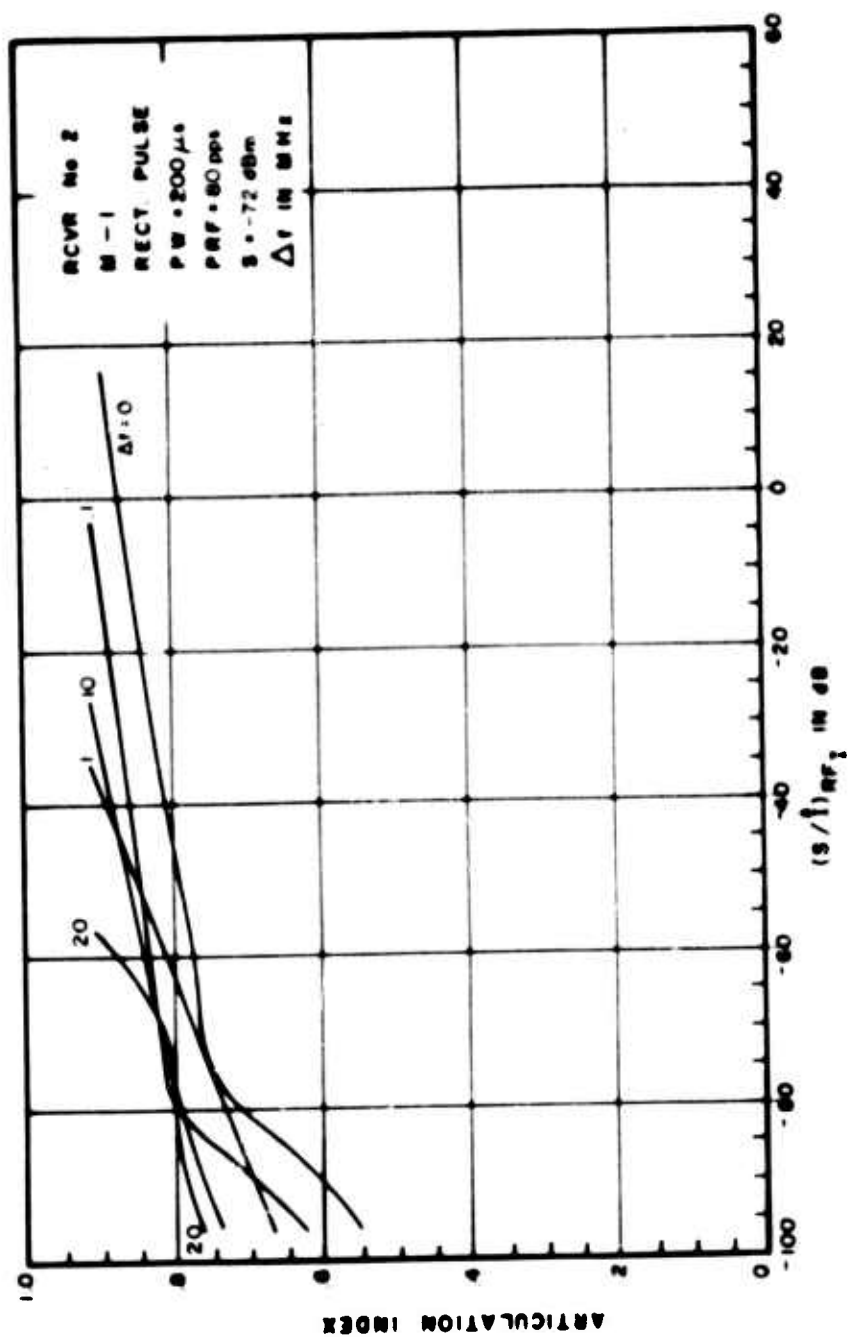


Figure III-92. Articulation Index for Pulsed Interference to an AM Receiver

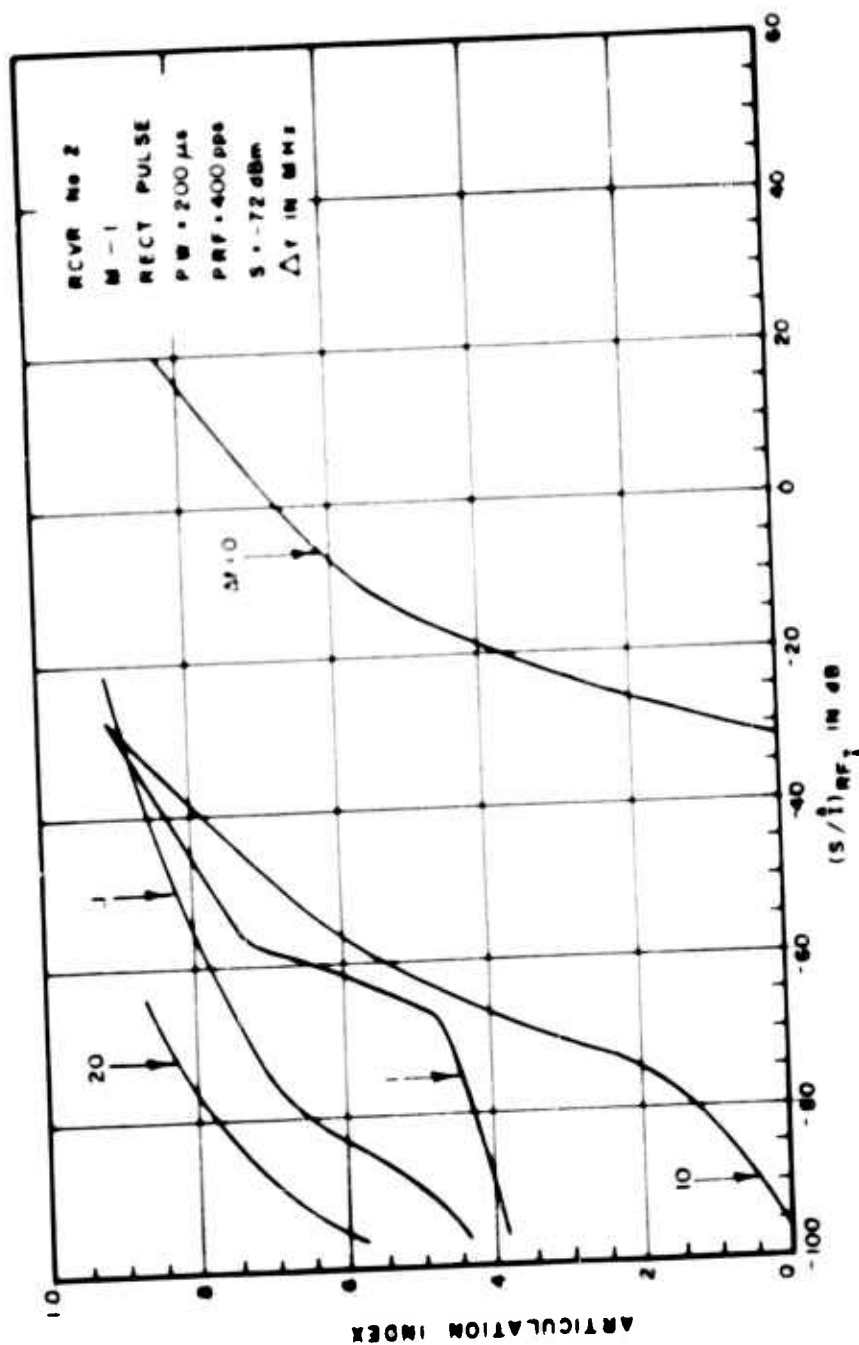


Figure III-93. Articulation Index for Pulsed Interference to an AM Receiver

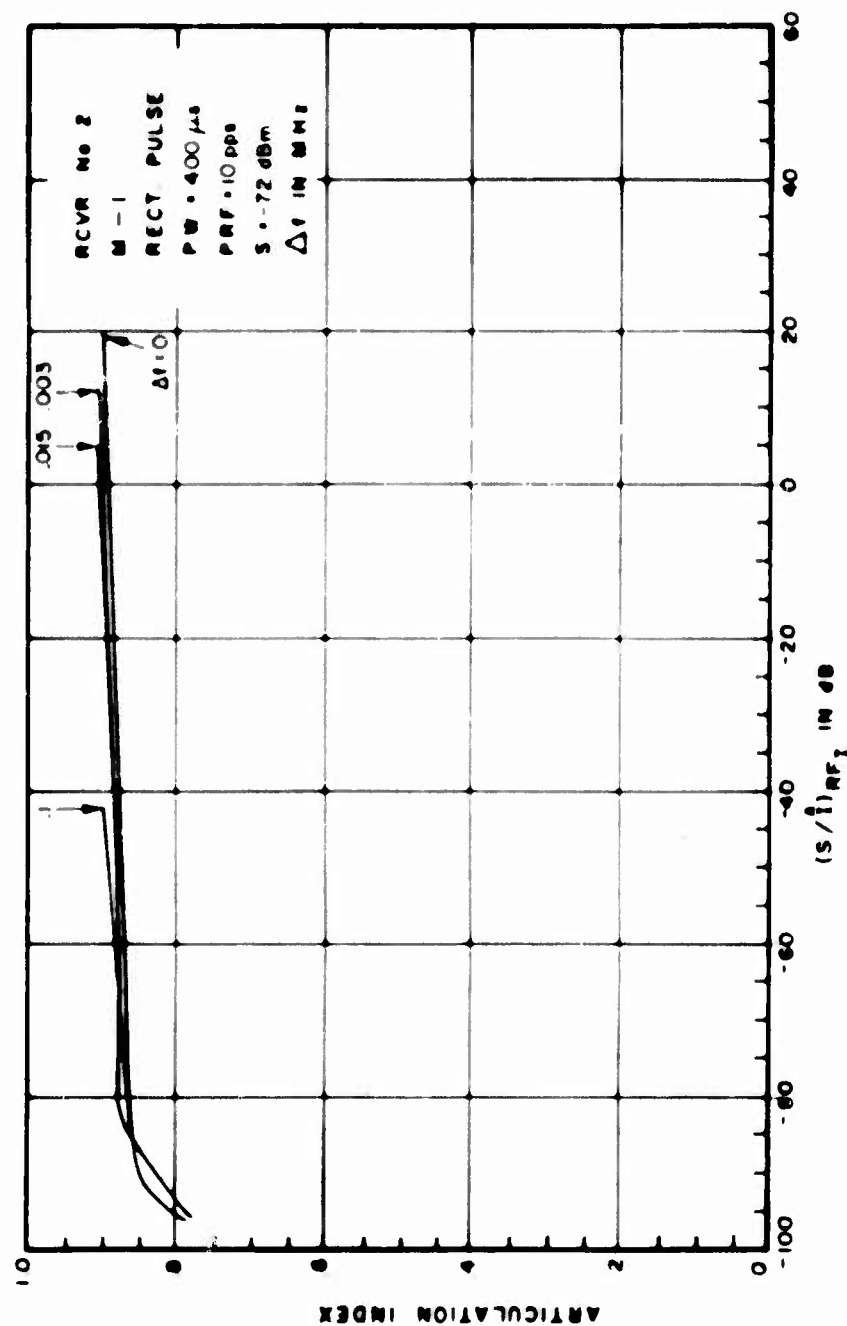


Figure III-94. Articulation Index for Pulsed Interference to an AM Receiver

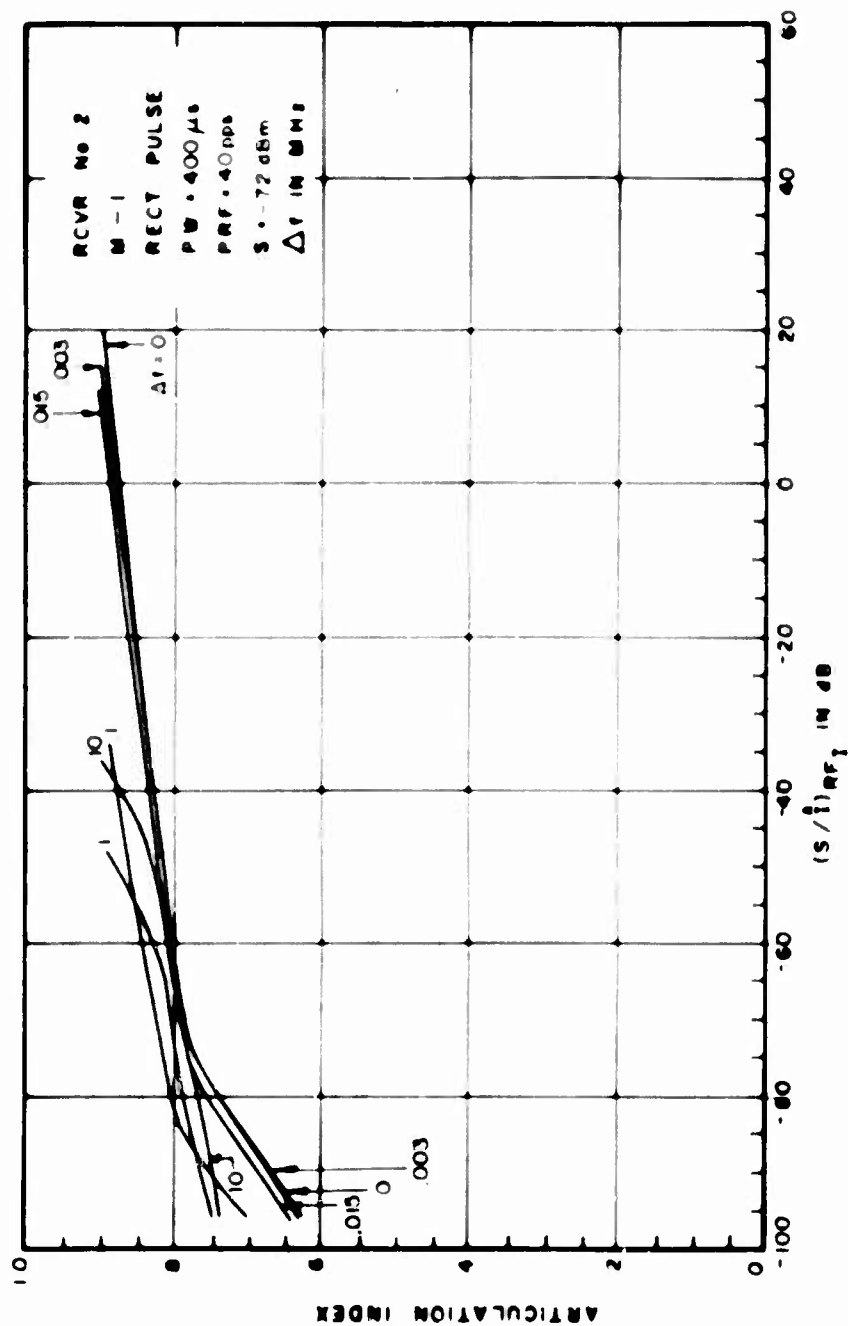


Figure III 95. Articulation Index for Pulsed Interference to an AM Receiver

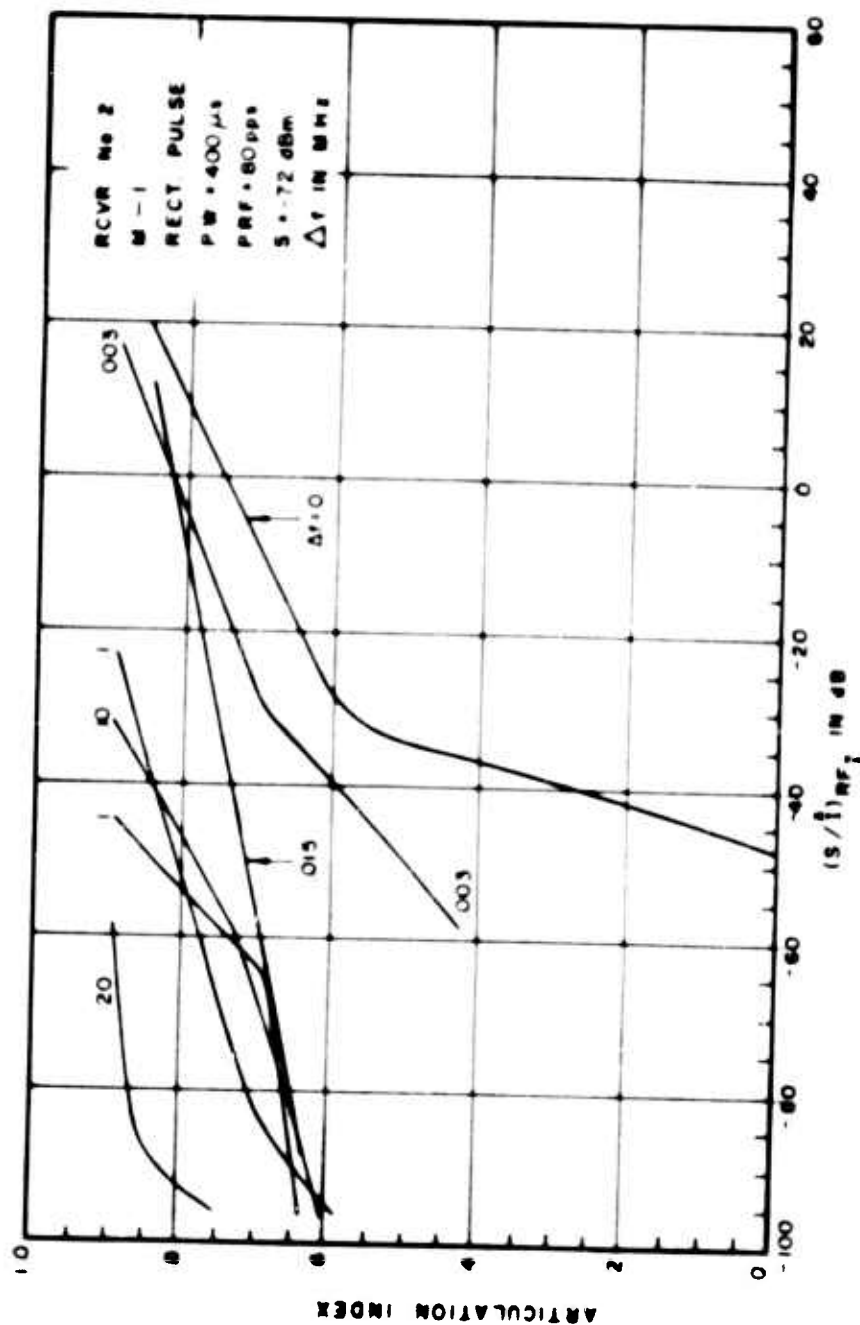


Figure III 96. Articulation Index for Pulsed Interference to an AM Receiver

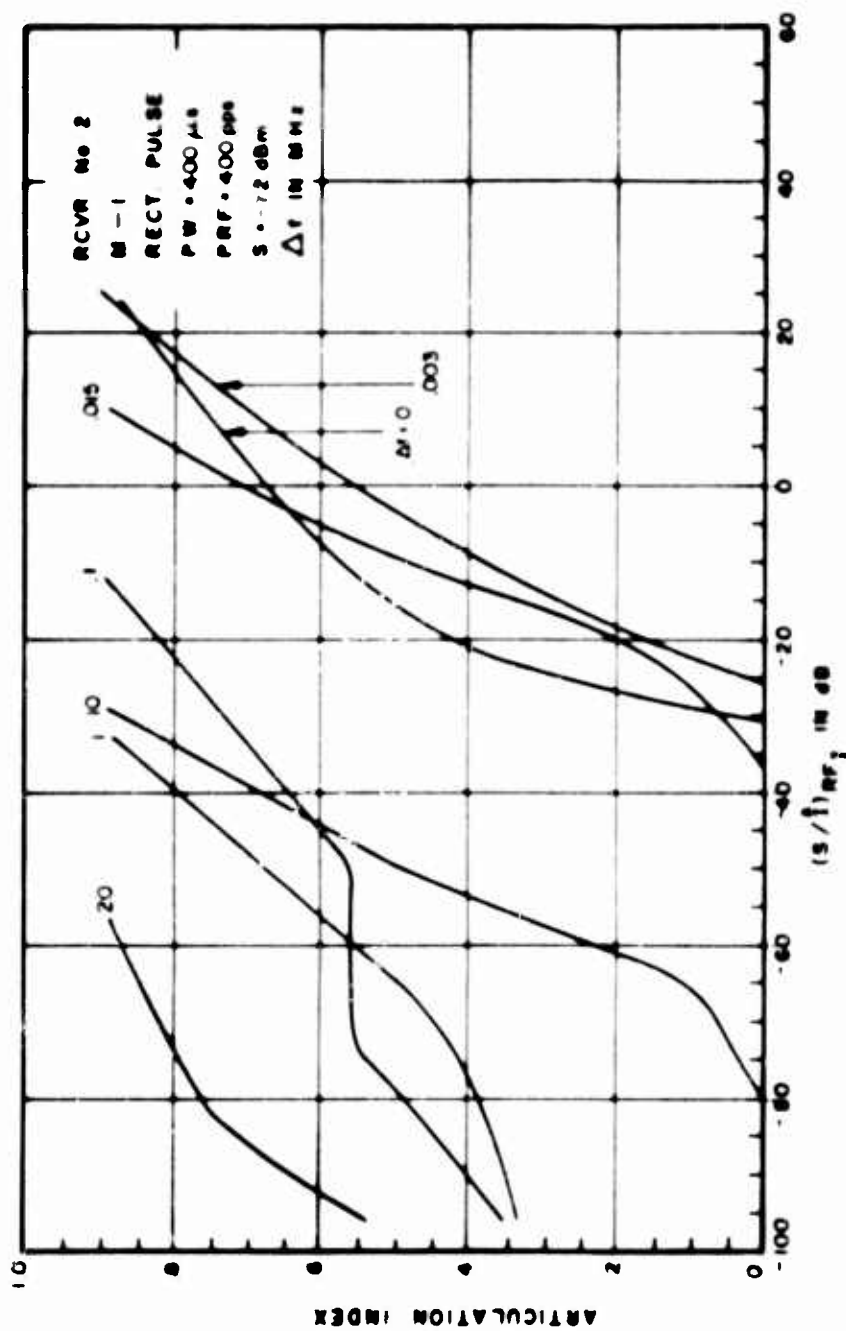


Figure III-97. Articulation Index for Pulsed Interference to an AM Receiver

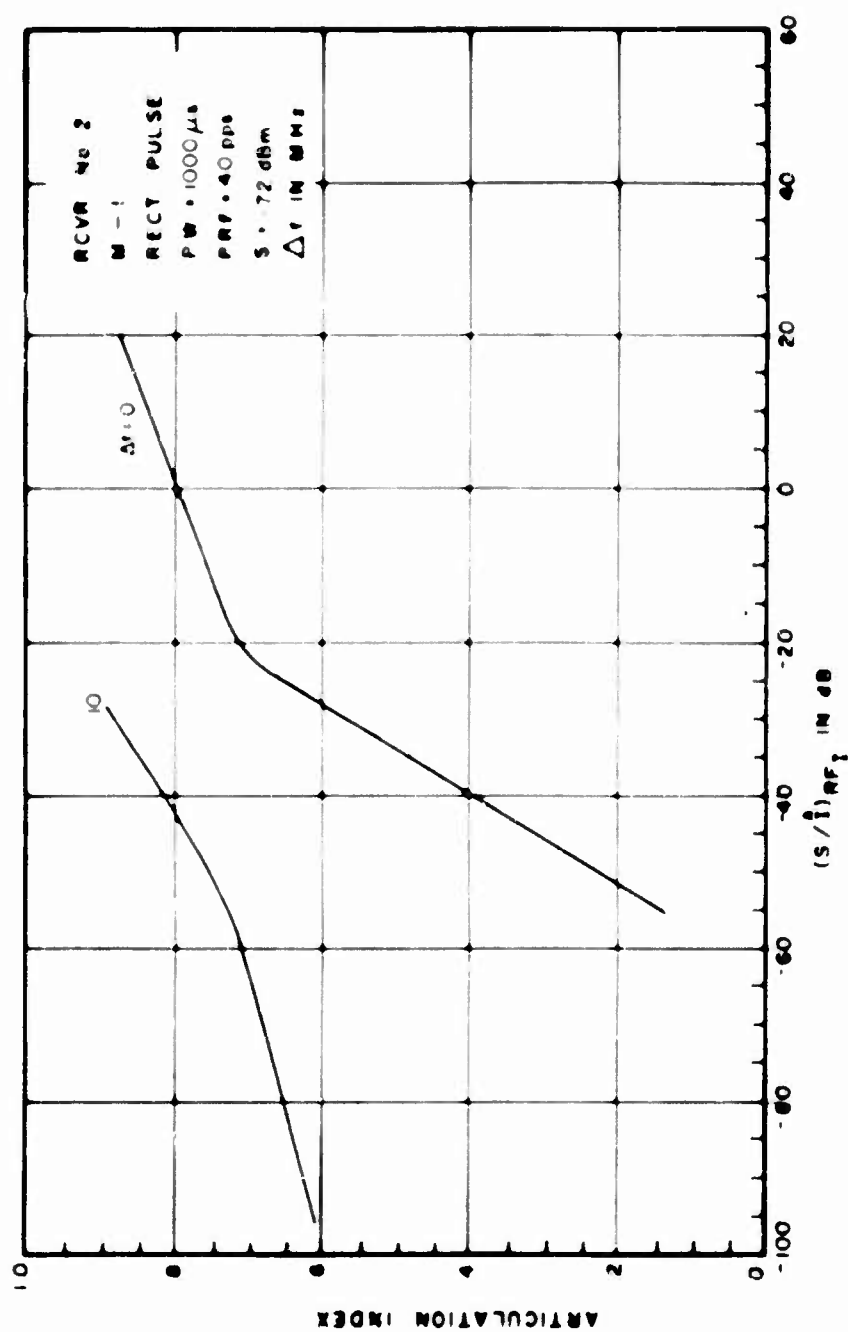


Figure III-98. Articulation Index for Pulsed Interference to an AM Receiver

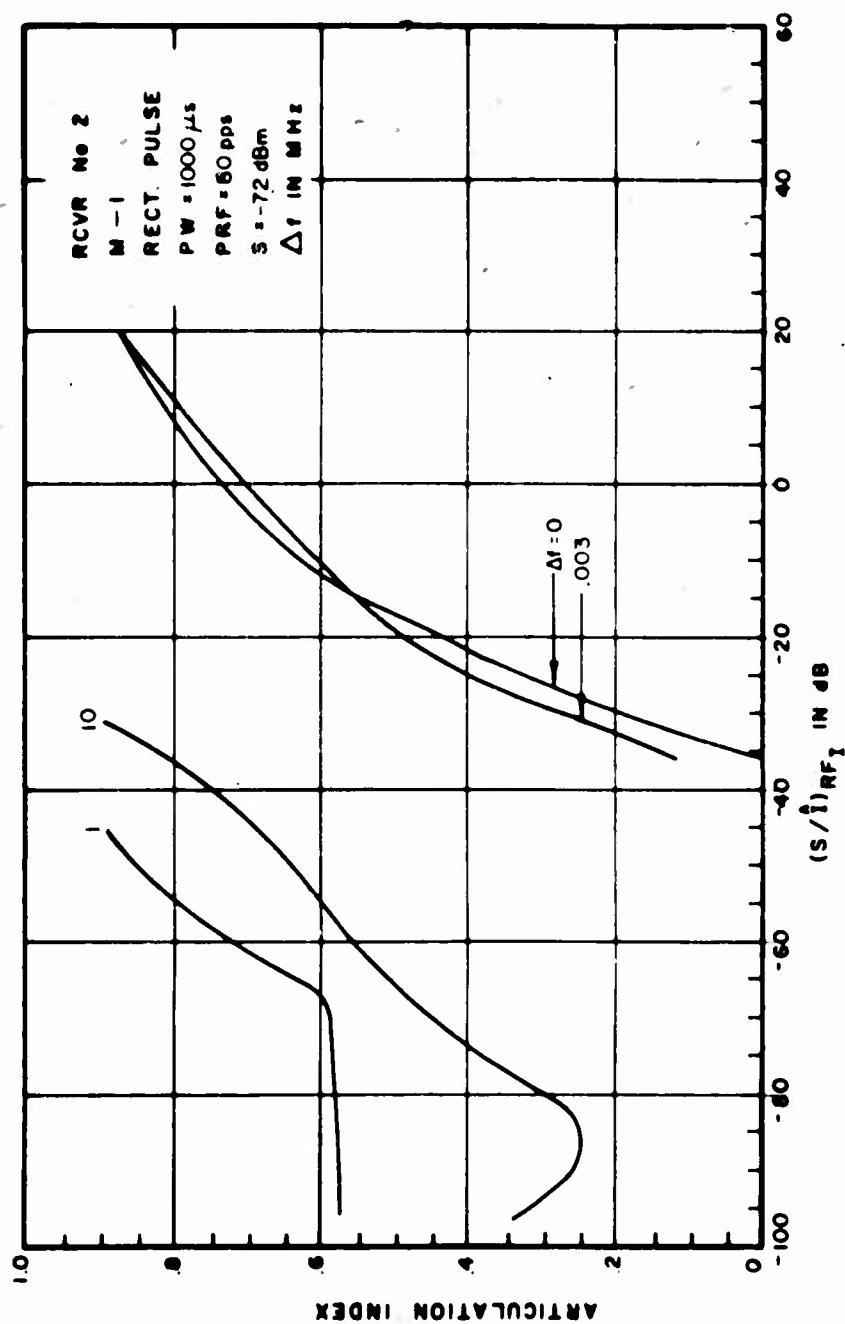


Figure III-99. Articulation Index for Pulsed Interference to an AM Receiver

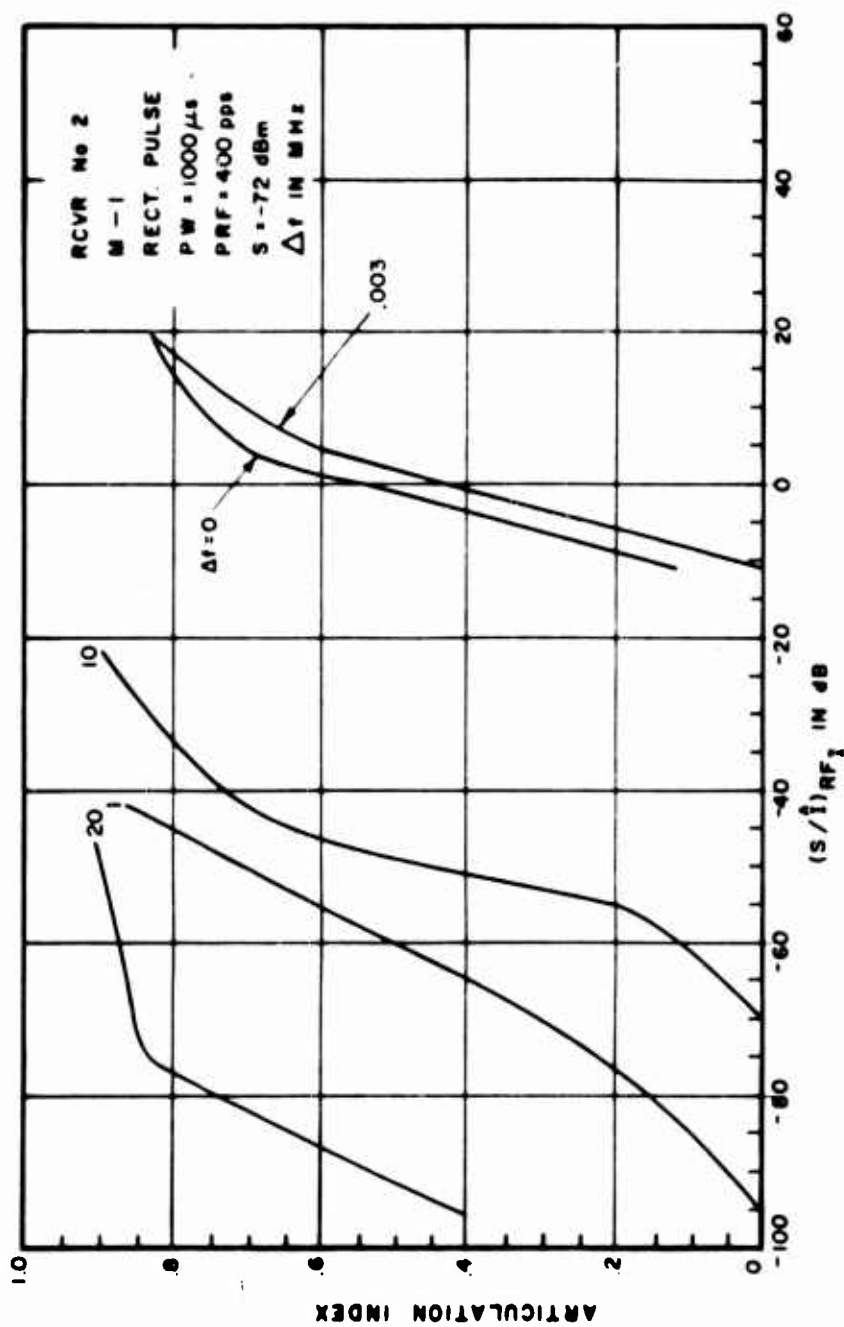


Figure III-100. Articulation Index for Pulsed Interference to an AM Receiver

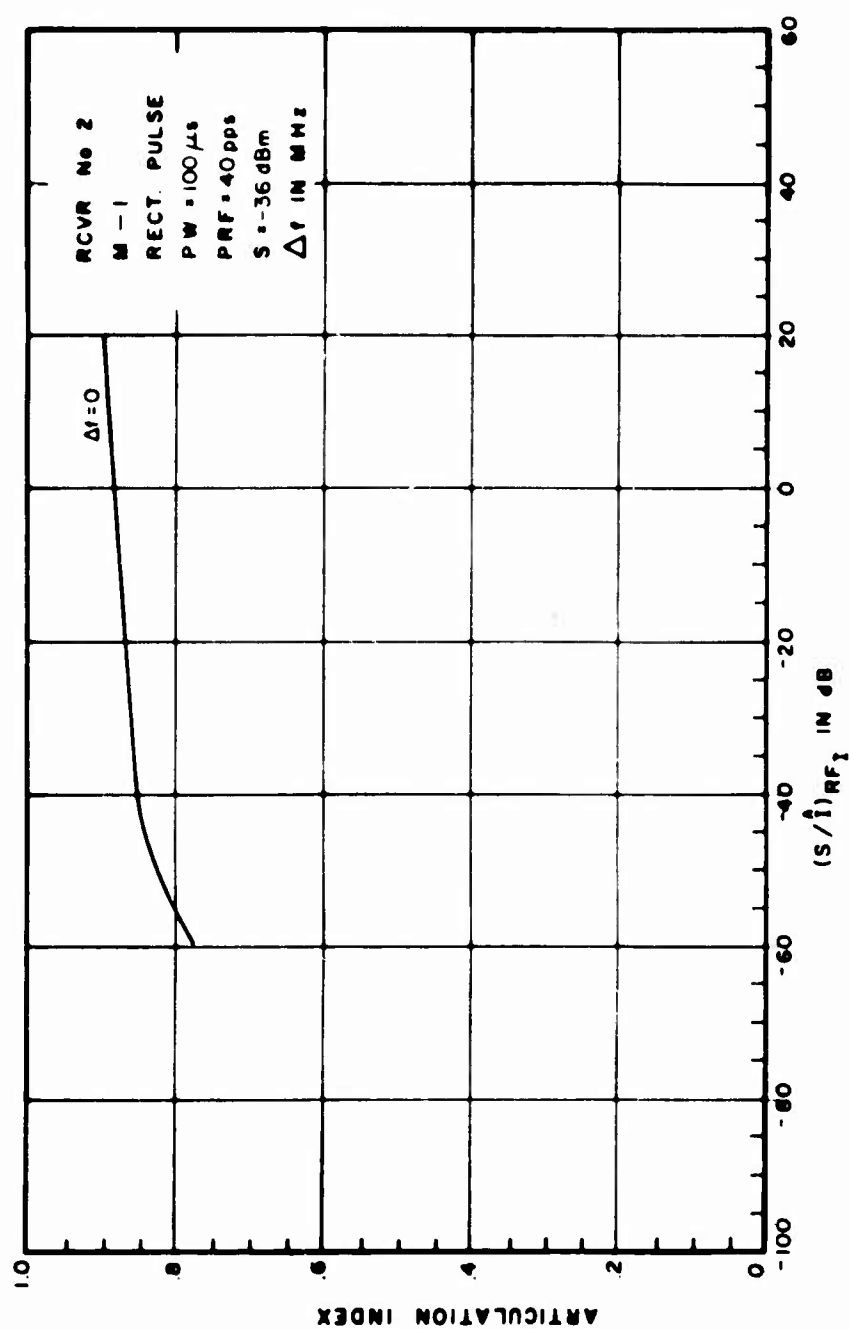


Figure III-101. Articulation Index for Pulsed Interference to an AM Receiver

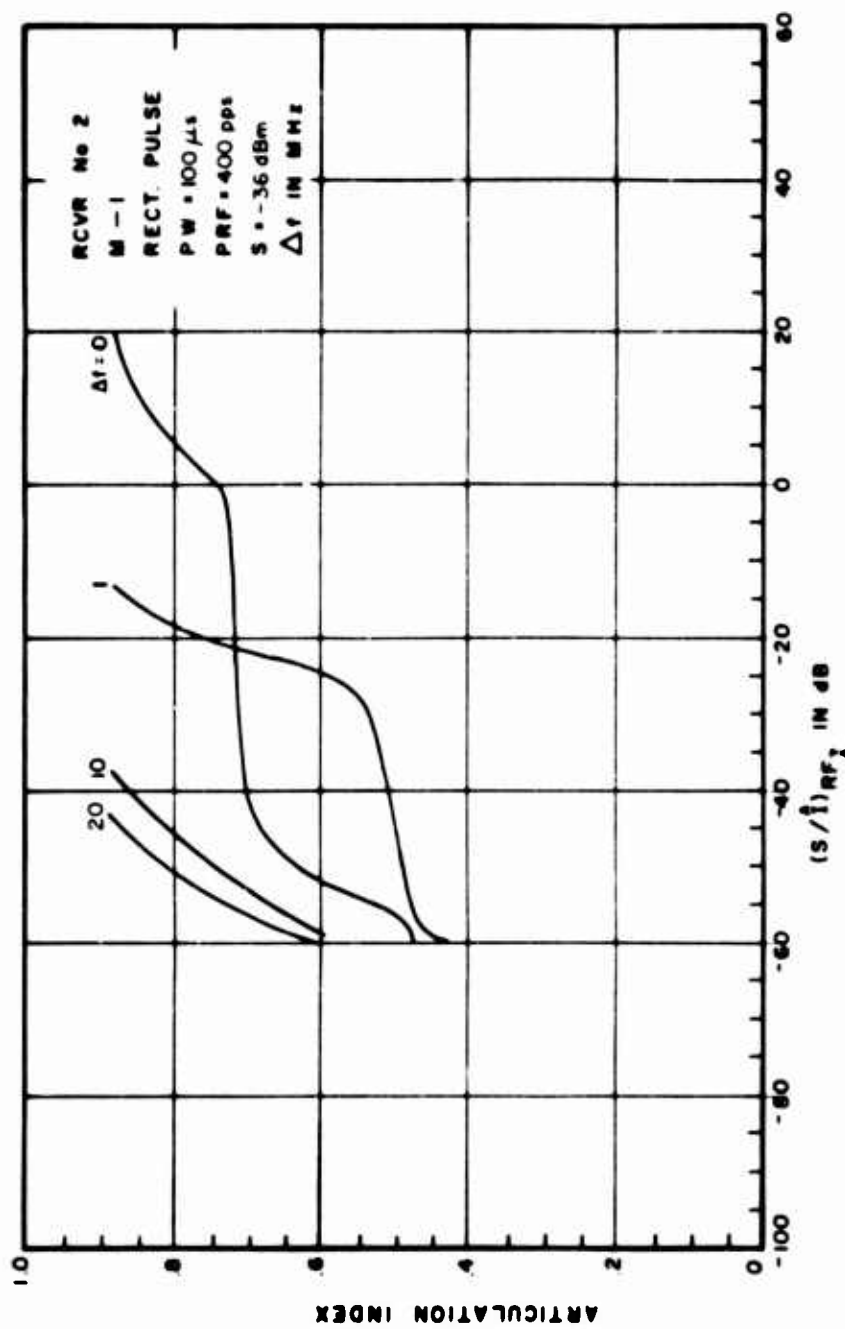


Figure III-102. Articulation Index for Pulsed Interference to an AM Receiver

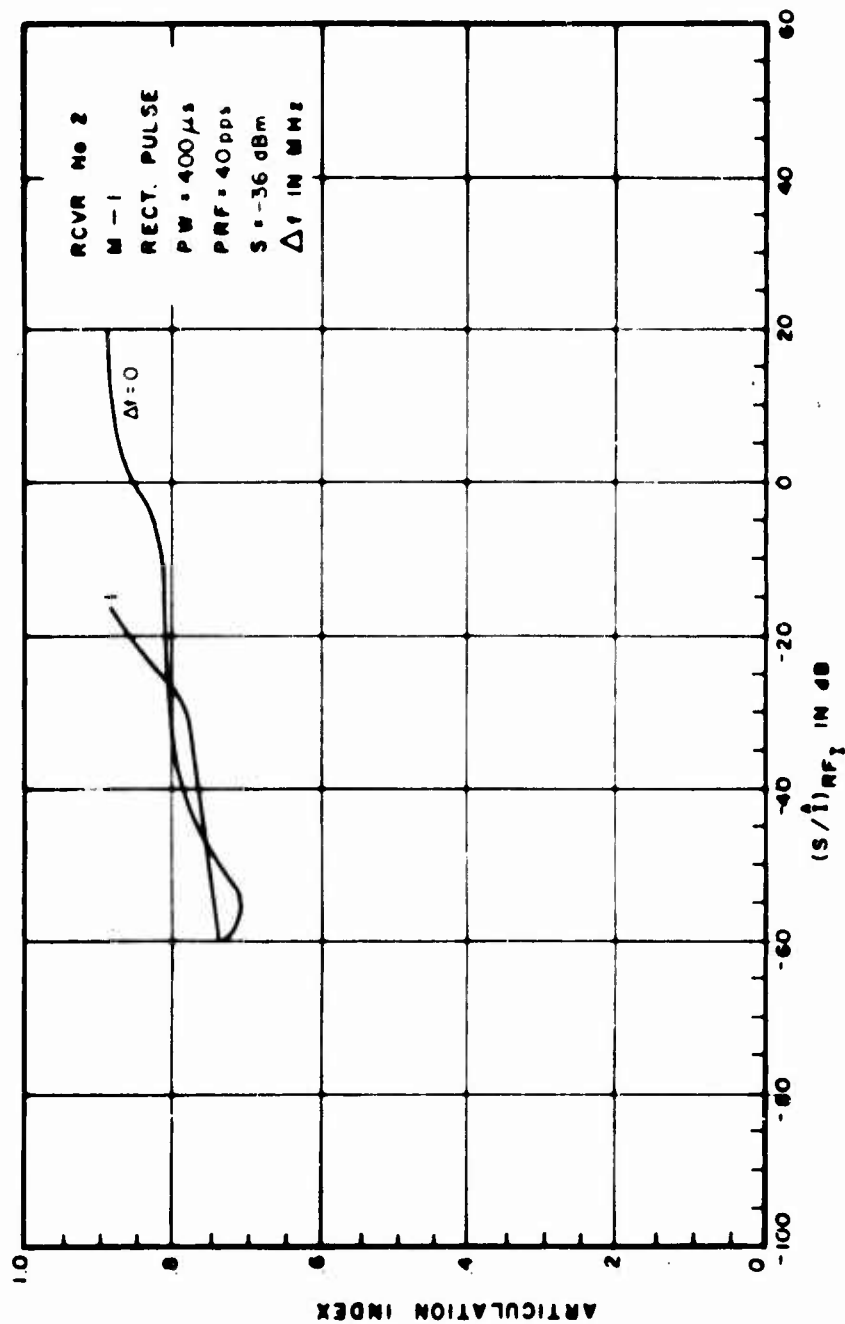


Figure III-103. Articulation Index for Pulsed Interference to an AM Receiver

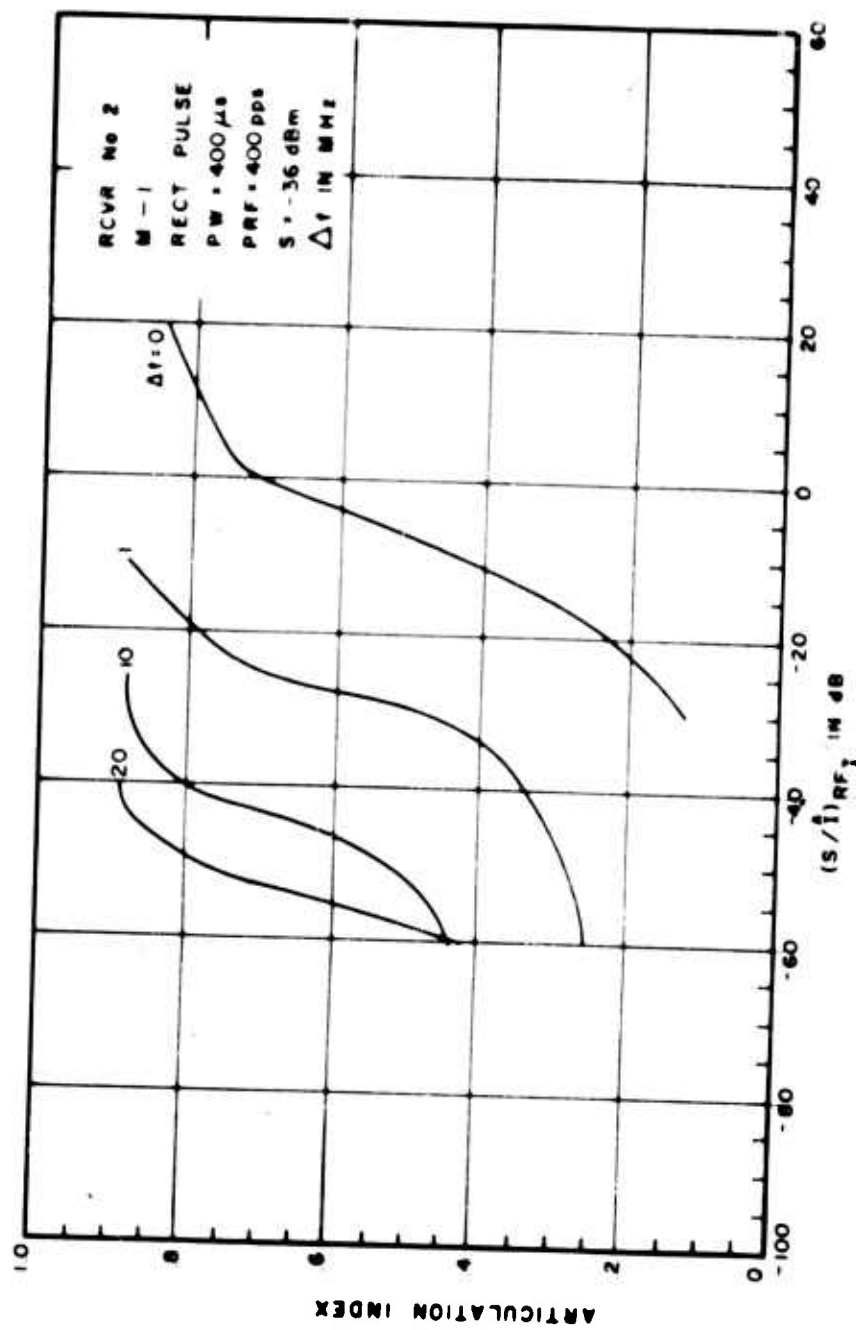


Figure III-104. Articulation Index for Pulsed Interference to an AM Receiver

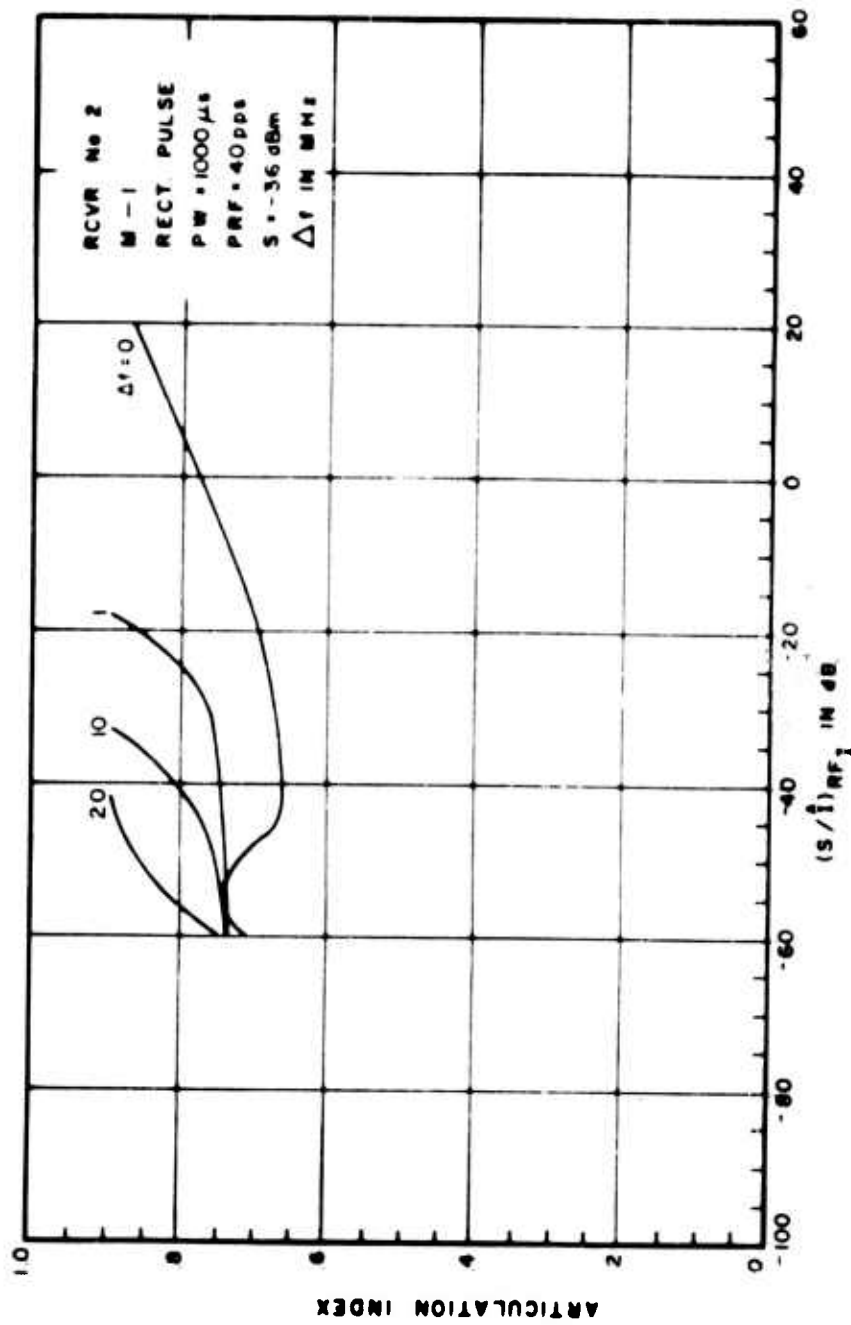


Figure III-105. Articulation Index for Pulsed Interference to an AM Receiver

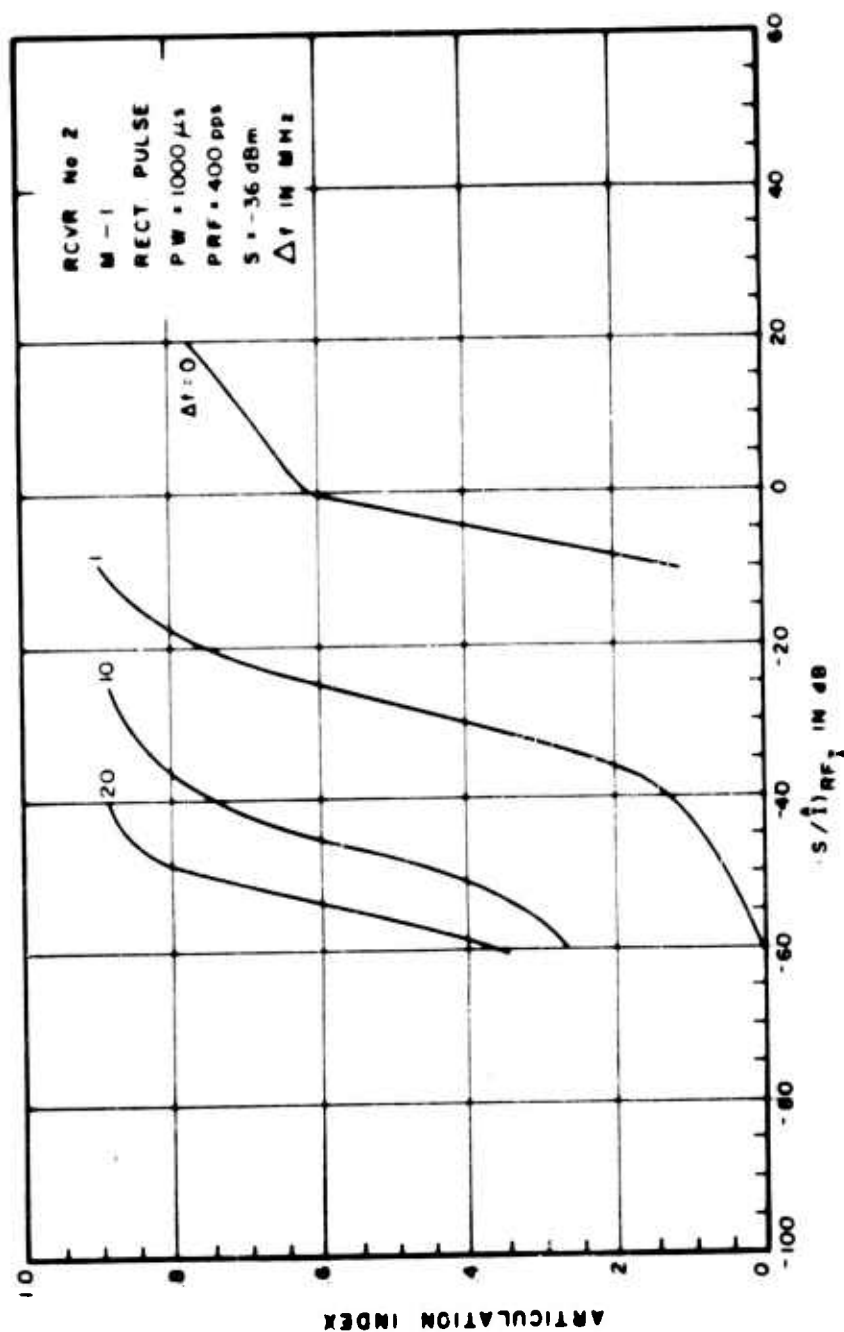


Figure III-106. Articulation Index for Pulsed Interference to an AM Receiver

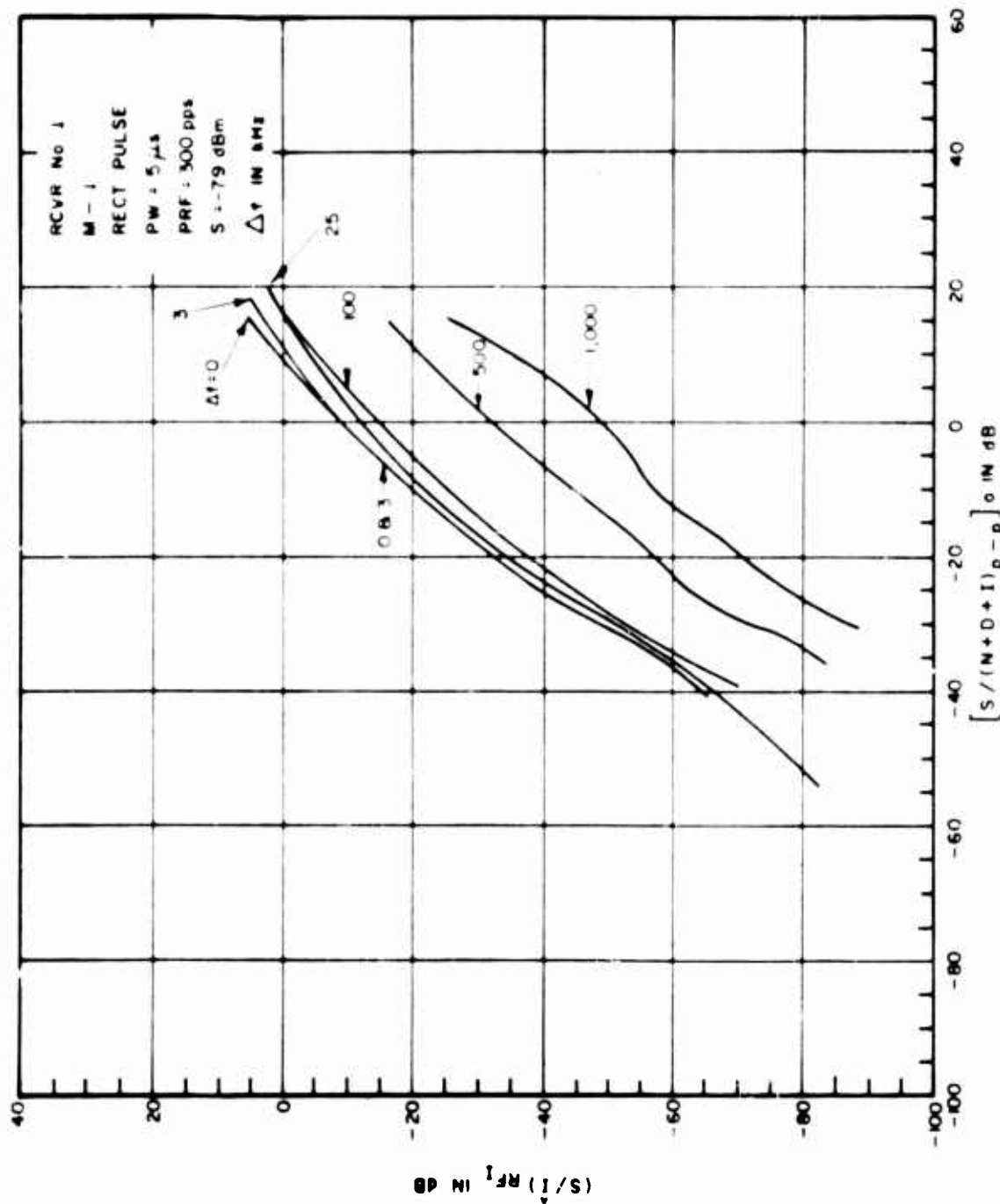


Figure III-107. Power Transfer Curves for Pulsed Interference to an AM Receiver

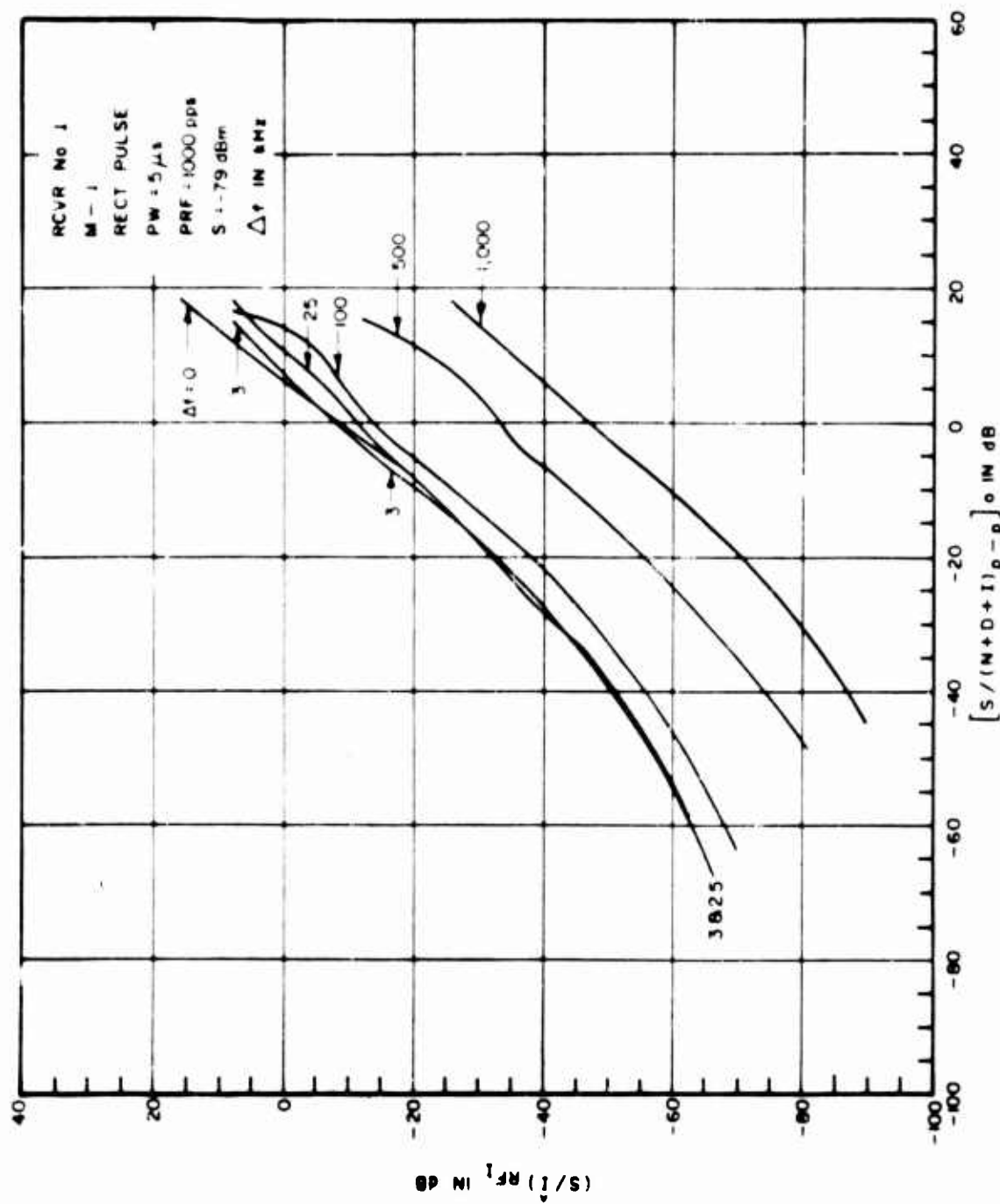


Figure III-108. Power Transfer Curves for Pulsed Interference to an AM Receiver

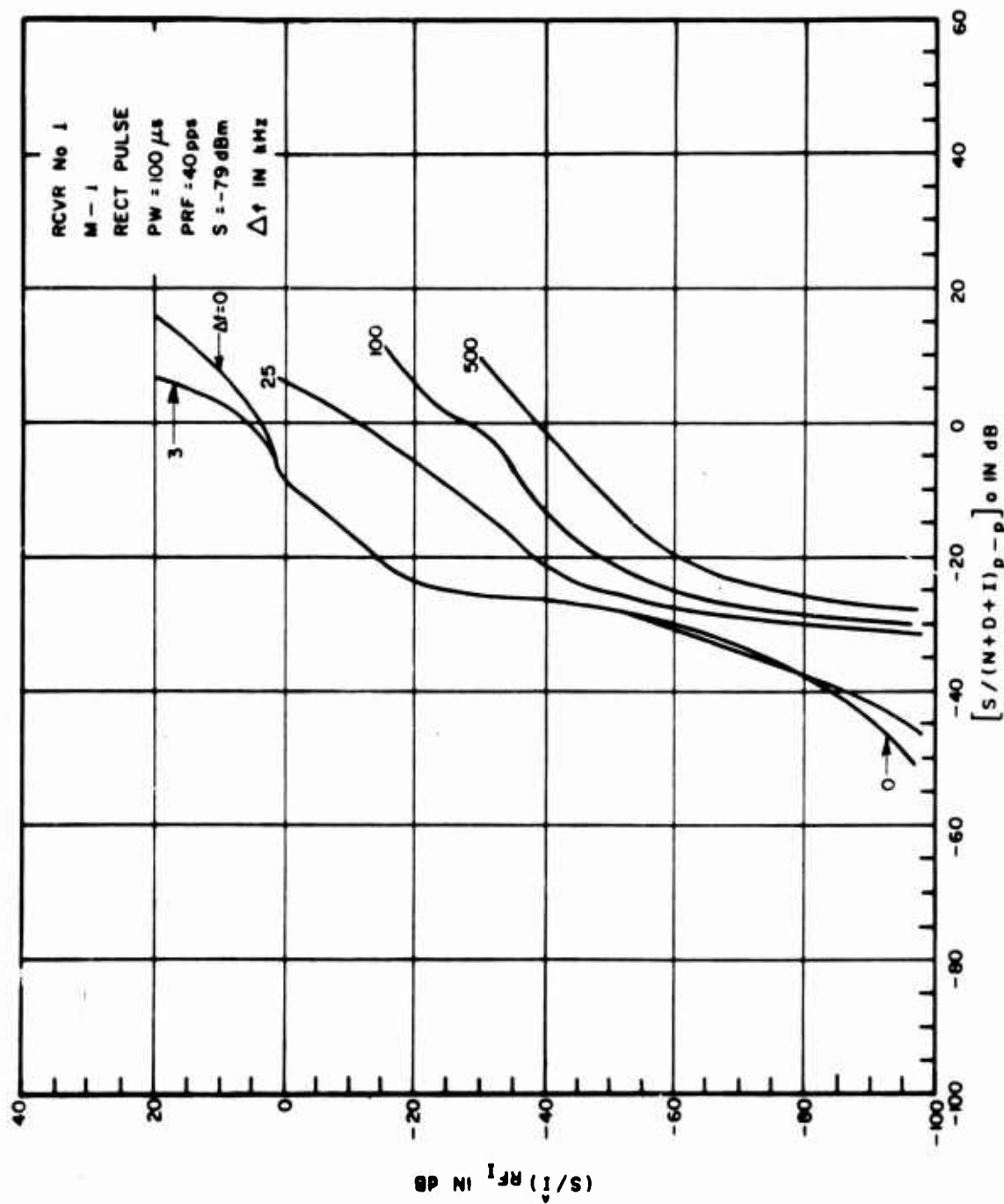


Figure III-109. Power Transfer Curves for Pulsed Interference to an AM Receiver

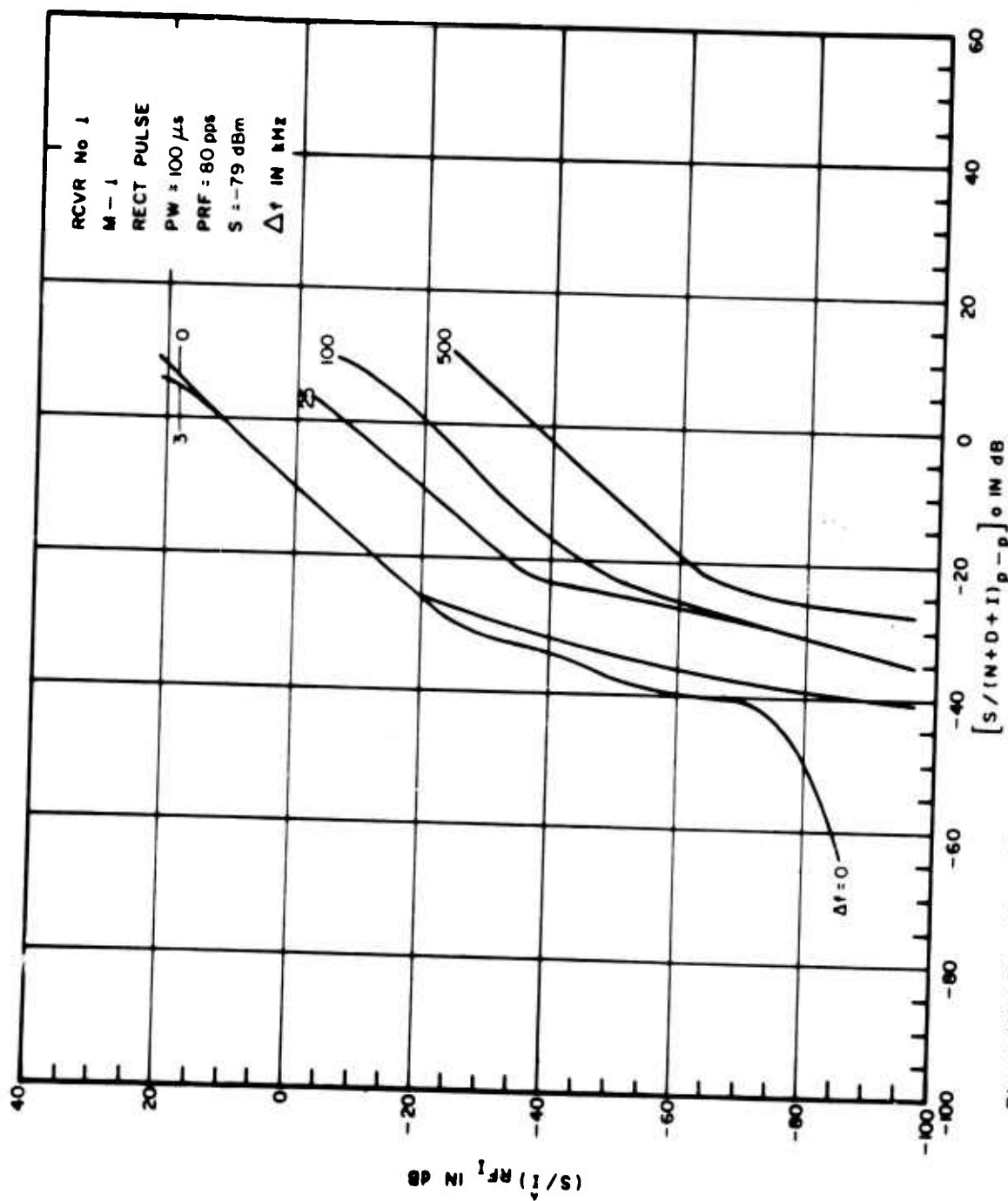


Figure III-110. Power Transfer Curves for Pulsed Interference to an AM Receiver

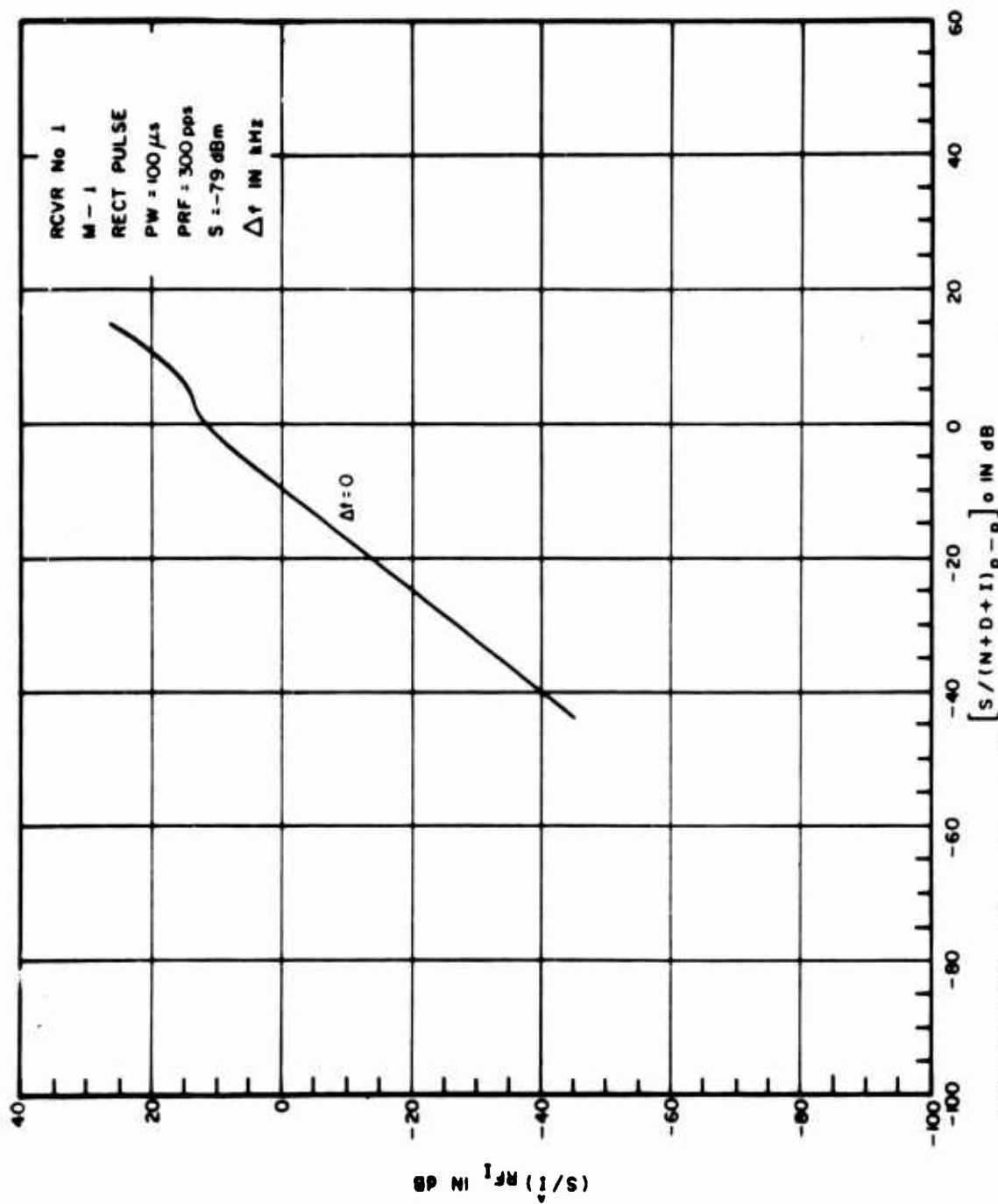


Figure III-111. Power Transfer Curves for Pulsed Interference to an AM Receiver

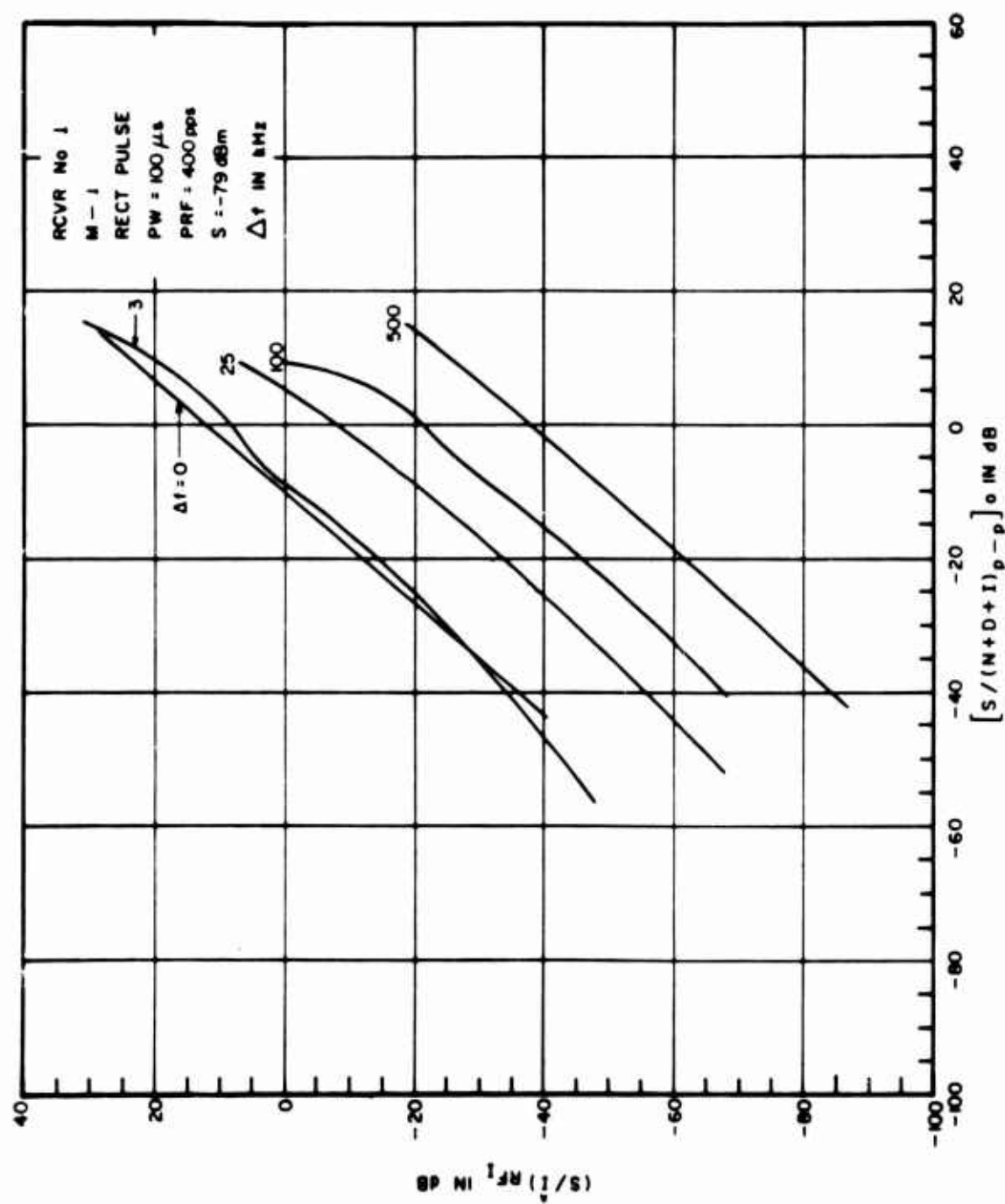


Figure III-112. Power Transfer Curves for Pulsed Interference to an AM Receiver

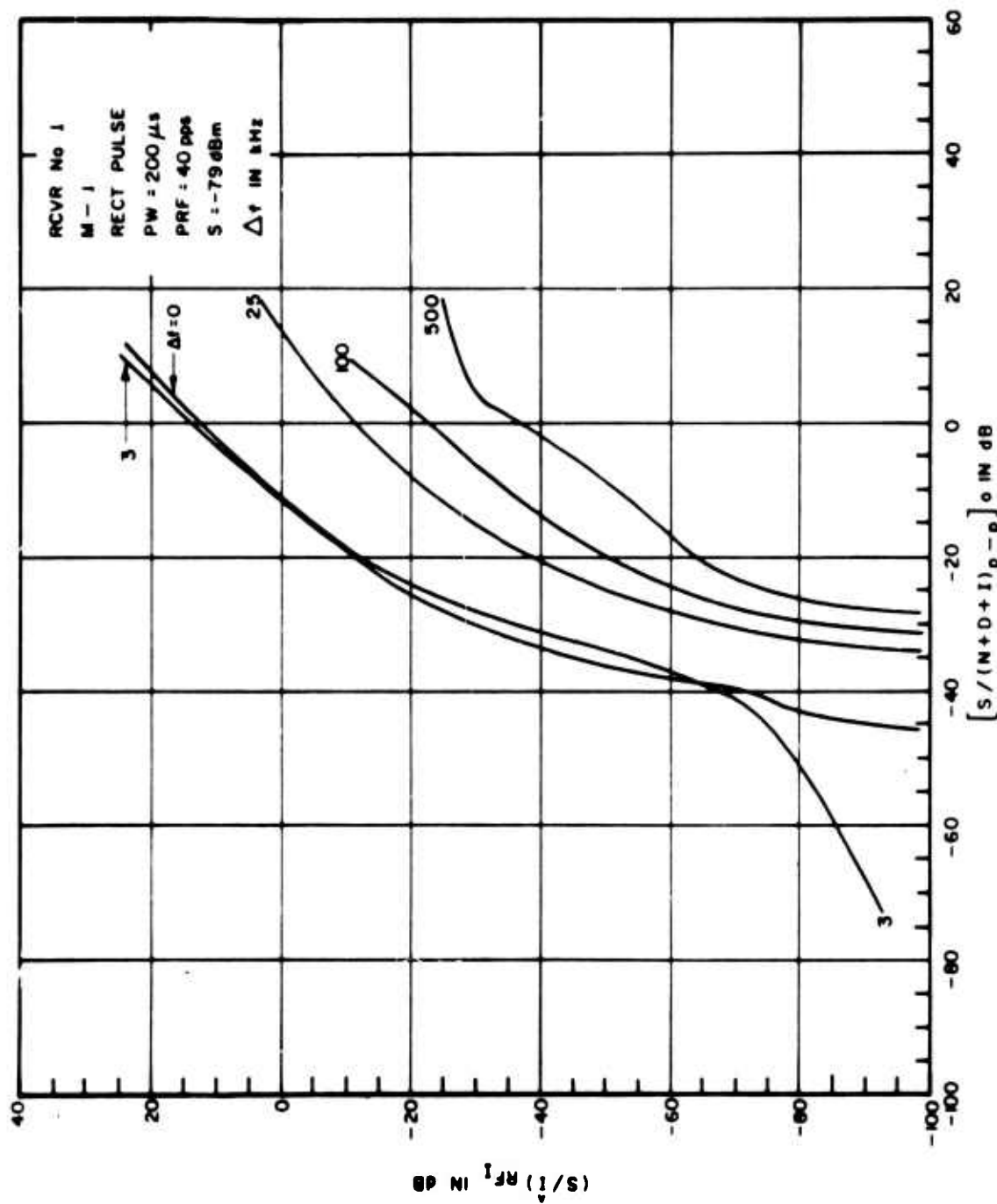


Figure III-113. Power Transfer Curves for Pulsed Interference to an AM Receiver

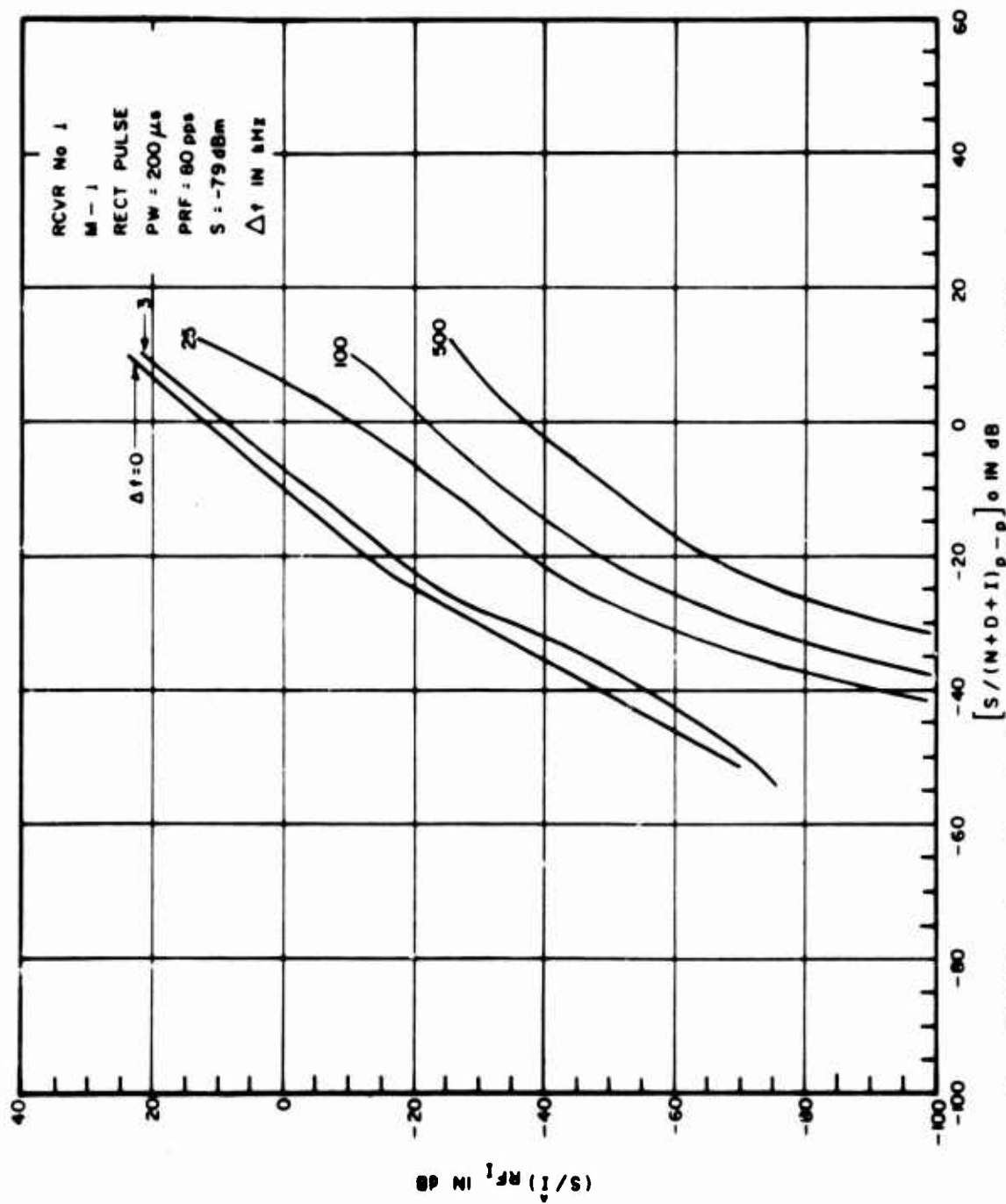


Figure III-114. Power Transfer Curves for Pulsed Interference to an AM Receiver

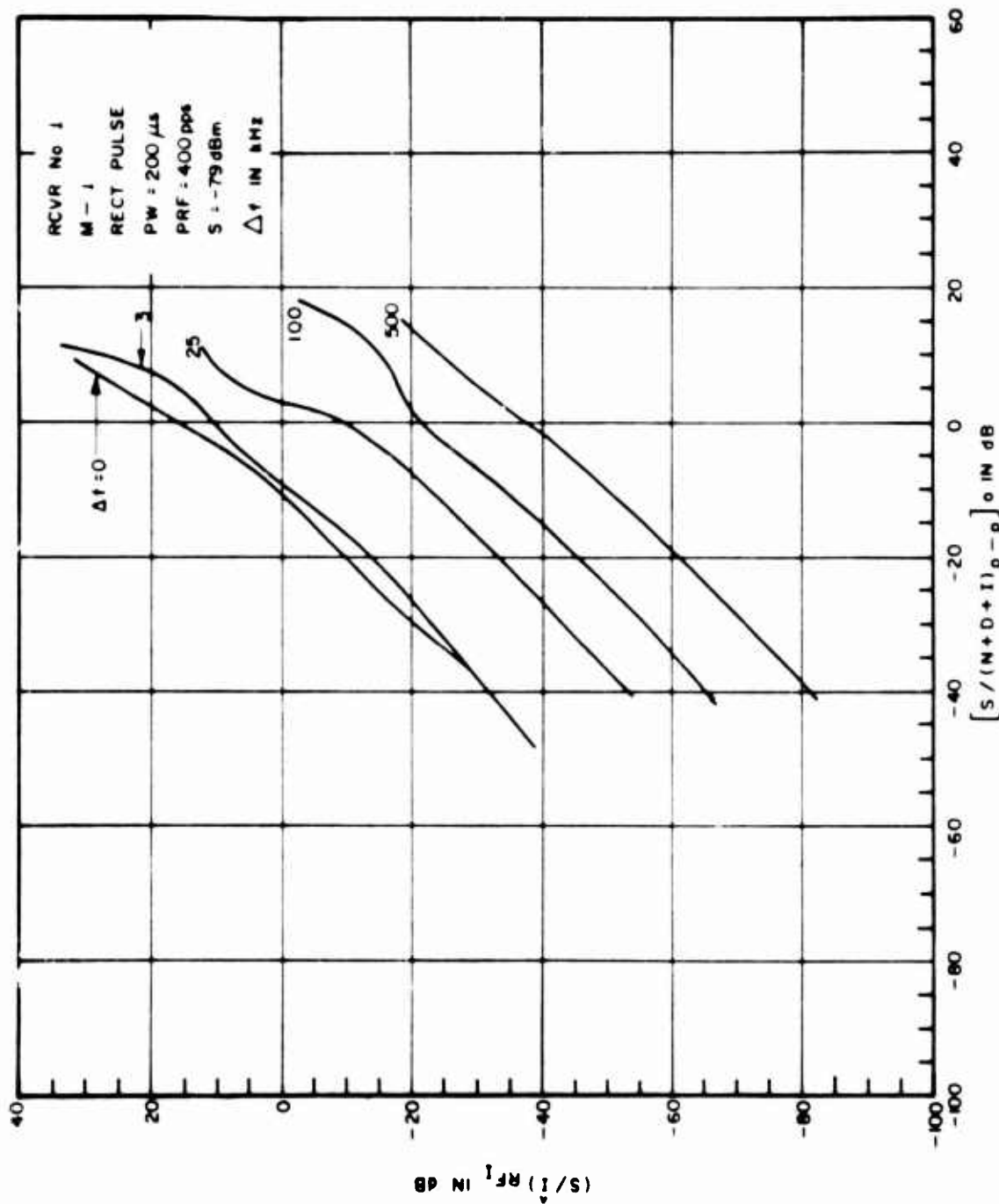


Figure III-115. Power Transfer Curves for Pulsed Interference to an AM Receiver

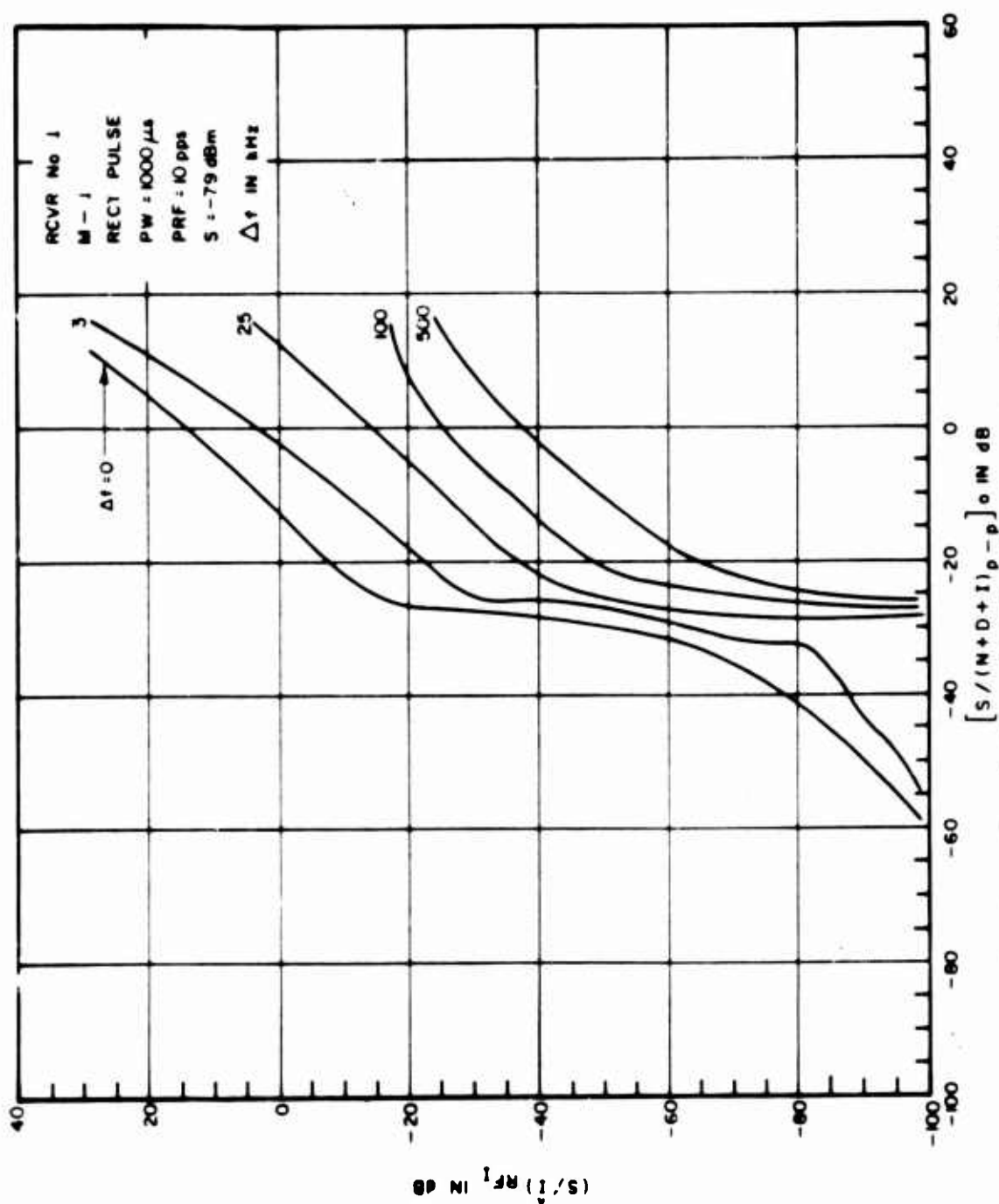


Figure III-116. Power Transfer Curves for Pulsed Interference to an AM Receiver

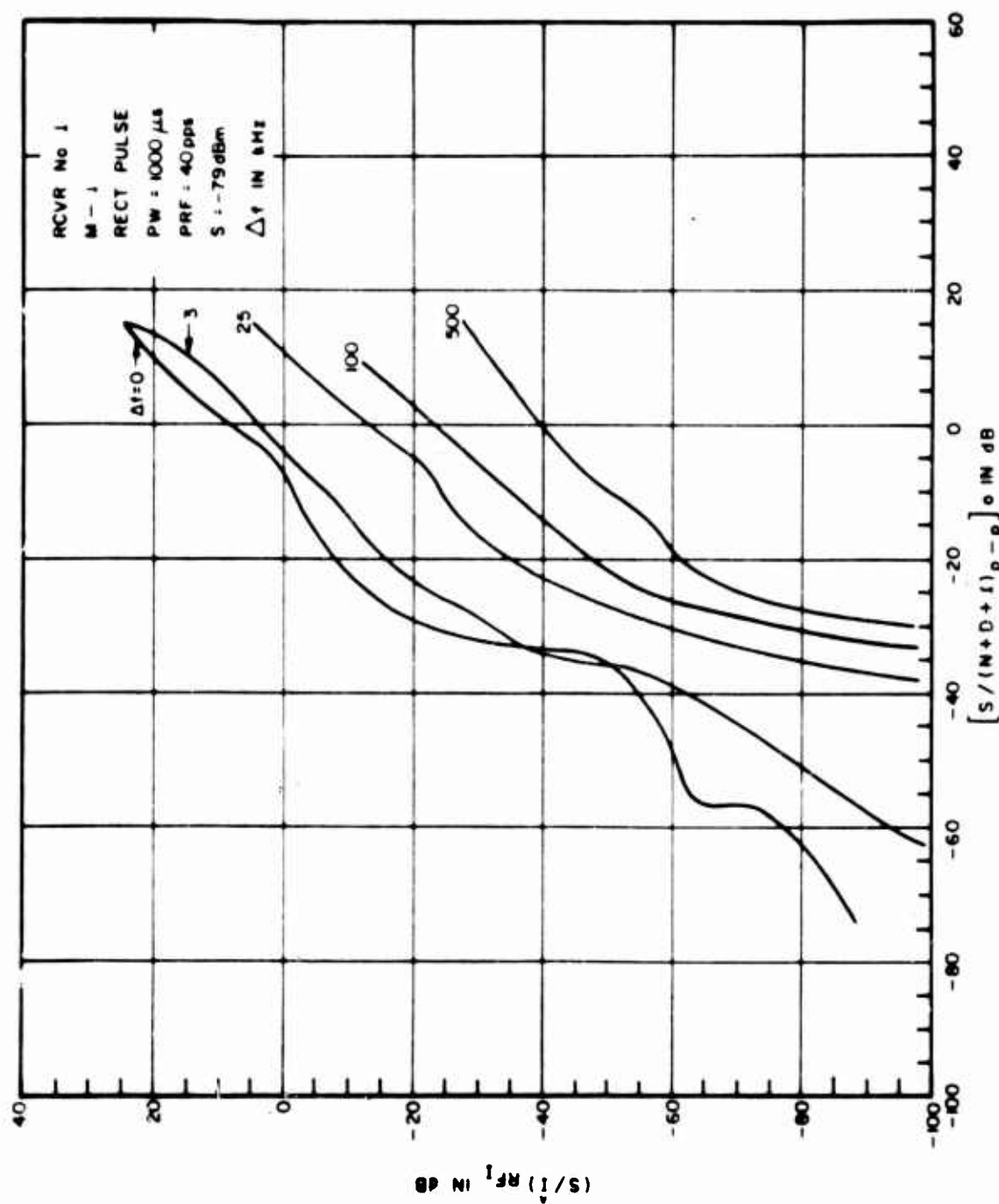


Figure III-117. Power Transfer Curves for Pulsed Interference to an AM Receiver

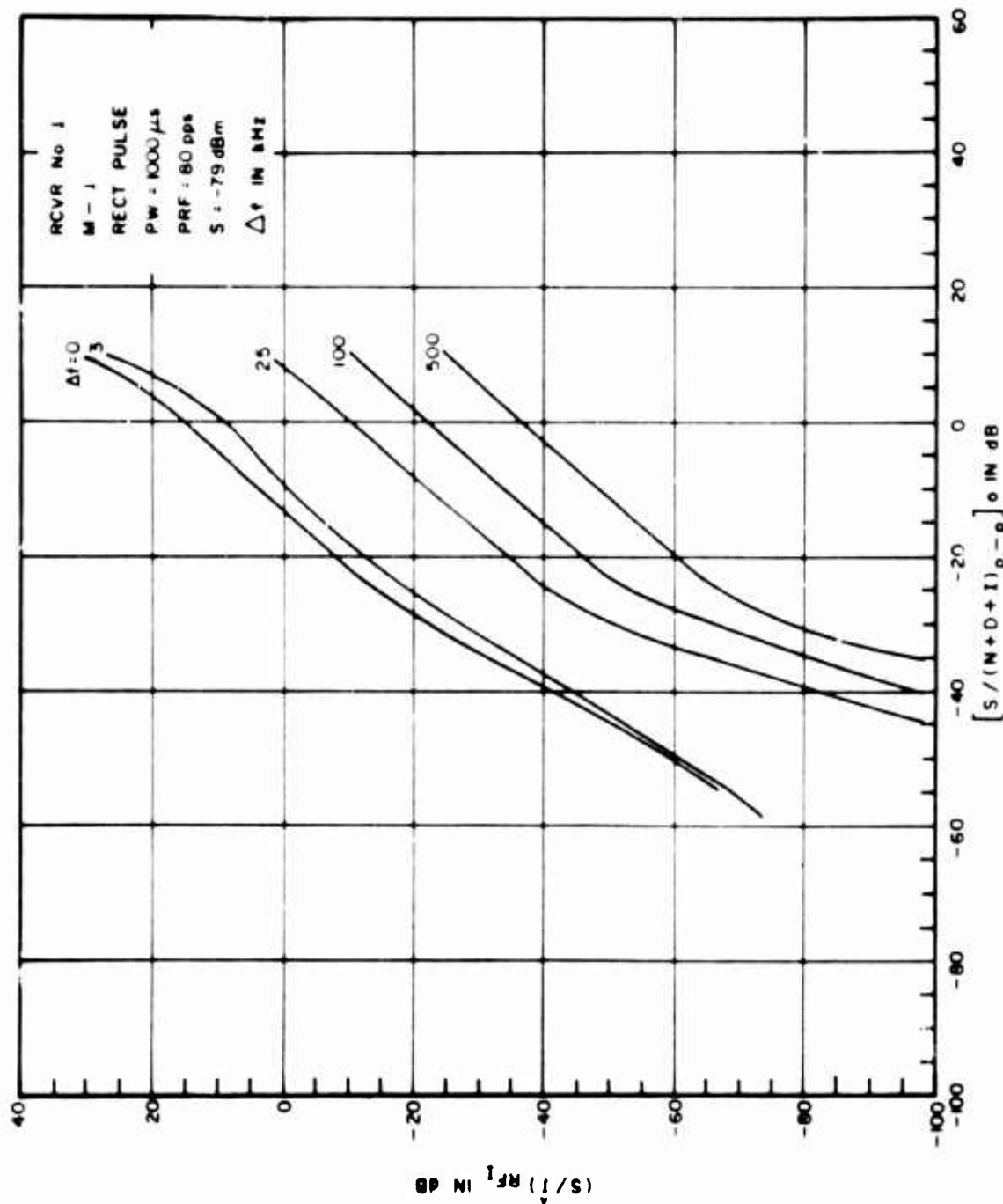


Figure III-118. Power Transfer Curves for Pulsed Interference to an AM Receiver

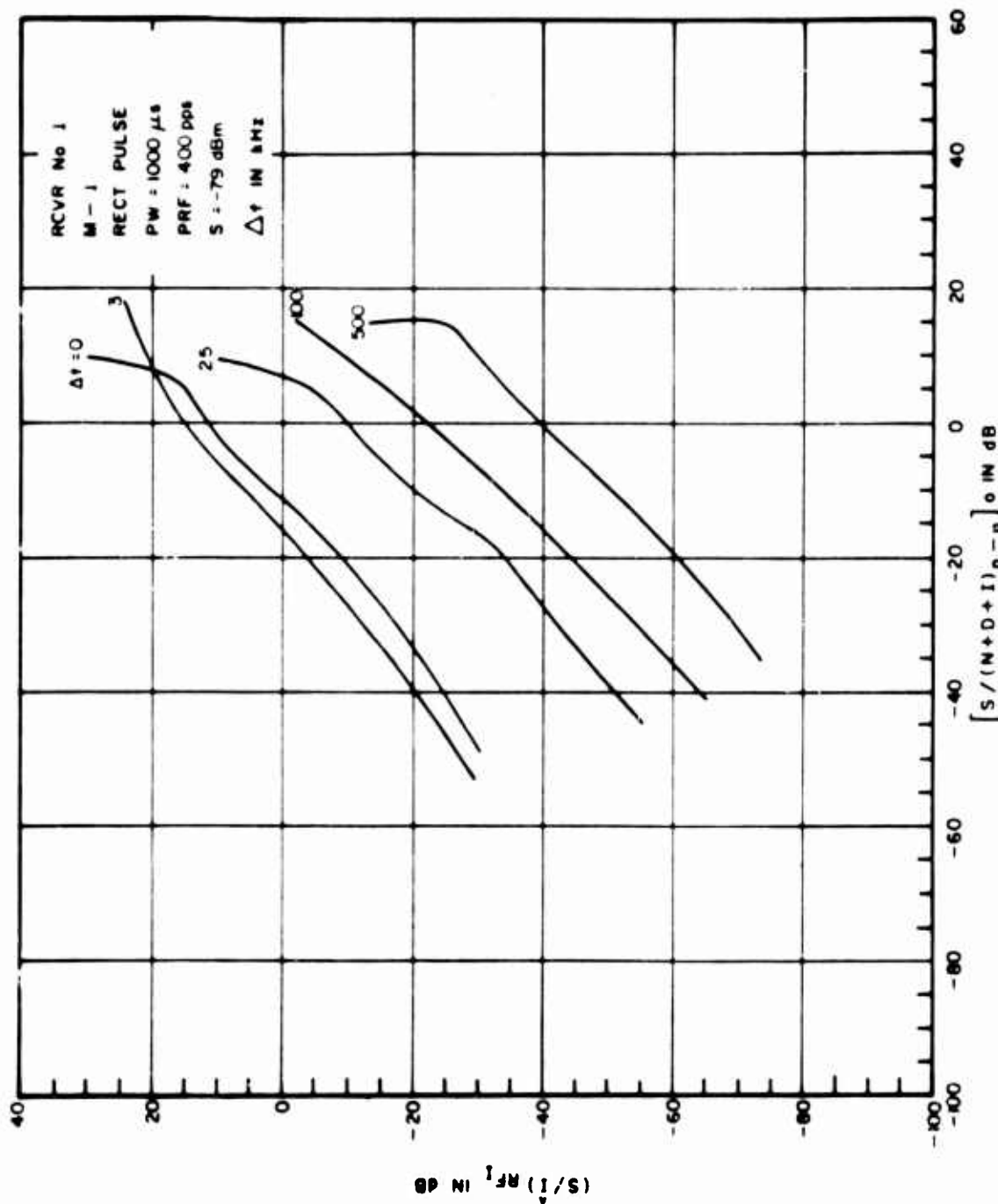


Figure III-119. Power Transfer Curves for Pulsed Interference to an AM Receiver

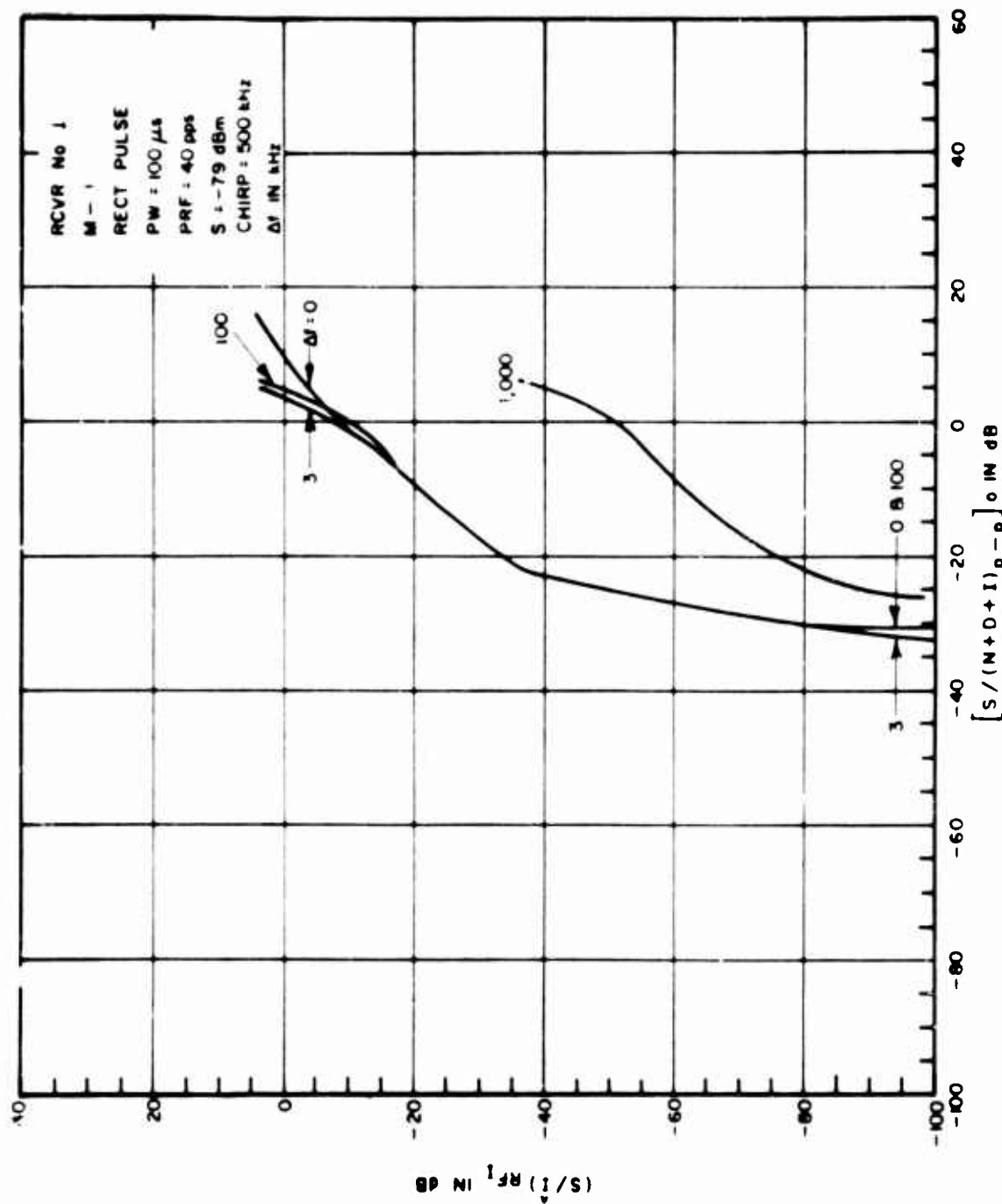


Figure III-120. Power Transfer Curves for Pulsed Interference to an AM Receiver

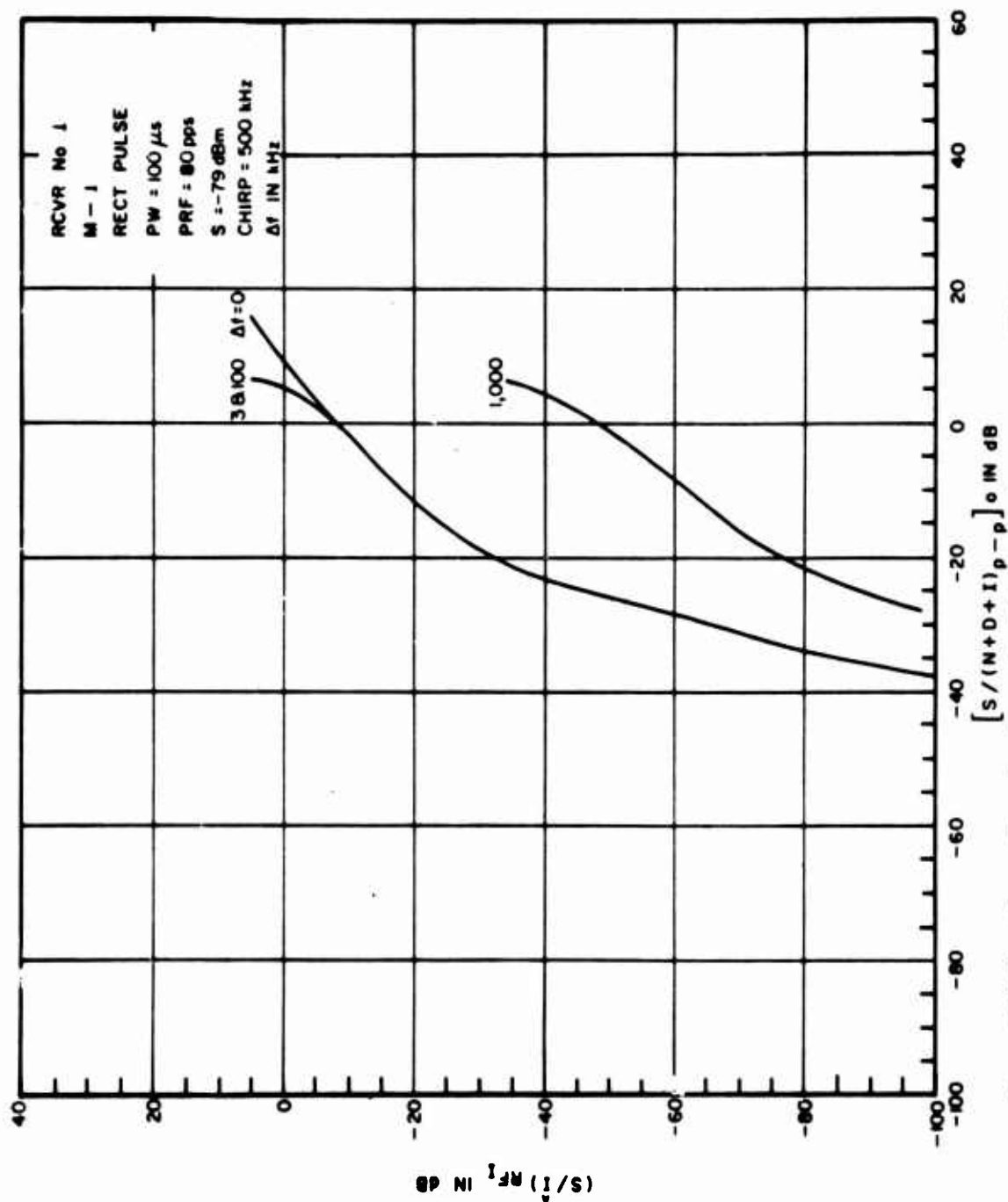


Figure III-121. Power Transfer Curves for Pulsed Interference to an AM Receiver

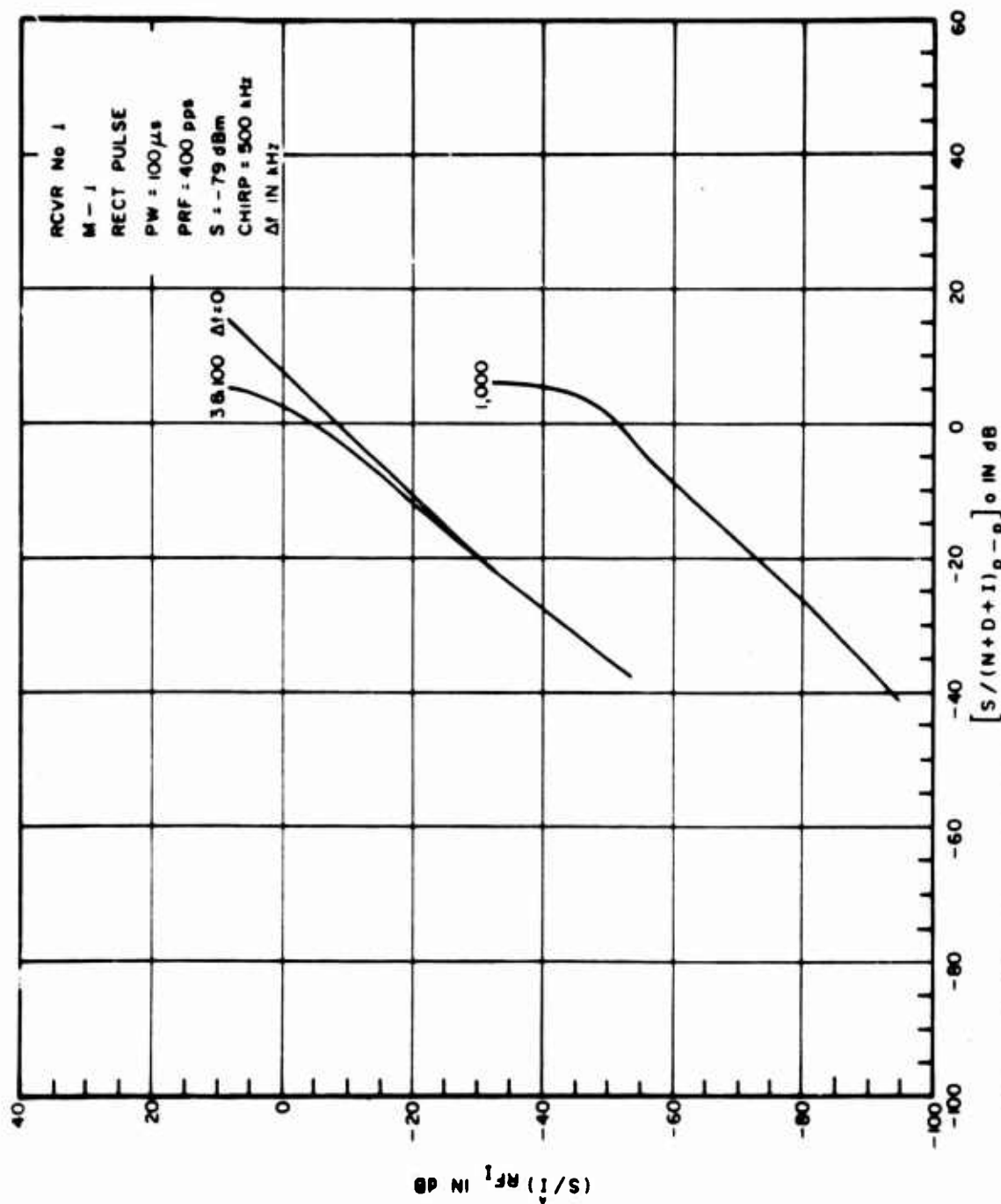


Figure III-122. Power Transfer Curves for Pulsed Interference to an AM Receiver

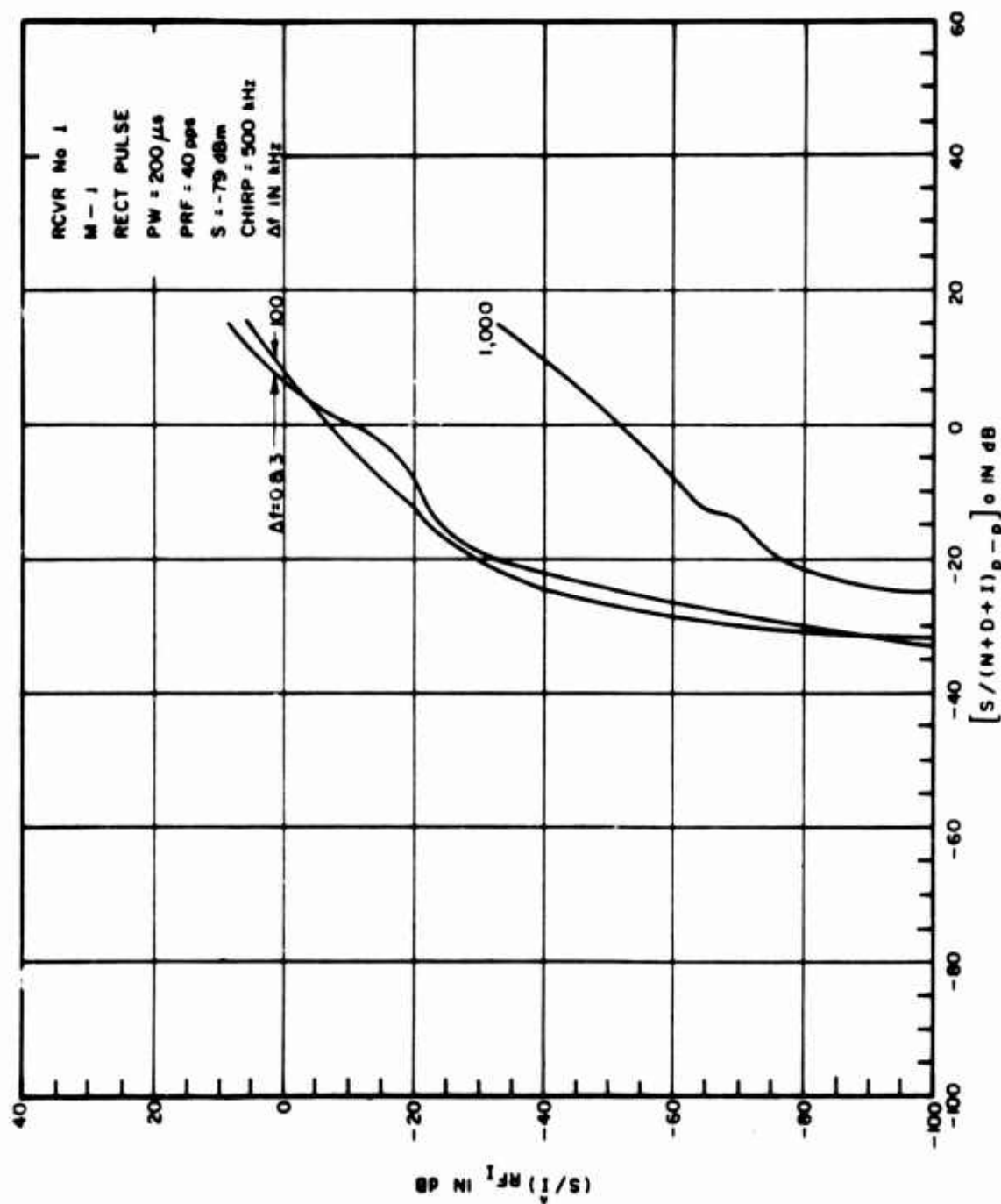


Figure III-123. Power Transfer Curves for Pulsed Interference to an AM Receiver

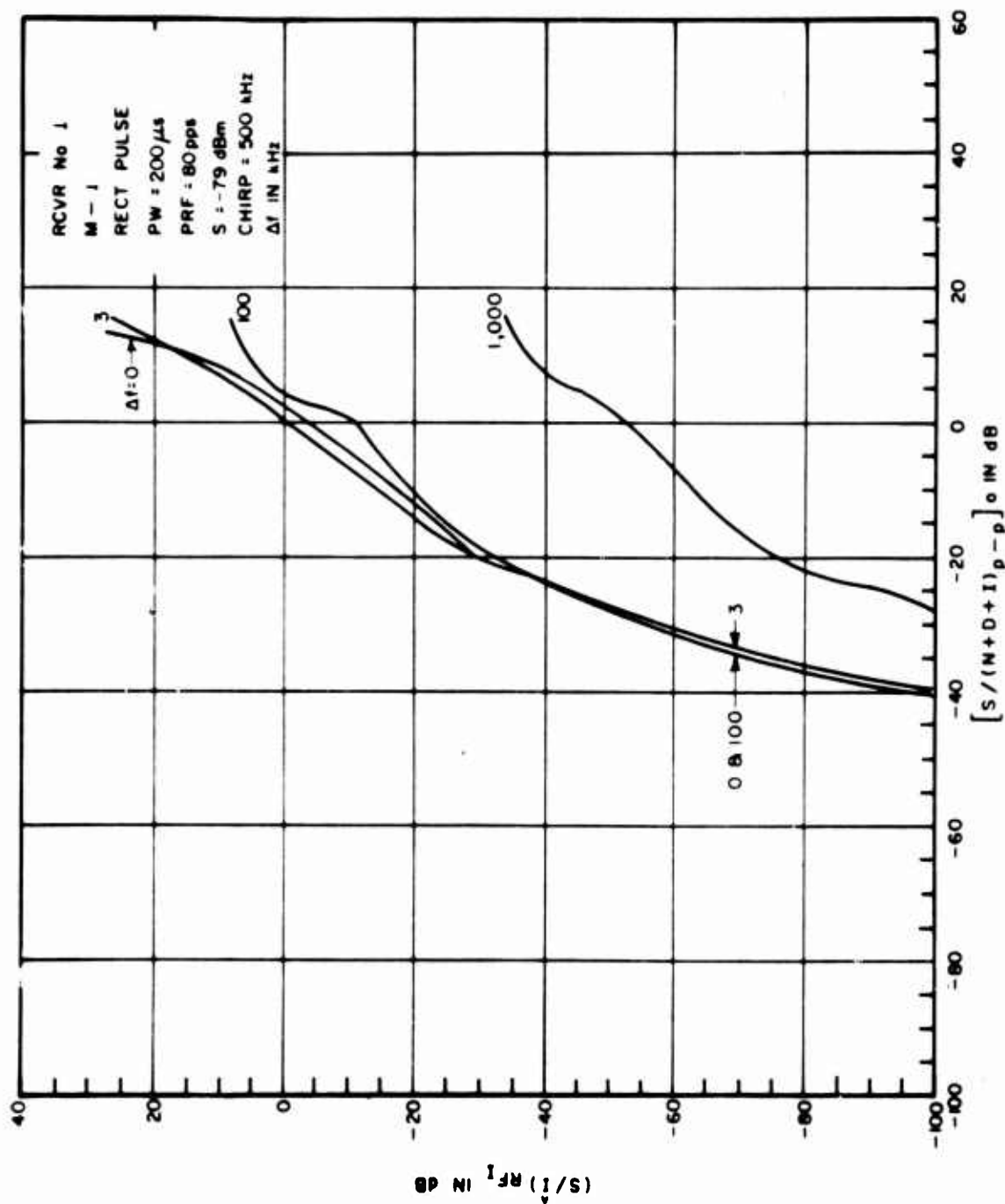


Figure III-124. Power Transfer Curves for Pulsed Interference to an AM Receiver

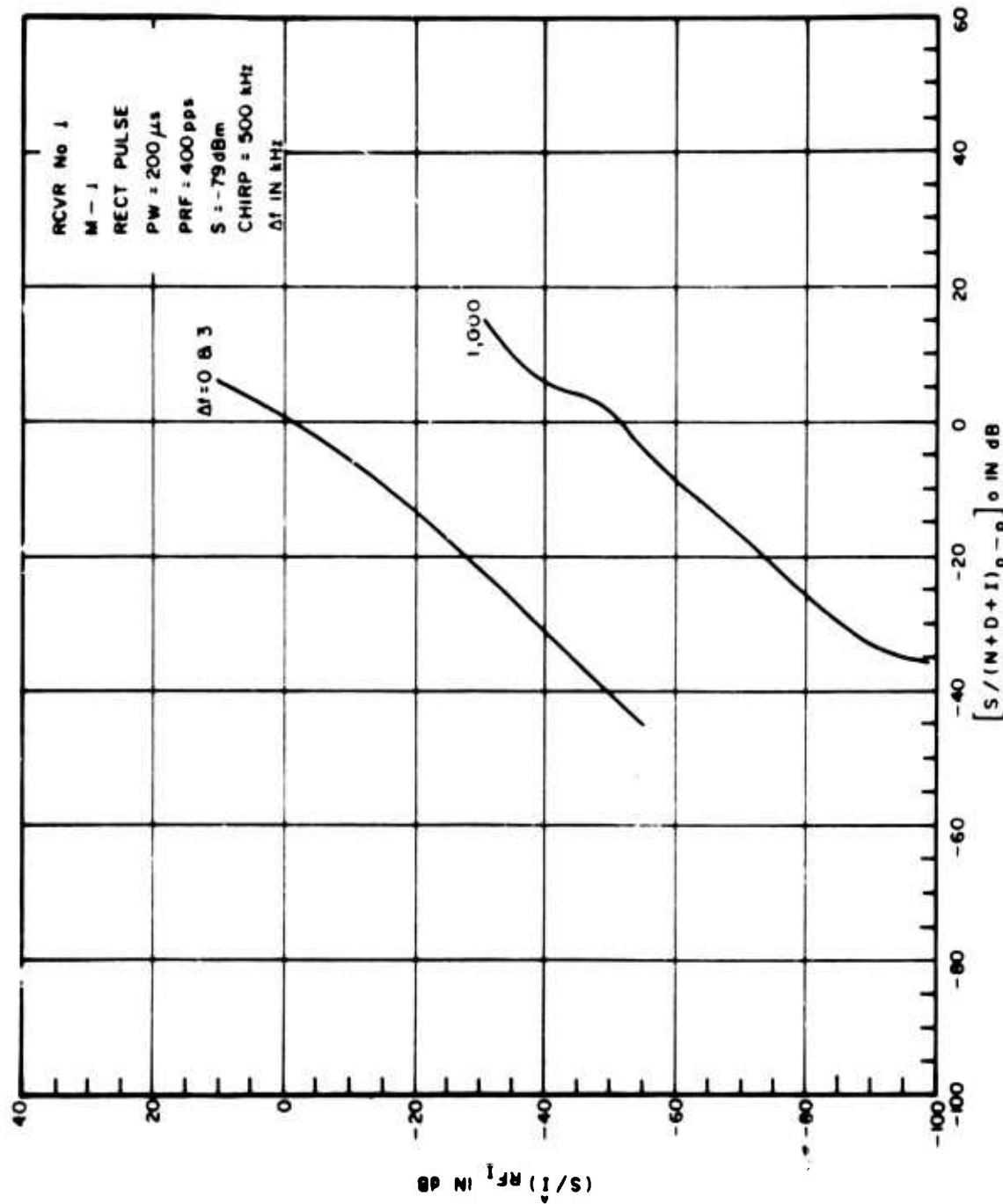


Figure III-125. Power Transfer Curves for Pulsed Interference to an AM Receiver

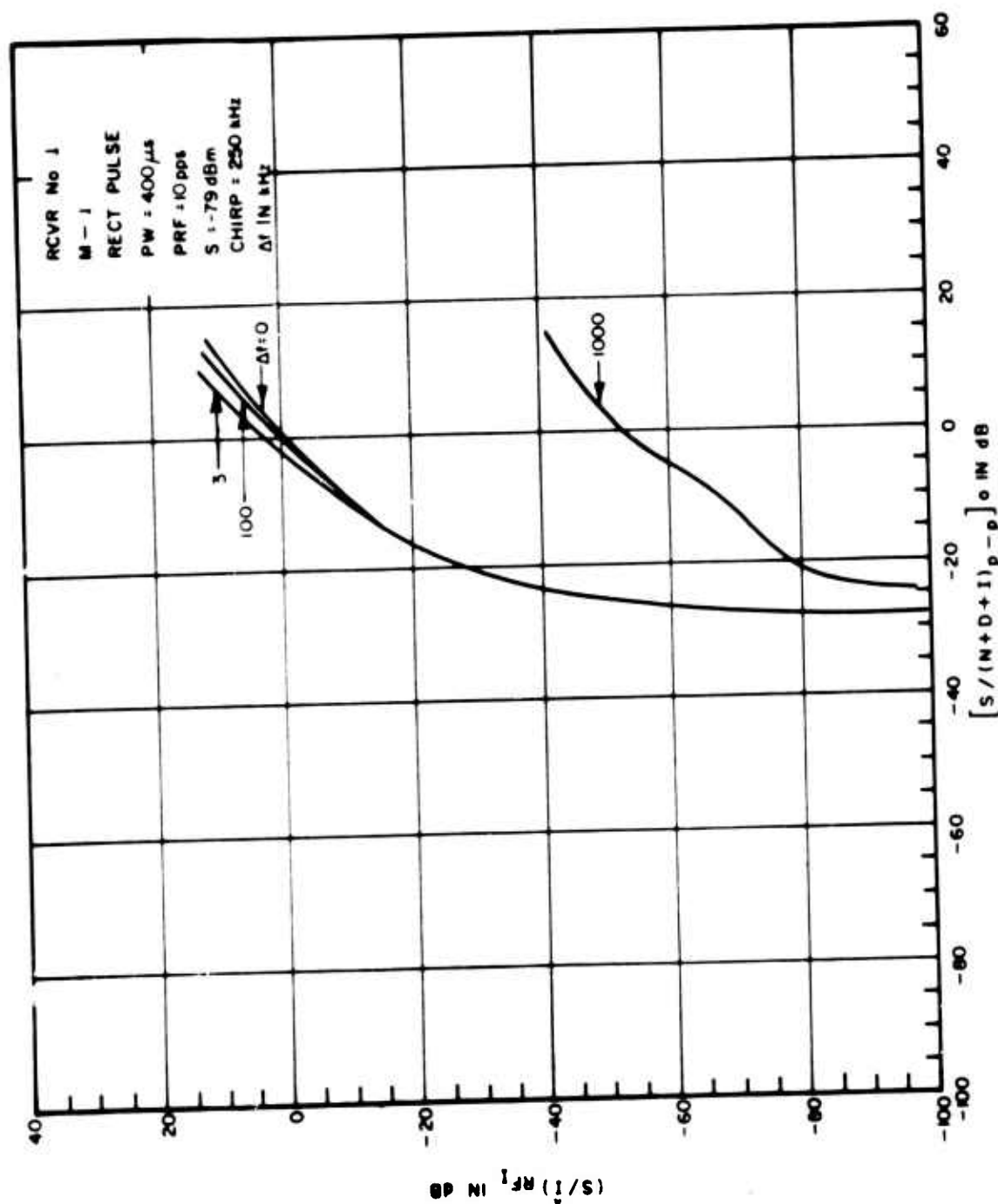


Figure III-126. Power Transfer Curves for Pulsed Interference to an AM Receiver

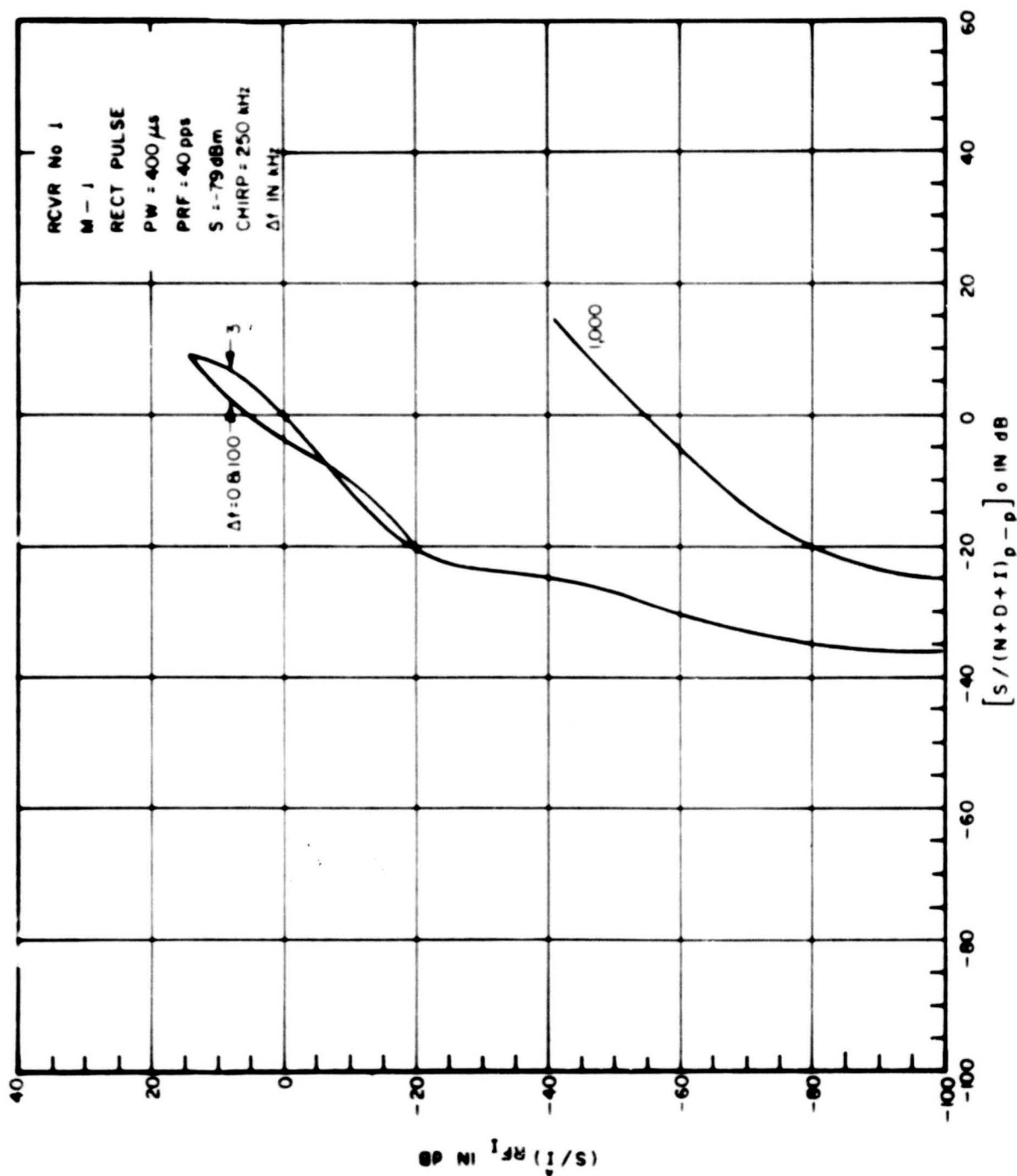


Figure III-127. Power Transfer Curves for Pulsed Interference to an AM Receiver

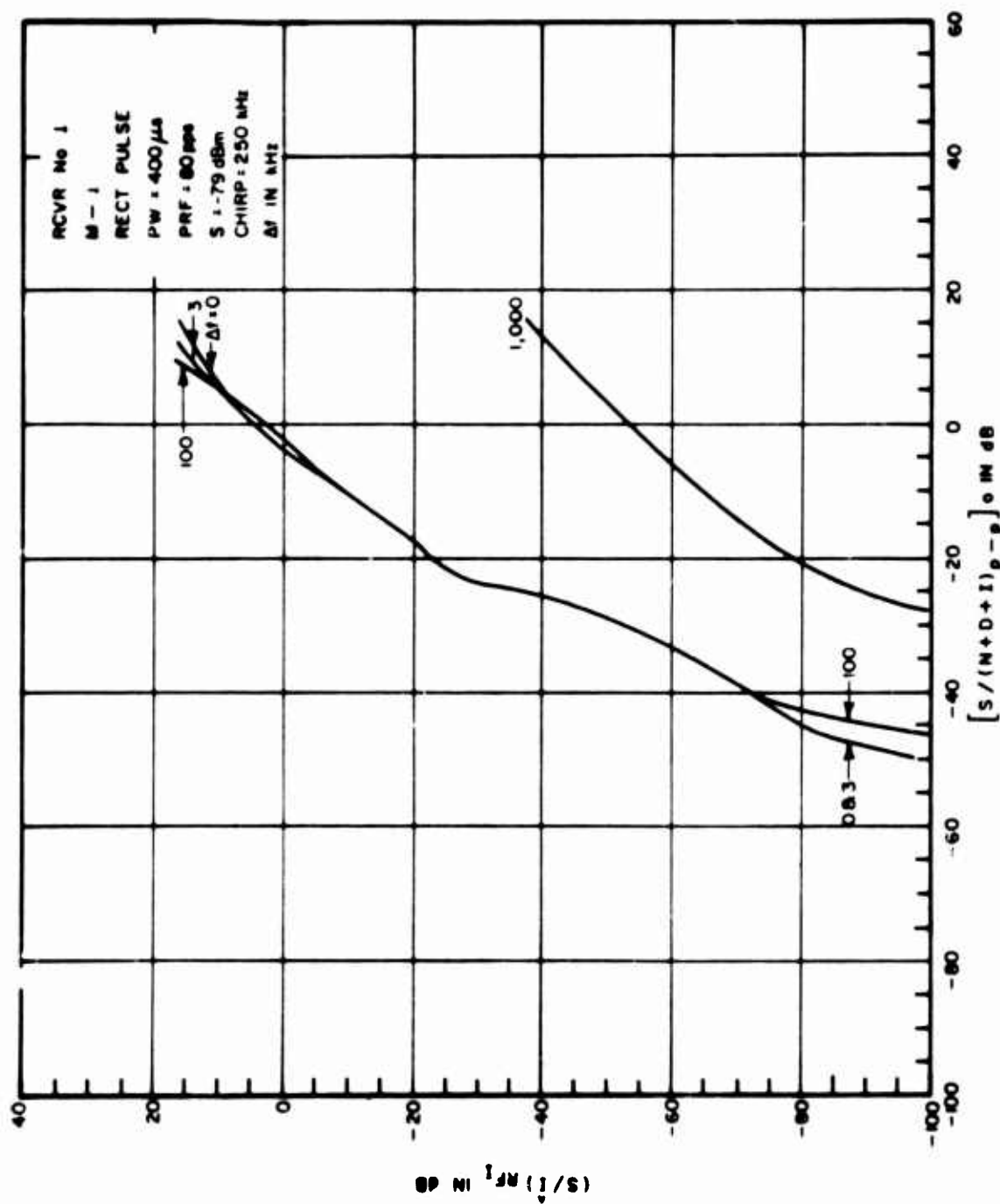


Figure III-128. Power Transfer Curves for Pulsed Interference to an AM Receiver

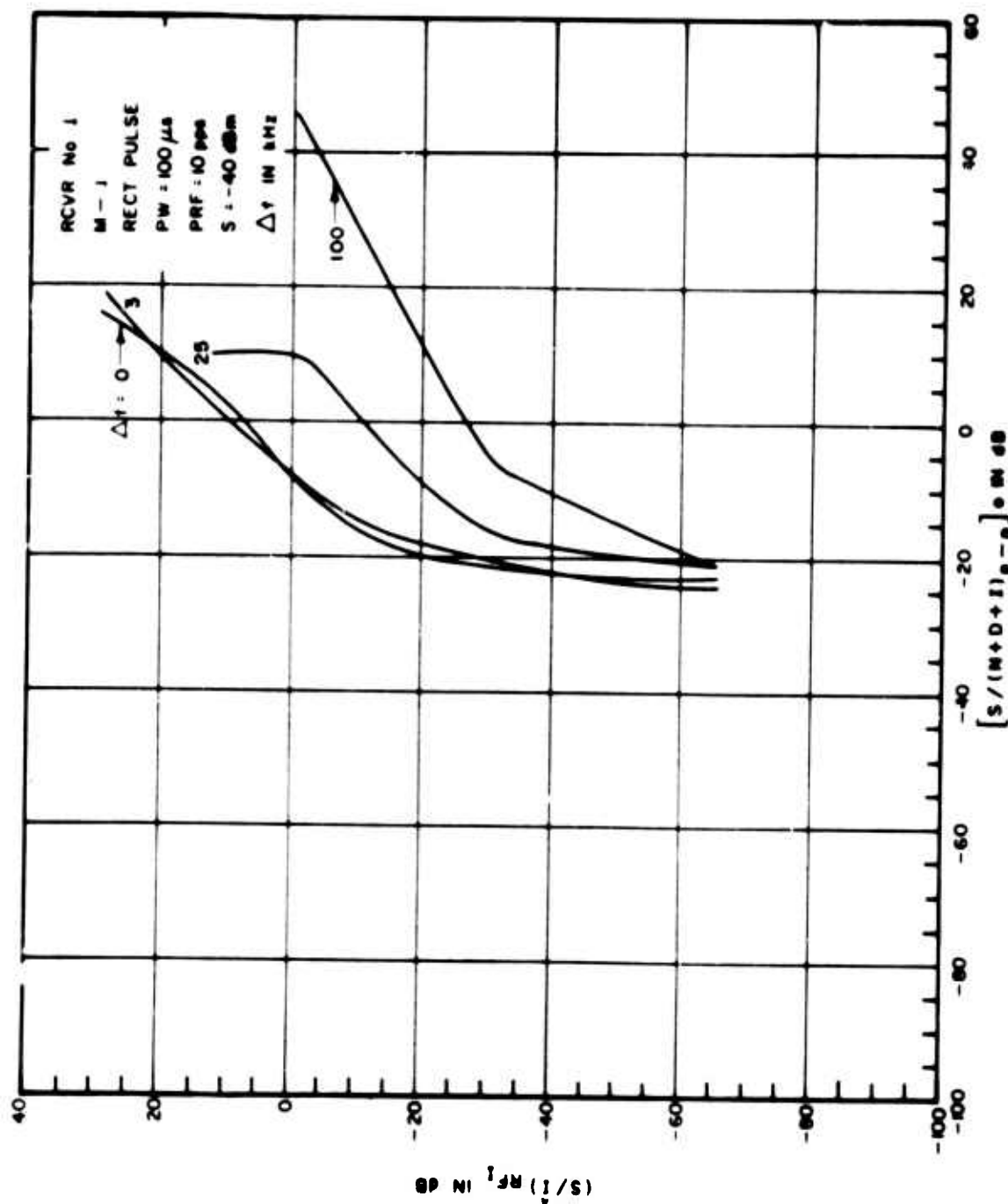


Figure III-129. Power Transfer Curves for Pulsed Interference to an AM Receiver

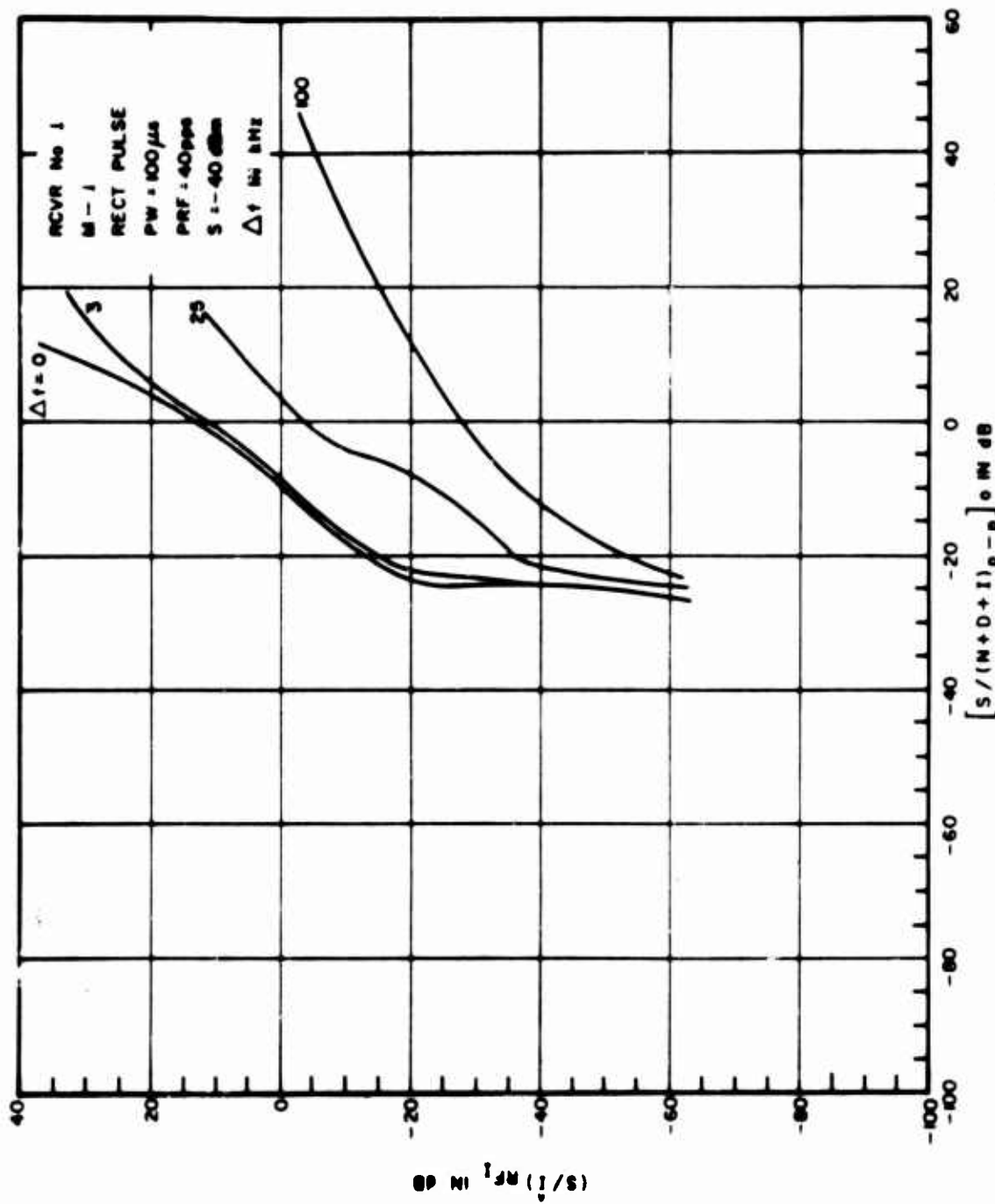


Figure III-130. Power Transfer Curves for Pulsed Interference to an AM Receiver

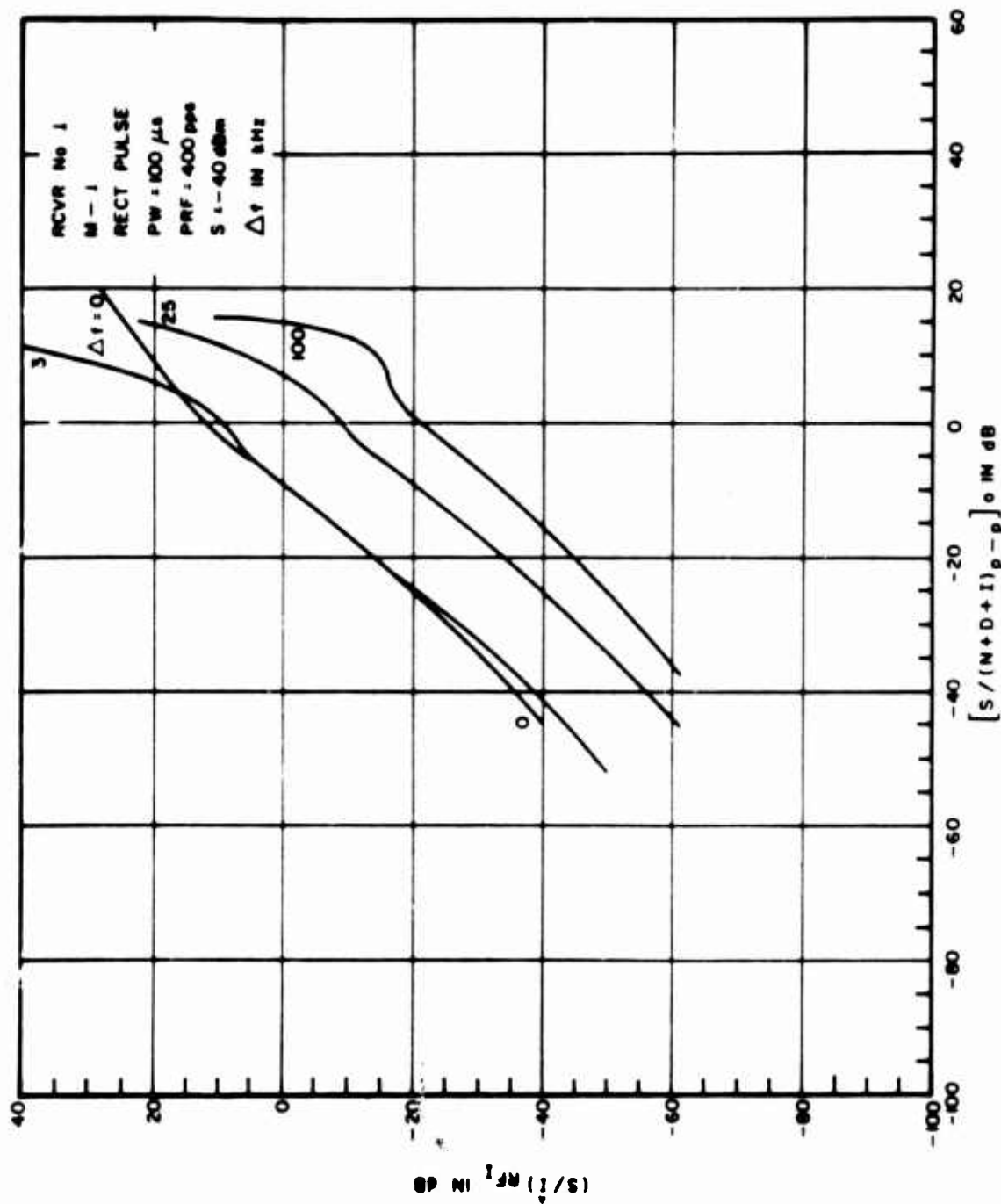


Figure III-131. Power Transfer Curves for Pulsed Interference to an AM Receiver

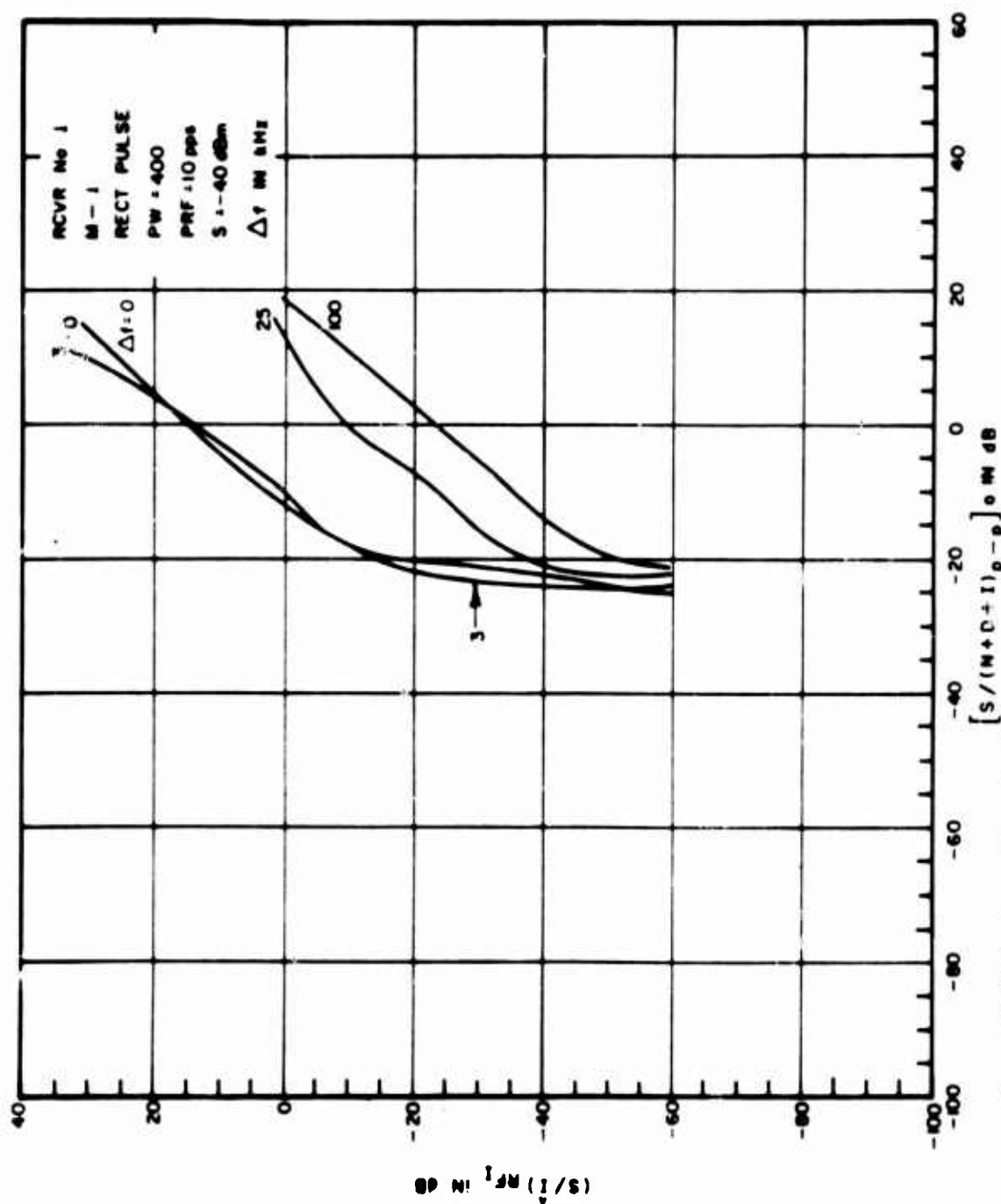


Figure III-132. Power Transfer Curves for Pulsed Interference to an AM Receiver

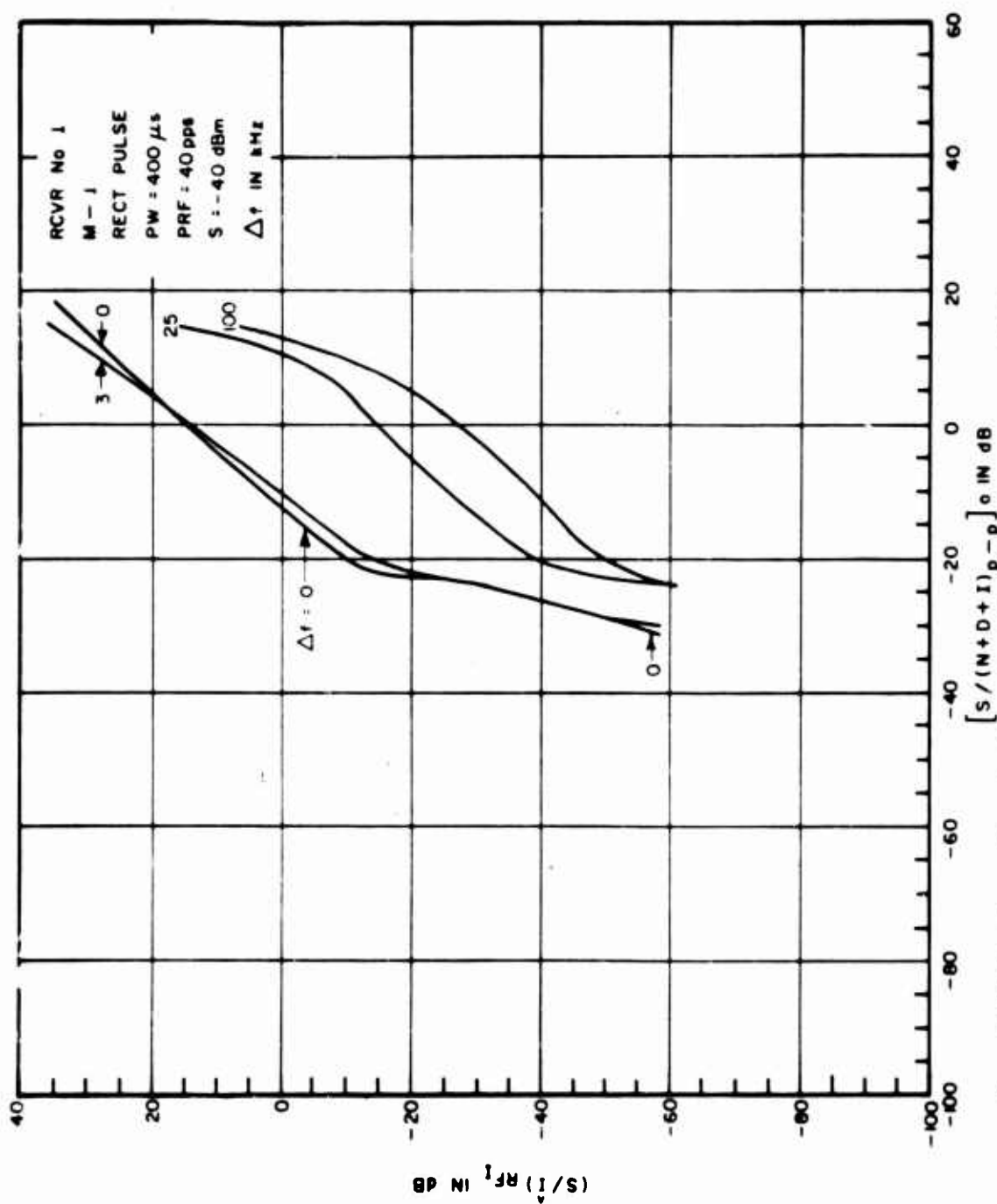


Figure III-133. Power Transfer Curves for Pulsed Interference to an AM Receiver

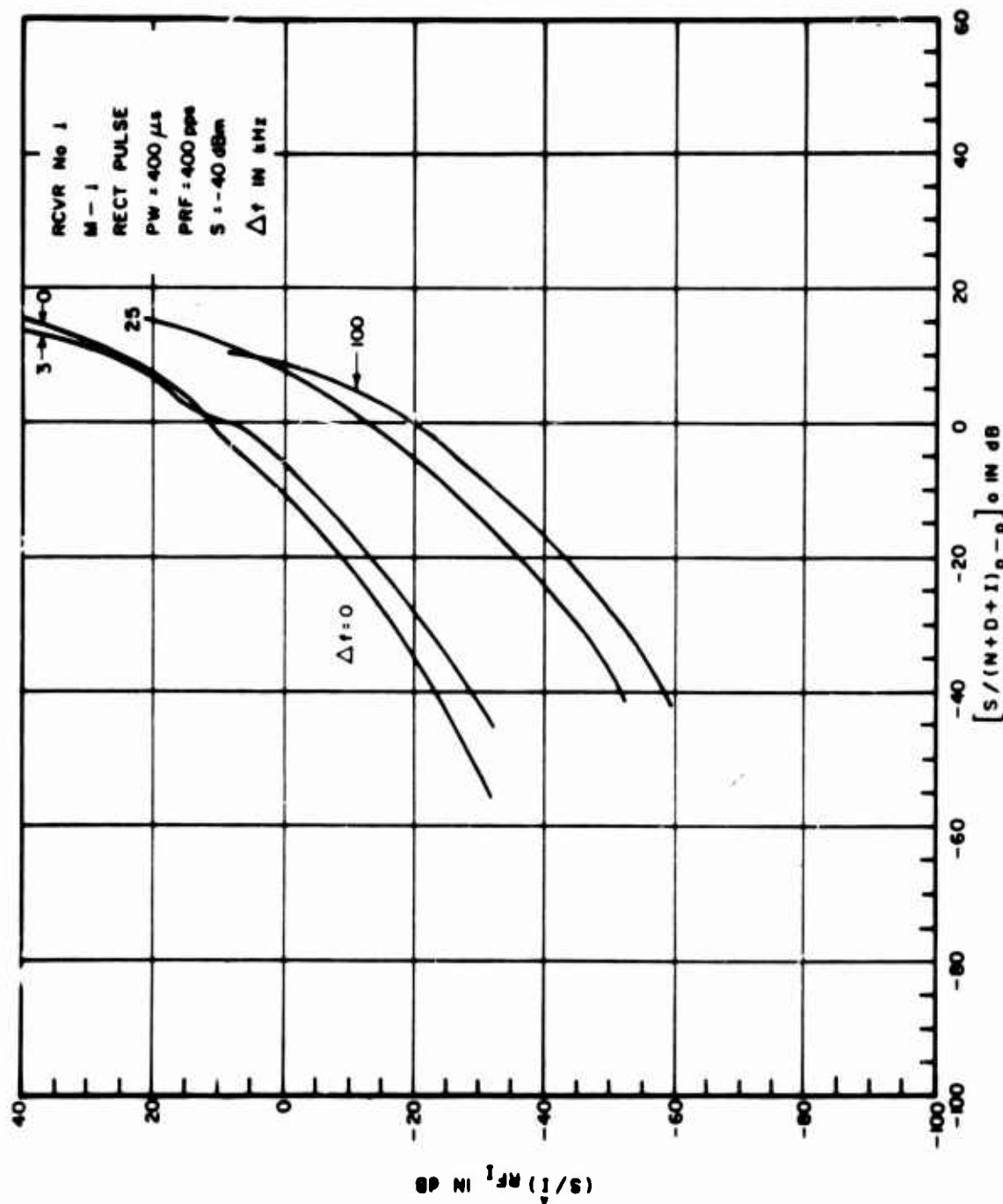


Figure III-134. Power Transfer Curves for Pulsed Interference to an AM Receiver

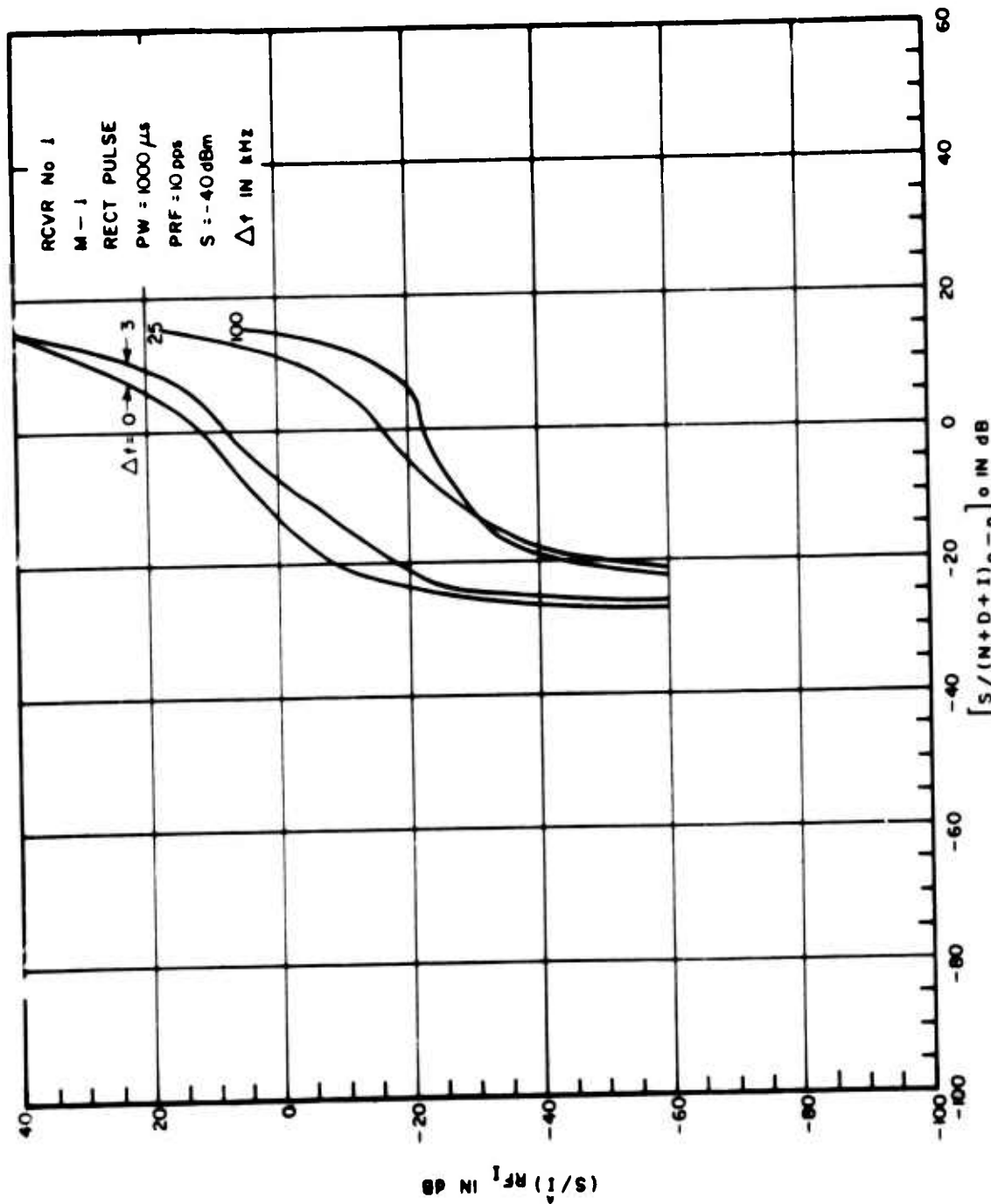


Figure III-135. Power Transfer Curves for Pulsed Interference to an AM Receiver

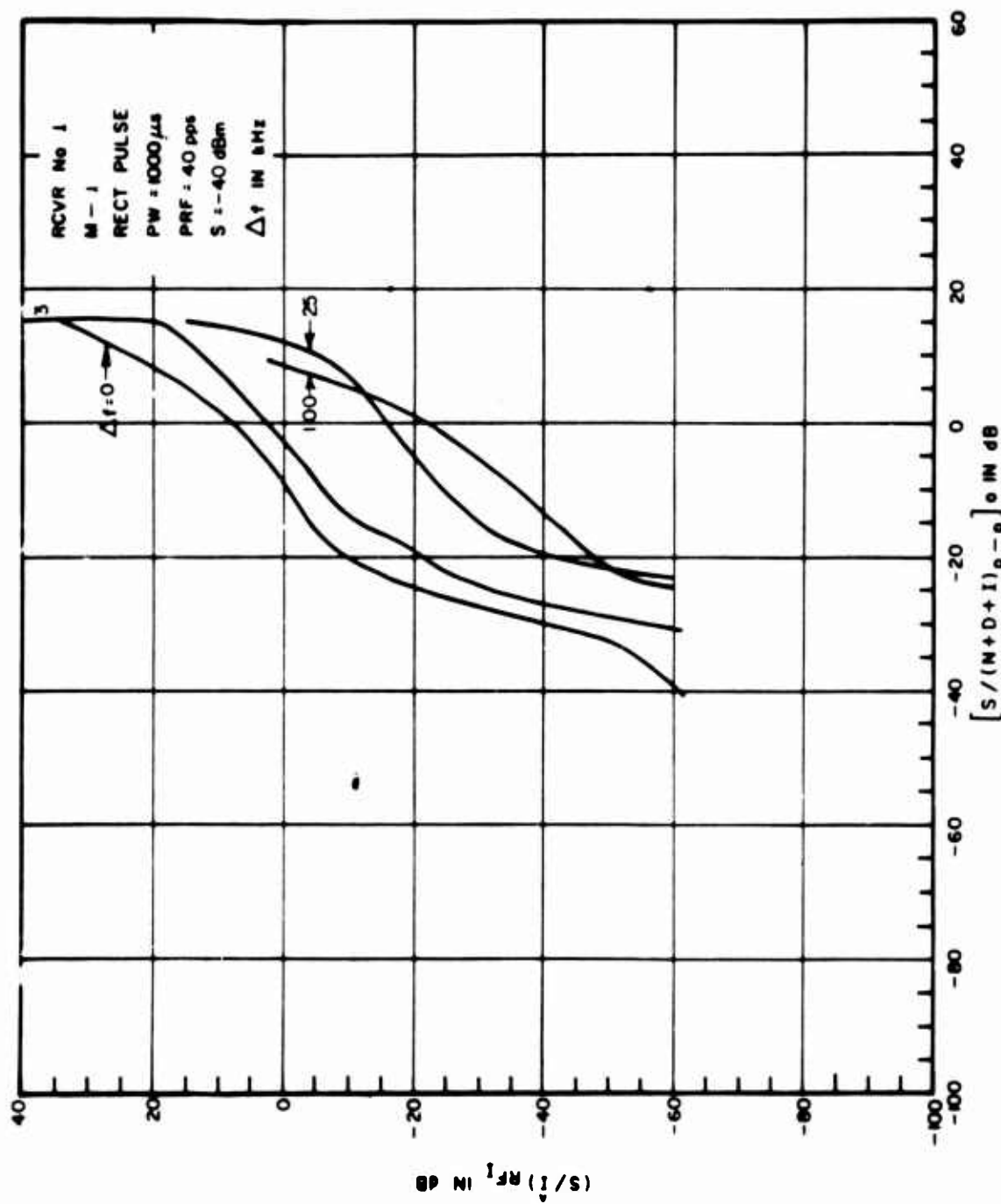


Figure III-136. Power Transfer Curves for Pulsed Interference to an AM Receiver

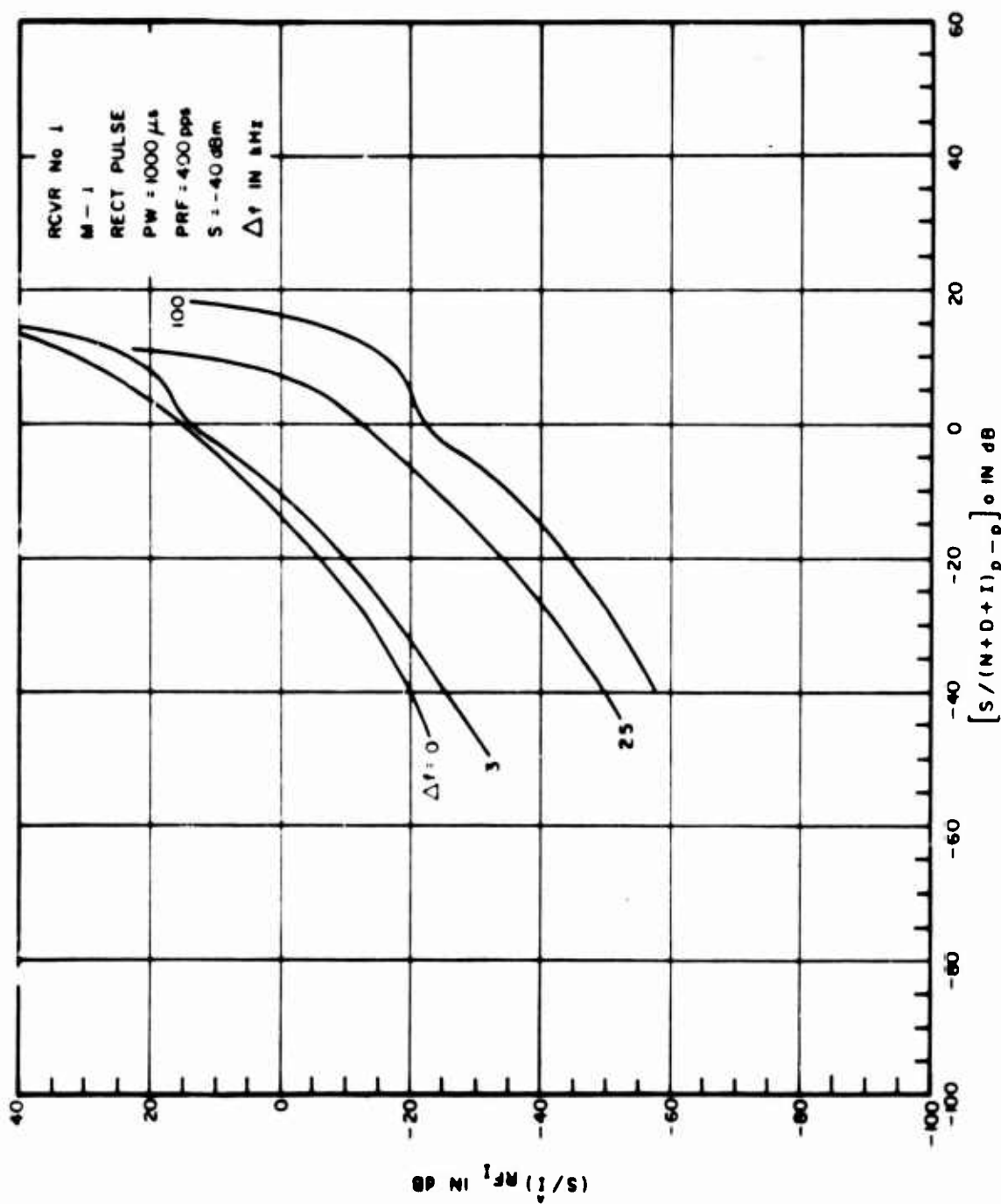


Figure III-137. Power Transfer Curves for Pulsed Interference to an AM Receiver

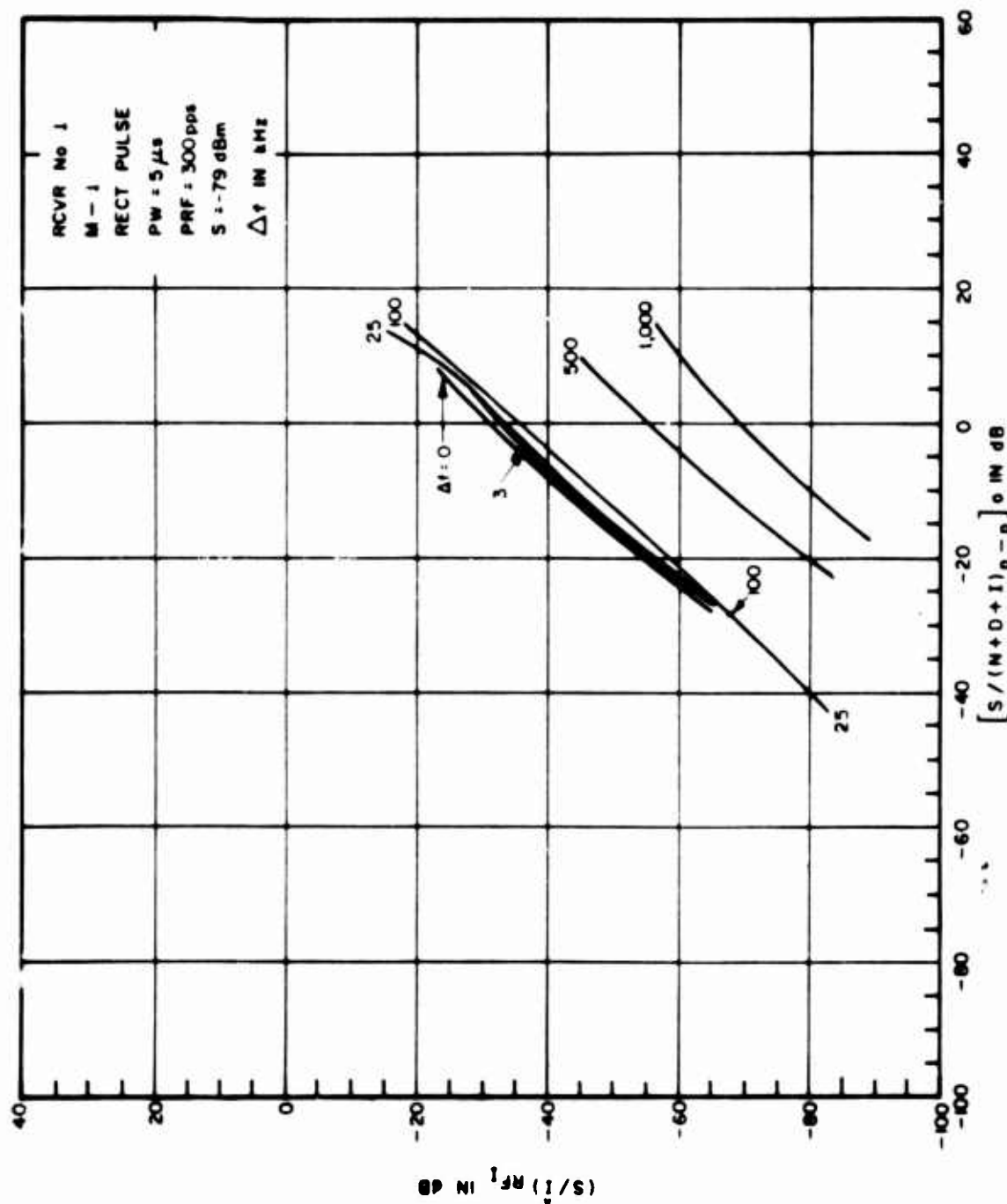


Figure III-138. Power Transfer Curves for Pulsed Interference to an AM Receiver

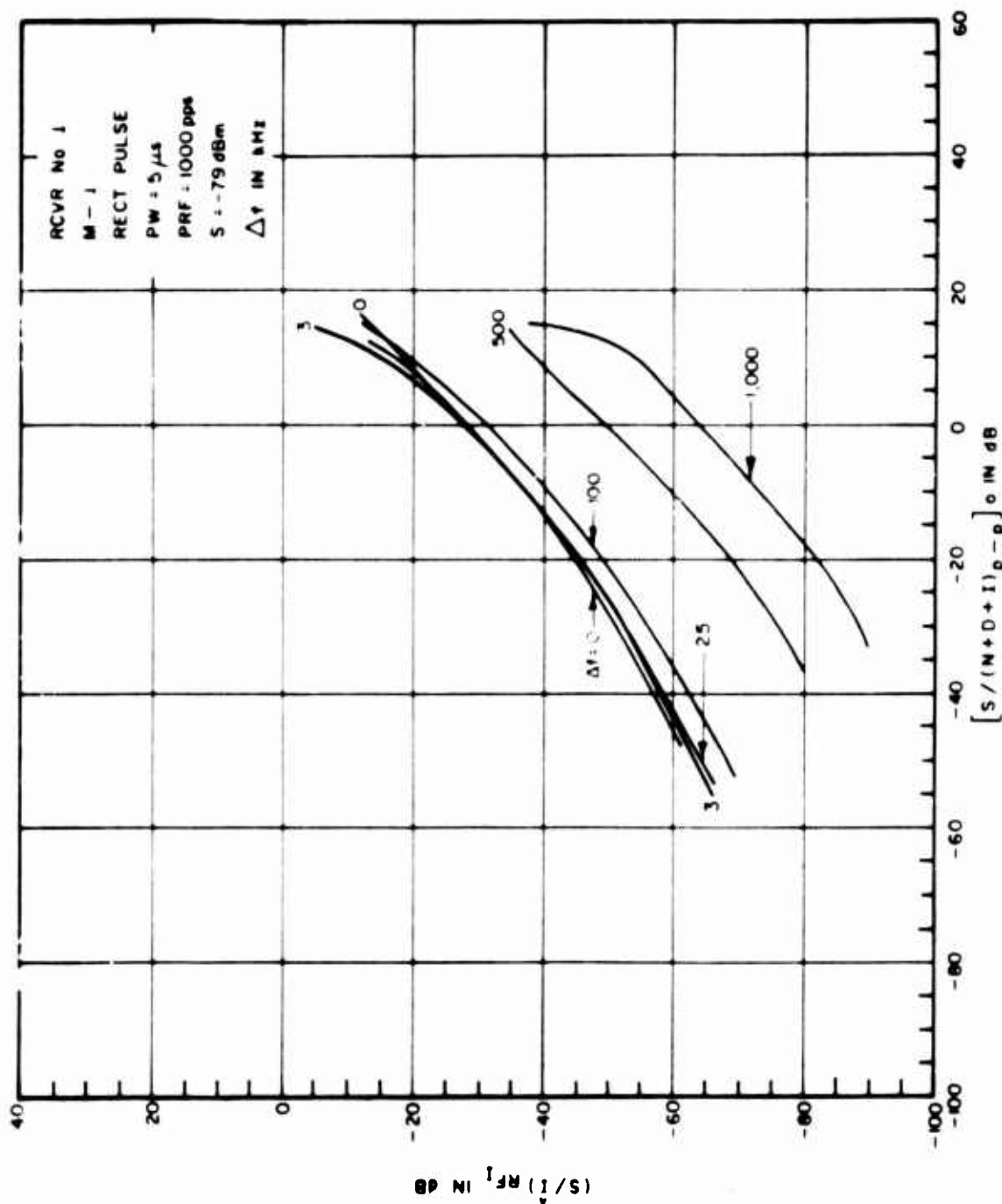


Figure III-139. Power Transfer Curves for Pulsed Interference to an AM Receiver

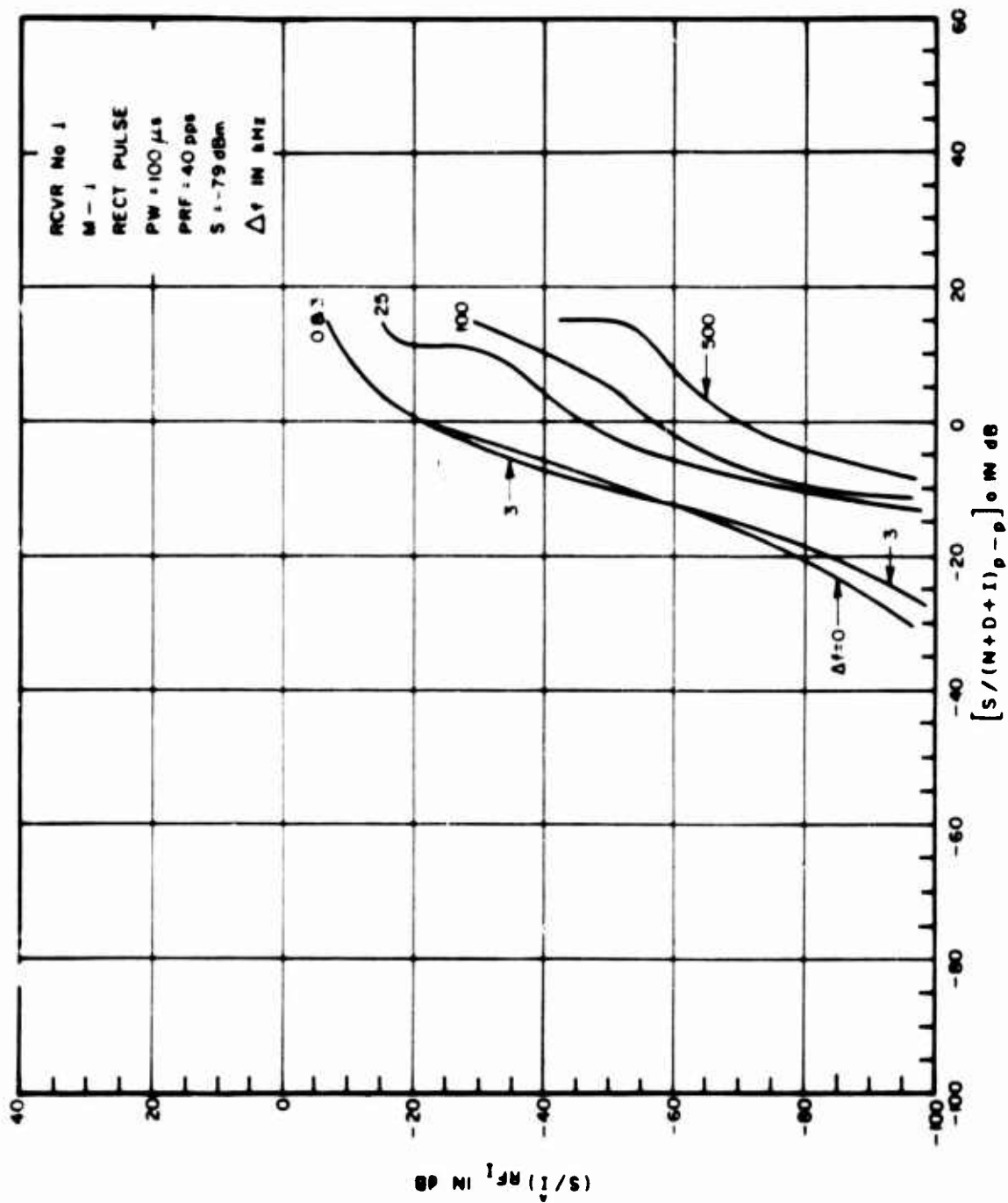


Figure III-140. Power Transfer Curves for Pulsed Interference to an AM Receiver

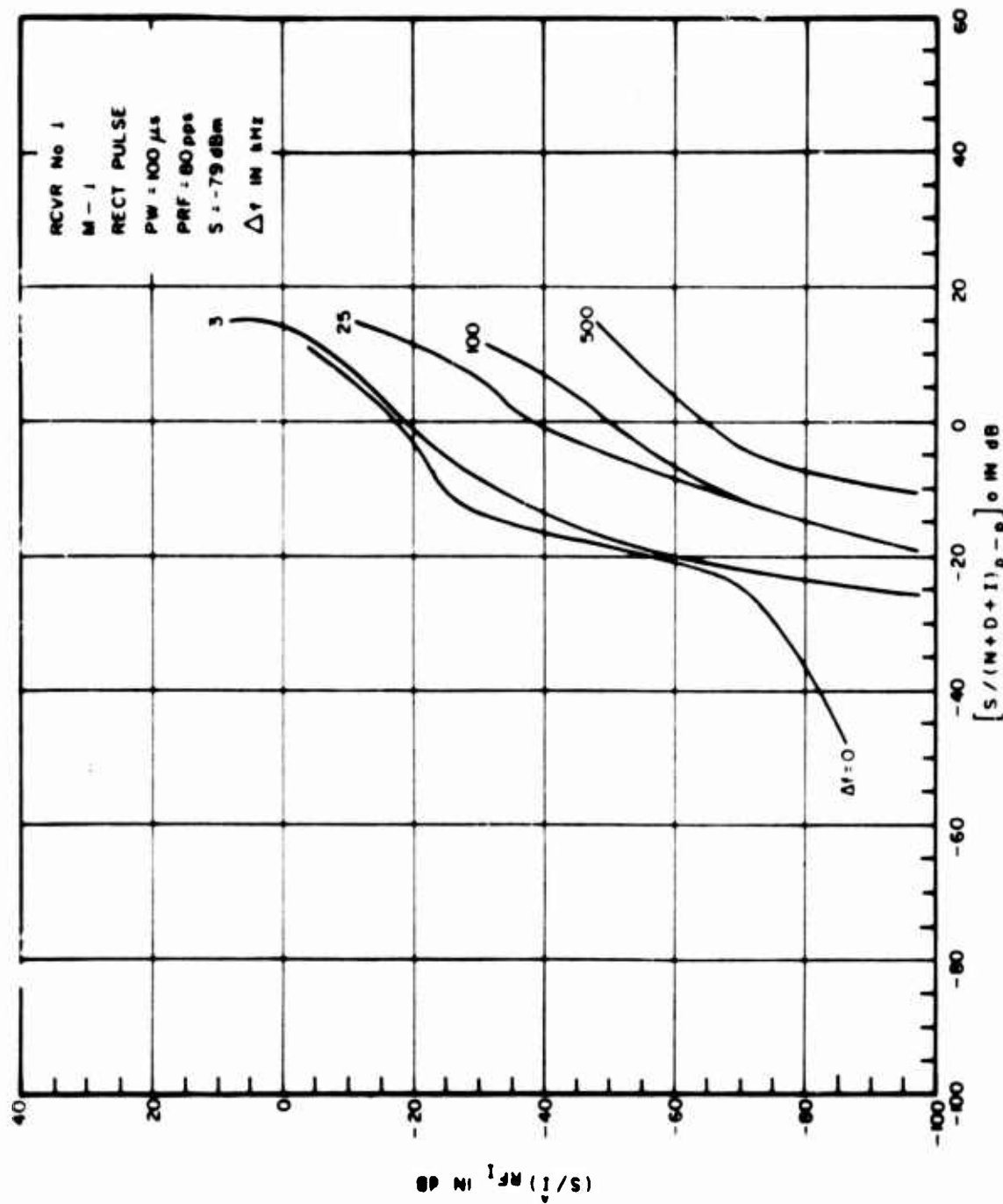


Figure III-141. Power Transfer Curves for Pulsed Interference to an AM Receiver

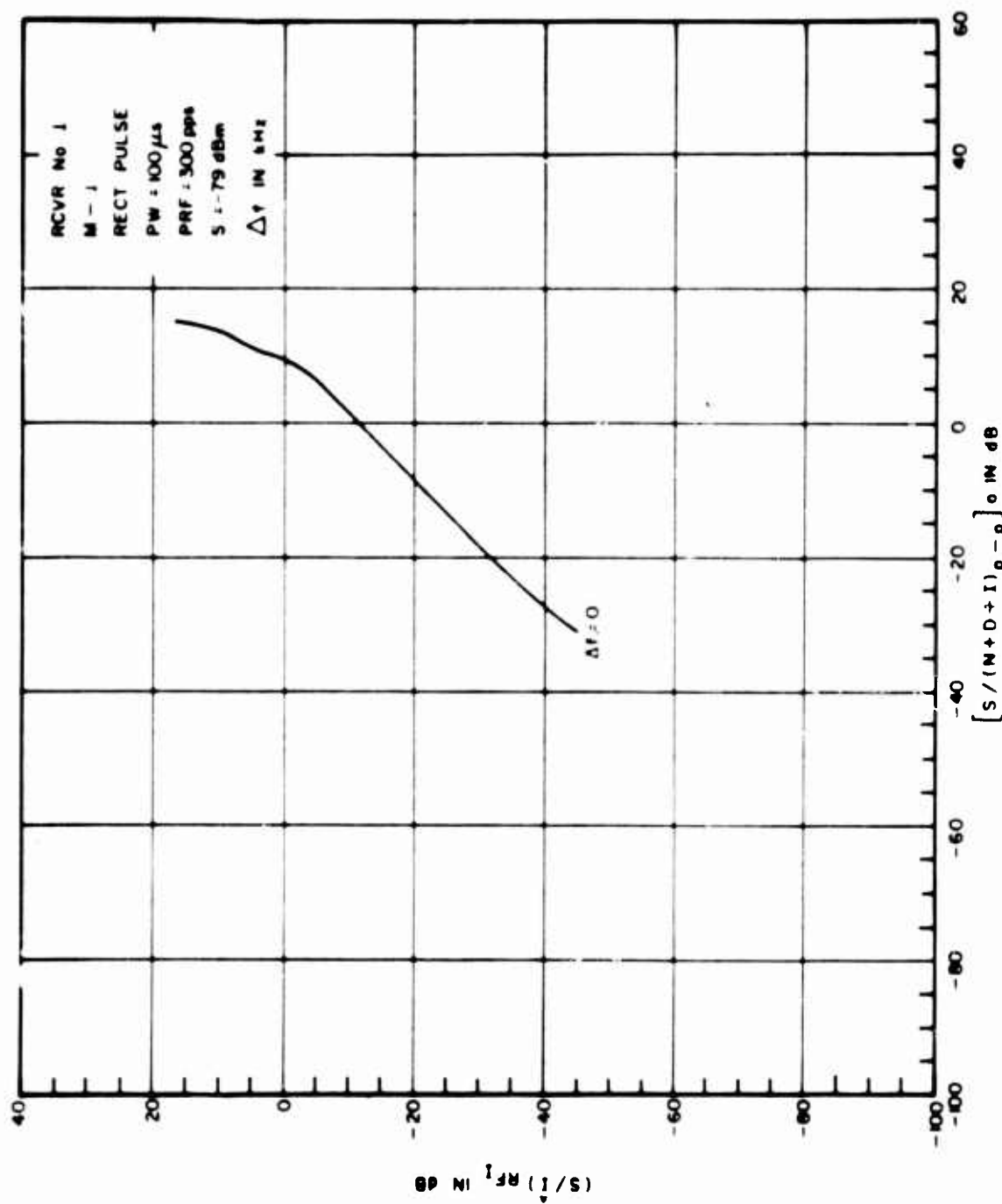


Figure III-142. Power Transfer Curves for Pulsed Interference to an AM Receiver

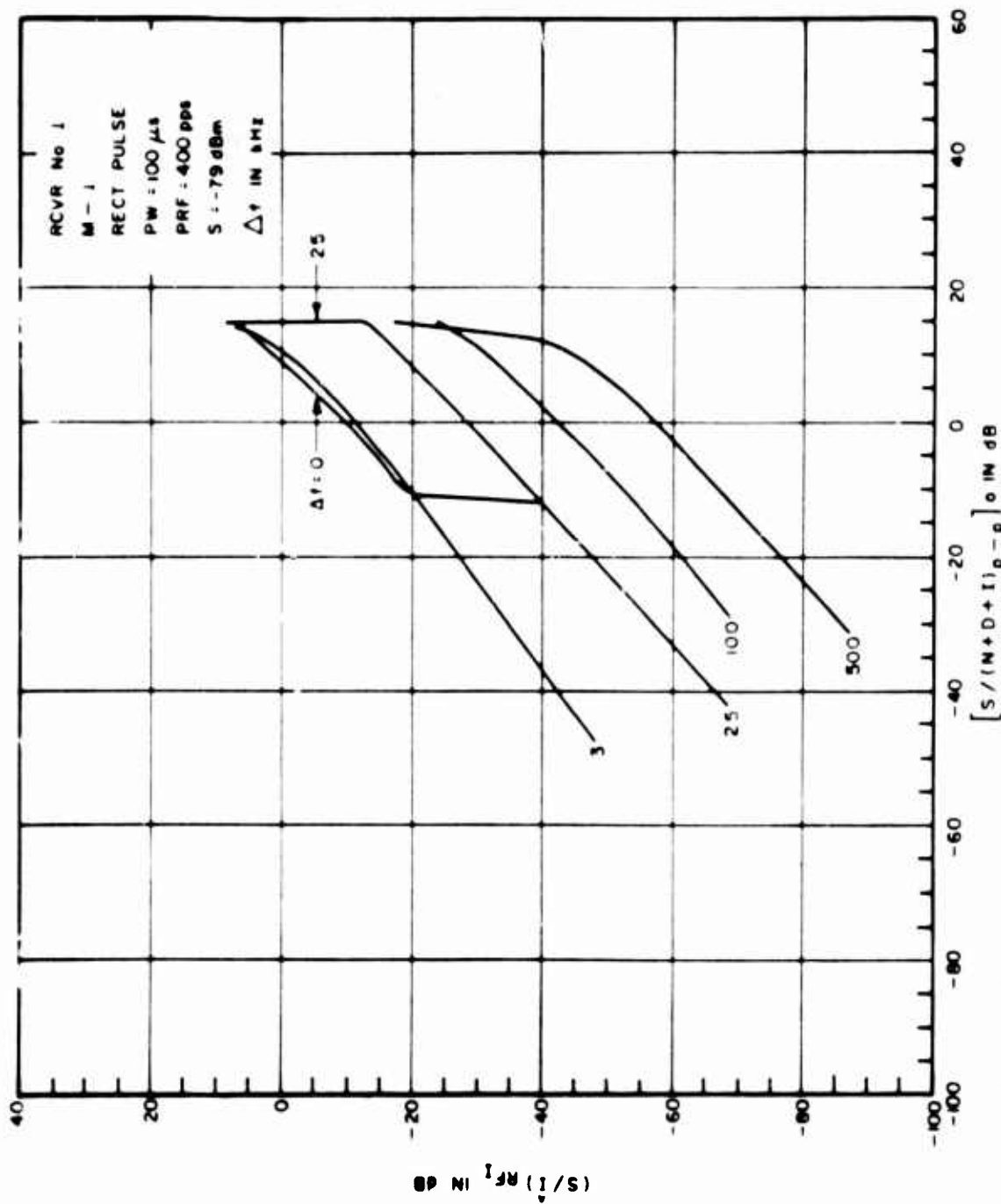


Figure III-143. Power Transfer Curves for Pulsed Interference to an AM Receiver

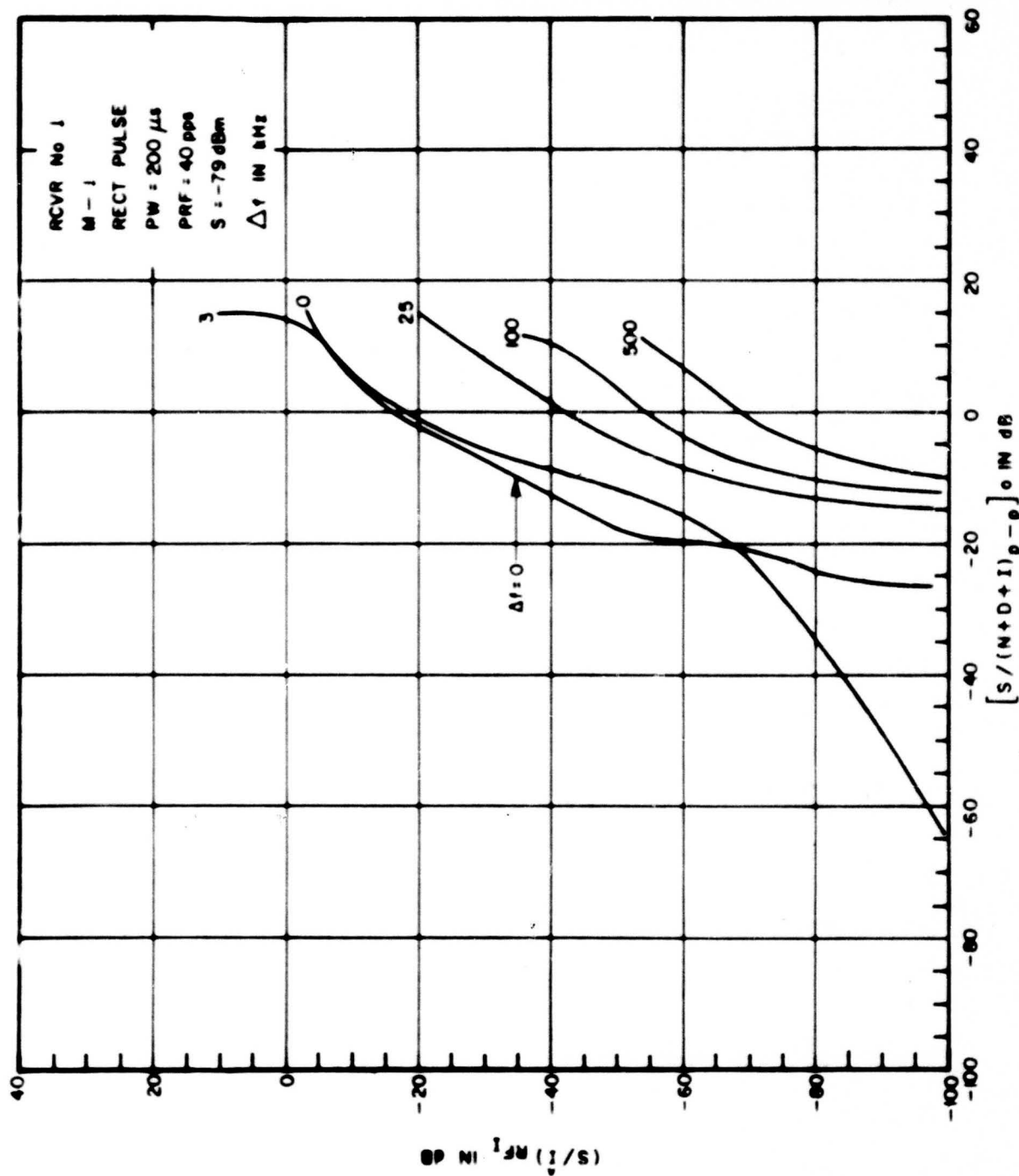


Figure III-144. Power Transfer Curves for Pulsed Interference to an AM Receiver

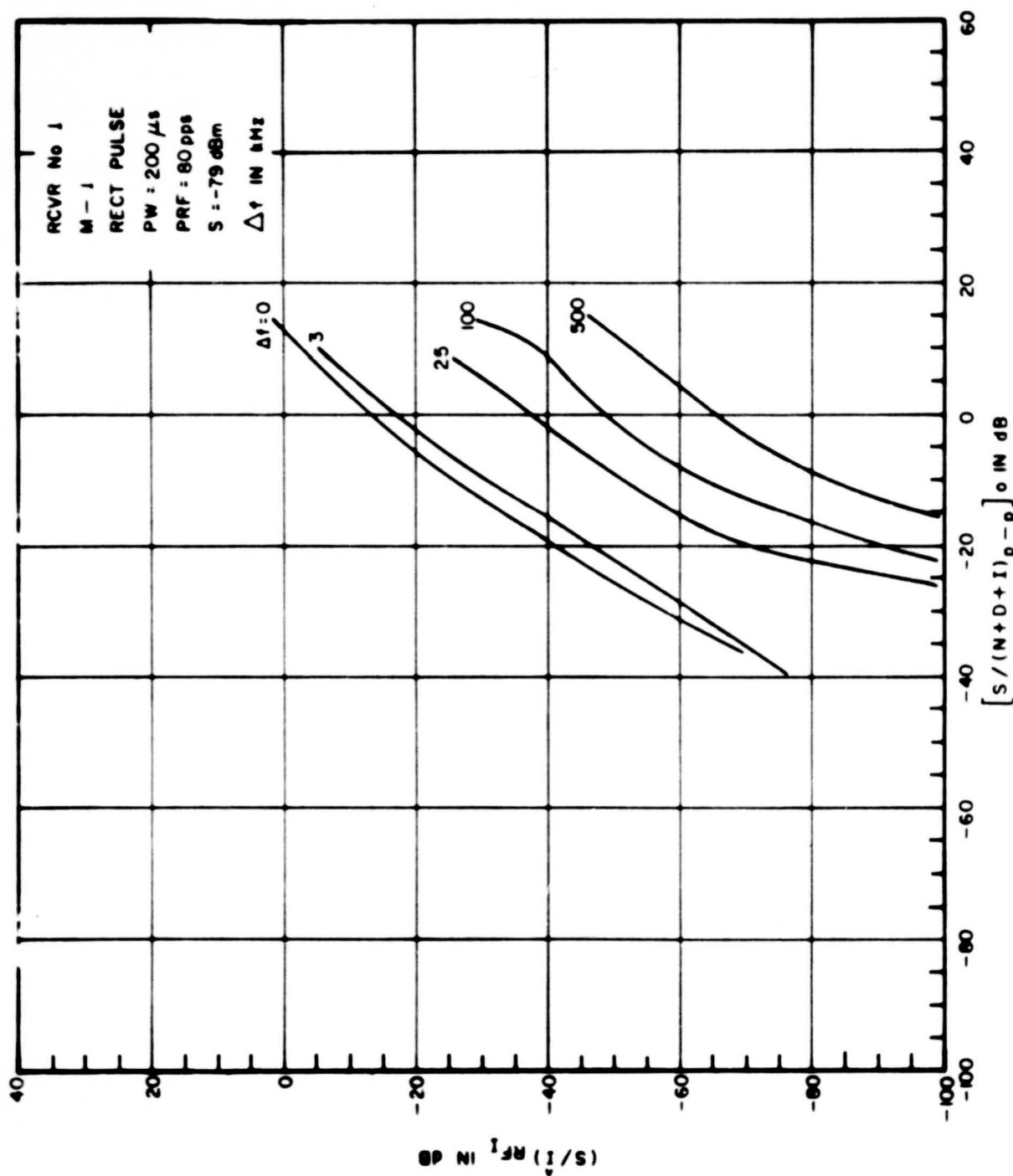


Figure III-145. Power Transfer Curves for Pulsed Interference to an AM Receiver

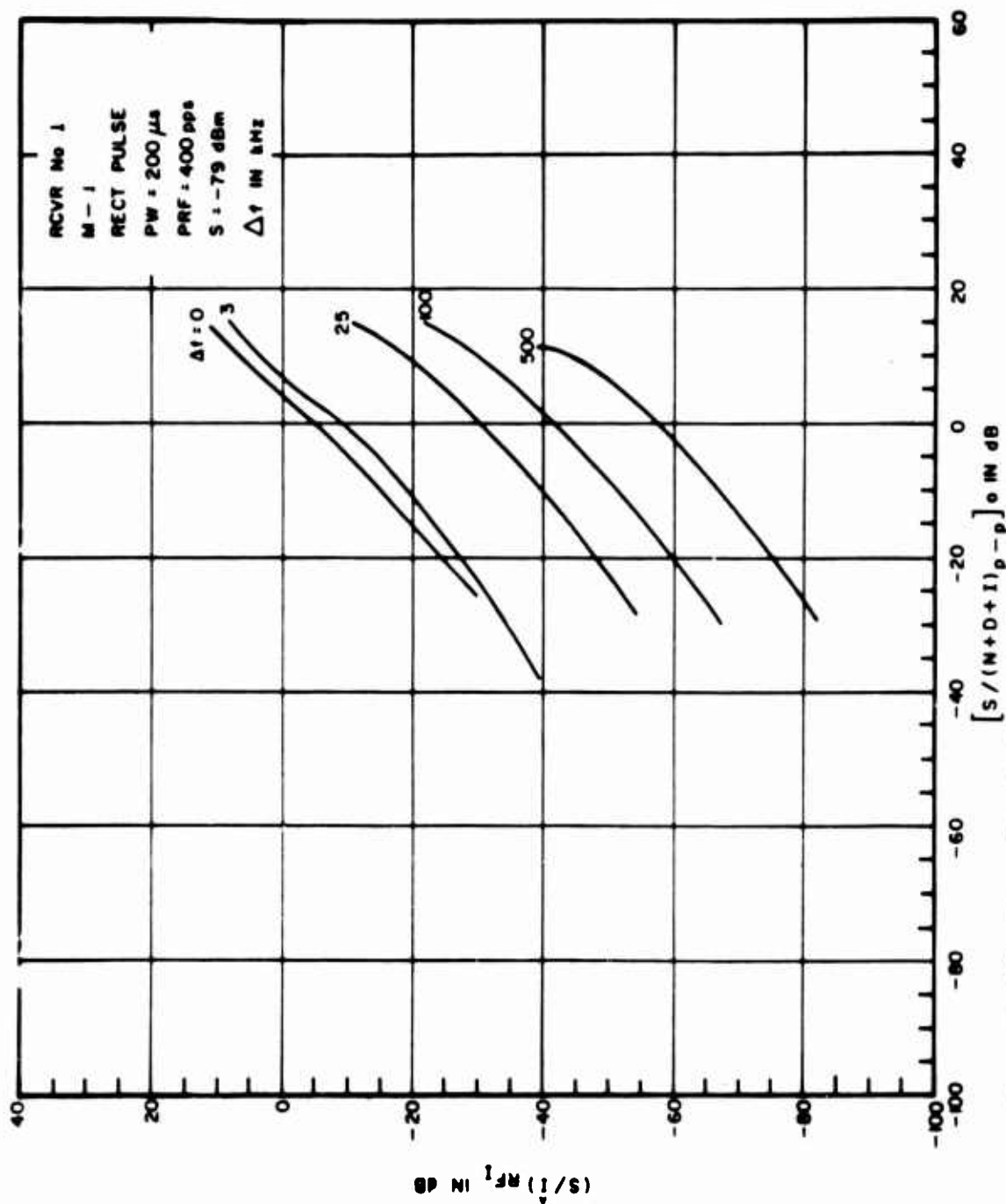


Figure III-146. Power Transfer Curves for Pulsed Interference to an AM Receiver

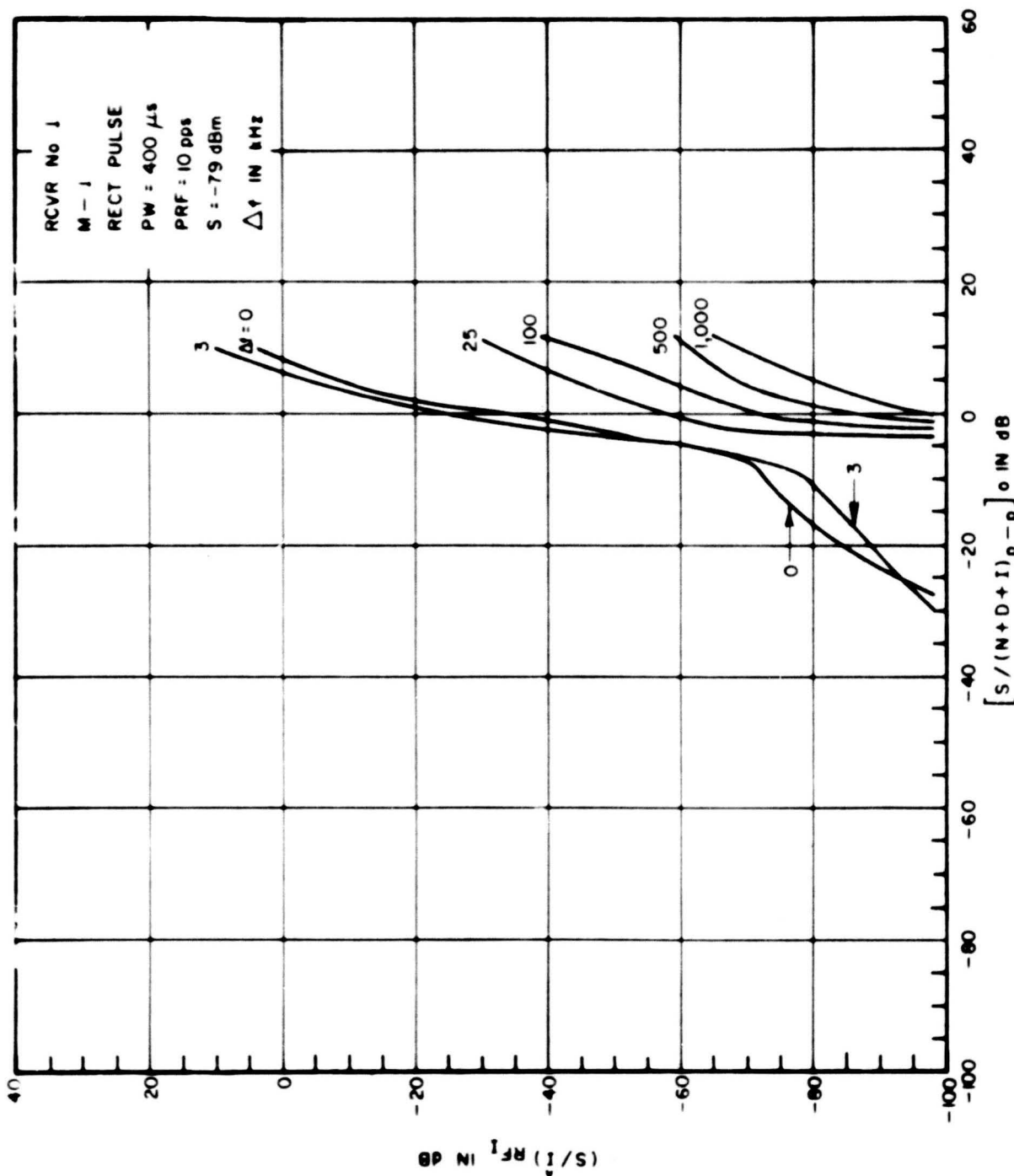


Figure III-147. Power Transfer Curves for Pulsed Interference to an AM Receiver

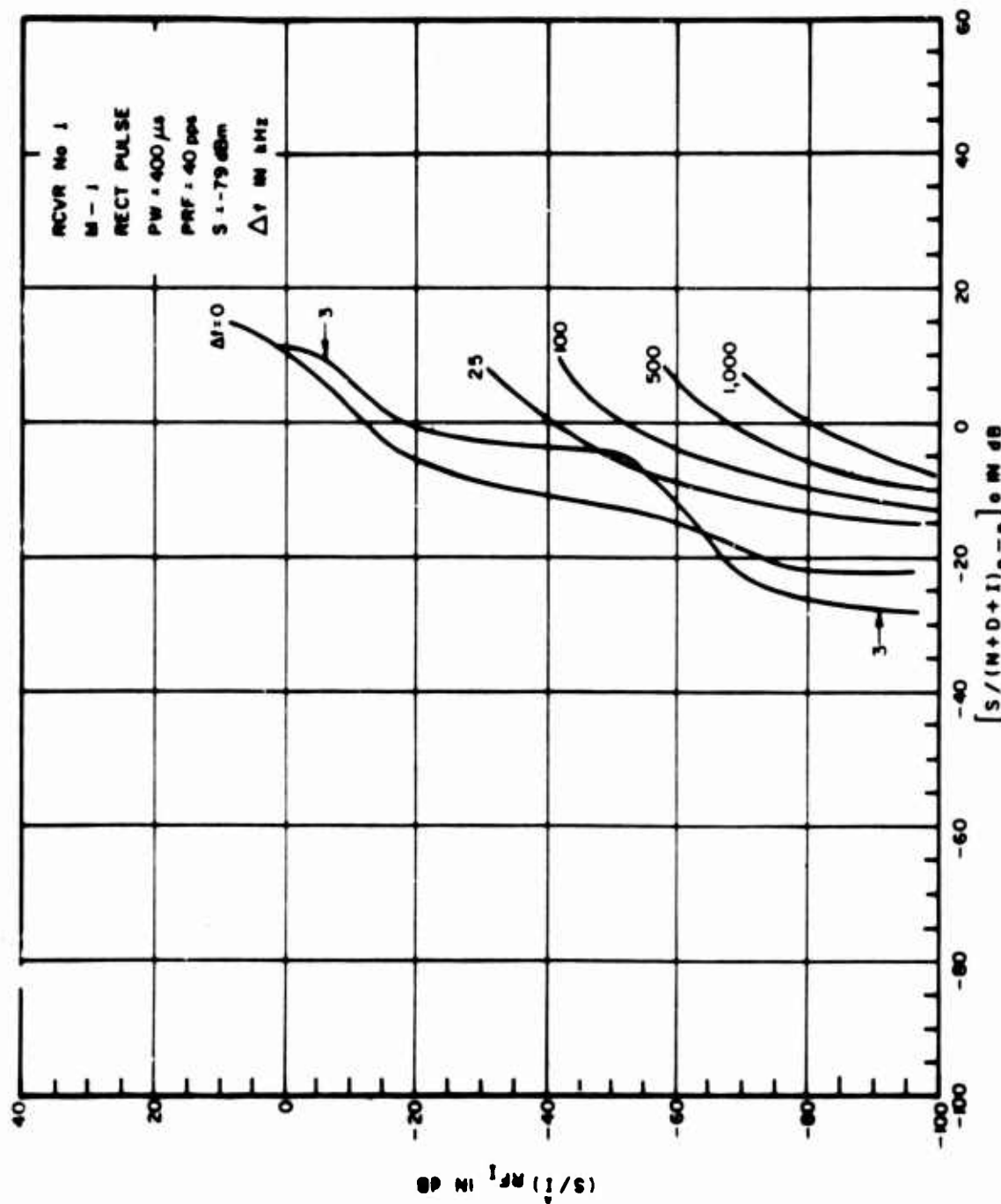


Figure III-148. Power Transfer Curves for Pulsed Interference to an AM Receiver

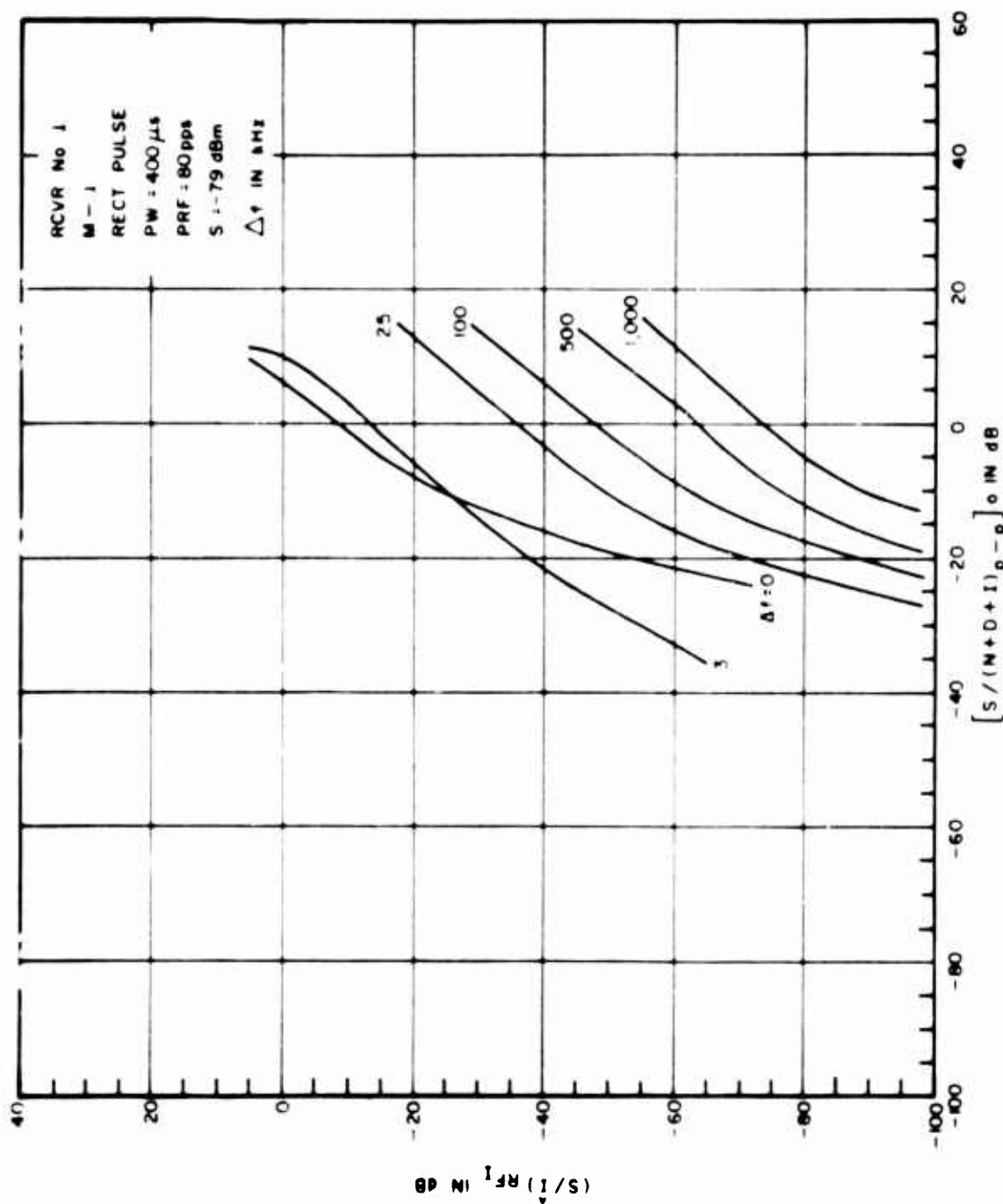


Figure III-149. Power Transfer Curves for Pulsed Interference to an AM Receiver

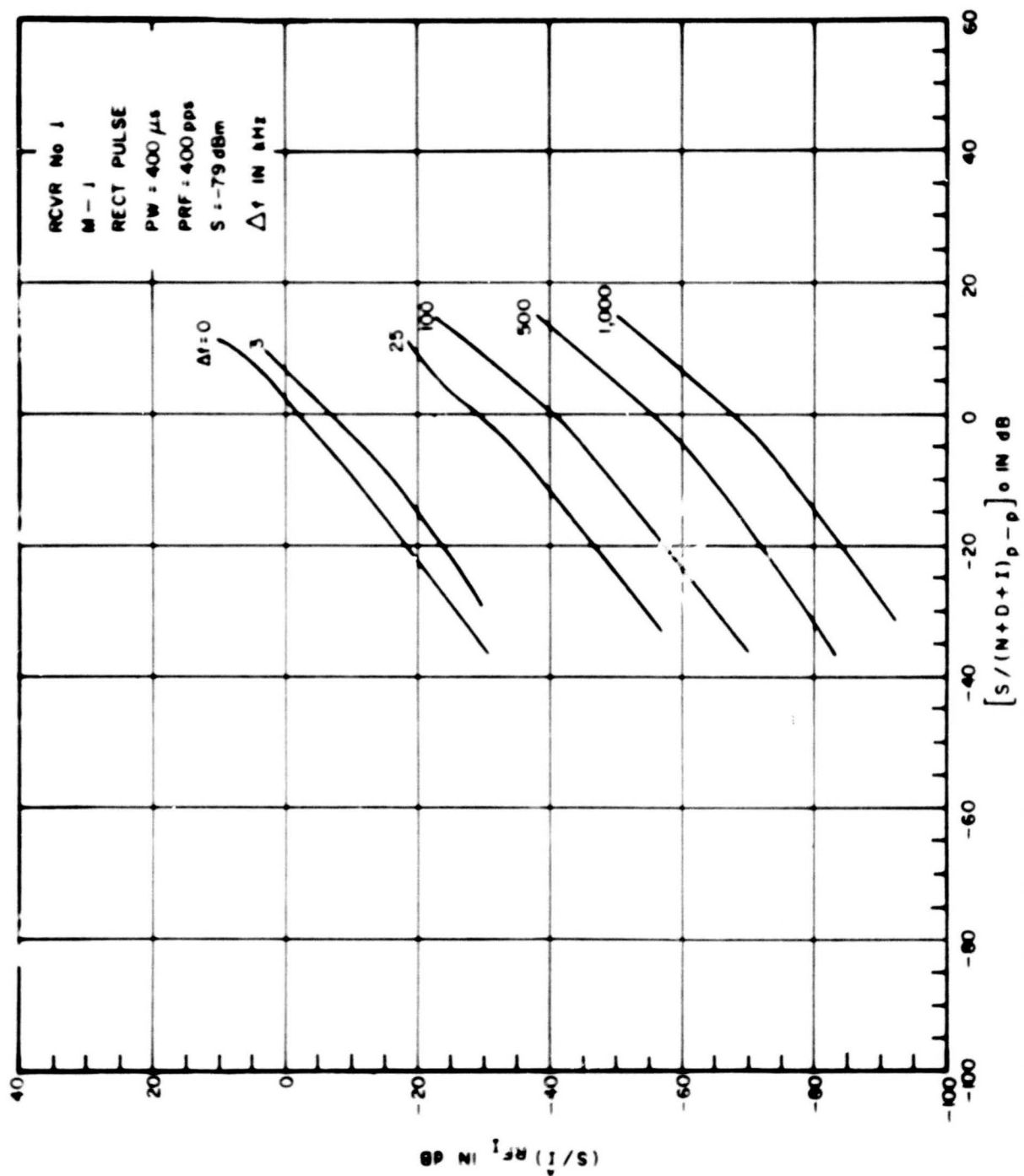


Figure III-150. Power Transfer Curves for Pulsed Interference to an AM Receiver

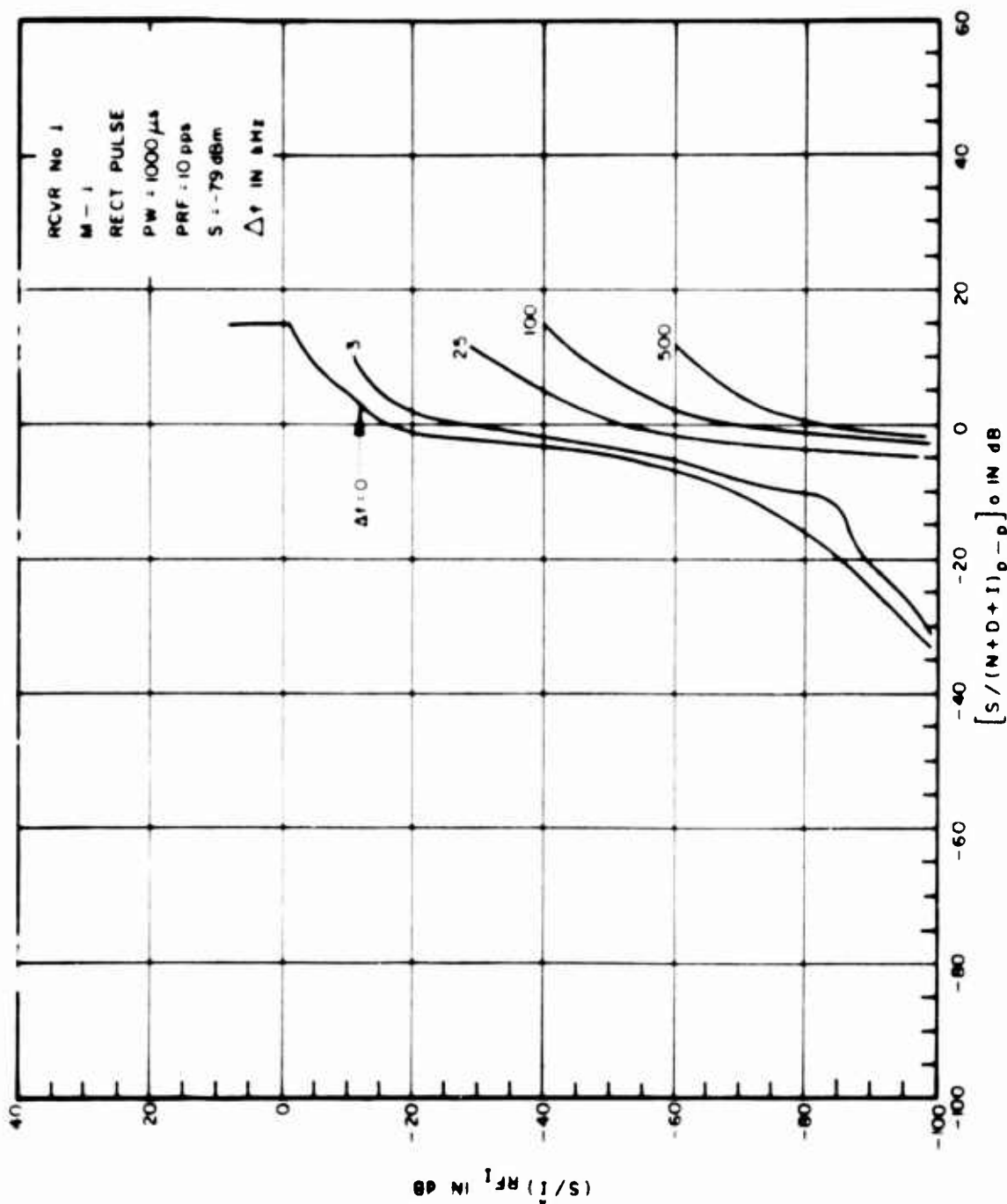


Figure III-151. Power Transfer Curves for Pulsed Interference to an AM Receiver

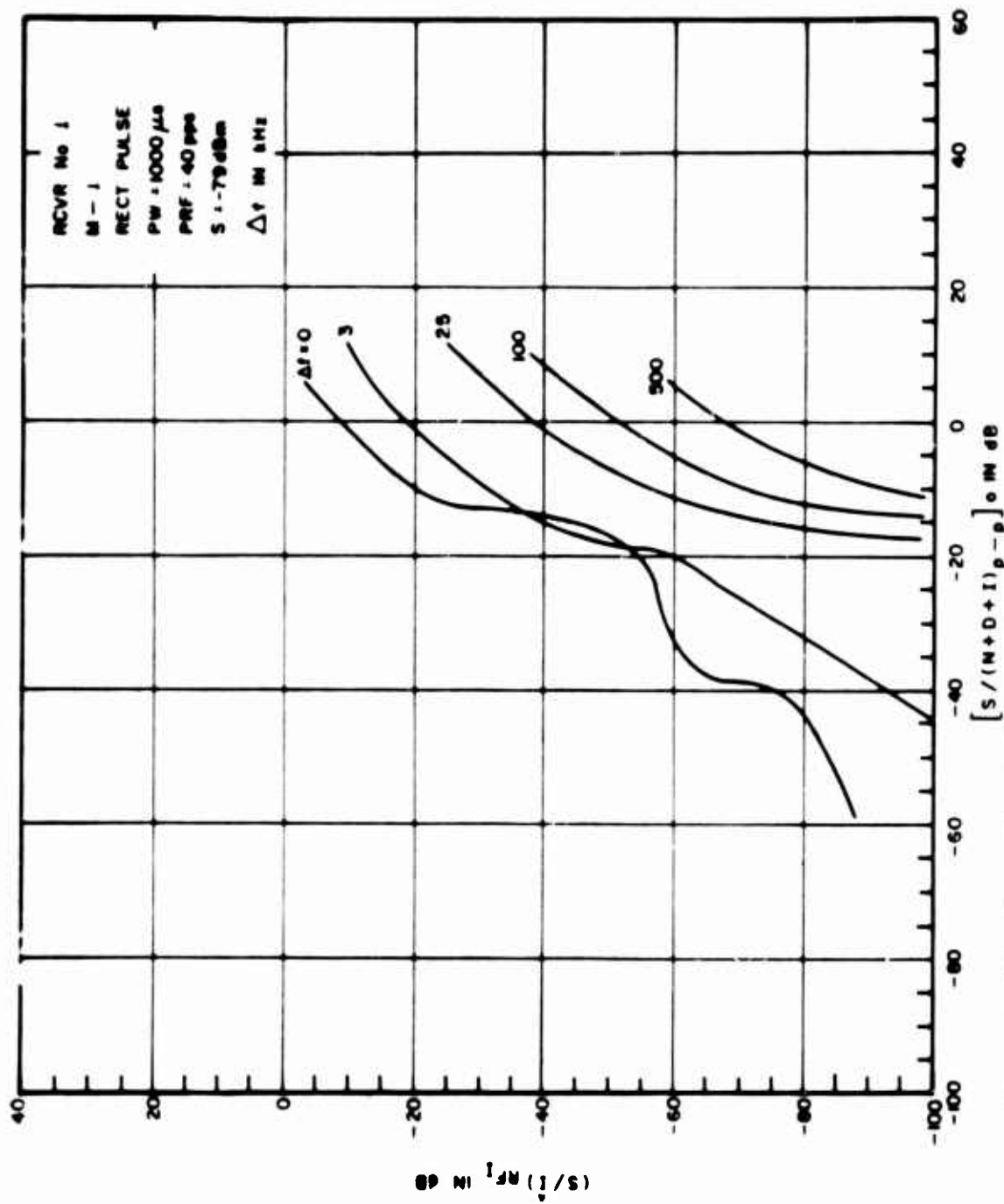


Figure III-152. Power Transfer Curves for Pulsed Interference to an AM Receiver

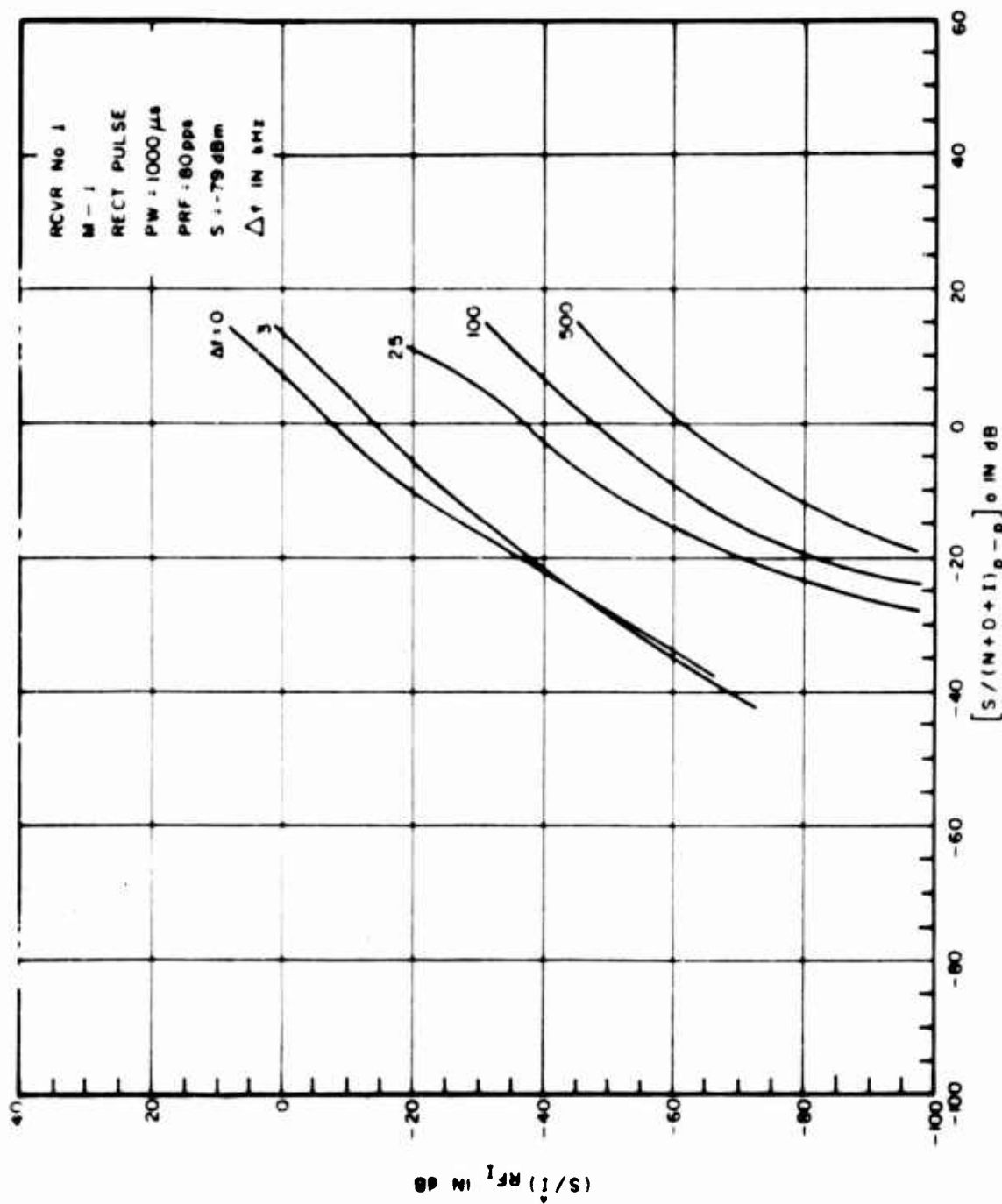


Figure III-153. Power Transfer Curves for Pulsed Interference to an AM Receiver

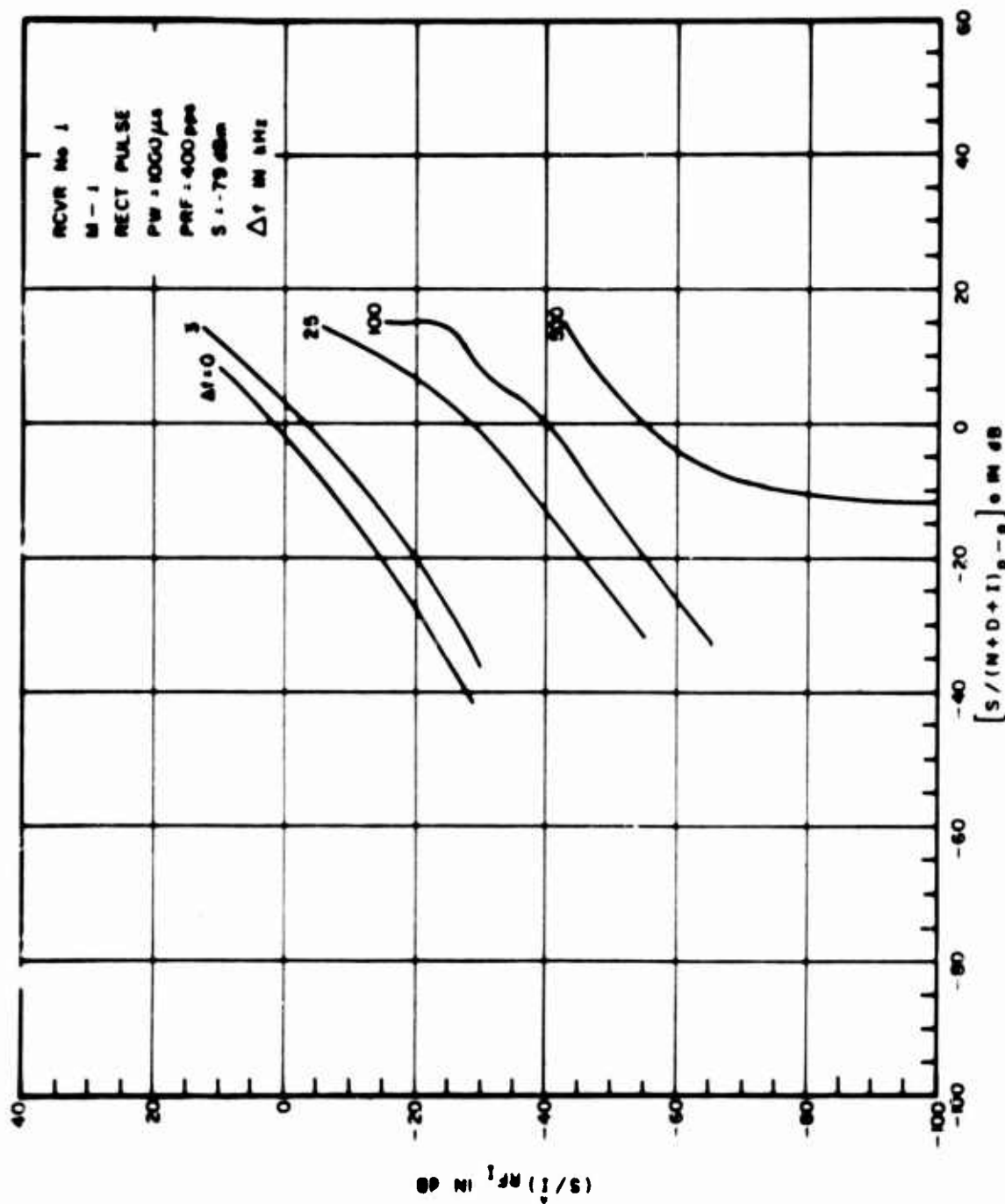


Figure III-154. Power Transfer Curves for Pulsed Interference to an AM Receiver

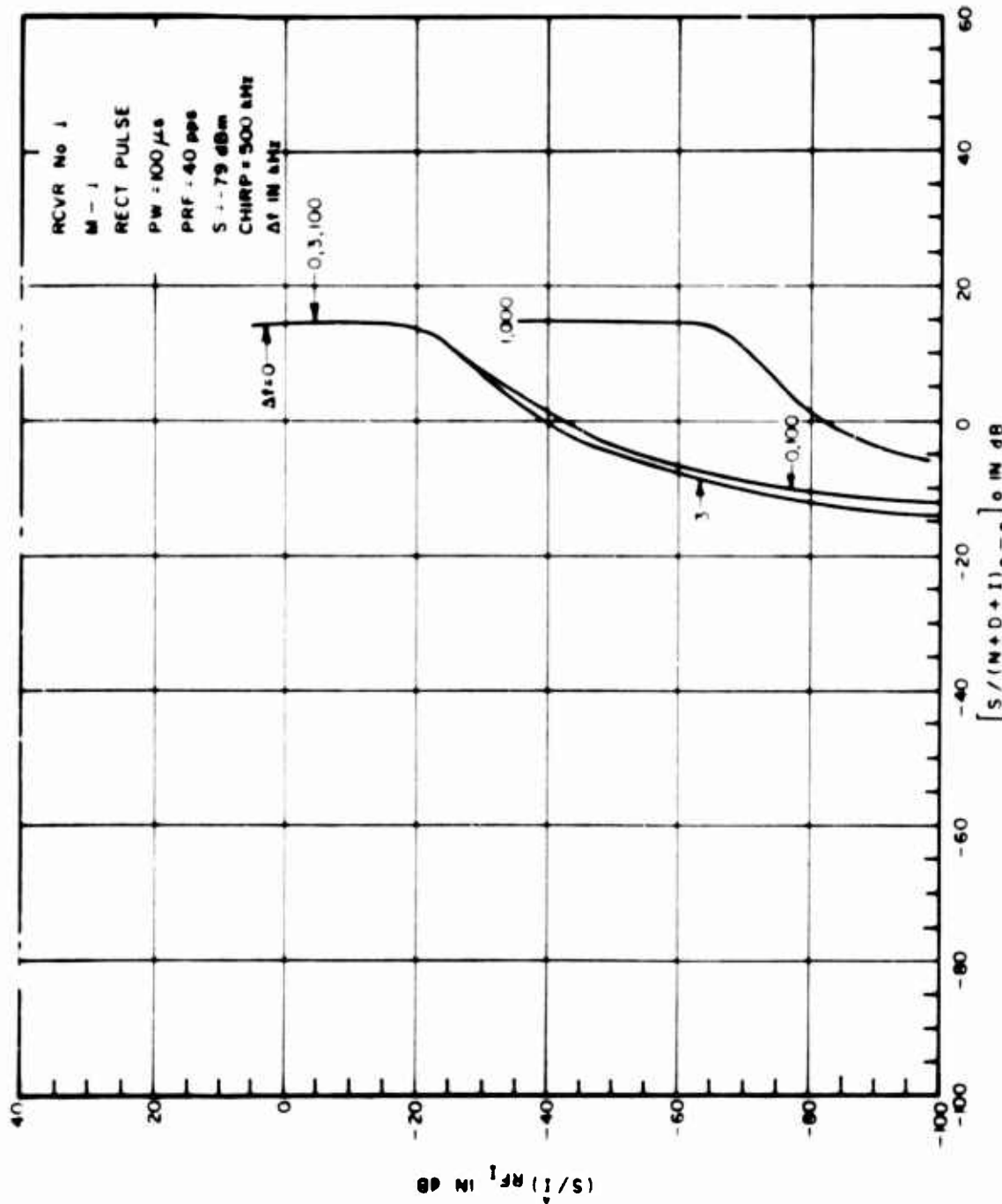


Figure III-155. Power Transfer Curves for Pulsed Interference to an A1 Receiver

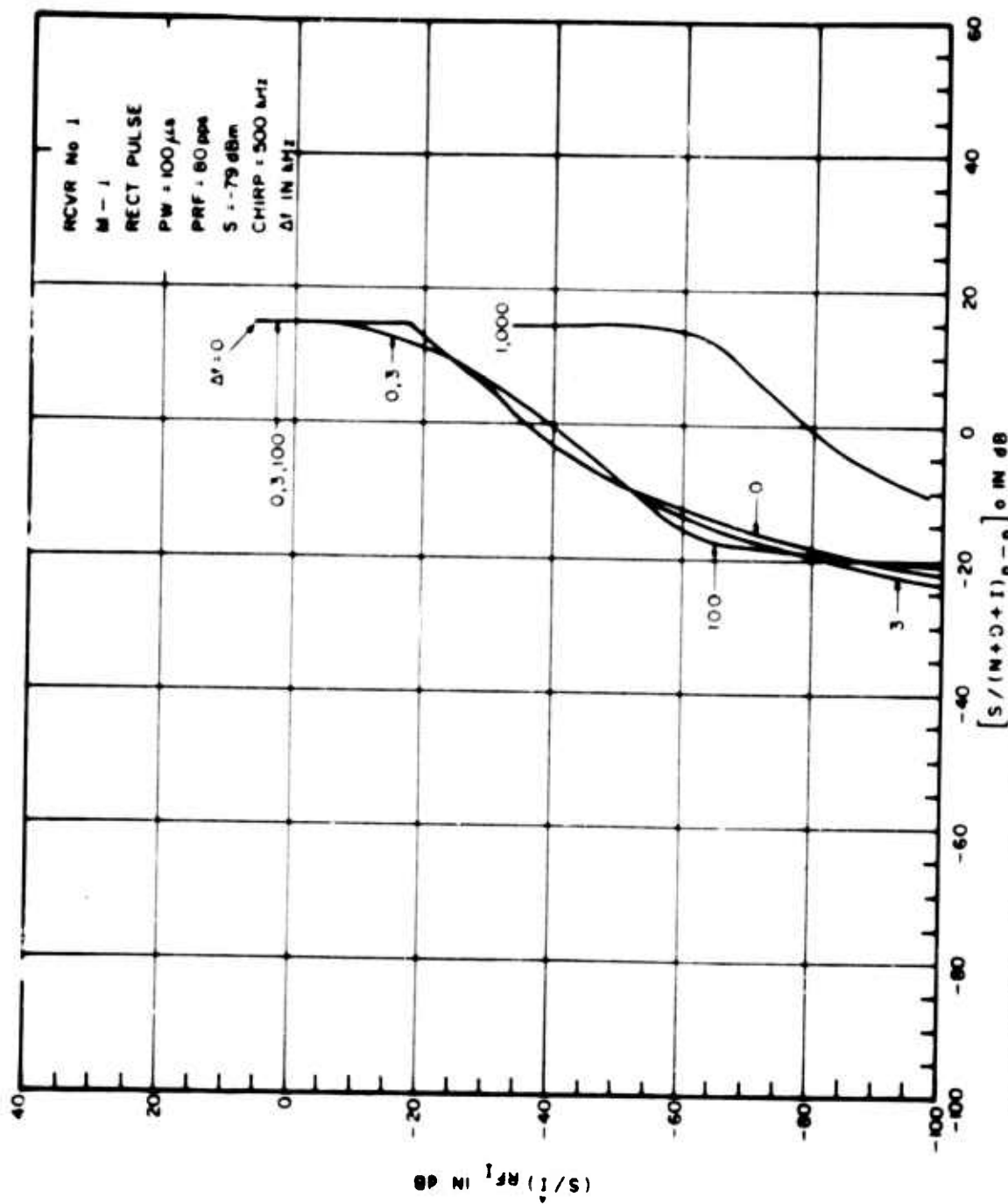


Figure III-156. Power Transfer Curves for Pulsed Interference to an AM Receiver

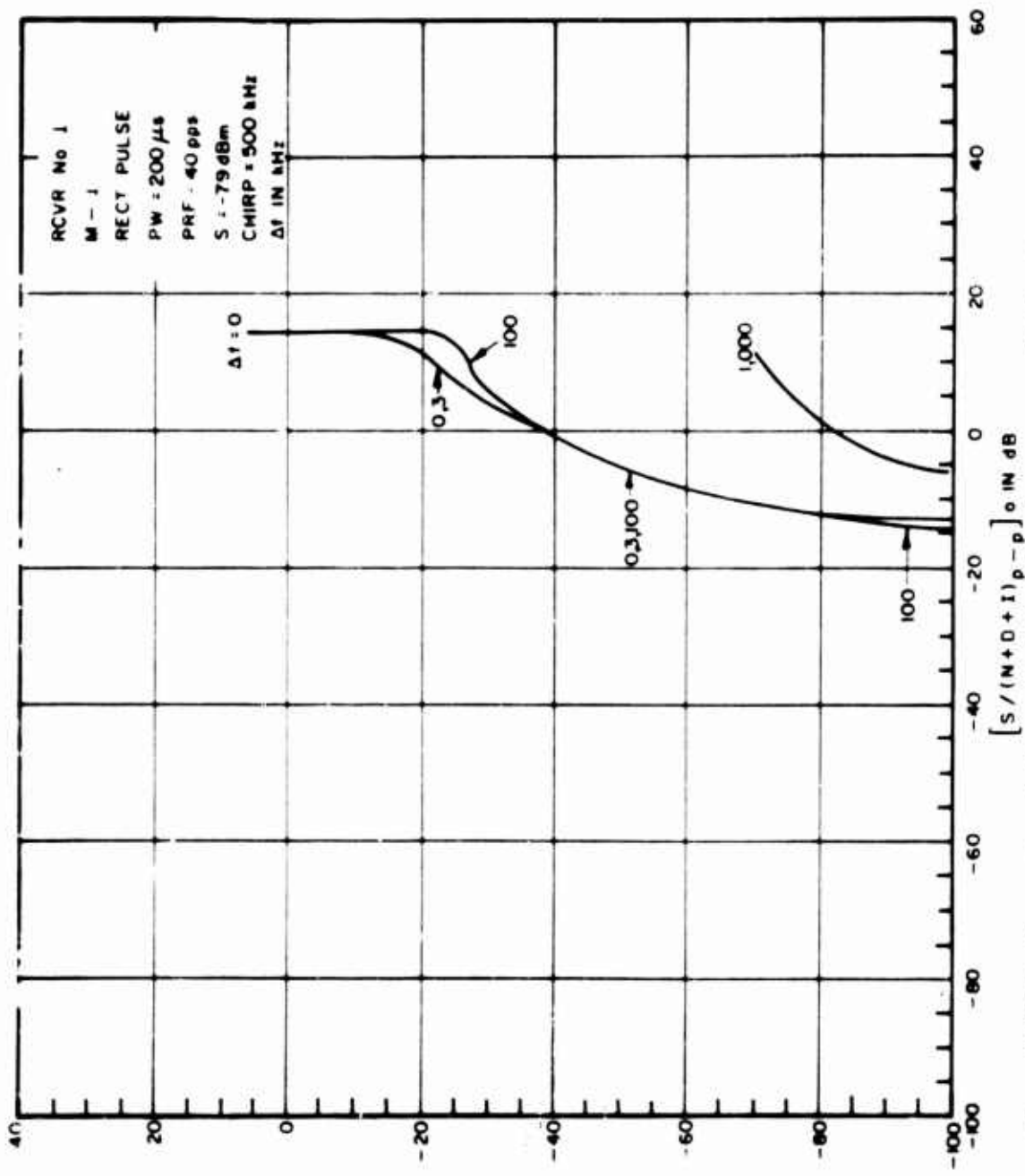


Figure III-157. Power Transfer Curves for Pulsed Interference to an AM Receiver

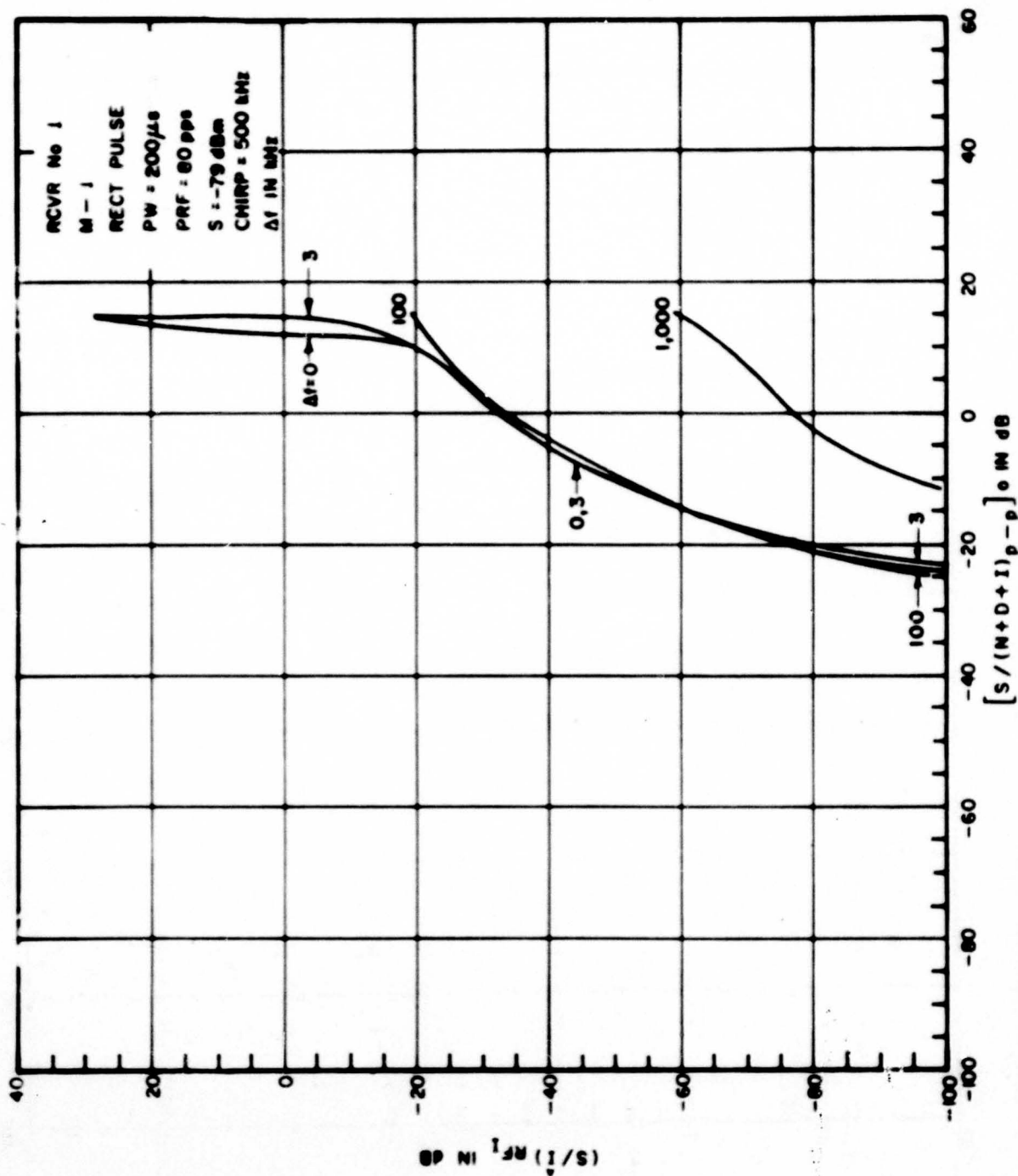


Figure III-158. Power Transfer Curves for Pulsed Interference to an AM Receiver

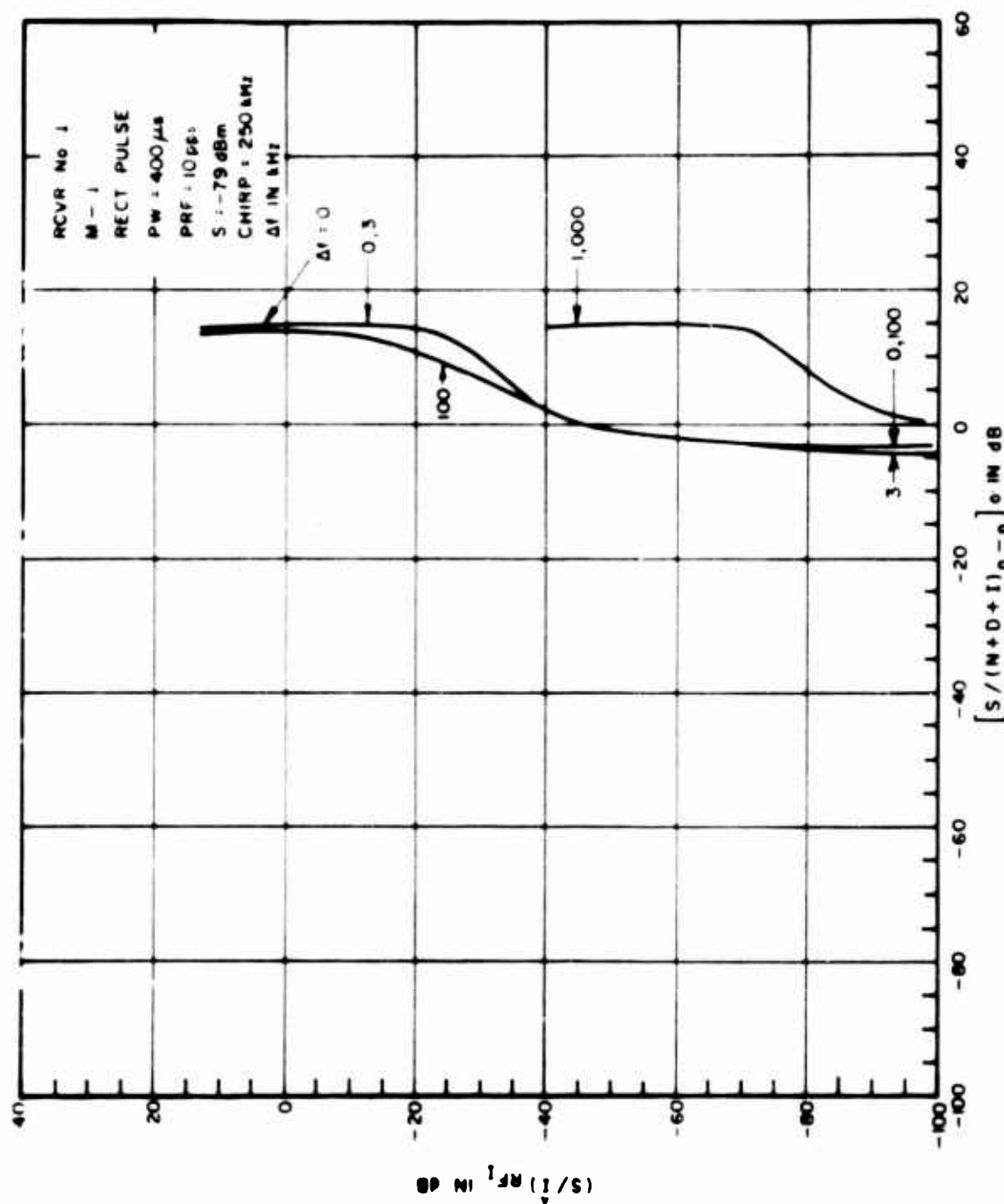


Figure III-159. Power Transfer Curves for Pulsed Interference to an AM Receiver

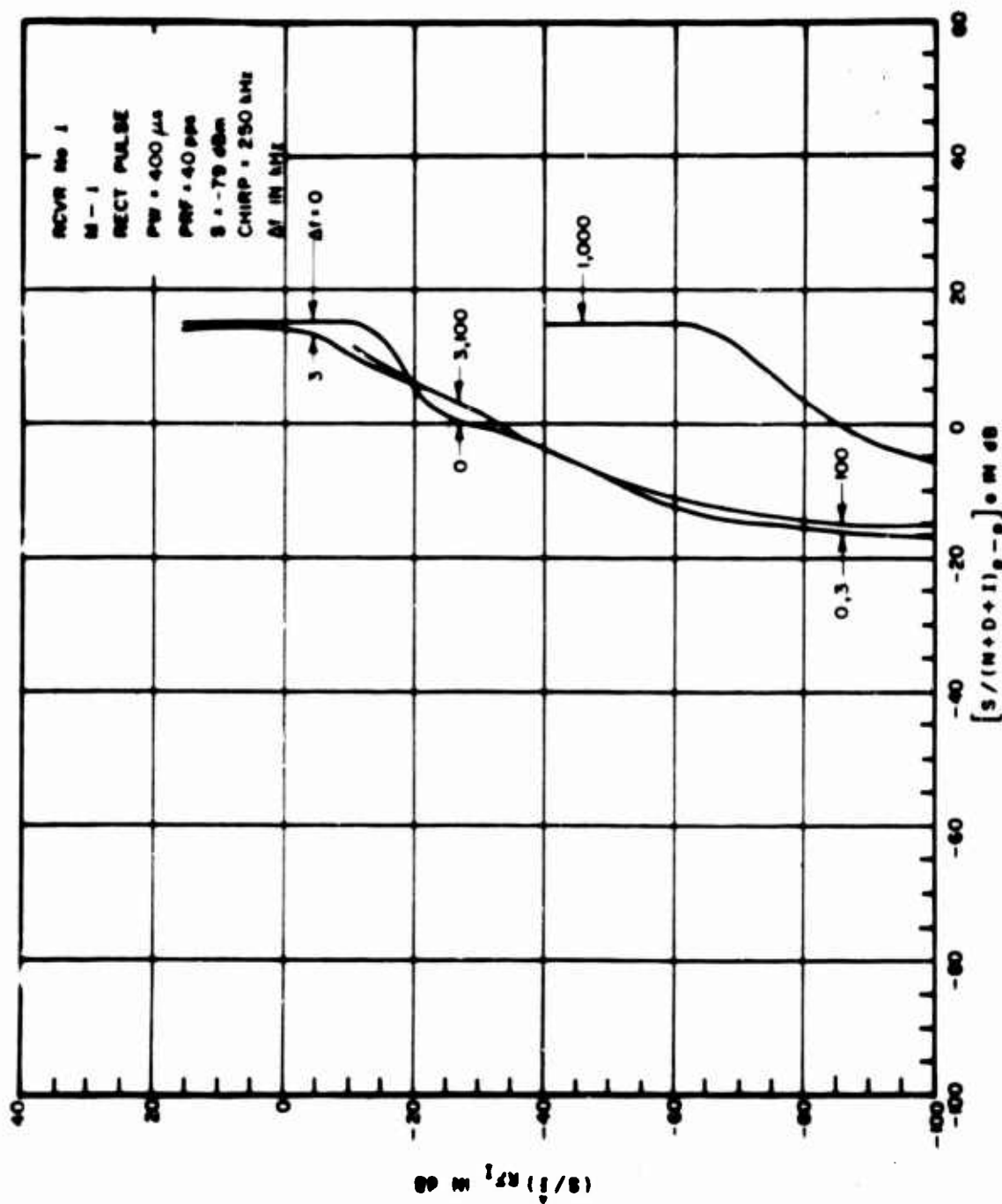


Figure III-160. Power Transfer Curves for Pulsed Interference to an AM Receiver

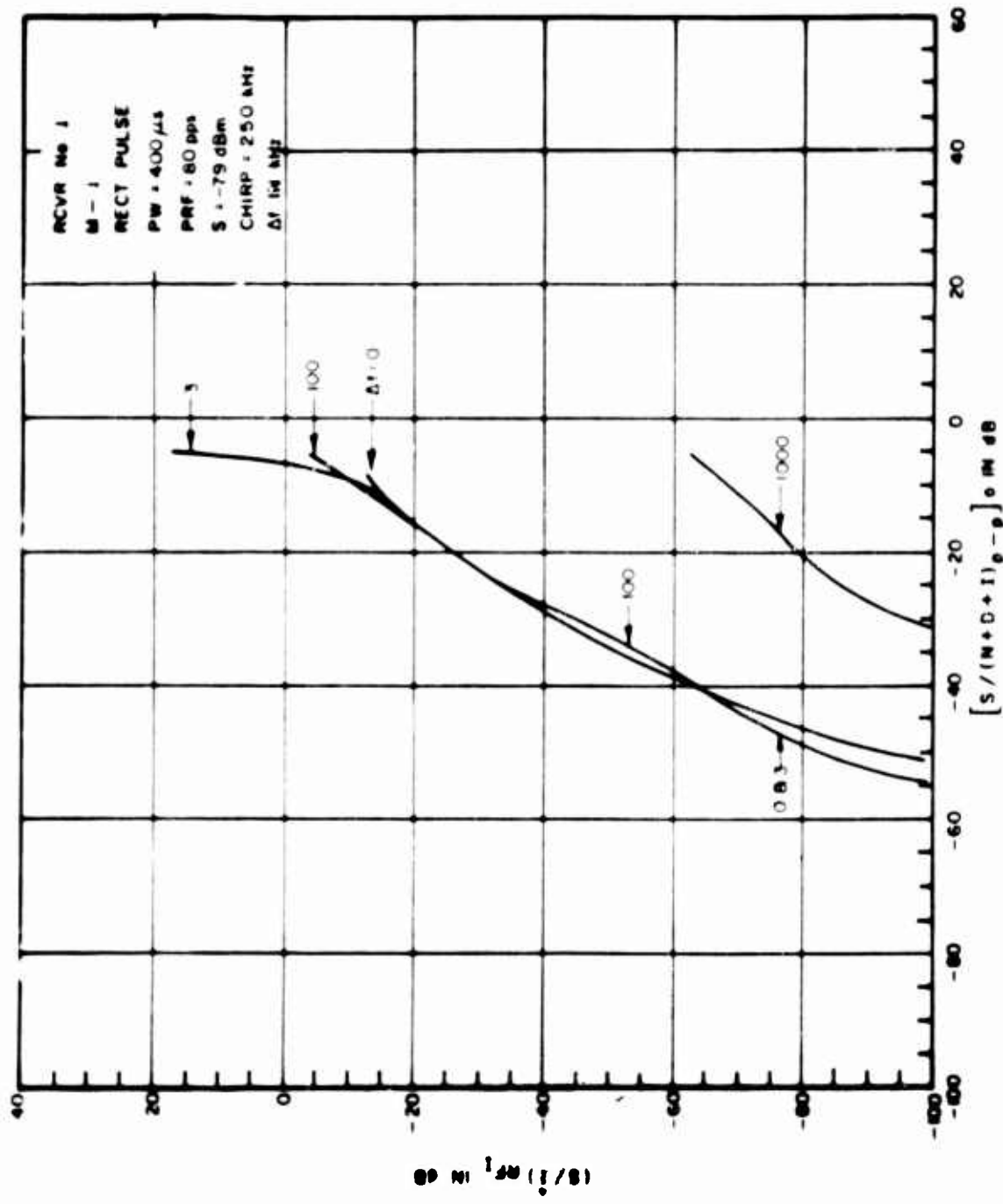


Figure III-161. Power Transfer Curves for Pulsed Interference to an AM Receiver

APPENDIX IV

DEGRADATION MEASURES

GENERAL

The following is a discussion of how the baseband output (desired and undesired signals) is measured to evaluate performance degradation of voice and digital systems. Reference 32 contains a general discussion of this topic.

This report specifically considers AM receiver degradation for voice systems. However, the receiver simulation model includes the basic structure, through the baseband filter, required for any AM system subjected to pulsed interference. It is, therefore, necessary to only add appropriate digital and analog degradation measures (to the simulation model) to evaluate the AM receiver with digital and analog modulation.

The "complete" mathematical modeling of a system's performance is the end objective of a prediction analysis. However, there does not exist one complete mathematical operation for analyzing all types of system performances and the best that can be accomplished is to use the measures that are most appropriate to a particular system (i.e., mean square measures, probability measures, etc.). The basic difficulty is to determine what exact type of evaluation should be associated with interference degradation. Although considerable research has been conducted on performance degradation evaluation the desired outputs for receiving systems still reduce to a few basic types. In particular, for voice systems, Articulation Score (the percent of words correctly received) is still used as the main intelligibility standard. For digital systems, the probability of detection and probability of false alarm are desired. For analog signals, the mean square error (or the RMS error) is usually desired.

The following discussion will specifically examine the performance measures of articulation score, articulation index, CORODIM and minimum interference thresholds for voice systems. Performance degradation of digital systems will be examined in terms of error probabilities as an example of how to extend the model developed in this report to other types of modulation.

ARTICULATION SCORE

The basic measure of the intelligibility of a voice system is in terms of the percent of words correctly understood over a channel perturbed by interference. This measure has been

designated as an articulation score (AS) and is usually conducted with specific types of words or syllables as well as specific system parameters. In an attempt to define the main voice parameters that are involved, workers in the field have conducted experiments by varying (at audio frequencies) the word content, bandwidth, audio (S/N) and the type of talkers and listeners that are involved. Through the above experiments, articulation scores have been obtained as functions of the above variables and, as one would expect, the scores increased with increasing bandwidth, number of syllables in the words, speaker-listener familiarity, and audio (S/N).

If the receiving system is subjected to a range of distortion or masking conditions, the AS may then be determined as a function of the interfering condition. Figure IV-1 presents typical AS curves for different PB (phonetically balanced) word groupings in which the interference was white noise of various bandwidths (reference 33). White noise, which contains a continuous uniform spectrum, is one of the most effective maskers of speech and is often used in speech intelligibility studies as a standard or reference interference.

The articulation testing procedure is not simple nor has it always been standardized. Because it deals with the performance of human beings, the tests can yield variable results in individual cases when improper statistical safeguards are not taken. It is generally necessary to use a number of listeners in order to obtain statistically meaningful results. Proper conduct of the test is tedious and time consuming. The situation is aggravated by the necessity of a training program for the listeners in order to eliminate the improvement noted for successive tests of most word lists. The test procedures, the material that is used, as well as the techniques employed to measure the average power of the desired and undesired signals vary between investigators.

Nevertheless, the tests provide the most valid objective method available for evaluating the intelligibility of speech communication components or systems. When the AS tests are carefully organized, the scores are repeatable 68% of the time within a 2 dB data spread.

This test was used as the basic standard of intelligibility for this study. However, since this method cannot be mechanized, it is advantageous to use other techniques that allow machine computation. A number of these techniques will be subsequently discussed.

SPECTRAL APPROACHES

There are a number of approaches that obtain a measure of the effects of undesired signals on speech communications systems by calculation and/or instrumentation of a criterion measure in each of a number of bands in the speech frequency spectrum. Included within the approaches, besides the better known articulation index (AI), are formant intelligibility and pattern correspondence index (PCI).

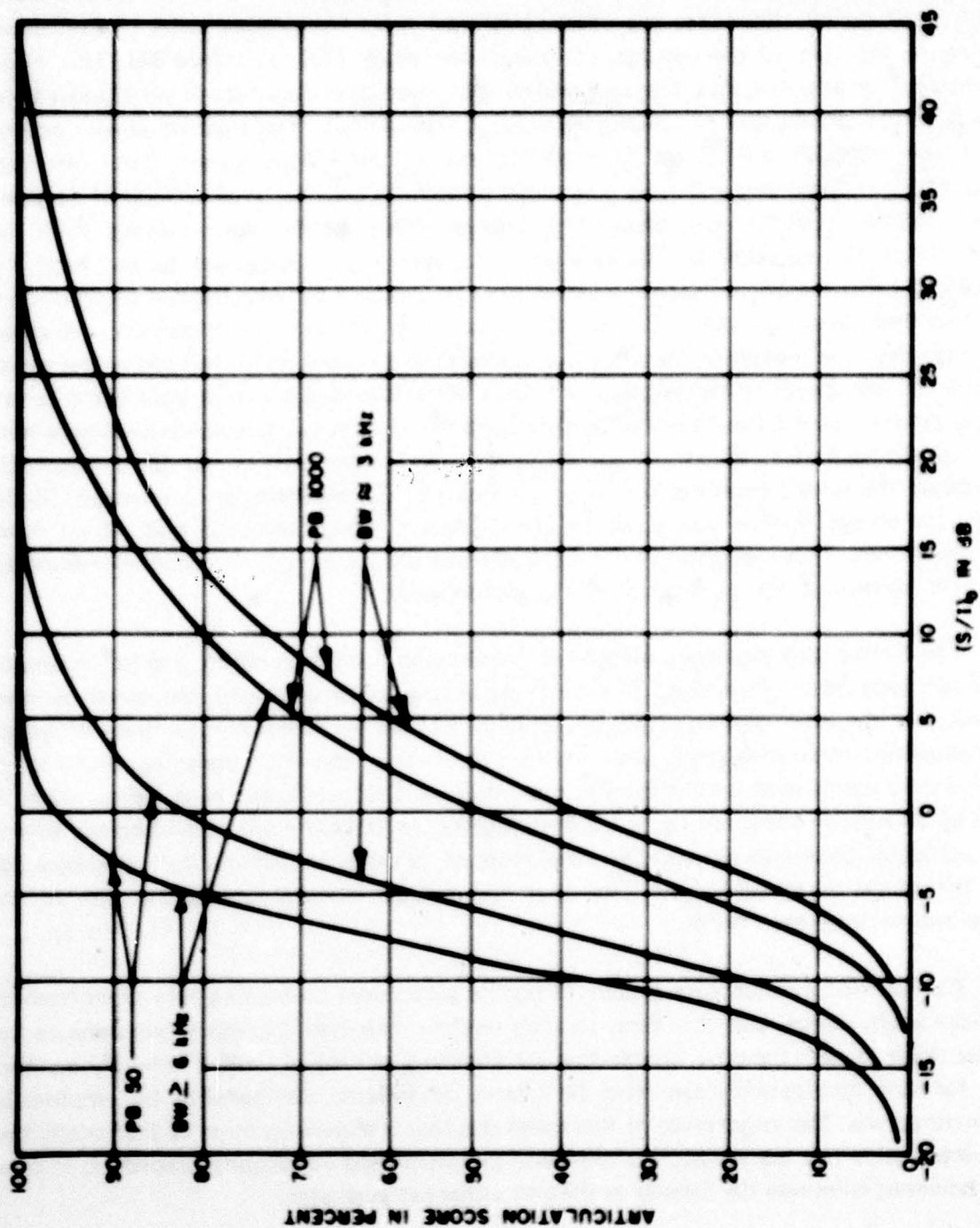


Figure IV-1. Articulation Score versus Noise Interference

All these methods operate on the short-term power spectrum to obtain a performance measure of speech. Basically, the procedures stem from the original work of French and Steinburg that led to the concept of articulation index (AI) (reference 34). This effort, essentially, determined that one can divide the speech spectrum into N contiguous bands which contribute equally to intelligibility (in terms of AS). The method ideally assumes there are negligible effects on intelligibility due to the speech sounds from one band masking, or in some way affecting, sound components of another band. Effects of noise and other factors (interference, distortion) prevent these bands from making their full contribution to intelligibility. The intensity of speech varies according to the band. For these and other reasons, a weighting factor must be included for each band in recognition of the fact that some bands do not make their maximum possible contribution to the speech intelligibility. The weighting factors vary for each band according to the ratio of the speech energy (in that band) to the hearing threshold. When the speech energy level in the band is 30 dB or more above the threshold level it contributes its maximum value and hence has a unit weighting factor. When the speech energy level is between 0 and 30 dB above the threshold, the band's contribution is in proportion to its maximum as its level is to 30 dB. When the energy level is below the threshold there is no contribution and the weighting factor vanishes. These weighting factors are additive and the sum can be used with empirical curves to determine the corresponding articulation score.

The French and Steinburg method is, however, still fairly complex and hence simpler methods have been developed. The next procedure to be discussed, the tonal method, asserts that the intelligibility of speech depends, not on the absolute magnitude of speech and undesired signal intensities, but rather on the amount by which the speech exceeds the auditory threshold level for a particular type of noise. This perception level is determined in each of 20 equally contributing bands covering 100 to 10,000 cps for standardized speech and particular undesired signals. The tonal method, "Formant intelligibility" (reference 35) has the property of additivity such that the overall intelligibility is the sum of the contributions from each band.

The formant intelligibility process is readily automated by feeding pure tones from an artificial voice source, one at a time, to each of the n channels. Listeners then measure the excess noise in each band by attenuating the standard test signal until it is barely audible. The formant intelligibility can then be related to syllabic intelligibility by empirically obtained curves. The importance of this method is that it eliminates most of the variabilities associated with the transmission process and eliminates the AS scoring procedure. It does not, however, eliminate the listener as the end subjective evaluator.

Other methods have therefore been developed which measure the effects of the undesired signals without subjective listener evaluation. Two of these other methods have

led to the development of testing machines by General Electronics Labs (GEL) based upon the assumption that speech intelligibility resides principally in the short time spectrum.

The first machine measures a number called the pattern correspondence index (PCI) (reference 36). This number is an index of the correspondence of the spectrum patterns of the interfered and non-interfered cases. The PCI is actually obtained by taking the average difference between three recorded sentences and the transmitted interfered sentences. The PCI, theoretically, has a monotonic relationship to articulation score and should be calibrated or tested for specific types of undesired signals. The device has, at least, been calibrated for white noise. It is postulated that this curve or type of curve is universal as a function of signal-to-noise, independent of the type of interference. If AS versus noise curves are available for the particular undesired signal case being investigated, a direct translation between PCI and AS can be made. This machine uses an autocorrelation measure of the desired signal and the corrupted output. Therefore, except for possible mechanical deficiencies this approach is adequate or inadequate depending on how optimum this measure is for the particular interference being considered.

The other machine, produced by GEL to mechanically measure voice intelligibility, is called the Voice Intelligibility Analysis Set (VIAS) (references 25 and 37). This device also operates on the principle, previously described, of dividing the spectrum into a number of unequal bandwidths (14) and measuring the relative desired to undesired signal ratio relative to the hearing threshold. The sum of the contributions from each band is then averaged over all 14 bands to produce the composite AI. The 14 VIAS frequency bands are shown in Figure IV-2 and the calculation of AI is depicted graphically in Figure IV-3. In order to perform this basic calculation, a synthetic desired speech signal, which consists of a triangle modulated 950 cycle tone, is transmitted over the test channel and is then measured by the recording portion of the device, in order to determine representative speech levels in the 14 bands. The average power (over a 17 sec. period) of the undesired signal in the 14 bands is then measured and from knowledge of the average desired signal in that band, the desired to undesired signal ratio is computed. The articulation index is then computed by summing the contribution from each of the 14 bands. VIAS incorporates empirically derived correction factors to account for the upward spread of masking. This is the phenomena in which interference at a low frequency masks a higher frequency portion of the voice spectrum. Correction must also be inserted for the receiver's frequency characteristics. The degree of correction must be determined by measurement on the system and then inserted manually. Reference 25, Appendix II, discusses this correction factor in detail. The important difference between the AI machines and the tonal method is the simplification to one test signal and the elimination of the subjective evaluation. This method implies that interfering effects are independent and consequently additive. This last statement is especially critical

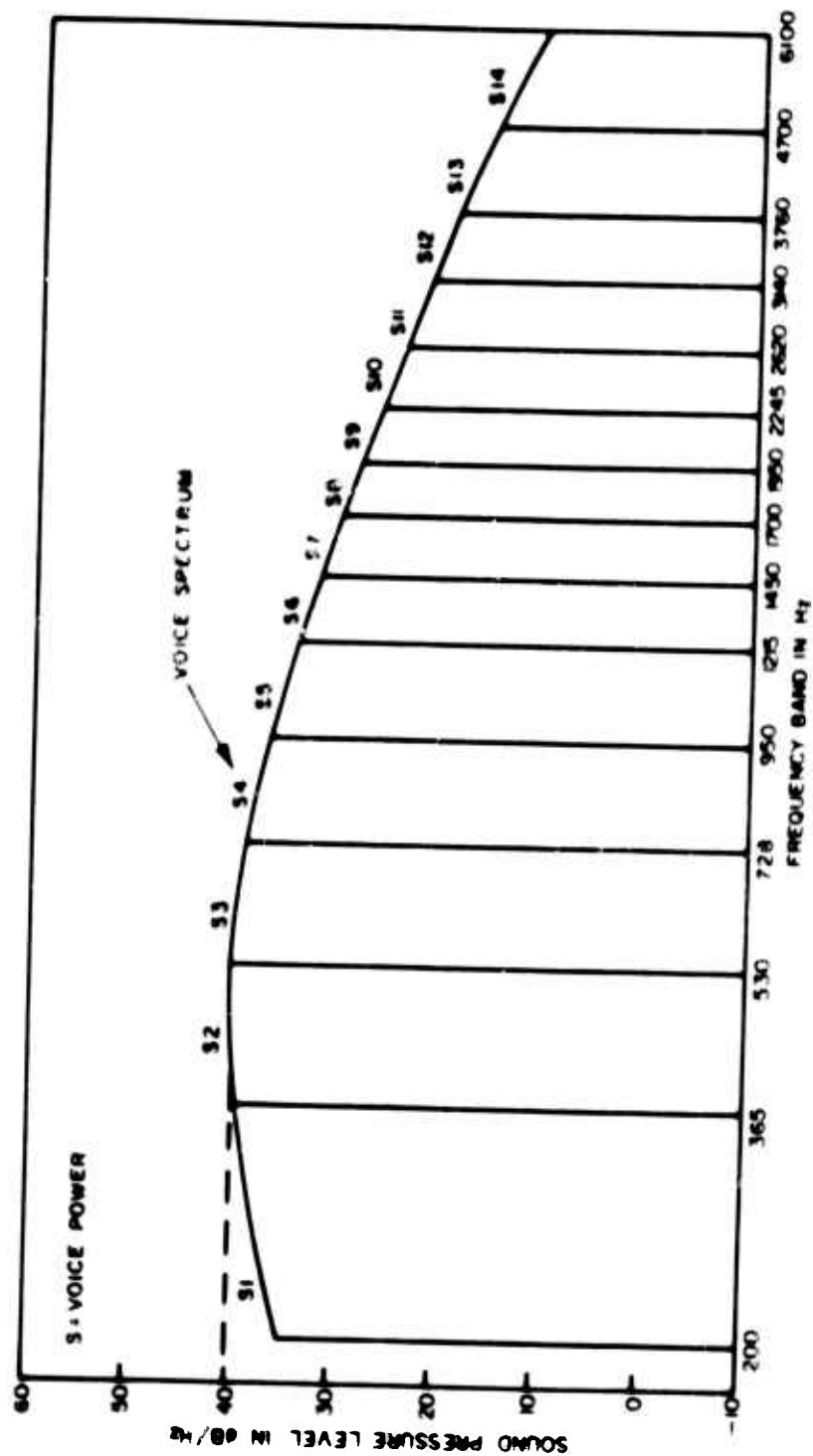


Figure IV-2. Long Term Speech Spectrum and Associated AI Bands

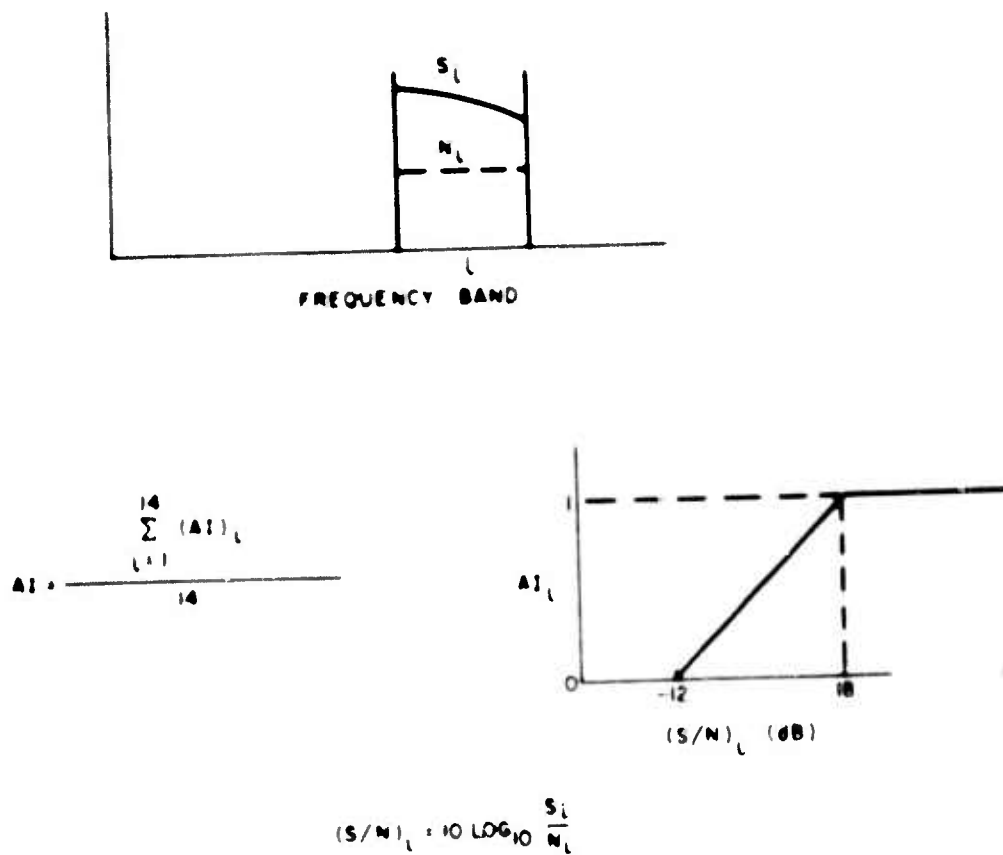


Figure IV-3. Theoretical Calculation of AI Score

since the use of a number based on this technique even for the simplest use (i.e., that of system comparison and not performance measurement) requires validation for situations in which the noise is not additive.

Another device that automatically calculates the AI, in a slightly different manner, is the Speech Communications Index Meter (SCIM) produced by Bolt, Beranek and Newman, Inc. (reference 38). The basic difference between this device and VIAS is the manner in which the synthetic voice signal is generated. In the SCIM machine, a noise spectrum is transmitted that has been frequency filtered or shaped to correspond to the average voice spectrum. This signal is then filtered into nine frequency bands and used to compute the desired to undesired signal ratios. This, therefore, ideally has an advantage over VIAS in that the actual synthetic signal power in band N is used and not an extrapolation of that signal. The SCIM machine also takes into account the upward spread of masking effect.

A new version of the automated AI calculator is the PSI/COMP machine. The performance of this machine should be very similar to the SCIM machine since it employs the same basic signal processing.

Degradation measurements involving a large number of parameter variations (PW, PRF, etc.) were desired for this investigation. Because of the time involved in testing AS with all these parameter variations, it was desired to use an automated measure. The VIAS AI scoring machine was subsequently chosen for these measurements. This device was chosen because preliminary investigation had shown that the PSI/COMP machine (and probably SCIM, since they are very similar) did not appear to respond correctly to pulsed interference.

Another concept called CORODIM (Correlation of the Recognition of Degradation with Intelligibility Measurements) has recently been developed (reference 39). This technique is similar to the previous methods in that the baseband power spectrum is again used as a basic measure. It differs from other automatic intelligibility measuring techniques in that it transmits a test signal composed of speech-like sounds representative of phoneme consonants. The degradation manifests itself as an "effective noise spectrum" which is measured and matched to one of a library of reference noise spectra. For each reference spectrum, data are stored relating phoneme recognition probability to speech-to-noise ratio. Thus, by means of the spectrum matching operation and a measurement of signal-to-noise ratio, each component sound of the test signal is assigned a probability of recognition. These values are weighted by phoneme probability of occurrence factors, summed and normalized to obtain a score representative of word intelligibility based on either initial or final consonant recognition. CORODIM evaluates scores for both the initial and final consonants and takes their product for the overall word intelligibility score.

The scores obtainable from CORODIM are directly comparable to listener panels, according to Philco, the developer. If sufficient audio spectra have been pretested, the AS results from CORODIM should also be valid for most (but not necessarily all) interfering signals. This technique, therefore, has an important theoretical advantage over all previous automated scoring techniques.

This technique was not used in this investigation and has been discussed because of its potential use in future voice degradation problems. In particular, it should be apparent that it is only necessary to couple the CORODIM process with the simulated receiver output to obtain simulated AS scores.

MINIMUM INTERFERENCE THRESHOLDS

A degradation threshold level is by implication: the level at which the interference is first observed. For the audio case being considered, the minimum interference threshold is the level at which the pulsed interference is first heard. Since this level is obtained through a subjective evaluation there is an inherent variability due to the human observer and also one due to the manner in which the threshold is defined to the observer. In particular, the threshold level can be determined by decreasing or increasing the interference level relative to a fixed desired signal level. In the first case the test begins with very noticeable interference and stops when the interference is just perceptible. In the second case the interference is increased until the subject records that the interference was first heard. The first method is more repeatable than the second, although care must be taken to insure that the level recorded is indeed the last level that can be heard. This is easily implemented by allowing the subject to adjust the interference level plus and minus the threshold level to definitely determine that the interference was and was not heard.

The test can also be made without the presence of a desired signal. This type of test would be used for high fidelity, TV, or stereo systems where the presence of interference during the time the desired signal is absent may be unacceptable. A lower threshold interference level would be required for this case than if the desired signal were present since the desired signal aids in making the presence of the interfering pulse.

The validity of this type of measurement is shown in Reference 40. Two separate listening crews were used to determine the threshold of perceptability (minimum interference threshold) for speech masked by noise. One crew contained three experienced listeners and the other contained eight inexperienced listeners. The signal (speech)-to-noise ratio (S/N) was then adjusted by each listener until he obtained the threshold of perceptability. With the exception of one individual in the crew of eight, the maximum variation in the S/N ratio required by each listener was 3 dB. The average difference in S/N between the two crews was less than 1 dB.

The minimum interference threshold approach was also used for this pulsed degradation investigation because it is repeatable and because it defines the region between no interference and slight interference.

ERROR PROBABILITIES

The evaluation of digital performance measures basically consists of computing error probabilities. In a general sense this consists of evaluating the categories of false acceptance and false dismissal. In the simplest type of detection problem (single alternative decision), false acceptance is equal to the probability of false alarm while that of false dismissal is equal to the quantity one minus the probability of detection. These can be considered by simply examining the probability densities for noise alone and for signal and noise at the receiver output (see Figure 4-22). In this figure $Q_n(x)$ refers to output noise distribution density while $P_n(x)$ is the output distribution density when signal, noise and interference are present. The false alarm probability α' is the area of $Q_n(x)$ above the decision threshold K' . The area of $P_n(x)$ above the threshold K' is the probability of detection. One minus this value or the area of $P_n(x)$ below the threshold K' is the false dismissal probability β' . These quantities can be stated mathematically as

$$\alpha' = \int_{K'}^{\infty} Q_n(x) dx \quad (IV-1)$$

$$\beta' = \int_{-\infty}^{K'} P_n(x) dx \quad (IV-2)$$

Both $P_n(x)$ and $Q_n(x)$ are output probability densities obtained by operating on the input probability densities with the receiver system structure. If, as an example, the receiver has an envelope detection-threshold type of structure the envelope of the input probability density distribution must be obtained in order to obtain $P_n(x)$ or $Q_n(x)$ before the false acceptance or false dismissal probabilities can be calculated. This operation is, in general, nonlinear.

The calculation of $Q_n(x)$ and $P_n(x)$ for specific a priori interference and noise assumptions generally involves untractable analysis problems. However, the modeling of the receiver structure and the simulation process described in Section 4 readily allow error probability evaluation. In particular, it is basically only necessary to count the number of undesired responses above a desired threshold (K') in the simulated receiver time amplitude output response to obtain false alarm probabilities. It is, of course, also necessary to properly randomize the input variables to obtain the desired output density function for these calculations. The false dismissal probabilities can also be obtained in a similar manner.

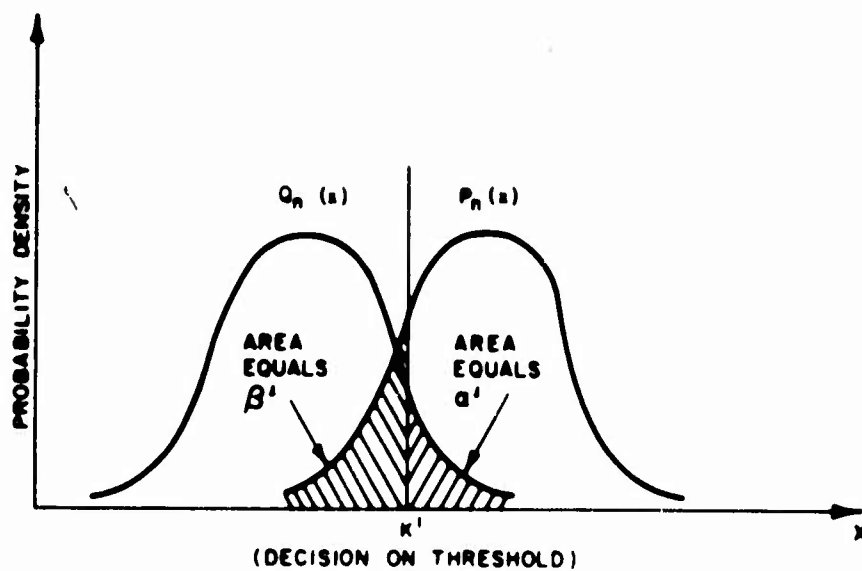


Figure IV-4. System Probability Density with Decision Regions

SUMMARY

This Appendix has discussed various degradation measures that are applicable to voice and digital systems. The measurements and analysis, discussed in this report, concentrate on voice modulation. In the voice area AS measurements are required as the basic intelligibility measure. However, when an investigation involving numerous parameters is to be undertaken an "available automated" measure such as the VIAS AI measure must be used to complete a testing program in a reasonable time. In addition, it is also desirable to subjectively measure the just perceptible "threshold" of interference since neither the AI or AS can accurately measure interference in this region. It is, therefore, required (because of the lack of a general measure) to use AS, AI and threshold measures to solve voice degradation problems. It is also apparent that, in general further investigation should be made of different automated measures of voice degradation. It appears that if it is desired to generally model voice intelligibility degradation the CORODIM and the PCI technique should be further investigated.

The application of the time waveform simulated output digital modulation was also discussed. In general, the solution to other types of degradation measures involves the appropriate operation on the output time waveform signals to obtain the degradation measure.

REFERENCES

1. R. Mayher, *Introduction to the Analysis of Interference to the Performance of Communications Systems*, ECAC-TR-65-1, May 1965.
2. R. Mayher and R. Serafin, *Interference Effects in Matched Filter Receivers*, ESD-TR-66-7, August 1966.
3. R. Mayher, *The Analysis of Interference to Phase and Frequency Feedback Systems*, ESD-TR-66-8, March 1967.
4. R. Mayher, *Basic Performance Thresholds*, ESD-TR-66-9, December 1966.
5. R. Mayher, *Interference Detection Modeling*, ECAC-TM-X003-18, November 1963.
6. W. J. Cunningham, S. J. Goffard and J. C. R. Licklider, *The Influence of Amplitude Limiting and Frequency Selectivity Upon the Performance of Radio Receivers in Noise*, Proceedings of the IRE, 1947.
7. F. Haber, *Receiver Susceptibility to RF Pulse Interference*, University of Pennsylvania, Philadelphia, Pennsylvania.
8. J. Molnar, *Intelligibility Tests on the R-361 (GRR-7) Receiver in the Presence of RF Pulse Interference*, RADC-TN-59-198, June 1959.
9. W. Duff, K. Heisler, Jr., et. al., *Voice Communication Degradation Study*, RADC-TR-67-546, February 1968.
10. Proposed MIL-STD-449(D), August 1969.
11. J. Herishen, *Diode Mixer Coefficients for Spurious Response Prediction*, ESD-TR-67-10, December 1967.
12. J. Sell, *The Spurious Response Measurement and Identification Problem*, ESD-TR-69-303, November 1969.
13. M. Lustgarten, *COSAM (Cosite Analysis Model)*, 1970 IEEE International Symposium on Electromagnetic Compatibility, July 1970.

REFERENCES (continued)

14. W. Rothlisberger, *Interference Prediction Model Development: Cosite Interference Prediction*, Bell Aerosystems Report No. A70009-371, November 1968.
15. W. Cochran, J. Cooley, D. Favin, H. Helms, R. Kaenel, W. Lang, G. Maling, Jr., D. Nelson, C. Rader, P. Welch, *What is the Fast Fourier Transform?*, Proceedings of the IEEE, October 1967.
16. R. Mayher, *Off-Tuning Effects Produced by Interference*, Ninth Tri-Service Conference on Electromagnetic Compatibility, October 1963.
17. R. Marcus and F. Stenwick, *Computer Program for Determining the Effects of Transfer Functions on a Pulsed RF Signal*, 1968 IEEE EMC Symposium, July 1968.
18. S. Seely, *Electron Tube Circuits*, McGraw Hill, 1958.
19. *Monosyllabic Word Intelligibility*, American Standards Association, Report No. 532-1960.
20. *General Test Standard*, Bell Aerosystems Company, RLP-B 2, 21 September 1966.
21. S. Stevens, J. Miller and I. Truscott, *The Masking of Speech by Sine Waves, Square Waves and Regular and Modulated Pulses*, The Journal of the Acoustical Society of America, Vol. 18, No. 2, October 1966.
22. G. Miller and J. Licklider, *The Intelligibility of Interrupted Speech*, The Journal of the Acoustical Society of America, Vol. 22, No. 2, March 1950.
23. D. Robertson, *A Comparison of the Procedures and Results of Intelligibility Tests for a Number of Interference Conditions*, ECAC Technical Memorandum No. X003 10, 16 April 1962.
24. Jansky and Bailey, *Interference Prediction Study*, Final Report, Vol. 1, Contract No. AF 30(602)1934, January 1960.
25. A. Thompson, *The Application of the Voice Interference Analysis System to the Prediction of Voice Intelligibility - Part I*, Bell Report No. A70009-280, November 1967.

REFERENCES (continued)

26. P. Newhouse, *Electromagnetic Compatibility Communications, Designers Digest*, Vol. 2, No. 12, pp. 34-38, December 1969.
27. P. Newhouse, *A Simplified Method for Calculating the Bounds in the Emission Spectra of Chirp Radars* ECAC-TR-70-273.
28. Mason, S., Zimmerman, H., *Electronics Circuits, Signals, and Systems*, John Wiley and Sons, Inc., New York, 1960.
29. Popoulis, A., *The Fourier Integral and Its Application*, McGraw-Hill Book Company, New York.
30. Panter, P., *Modulation Noise and Spectral Analysis*, McGraw-Hill Book Company, New York.
31. Stein, S., Jones, J. J., *Modern Communication Principles*, McGraw-Hill Book Company, New York, 1967.
32. G. Hawthorne, Jr., W. Jones, Jr., S. Robinette, Jr., V. Smith, Jr., W. Warren, Jr., and W. Wright, *Final Report - Volume I Performance of Communications Systems in the Presence of Interference*, RADC-TR-59-133A.
33. D. Robertson, *A Comparison of the Procedures and Results of Intelligibility Tests for a Number of Interference Conditions*, ECAC Technical Memorandum No. X003-10, April 1962.
34. N. French, J. Steinberg, *Factors Governing the Intelligibility of Speech Sounds*, Journal of the Acoustical Society of America, Vol. 19, pp. 90-119.
35. A. Tkachenko, *Tonal Method for Determining the Intelligibility of Speech Transmitted by Communications Channels*, Soviet Physics - Acoustics, Vol. 1, No. 2 (January - June 1955).
36. J. C. R. Licklider, A. Bisberg and H. Schwarzlander, *An Electronic Device to Measure the Intelligibility of Speech*, 1959 Proceedings of the National Electronic Conference, No. 15, 1959.

REFERENCES (continued)

37. R. Fitts, *Electronic Evaluation of Voice Communications Systems*, RADC-TDR-63-355, August 1963.
38. C. Hudson, W. Limburg, *Loss of System Effectiveness due to Electromagnetic Interference*, Tenth TriSource Conference on Electromagnetic Compatibility, Chicago, Illinois, November 1964.
39. G. Strohmeyer, J. Richards, J. Schultz, *Voice Quality Determination Study*, RADC-TR-67-319, August 1967.
40. J. Egan, *Articulation Testing Methods II*, OSRD Report No. 3802, Research on Sound Control Psycho-Acoustic Laboratory, Harvard University, Cambridge, Massachusetts, 1 November 1944.

DISTRIBUTION LIST FOR
ANALYSIS OF PULSED INTERFERENCE
TO AMPLITUDE MODULATED (AM) RECEIVERS
ESD TR 70 207

DOD AND OTHERS	No. of Copies	NAVY (Continued)	No. of Copies
JCS (J-6/SSD01) DOD Pentagon Washington, D.C. 20330	1	Commander (AIR 53356A J. Fisher) Naval Air Systems Command Washington, D.C. 20360	1
Hqs ESD (TRI) L.G. Hanscom Field Bedford, Massachusetts 01730	3	Commander (LEX 0512/C Neill) Naval Electronic Systems Command Washington, D.C. 20360	1
OSD (ODDRAE) Attn: Col James H. Terrell DOD Pentagon Washington, D.C. 20301	1	Western Area Frequency Coordinator Attn: E. Angle Point Mugu, California 93042	1
DOC Cameron Station Alexandria, Virginia 22314	20	Superintendent Naval Postgraduate School Monterey, California	1
Director Defense Communications Agency Attn: Mr Samuel Ed. Probst, Code 513 Washington, D.C. 20305	1	AIR FORCE	
Director National Security Agency Attn: K 304 Fort George G. Meade, Maryland 20755	2	Hq USAF (PRCF) Room 2303, Tempo 8 Building 3500 Newark Street, N.W. Washington, D.C. 20330	1
Department of Transportation Federal Aviation Administration Attn: RD-510 Washington, D.C. 20590	4	Hq AFCS (DONRF) Richards-Gebaur, Mo. 64030	1
National Aeronautics and Space Administration Goddard Space Flight Center Attn: Code 551 Greenbelt, Maryland 20771	1	Hq RADC (RCCI) Griffiss AFB New York 13440	1
NAVY		MARINE CORPS	
Chief of Naval Operations (OP-03E) Navy Department Washington, D.C. 20350	1	Commandant of the Marine Corps (A04C) Headquarters, U.S. Marine Corps Washington, D.C. 20380	1
Chief of Naval Operations (OP-094F) Navy Department Washington, D.C. 20350	1	Commanding General Marine Corps Development Center MCDEC (C E Div.) Quantico, Virginia 22134	1
Commander, Naval Communications Command Naval Communications Command Headquarters 4401 Massachusetts Ave., N.W. Washington, D.C. 20390	1	Commander (Code 1270) Naval Electronics Laboratory Center San Diego, California 92152	1
Commander, Naval Ship Engineering Center Attn: Code 6179C07 Center Building Prince George's Center Hyattsville, Maryland 20782	1	ARMY	
		U.S. Army Safeguard System Office Attn: CSSSO-TDE 1320 Wilson Blvd. Arlington, Virginia 22209	1
		Joint Chiefs of Staff Joint Continental Defense Systems Integration Planning Staff Attn: LTC Finch/JSSC-C 1320 Wilson Blvd. Arlington, Virginia 22209	1

DISTRIBUTION LIST (continued)

	No. of Copies		No. of Copies
ARMY (continued)		INTERNAL	
Headquarters, Department of the Army Office of Assistant Chief of Staff for C-E Attn: CEED-7c Washington, D. C. 20314	1	ACO-3 (Lustgarten)	1
		ACOE-A	1
		ACOE-E	1
		ACOE-S	1
		ACOP-A	2
		ACOP-F	3
Commanding General U. S. Army Safeguard System Command Attn: SSC-STE (Welmer) P. O. Box 1500 Huntsville, Alabama 35807	1	ACOP-C	1
		ACOAT	5
		ACV	2
		ACX	1
		ACY	5
		ACZ	1
Commanding General U. S. Army Safeguard System Command Attn: SSC-DER (Odom) P. O. Box 1500 Huntsville, Alabama 35807	1	R. Hinkle	1
		W. Hatch	1
		R. Mayher	5
		J. Harshen	1
		D. Hughes	1
Commanding General U. S. Army Safeguard System Command Attn: Mr. W. Lawson P. O. Box 1500 Huntsville, Alabama 35807	1	E. Harrison	1
		R. Meyers	1
		R. Seach	1
Commanding General U. S. Army Missile Command Attn: AMCPM-MD/J. Brower Huntsville, Alabama 35809	1		
Commanding General U. S. Army Test and Evaluation Command Attn: AMSTE-EL Aberdeen Proving Ground, Maryland 21005	1		
Commanding General U. S. Army Electronics Command Attn: AMSEL-NL-C Fort Monmouth, New Jersey 07703	1		
Commanding Officer U. S. Army Electronic Proving Ground Attn: STEEP-EM Fort Huachuca, Arizona 85613	1		
Commanding General U. S. Army Strategic Communications Command Safeguard Communications Agency Attn: SCCX-SA-EED/B. Dycus Fort Huachuca, Arizona 85613	1		